Representative UKCS Seismic Survey Modelling

OESEA-17-81

Submitted to:

John Hartley
Hartley Anderson Limited
on behalf of the UK Department for Business, Energy and Industrial Strategy

Authors:

Michael Wood
Michael Ainslie
Alexander von Benda-Beckmann
Mark Prior
Rasmus Sloth Pedersen

10 September 2020

P001385
Document 01719
Version 1.0

JASCO Applied Sciences (UK) Ltd
The Roundel, St Clair's Farm
Wickham Road, Droxford
Hampshire, SO32 3PW UK
Tel: +44 (0) 1489 878439
www.jasco.com

Suggested citation:

Wood, M.A., M. A. Ainslie, A. M. von Benda-Beckmann, R. S. Pedersen, and M. K. Prior. 2020. Representative UKCS Seismic Survey Modelling*: OESEA-17-81*. Document 01719, Version 1.0. Report by JASCO Applied Sciences, TNO, and Irwin Carr Consultants for the UK Department for Business, Energy and Industrial Strategy's Offshore Energy Strategic Environmental Assessment programme

Disclaimer:

The results presented herein are relevant within the specific context described in this document. They could be misinterpreted if not considered in the light of all the information contained in this document. Accordingly, if information from this document is used in documents released to the public or to regulatory bodies, such documents must clearly cite the original document, which shall be made readily available to the recipients in integral and unedited form.

Contents

Figures

Tables

1. Introduction

This report contains the outputs of the project: “Modelling of Received Levels by Marine Mammals during Geophysical Surveys”, a study funded by the Department for Business, Energy and Industrial Strategy (BEIS) under the Offshore Energy SEA Programme and managed by Hartley Anderson Ltd (OESEA-17-81).

As part of marine seismic surveys significant acoustic levels are generated in the water. Current practices typically involve an assessment of the environmental impact of this type of activity and results typically form an integral part of the ‘noise risk assessment’. This assessment considers the potential consequences of the sound exposure against the likelihood of occurrence. Crucial to this, is the prediction of the acoustic levels in the water given the sound source and the environment in which it propagates. In most cases, this requires underwater acoustic modelling to take place. The results of the sound level predictions are then compared against scientifically established impact threshold criteria to determine the level of impact. Although seemingly straightforward, noise risk assessments in practice are complex and can vary significantly in levels of detail.

The aim of the modelling study is to provide robust examples of sound generated during typical geophysical survey scenarios to inform the development of guidance for noise risk assessments. This is through modelling studies representative of those undertaken on the UK continental shelf (UKCS). Multiple sound sources associated with the activities are investigated and the modelled locations are selected to be based on different region that provide contrasting environmental conditions. The underwater acoustic modelling in this report was carried out by JASCO Applied Sciences, TNO, and Irwin Carr Consultants, using multiple different acoustic models and modelling approaches to provide a set of baseline results. Based on these results, multiple single aspect modelling studies were carried out to focus on specific facets of the modelling, such as the source, environment, and receiver, to investigate the relative importance of the inputs to the modelling.

2. Project Overview

The work was performed in three phases: defining source characteristics, baseline acoustic modelling to determine the distance to thresholds for a set of typical scenarios, and lastly modelling variants of the baseline scenarios to quantify the relative importance of different factors on distance estimates.

The report is organised as follows: Section 3 provides an overview of the metrics for which results are presented, and include sound exposure level (SEL) and peak sound pressure level ($L_{p,\mathrm{pk}}$) metrics. Section 4 presents the work from Phase 1 that describes the airgun array sources, and the source modelling results. Sections 5 to 8 comprise the Phase 2 work. Section 5 provides details of the environmental properties for each of the scenarios. Four environments are defined that are based on general locations within the UK continental shelf (UKCS). The environments defined are: Irish Sea, North Sea Shallow, North Sea Deep, and Faroe-Shetland Channel. The choice of location, geoacoustic properties, and sound speed profiles are presented for each of these environments. Section 6 provides descriptions of the soft-start approach for each of the arrays and the survey designs to encompass 24 hours of operation required for the calculation of cumulative SEL to compare against identified impact thresholds. A description of the numerical models employed and the individual modelling processes are described in Section 7. The results and brief discussion of the numerical modelling is presented in tabular form in Section 8. Finally, the work from Phase 3 is covered in Sections 9 to Section 12. Section 9 presents results exploring the use of simple, commonly-used “N log(R)” expressions for the propagation modelling. Section 10 includes the model variants using static receivers; this includes: using a source model with greater higher-frequency energy, seasonal variation, taking maximum levels over the entire water column, the inclusion of surface roughness, and consideration of a change in geoacoustics. Sections 11 and 12 investigate the use of moving receivers with prescribed motions and those based on behavioural definitions respectively, and the acoustic effects in each case. Final discussions and conclusions are covered in Section 13. Underwater acoustical terminology throughout follows ISO (2017) and Ainslie et al. (2018).

2.1. Modelled Scenarios

In this project, six baseline scenarios were considered using sources and locations representative of survey operations on the UKCS. Scenario 1 considers a site survey, Scenario 2 investigates the sound fields from a VSP source array, and Scenarios 3 through 6 describes a regional seismic source array in four distinct regions around the UK. The environment for Scenarios 1 and 2 was selected as that supporting the largest impact from initial modelling of Scenarios 3 to 6 and so are representative of the most conservative case of the considered environments. The scenarios are listed in Table 1.

Table 1. Baseline scenarios for the geophysical modelling study.

Scenario	Survey type	Source characteristics	Survey characteristics	Environment
1	Site seismic survey	Array volume: 160 in³ Pulse interval: 3 s Pulse spacing: 6.25 m Depth: 3 m	Line length: 4 km Inter-line distance: 50 m Inter-track dist.: 2 km Line duration: 32 min Line turn dur.: 34 min	North Sea Deep
2	VSP	Array volume: 750 in³ Pulse interval: 20 s (static) Depth: 5 m	Vessel speed: Static	North Sea Deep
3	Reservoir & Regional seismic surveys (2D, 3D, 4D)	Array volume: 4130 in³ Pulse interval: 10 s Pulse spacing: 25 m Depth: 7 m	Line length: 20 km Inter-line distance: 300 m Inter-track dist.: 9.9 km Line duration: 144 min Line turn dur.: 120 min	Irish Sea
4				North Sea Shallow
5				North Sea Deep
6				Faroe-Shetland Channel

3. Impact Thresholds

The modelling study investigates modelled ranges to the permanent threshold shift (PTS) onset levels as recommended by NMFS (2016, 2018) for auditory groups represented in UK waters. These internationally recognised thresholds are supported by the latest scientific evidence and are appropriate for the sound sources and operations considered in this project. Additional results that consider the modelled ranges to temporary threshold shift (TTS) onset levels are included where studies into certain investigated factors are not evident close to the source, but at ranges more representative of those associated with TTS onset levels. Further PTS and TTS levels using older thresholds and weightings by Southall et al. (2007) are provided to allow for further comparisons with existing literature; the additional results are presented in appendices as indicated by the text. It should be noted that the NMFS 2018 thresholds are identical to those published in 2016, and later published by Southall (2019), although the latter reference included a change in terminology for the auditory groups; it is the auditory groups as defined by NMFS that are used here.

Table 2 lists the PTS thresholds for which maximum ranges are provided for the seismic survey modelling work. The PTS thresholds are in terms of both peak sound pressure level ($L_{p,\mathrm{pk}}$), and cumulative sound exposure level (SEL_{24h}). Modelling results in this report are analysed based on the thresholds shown in Table 2. The NMFS weightings are presented in Appendix A.1, and the Southall M-weightings are presented in Appendix A.2. The associated temporary threshold shift (TTS) levels are presented in Appendix A.3.

Table 2. PTS onset thresholds from NMFS (2018). Frequency-weighting is specified by NMFS (2018). The subscript “24h” indicates accumulation of sound exposure over 24 hours.

Marine mammal group	$L_{p,\mathrm{pk}}$ dB re 1 µPa	NMFS-weighted SEL_{24h} dB re 1 µPa²s
Low-frequency cetaceans	219	183
Mid-frequency cetaceans	230	185
High-frequency cetaceans	202	155
Phocid pinnipeds in water	218	185

4. Airgun Array Sources

4.1. Airgun Array Source Model

A single source model was selected to generate the source characteristics of all the arrays to be modelled in the study. The source model used was the Airgun Acoustic Source Model (AASM; (MacGillivray 2006), revised 2014), which has been developed by JASCO Applied Sciences. It is noted that other airgun array source models do exist and the effect of the choice of source model is discussed in Section 10.1.

AASM generates source functions based on the physics of the airgun array rather than from back-propagated recordings in specific environments; consequently, it is much more versatile and able to model virtually any type of airgun array geometry, regardless of environment. The output from the model is used routinely for standard survey geometries and has also been used for novel, bespoke and research airgun array studies. Modelling studies were undertaken by JASCO in 2011 using AASM for the E&P Sound and Marine Life Joint Industry Programme (JIP) specifically to characterise a much broader frequency range of radiated sound from conventional airguns to better inform global impact modelling studies.

Input data for AASM include the airgun array geometry which is one of the principal controlling parameters for the calculated directivity of each pulse. Array geometries are selected to optimise the directivity of the radiated impulse to match the water depth, survey type and sub-bottom penetration requirement. These optimised geometries are not unique to the UKCS as they are used in many other regions with similar water depths and basin geologies.

The output of AASM comprises the individual source pressure waveforms of each airgun. The treatment of the output, however, varies across propagation models. It is computationally more efficient to generate a single ‘point source’ representation of the array than to model the propagation from each individual airgun. Potential issues that may arise when representing the source in this way are that it is easy to lose information for both directivity in vertical and horizontal planes and in phase difference phenomena caused by the geometry that is vital for accurate representation of the time domain signal. Further details of how each model treats the source is discussed with other model details in Section 7.3.

4.1.1. Model description

AASM is a combined deterministic and stochastic model that treats separately the low-frequency and high-frequency components of signals produced by airgun arrays to produce the source levels and directivity from this type of source. The low-frequency module solves a set of parallel differential equations that govern the airgun bubble oscillations and accounts for additional physical effects, including pressure and motion interactions between airguns, port throttling, and bubble damping. It includes effects from surface-reflected pressure waves, heat transfer from bubbles to the surrounding water, and movement of the bubbles due to buoyancy. The high-frequency module in AASM simulates the high-frequency spectra of individual airguns in an array using a multivariate statistical model derived from measurements. The output of the model is a set of notional source signatures, corresponding to the individual airgun signals, which are then used to compute the far-field signature of the array in any direction. These “notional” signatures for each array element are based on:

- Array layout;
- Volume, tow depth, and operating pressure of each airgun; and
- Interactions between airguns in the array.

These notional signatures are the source waveforms of the individual airguns, and they account for the interactions with the other airguns in the array. The signatures are summed with the appropriate phase delays to obtain the far-field source signature of the entire array in all directions. This far-field array signature is filtered into decidecade[1] (equivalent to 1/3-octave) passbands to compute the source levels of the array as a function of frequency band and azimuthal angle in the horizontal plane (at the source depth). The array can then be treated as a directional point source in the far field.

In the near field, on the other hand, the airgun array appears as a collection of distinct sources, making the point-source representation inapplicable. Near-field conditions exist at distances less than the (frequency-dependent) Fresnel distance[2], R_{nf}, defined as

$$R_{\mathrm{nf}} < \frac{l^2}{4\lambda}$$

where λ is the sound wavelength and l is the longest dimension of the array (Lurton 2002). In addition, the minimum extent of the near field is determined by the physical size of the array, with $l/2$ suggested as a transition range by ANSI (R2003). For example, for the Regional Survey airgun array in this work, l = 16.8 m so near-field conditions exist at ranges less than 8 m at 10 Hz and 47 m at 1000 Hz.

The interactions between individual elements of the array create directionality in the overall acoustic emission. Generally, this directionality is prominent mainly at frequencies in the mid-range between tens of hertz to several hundred hertz. At lower frequencies, with acoustic wavelengths much larger than the inter-airgun separation distances, the directionality is small. At higher frequencies, the pattern of lobes is too finely spaced to be resolved and the effective directivity is less.

Although airgun signatures are highly repeatable at the low frequencies, extensive measurements from the Svein Vaage source characterization study Mattsson and Jenkerson (2008) have demonstrated that the high-frequency (>1 kHz) spectrum for single airguns includes a significant random component (Figure 1). Furthermore, for an array of airguns, the far-field directivity pattern of the source is sensitive to small random changes in the firing times and relative positions of the individual airguns. Despite the influence of these stochastic effects, the source spectrum and directivity pattern of an airgun array converges to a stable mean value when averaged over many shots. Thus, to treat these stochastic components of the airgun array source level rigorously, AASM uses a Monte-Carlo approach: the physical model is run many times with small random perturbations to the high-frequency spectrum and airgun firing times (MacGillivray 2019). The results are then averaged to produce a smoothed spectrum representative of the long-term average source level.

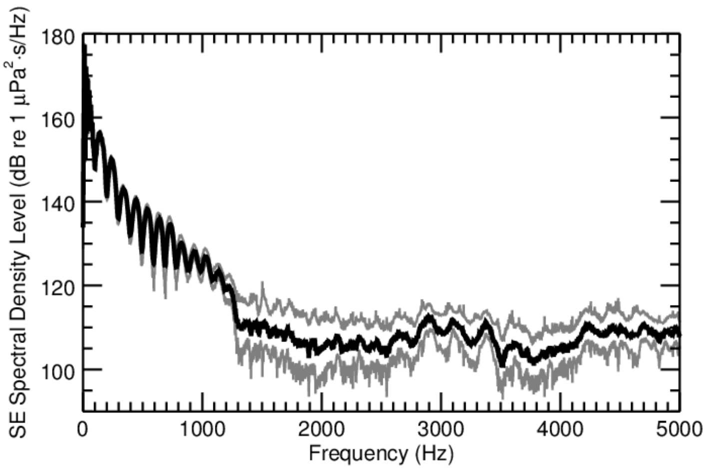

Figure 1. Mean and standard deviation sound exposure (SE) spectral density level of 30 shots from a 3.28 L (200 in³) Bolt 1900LLX airgun, from the Svein Vaage broadband airgun study, measured at 14.9 m range (reproduced from MacGillivray (2019)).

[1] A decidecade is one tenth of a decade and is approximately equal to one third of an octave (1/3-octave).
[2] Other definitions exist for the far-field range based on different assumptions with it being defined in ANSI (R2003) as $R > \pi l^2/4\lambda$ and ISO (2017) as $R > \pi l^2/\lambda$.

The output is a directional high-frequency component to the source that is representative of the geometry of the source whilst avoiding unrealistic, highly precise, beam pattern interference resulting from an ideal model. The mean high-frequency spectra from the stochastic model augment the low-frequency signatures from the physical model, allowing AASM to predict airgun source levels at frequencies up to 25,000 Hz.

Both the high- and low-frequency components of the model are tuned to fit a large library of high-quality seismic source signature data obtained from the Joint Industry Program (JIP) on Sound and Marine Life (Mattsson and Jenkerson 2008).

4.2. Airgun Array Source Characteristics

Three different sources were agreed upon by the project steering group to match the survey type specified in the scope of work. A key requirement was for each of the sources to be representative of real-world arrays used on the UKCS.

The sources for the site survey and the VSP are relatively simplistic arrays representative of source arrays routinely used for UKCS surveys. For the regional survey, the source chosen is a 4130 in³ array modelled for an International Association of Oil and Gas Producers (IOGP) Sound and Marine Life Joint Industry Programme study in the North Sea (Zeddies et al. 2017, Matthews et al. 2018); across the UKCS, much smaller and larger arrays may be deployed (the range of array volumes reported to BEIS in 2014–2016 ranged from 2380 in³ to 6300 in³) but this intermediate size is representative of the majority (70%) of surveys The design of each array is presented in subsequent sections, along with the source modelling outputs. All are assumed to be operating at a pressure of 2000 psi (13790 kPa). The coordinate system follows a right-hand rule with positive Z indicating increasing depth; all arrays are towed in the positive X direction. The sources are summarised in Table 3.

Table 3. Chosen airgun arrays for each survey type in the modelling project.

Survey Type	Array volume (in³)	Number of active guns	Source depth (m)
Site survey	160	4	3.0
VSP Survey	750	3	5.0
Regional Survey	4130	31	7.0

4.3. Modelled Airgun Arrays

Due to the multiple elements comprising the airgun arrays and the acoustic interaction between them, the sound energy propagating from the arrays is not omnidirectional but varies according to horizontal and vertical angles. Modelling results of levels and spectra for the three sources at full operating volume are presented in principal directions. For the site survey and regional survey sources these are:

- Endfire: fore and aft directions;
- Broadside: port and starboard directions;
- Vertical: directly down; results are shown for both with and without the reflection (ghost) – as the reflection is inherent in the acoustic models used, only the without ghost outputs are used in modelling.

As the geometry of the VSP array does not lend itself to a ‘forward’ direction, the following terms are used:

- In-plane: horizontal sound in the same plane as the array elements;
- Perpendicular: horizontal sound perpendicular to the array element plane;
- Vertical: directly down without any reflection from the sea surface.

4.3.1. Site survey source

The source used for the site survey scenarios is the 4 × 40 in³ array described in Table 4 and shown in Figure 2.

The horizontal directivity of the array as a function of frequency is shown in Figure 3 and the signatures and spectra in broadside, endfire, and vertical directions are shown in Figure 4.

Table 4. The geometry of the 160 in³ site survey array.

Gun	*X* (m)	*Y* (m)	*Z* (m)	Volume (in³)
1	1.25	0.0	3.0	40
2	0.25	0.0	3.0	40
3	-1.25	-0.4	3.0	40
4	-1.25	0.4	3.0	40

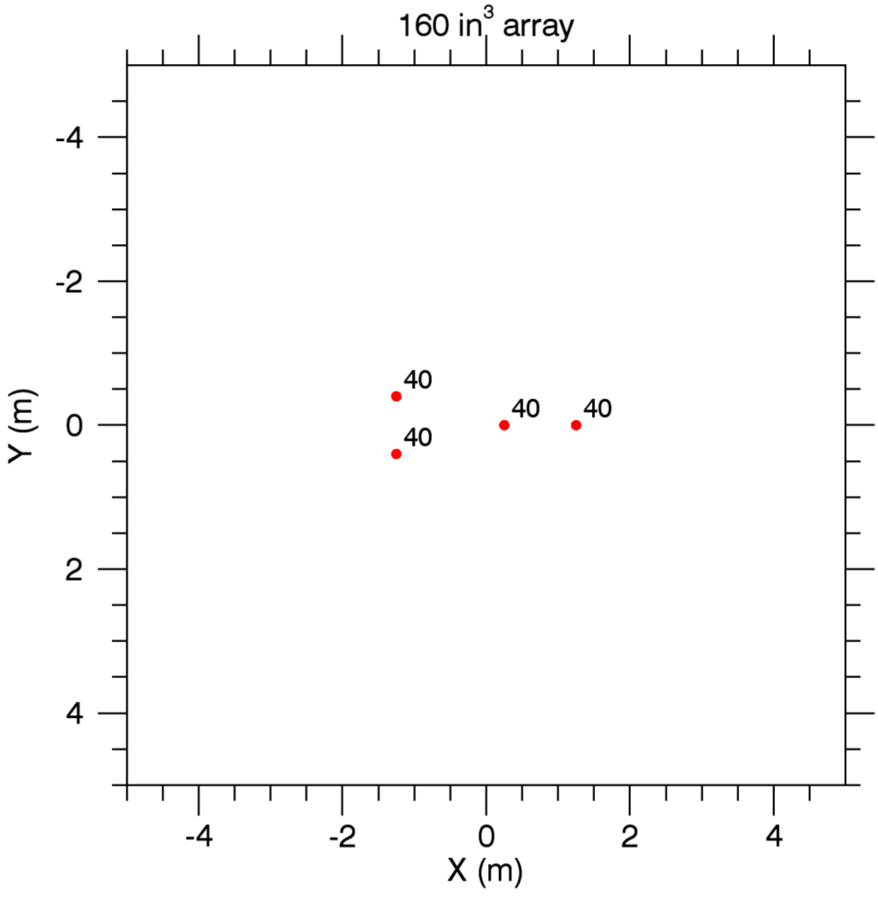

Figure 2. Plan view of the 160 in³ site survey array.

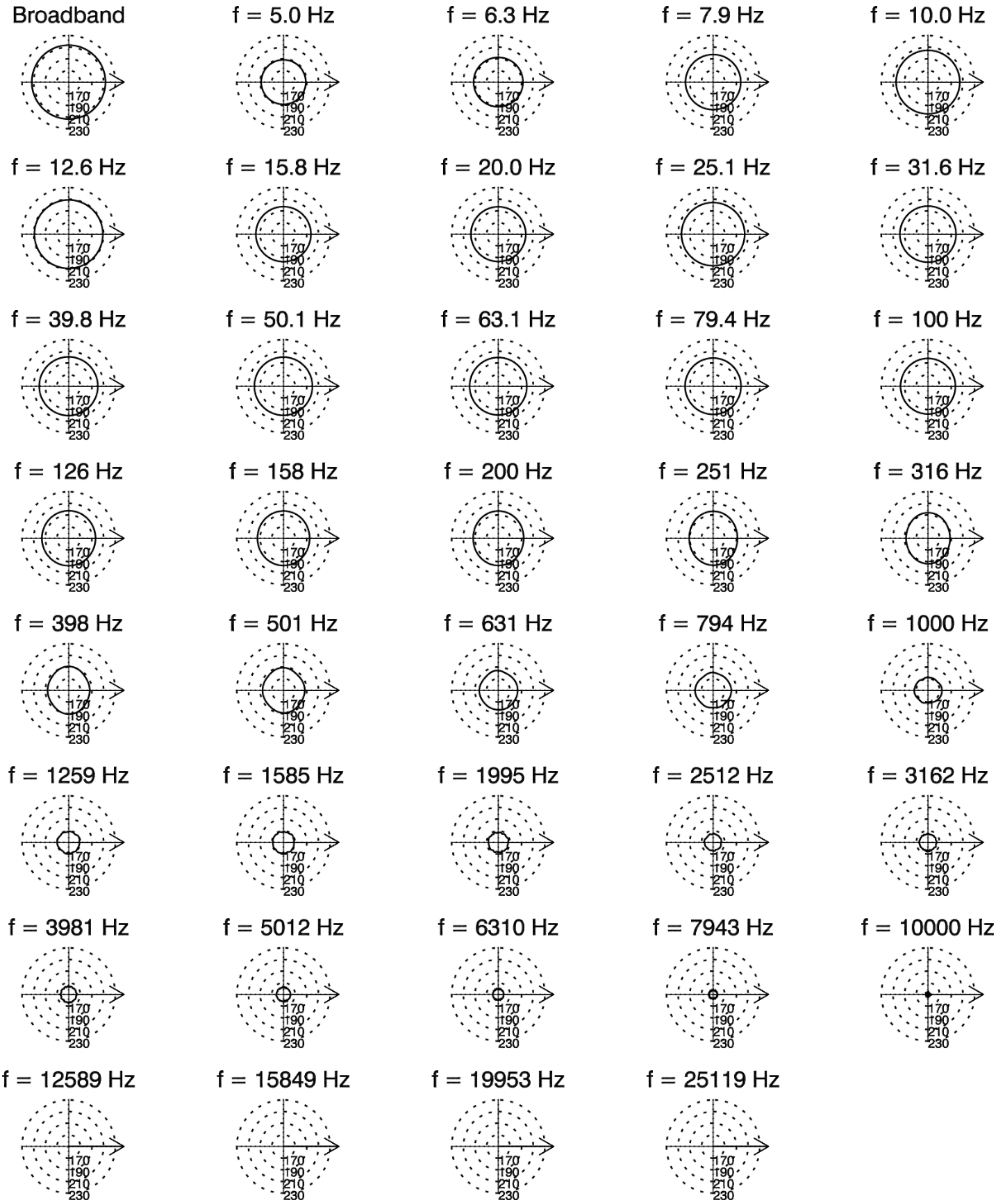

Figure 3. Horizontal energy source level (dB re 1 µPa²m²s) in decidecade bands as a function of azimuth and frequency for the 160 in³ site survey array. The arrow indicates the direction of travel.

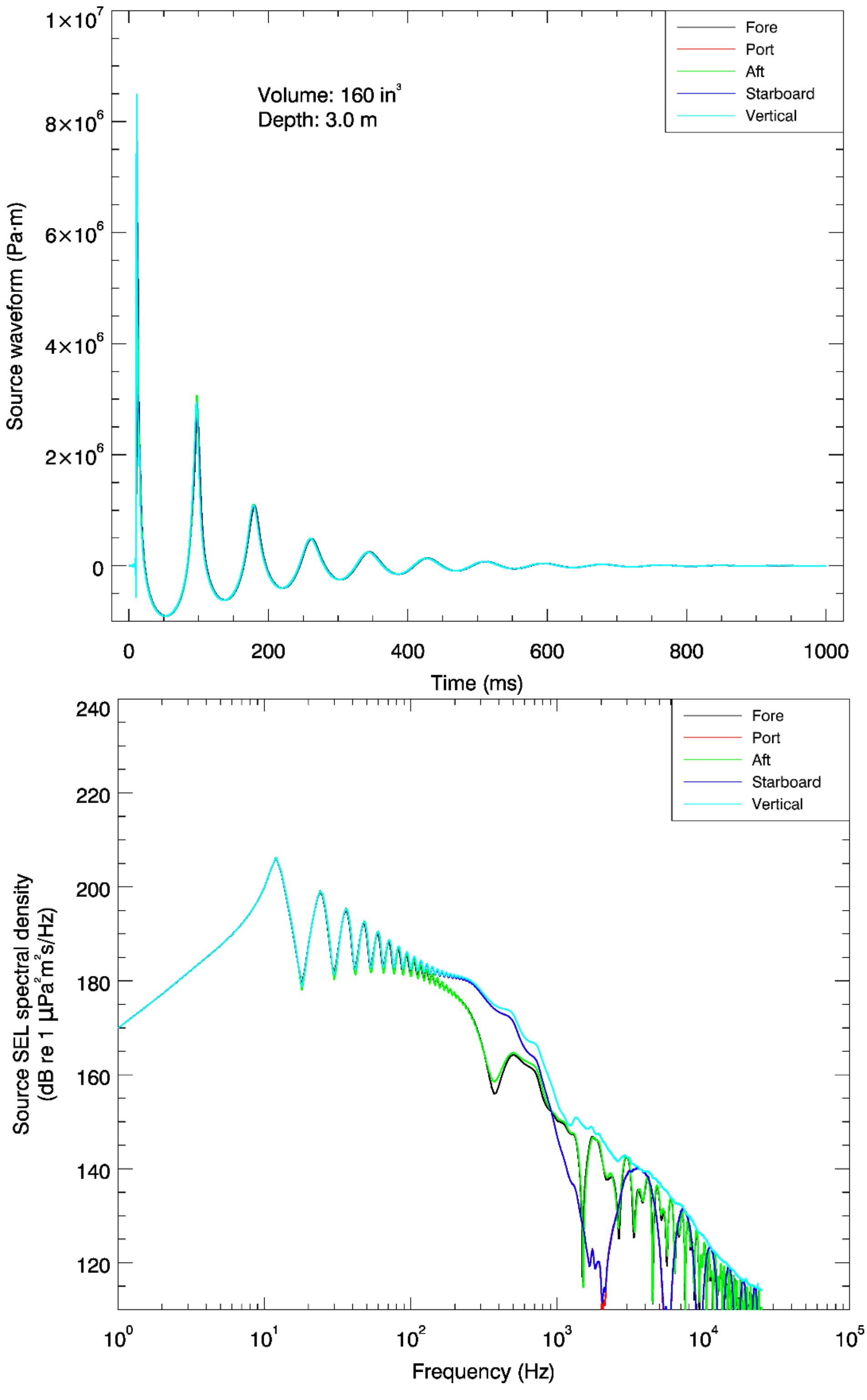

Figure 4. Source waveforms of individual airguns (Pa m) and energy source spectral density level (dB re 1 µPa^2m^2s/Hz) of the 160 in^3 site survey array.

4.3.2. VSP array source

The source employed for the VSP scenario is the 3 × 250 in³ array described in Table 5. The configuration is as a 3-element airgun cluster mounted on a frame and deployed from a rig; Figure 5 shows the side view of the gun positions with the three guns residing on the $X = 0$ plane.

The directivity of the array as a function of frequency is shown in Figure 6 and the signatures and spectra in horizontal (in-plane and perpendicular) and vertical directions are shown in Figure 7.

Table 5. The geometry of the 750 in³ VSP survey array.

Gun	X (m)	Y (m)	Z (m)	Volume (in³)
1	0.0	0	4.31	250
2	0.0	0.6	5.35	250
3	0.0	-0.6	5.35	250

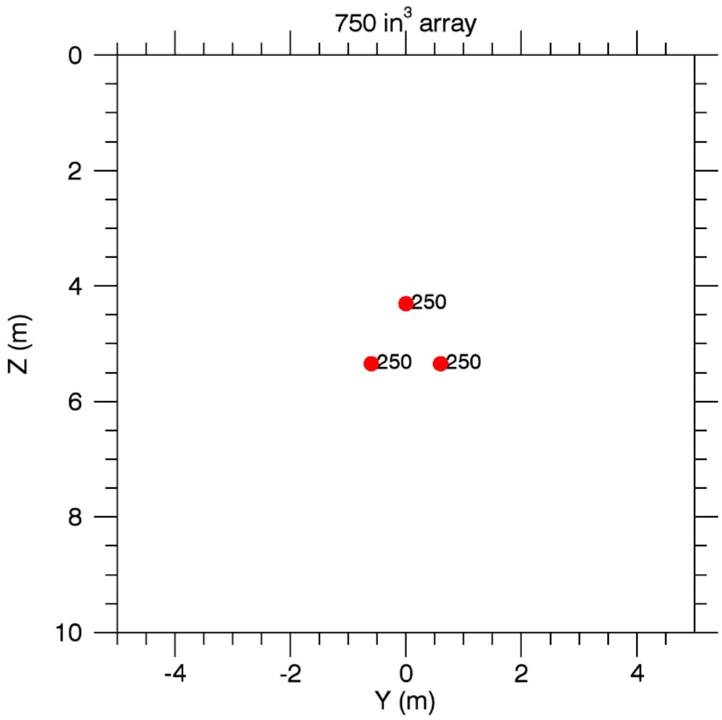

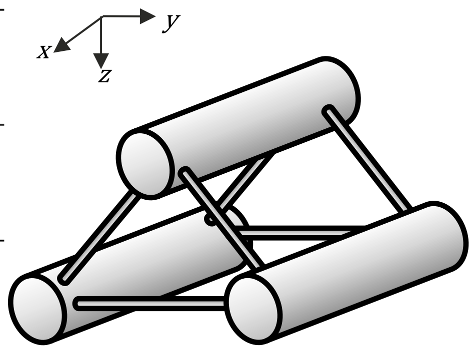

Figure 5. Side view and isometric view (not to scale) of the 750 in³ VSP array.

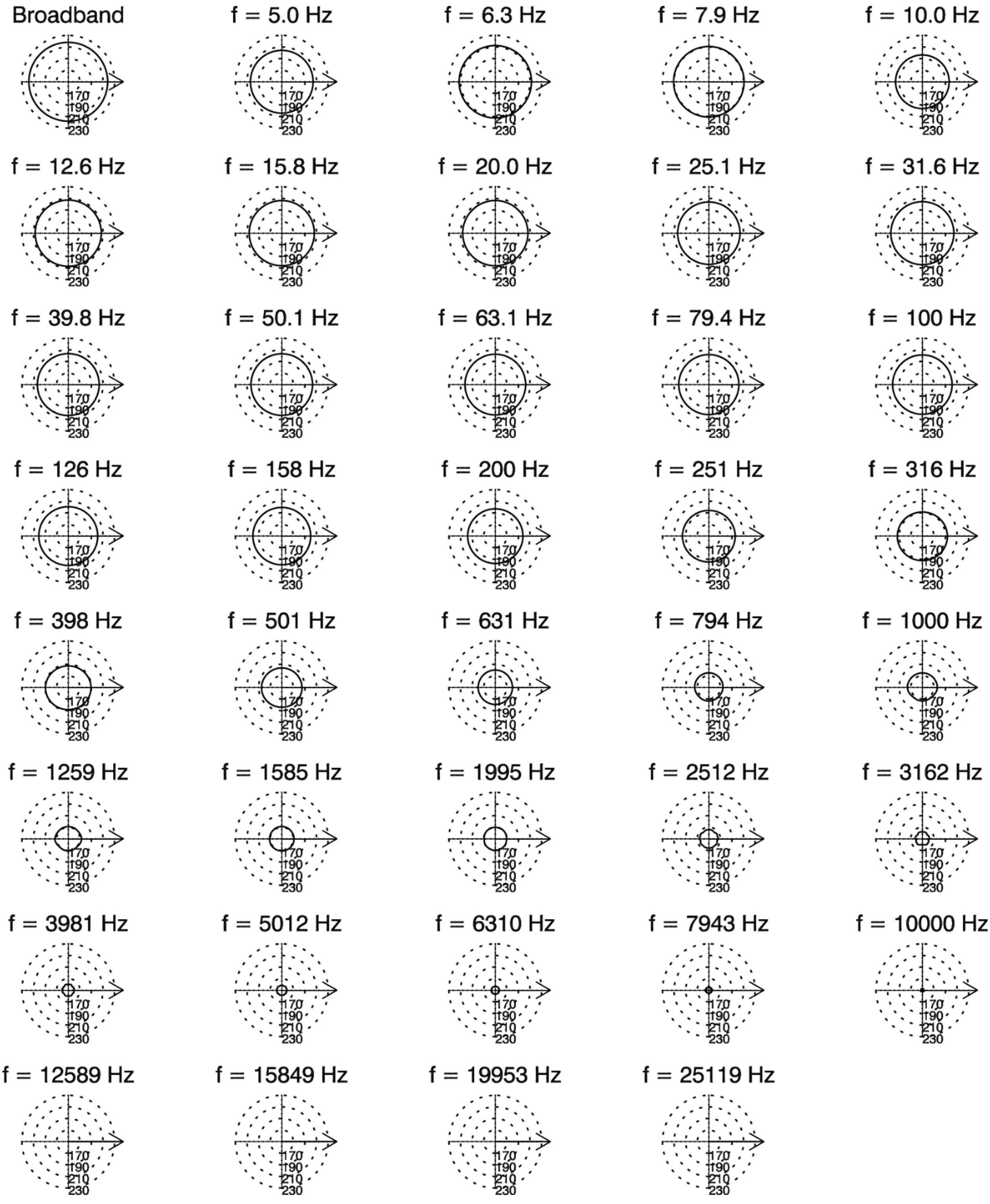

Figure 6. Horizontal energy source level (dB re 1 µPa²m²s) in decidecade bands as a function of azimuth and frequency for the 750 in³ VSP array. The arrow is in the positive x-direction as per Figure 5.

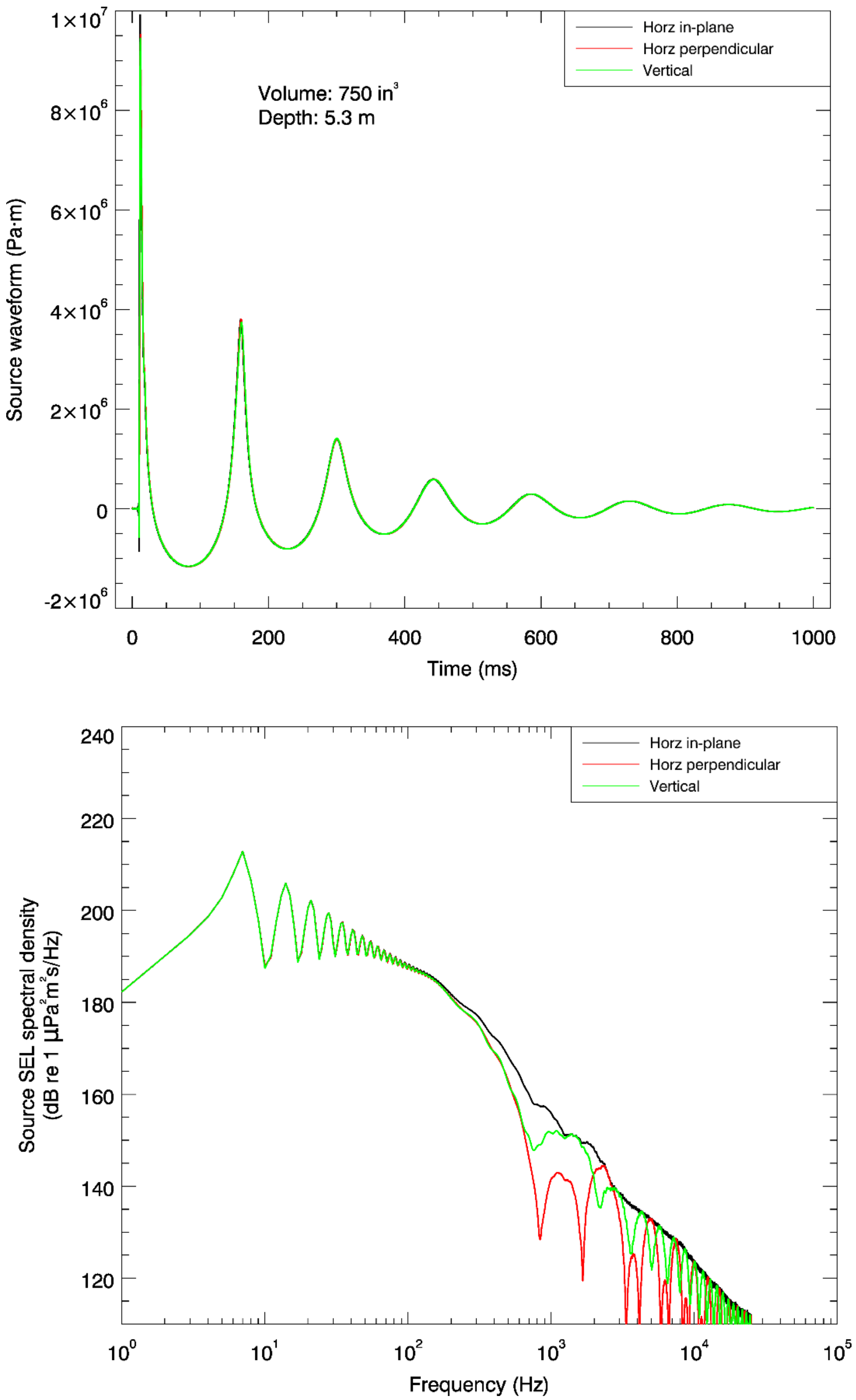

Figure 7. Source waveforms of individual airguns (Pa m) and energy source spectral density level (dB re 1 µPa^{2}m^{2}s/Hz) of the 750 in^3 VSP array.

4.3.3. Regional survey source

The source for the regional survey scenarios is the 4130 in³ array described in Table 6 and shown in Figure 8.

The directivity of the array as a function of frequency is shown in Figure 9 and the signatures and spectra in broadside, endfire, and vertical directions are shown in Figure 10.

Table 6. The geometry of the 4130 in³ regional survey array.

Gun	*X* (m)	*Y* (m)	*Z* (m)	Volume (in³)
1	0	8.4	7	150
2	0	7.6	7	150
3	-3	8.4	7	60
4	-3	7.6	7	60
5	-5	8	7	40
6	-7	8	7	70
7	-9	8.4	7	100
8	-11	8.4	7	90
9	-11	7.6	7	90
10	-14	8.4	7	250
11	-14	7.6	7	250
12	0	0.4	7	100
13	0	-0.4	7	100
14	-3	0	7	90
15	-5	0	7	60
16	-7	0	7	70
17	-9	0	7	100
18	-11	0.4	7	150
19	-11	-0.4	7	150
20	-14	0.4	7	250
21	0	-7.6	7	150
22	0	-8.4	7	150
23	-3	-7.6	7	150
24	-5	-8	7	90
25	-7	-8	7	70
26	-9	-7.6	7	70
27	-9	-8.4	7	70
28	-11	-7.6	7	250
29	-11	-8.4	7	250
30	-14	-7.6	7	250
31	-14	-8.4	7	250

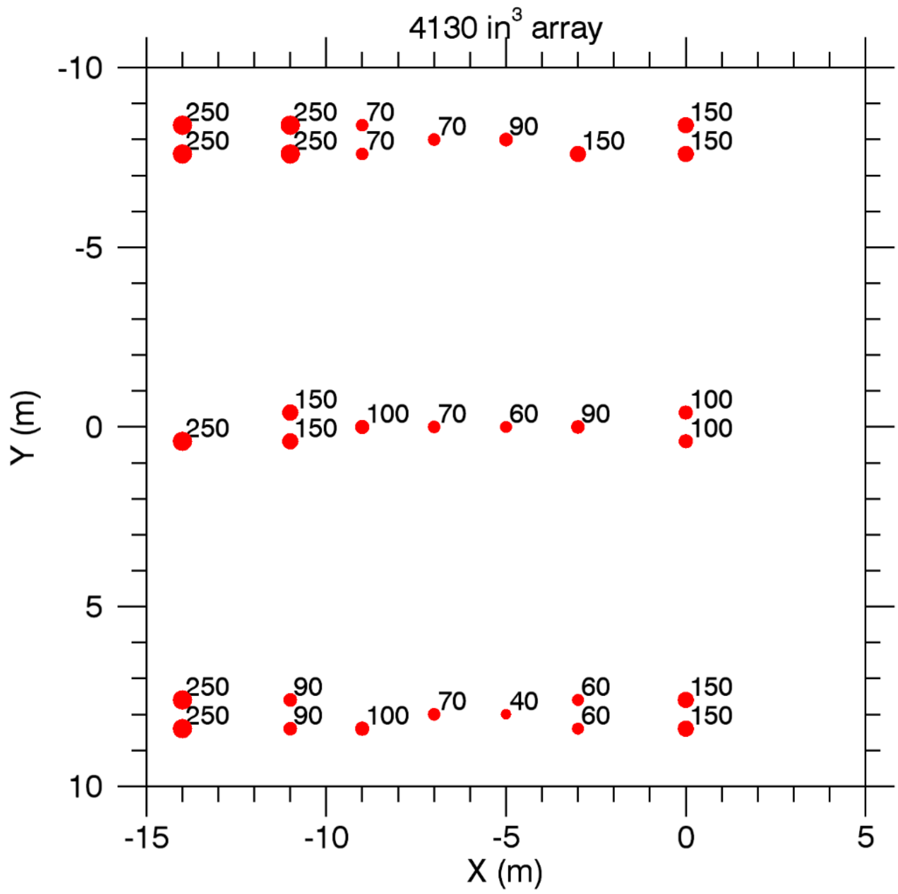

Figure 8. Plan view of the 4130 in³ regional survey array.

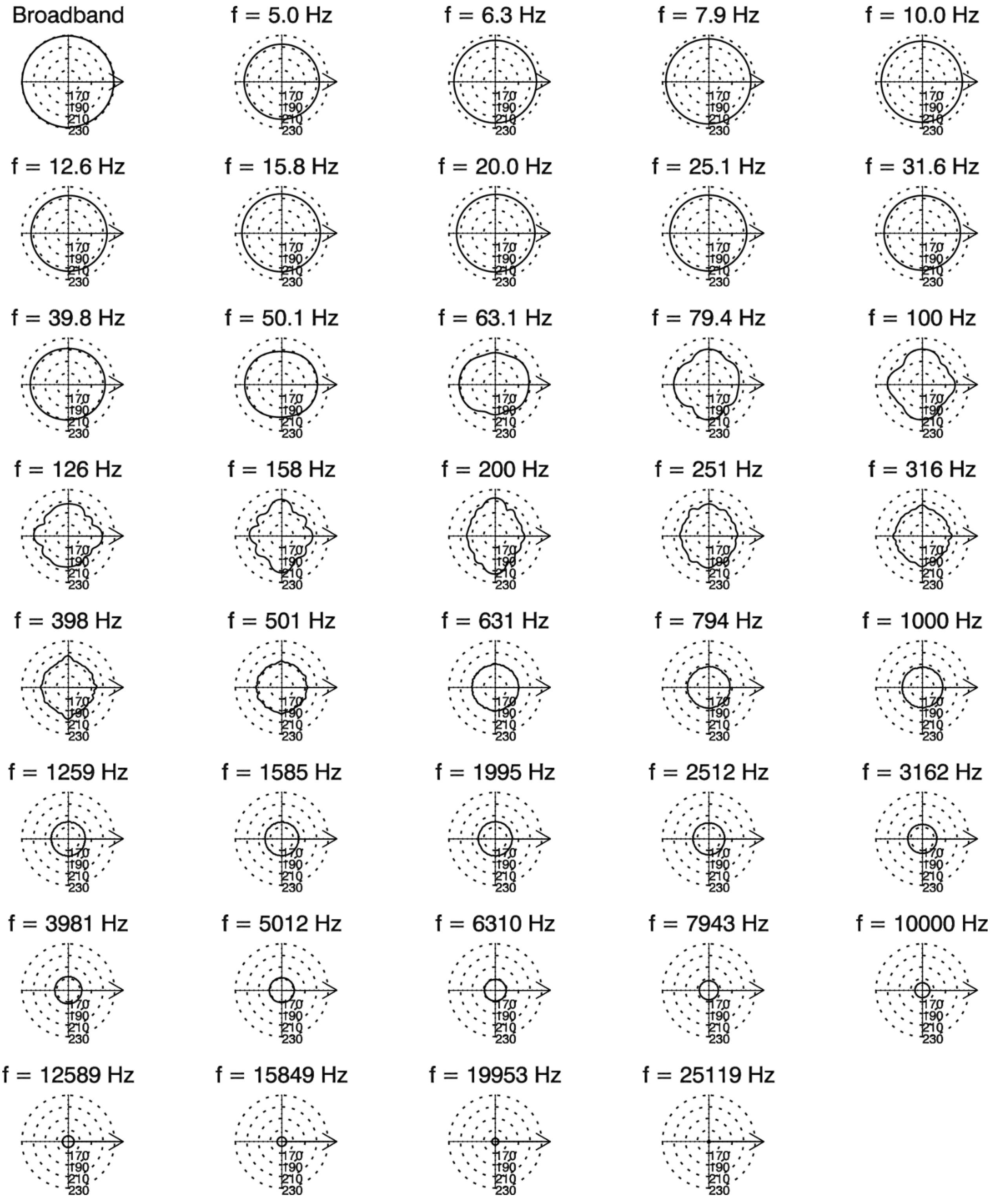

Figure 9. Horizontal energy source level (dB re 1 µPa²m²s) in decidecade bands as a function of azimuth and frequency for the 4130 in³ regional survey array.

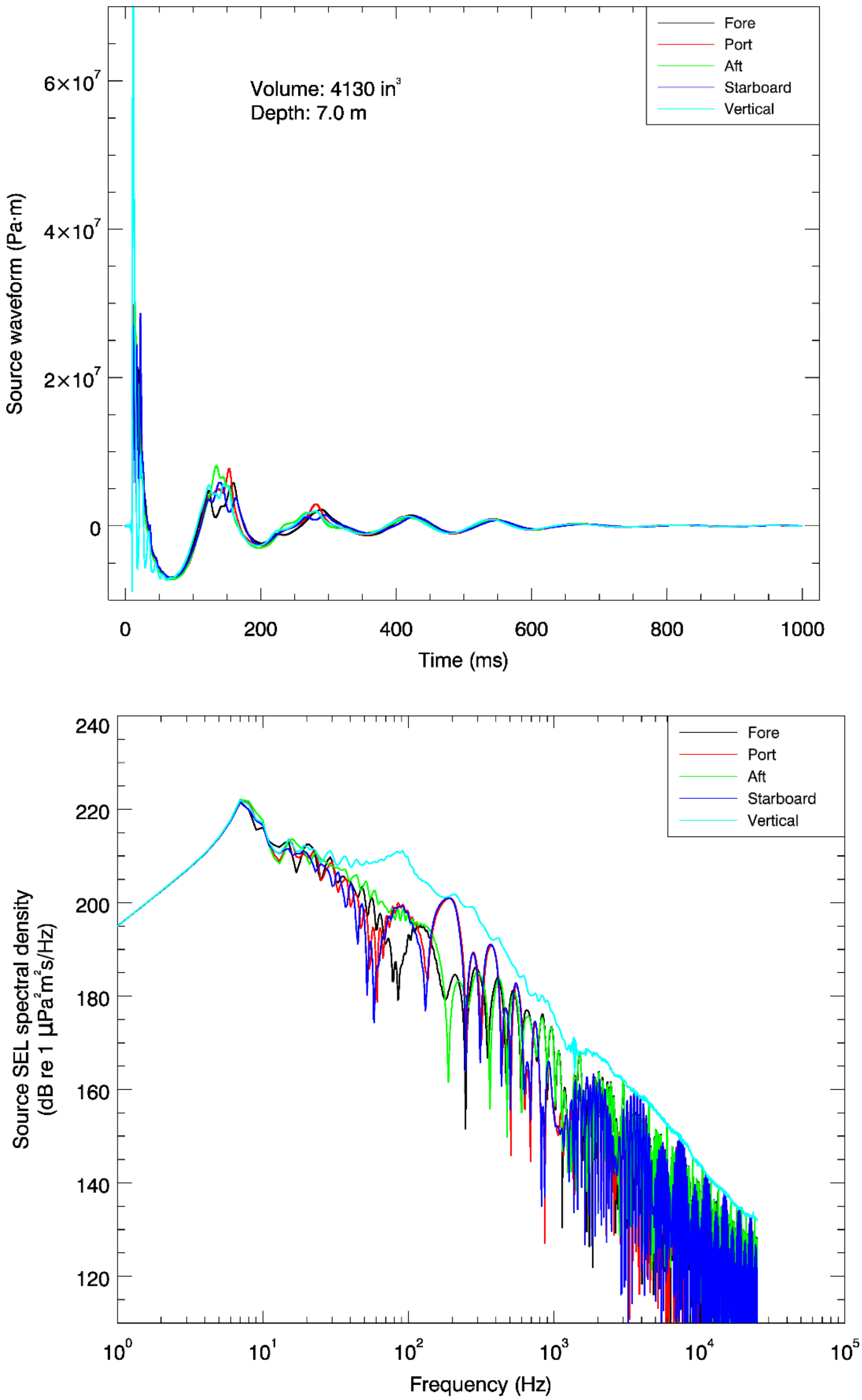

Figure 10. Source waveforms of individual airguns (Pa m) and energy source spectral density level (dB re 1 $\mu Pa^2m^2s/Hz$) of the 4130 in^3 regional survey array.

4.4. Source Level Summary

A summary of the source levels for the modelled arrays is shown in Table 7. Values are presented for zero to peak source level ($L_{S,pk}$) and energy source level ($L_{S,E}$) in principal directions. The source levels in decidecade bands are provided in Appendix F.

Table 7. Modelled source levels for the three airgun array sources. Levels shown for 160 in^3 site survey array at 3 m tow depth, the 750 in^3 VSP array at 5 m deployment depth, and the 4130 in^3 regional survey array at 7 m tow depth. Source levels are per-pulse and unweighted.

Direction	$L_{S,pk}$ (dB re 1 µPa·m)			$L_{S,E}$ (dB re 1 µPa²·m²·s)		
	Site survey	VSP	Regional survey	Site survey	VSP	Regional survey
Broadside / in-plane†	238.2	239.6	249.5	213.6	218.1	229.4
Endfire / perpendicular†	235.8	239.9	246.6	213.1	218.2	228.7
Vertical (no ghost)	238.6	239.5	258.3	213.7	218.1	232.5
Vertical (with ghost)	238.6	239.5	258.3	212.5	216.7	234.1

† In-plane and perpendicular directions are used for the VSP array only.

4.5. Sound Source Discussion

There are characteristics to the seismic sources that are common across all those discussed in the previous sections. Airgun arrays are typically low-frequency sources due to their need to penetrate the seabed and underlying geology. Consequently, the decidecade bands containing the greatest energy are typically below 20 Hz. The influence of the environment, however, determines the frequencies that have the lowest propagation loss; this frequency varies from scenario to scenario and depends on the water depth and the seabed properties. These other factors are explored in subsequent phases of the study.

The time series of each of the model outputs shows the typical signature formed of the initial pulse, due to the constructive nature of the simultaneous activation of individual air guns, and then a period of clear bubble oscillation. The source arrays are typically designed to reduce the trailing oscillations whilst maintaining a high amplitude broadband pulse output signal. This is achieved more effectively in the larger arrays as bubbles from individual air guns of various volumes are selected to cancel each other out, resulting in a broadband frequency spectrum without frequency notches resulting from interference patterns.

The source model considered here includes full vertical and horizontal directivity patterns for the modelled arrays. Where there are few elements in the airgun array, the combined source output is close to being omnidirectional as shown for both the VSP and site survey arrays. Where more elements are included, such as in the regional array, the arrival time difference between sources at different angles can generate strong directivity patterns that are typically strongest in the endfire and broadside directions. The inclusion of more elements at the same depth and activated simultaneously increases the difference between the vertical sound level and horizontal due to constructive interference in the vertical direction.

The directivity patterns of the site survey, the VSP, and the regional arrays are shown in Figures 3, 6 and 9 respectively. In the case of the 160 in^3 site array and the 750 in^3 VSP array, little directivity is observed in the modelling results; consequently, the bearing of any survey lines is unlikely to make any significant difference to the observed sound field with all else being equal.

More detailed directivity is realised in the case of the regional array. As seen in Figure 9, the patterns are more distinct from 50 Hz to 400 Hz. Energy within this frequency band often propagates effectively in ocean environments as at lower frequencies shallow water depths can result in a low-frequency cut-off due to the water depths not supporting wavelengths over a certain size. In addition, energy at these frequencies is also not significantly affected by medium losses nor scattering losses from a rough sea surface over the likely range of interest. Consequently, the resulting broadband sound fields reflect the mid-frequency directivity patterns, with ranges to specific isopleths typically being greatest in the broadside directions.

It should be noted again, that although a fully directional multi-element source function can be generated, acoustic propagation models vary in their usage of the source function in that they may include full directivity, horizontal variation only, vertical variation only, or a single value omnidirectional source level. Details of how each model in this report use the source functions is detailed in Section 7.

5. Environments for Representative Seismic Modelling

Representative general locations were selected by the steering group to provide environmental data for the baseline scenarios modelled in Phase 2. This section provides the locations of each and the associated pertinent environmental data used in the baseline modelling.

Figure 11 shows the water depths around the UK banded with bathymetry data sourced from EMODnet (2016). For each identified general region, nominal survey blocks were drawn that encompass the target water depth and the identified sediment type; sediment descriptions have been sourced from the British Geological Survey Marine Sediments 250k dataset (2018).

Sound speed profiles were determined by sourcing data from GDEM (Teague et al. 1990). GDEM provides monthly salinity and temperature profiles worldwide at a resolution of 0.25° in both longitude and latitude. From the salinity and temperature profiles, sound speed profiles are calculated according the formula by Coppens (1981). As the sound speed of the loose sediment layer is directly related to the sound speed of the water above it, respective geoacoustic profiles were also calculated for each month. A preliminary modelling study was performed at each modelling site to determine the month of greatest propagation over the range of a few kilometres (Appendix B). The coordinates for the studied areas are supplied in Appendix C. Throughout Phase 2 it was assumed that a single sound speed profile and single geoacoustic profile existed across each modelling scenario region. The tabulated sound speed profiles for all sites are shown in Appendix D.

Geoacoustics for each region were calculated from a single value: the representative grain size of surficial sediments. The grain size is determined from lithographic descriptions by using the Wentworth scale and shown in phi units (grain size, $\phi = -\log_2(D/D_0)$ where D is the median grain diameter in mm, and D_0 is the reference diameter of 1 mm). The phi scale is used in preference over existing ISO standards for grain sizes as the employed equations for geoacoustic properties are based on this scale.

The minimum requirements for the geoacoustic properties are for the density, compressional wave speed, and compressional wave attenuation to be defined. However, in some models, the shear wave properties of the sediment can also be included. Typically, the effect of shear wave propagation is small for wave speeds less than 200 m/s, but for higher shear speeds it can increase bottom loss at subcritical and intermediate grazing angles (Jensen et al. 2011). Sediment shear wave speeds are based on rounded results by Holzer et al. (2005) for the different sediment classes; the values used are presented in Table 8 with results for coarse sediments being the same as for sand. For Phase 2, no layering of sediments nor depth dependence in sediment properties has been considered.

Table 8. Shear wave speeds of different sediments based on rounded values from Holzer et al.(2005).

	Clay	Silt	Sand
Shear wave speed (m/s)	100	200	300

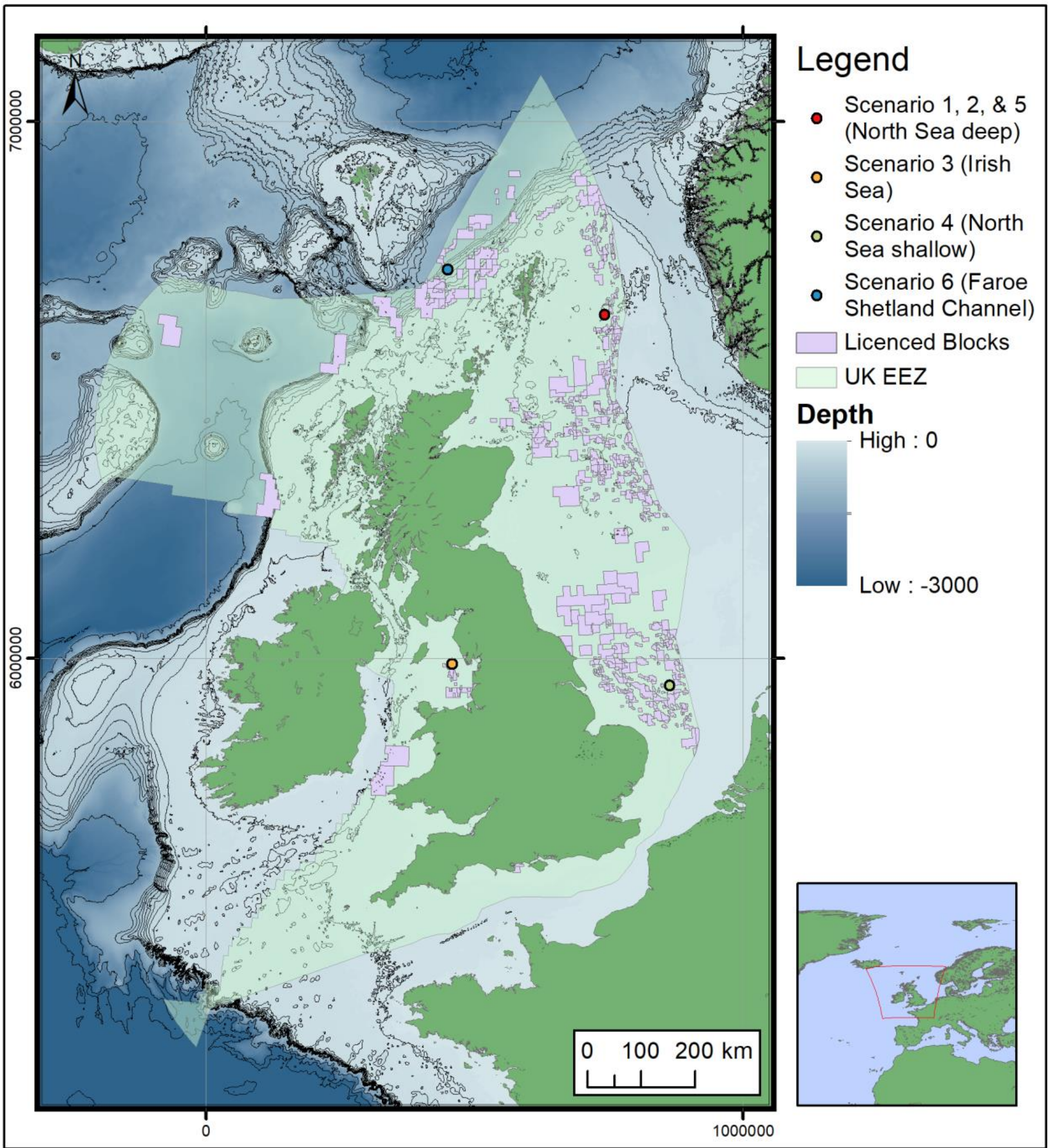

Bathymetry overview	Datum: WGS84 Projection: UTM30 North	JASCO APPLIED SCIENCES
Representative UKCS Seismic Survey Modelling	Created: Dec 2018	

Figure 11. Water depths on the UK continental shelf and scenario locations.

5.1. Specific Scenario Environments

5.1.1. Irish Sea

The Irish Sea region is used for Scenario 3, and is the shallowest selected for this study with a target modelled water depth of between 20 and 30 m. The surficial sediment has been identified as mud.

Based on the preliminary modelling study, the monthly sound speed profiles that generated the greatest propagation was from December to February; the selected SSP for modelling is December and is shown in Figure 12. The surficial sediment is principally sandy mud and muddy sand. Based on the Folk classification of sediments, mud can be interpreted as sediments with a grain size of between 4ϕ and 10ϕ (ranging from silt to clay). Due to the preponderance of sand in the region it is reasonable to assume that the grain sizes be skewed towards the larger grain sizes within the range for mud; consequently, geoacoustic properties are calculated according to Ainslie (2010) using a grain size of 5ϕ. The geoacoustic properties used for the modelling in the Irish Sea region are presented in Table 9. The bathymetry for the area is shown in Figure 13.

Table 9. Geoacoustic properties for the Irish Sea modelling region.

Depth below seafloor (m)	Material	Density (g/cm^3)	P-wave speed (m/s)	P-wave attenuation (dB/λ)	S-wave speed (m/s)	S-wave attenuation (dB/λ)
0+	Coarse/medium Silt	1.693	1577.4	0.71	200.0	3.65

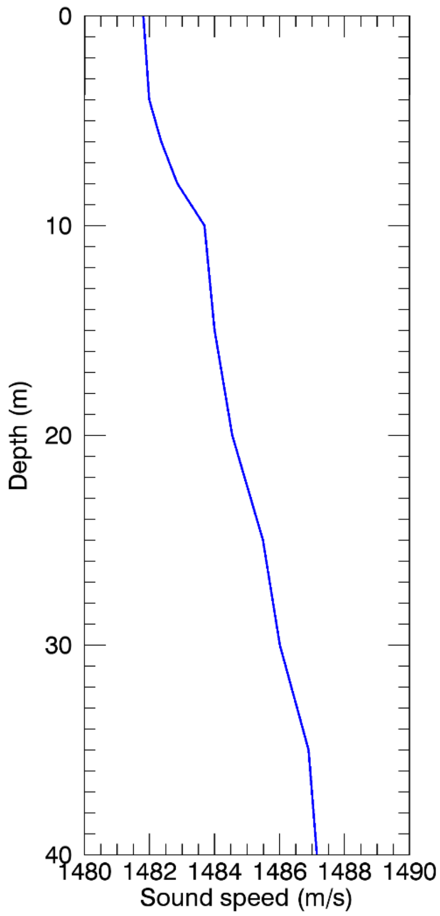

Figure 12. The sound speed profile for the Irish Sea region for December.

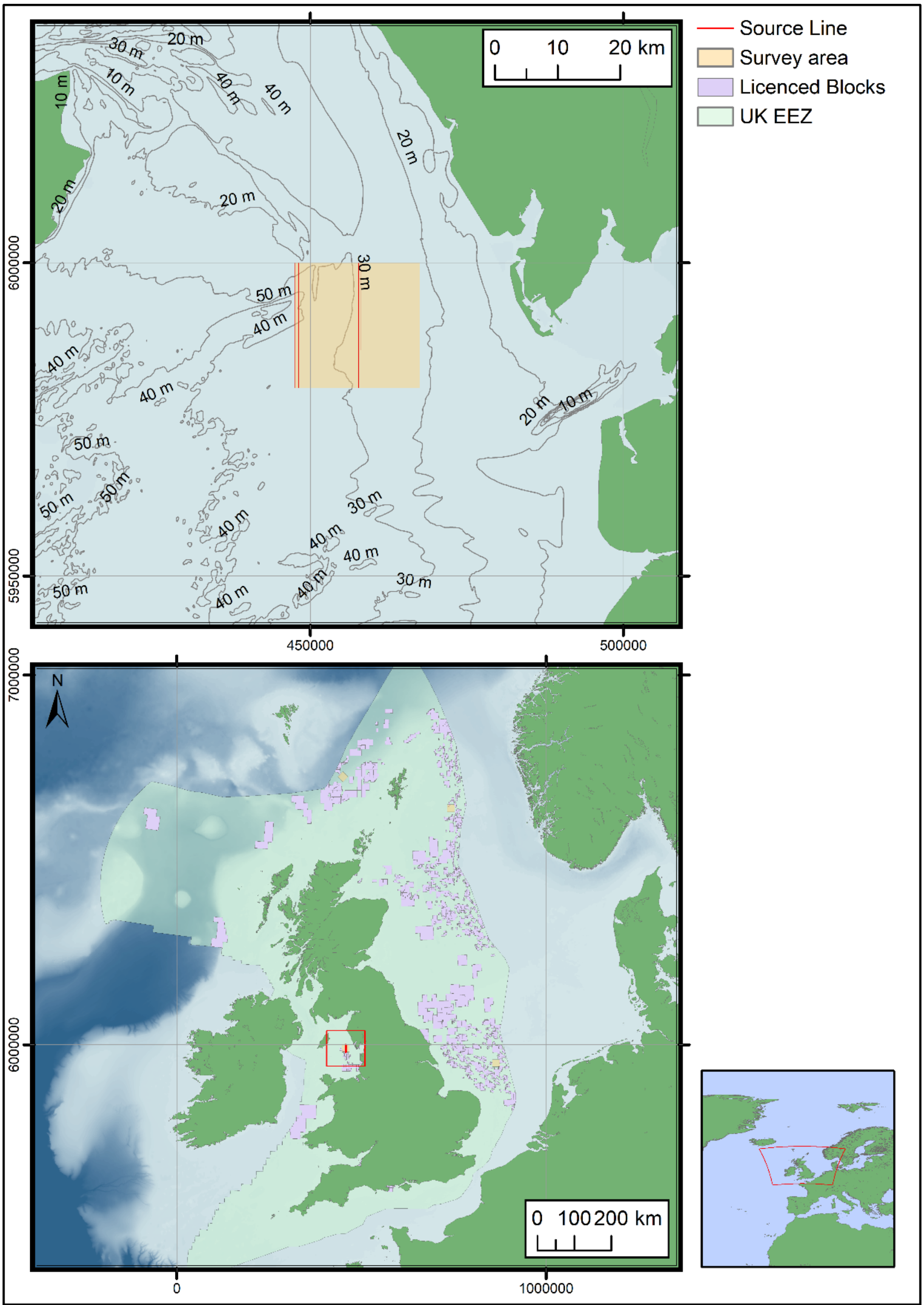

Irish Sea survey area and bathymetry	Datum: WGS84 Projection: UTM30 North	JASCO APPLIED SCIENCES
Representative UKCS Seismic Survey Modelling	Created: Aug 2020	

Figure 13. Bathymetry and modelled survey lines (Scenario 3) for the Irish Sea region.

5.1.2. North Sea Shallow

The North Sea Shallow region fulfils the requirements for Scenario 4. The depths in the region are principally between 25 and 35 metres. The target sediment for the scenario is sand.

Based on the preliminary modelling study, the monthly sound speed profiles that generated the greatest propagation were from January to March; the profile for January is shown in Figure 14. Geoacoustic properties are calculated according to Ainslie using a grain size of 1.5ϕ (medium sand); these are presented in Table 10. The bathymetry for the area is shown in Figure 15.

Table 10. Geoacoustic properties for the North Sea Shallow modelling region.

Depth below seafloor (m)	Material	Density (g/cm^3)	P-wave speed (m/s)	P-wave attenuation (dB/λ)	S-wave speed (m/s)	S-wave attenuation (dB/λ)
0+	Medium sand	2.143	1766.0	0.88	300.0	3.65

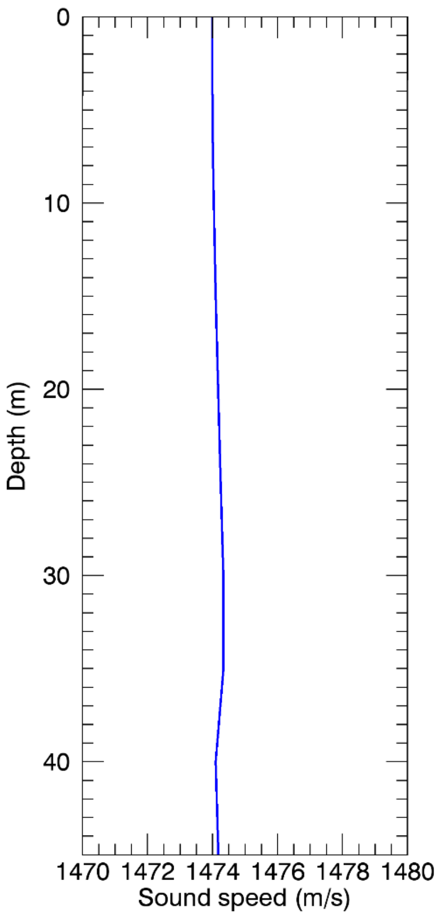

Figure 14. The sound speed profile for the North Sea Shallow region for January.

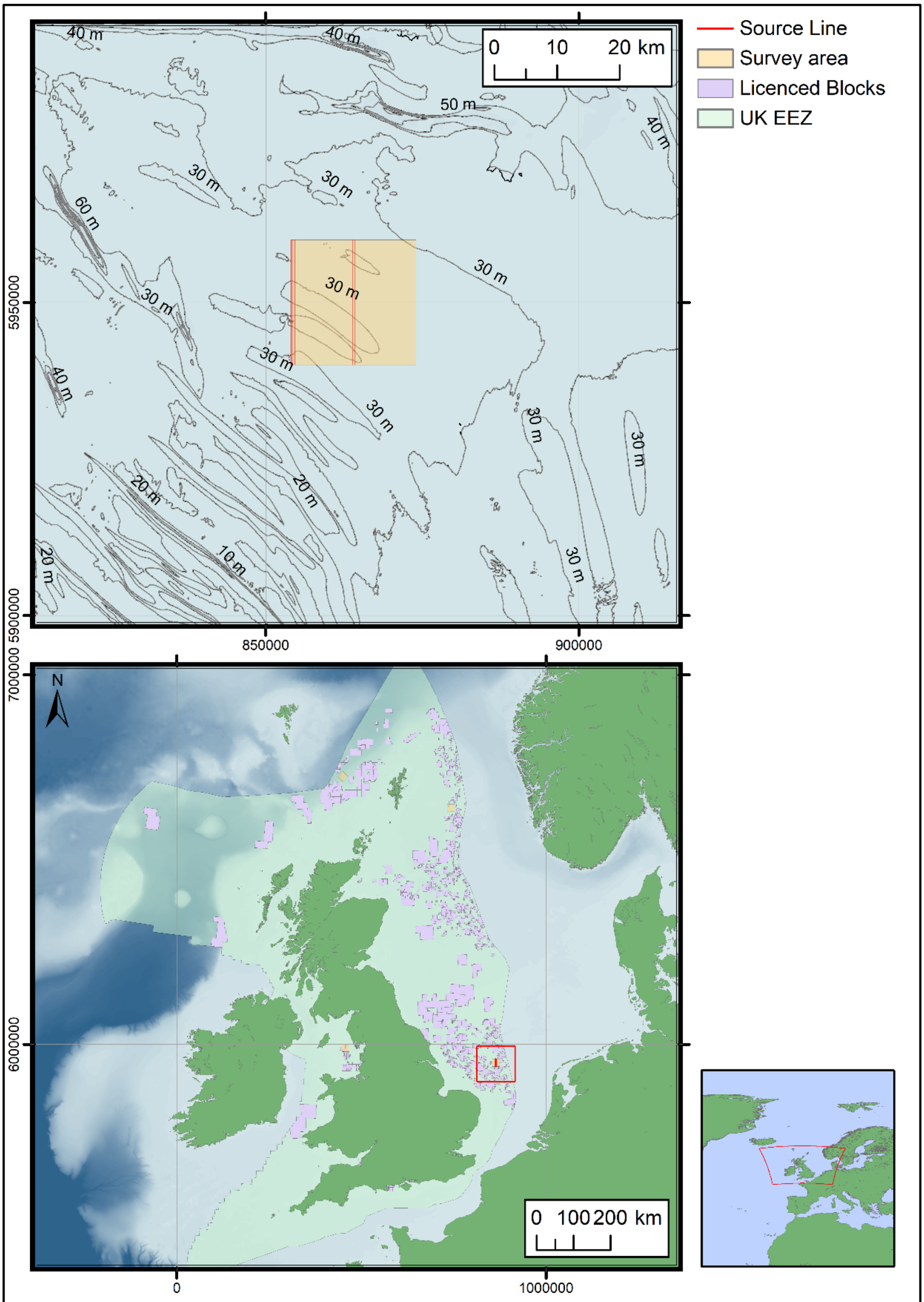

North Sea Shallow survey area and bathymetry	Datum: WGS84 Projection: UTM30 North	JASCO APPLIED SCIENCES
Representative UKCS Seismic Survey Modelling	Created: Aug 2020	

Figure 15. Bathymetry and modelled survey area for the North Sea Shallow region.

5.1.3. North Sea Deep

The North Sea Deep region fulfils the requirements for Scenario 5 and is additionally used for Scenarios 1 and 2. The depths in the region are principally between 100 and 120 metres; the target sediment is sand.

Based on the preliminary modelling study, the monthly sound speed profile that generated the greatest propagation was between January and March; the sound speed profile for January is shown in Figure 16. Geoacoustic properties are calculated according to Ainslie using a grain size of 1.5ϕ (medium sand); these are presented in Table 11. The bathymetry for the area, and the modelled survey lines for Scenario 5 are shown in Figure 17.

Table 11. Geoacoustic properties for the North Sea Deep modelling region.

Depth below seafloor (m)	Material	Density (g/cm^3)	P-wave speed (m/s)	P-wave attenuation (dB/λ)	S-wave speed (m/s)	S-wave attenuation (dB/λ)
0+	Medium sand	2.145	1773.7	0.88	300.0	3.65

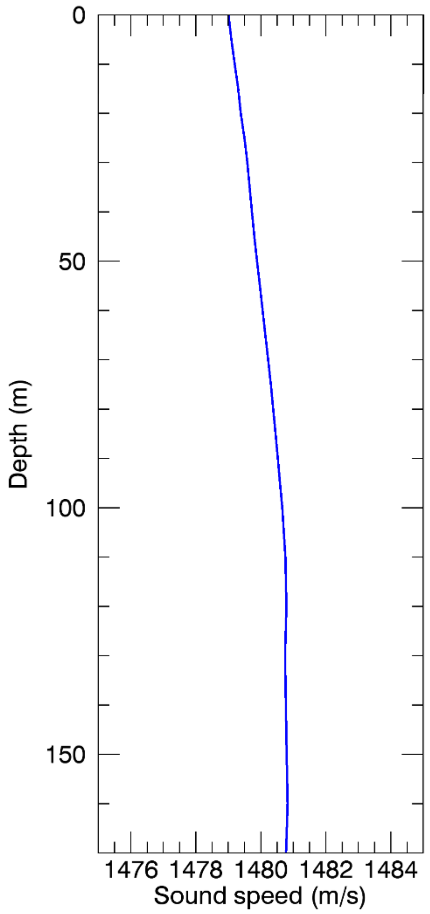

Figure 16. The sound speed profile for the North Sea Deep region for January.

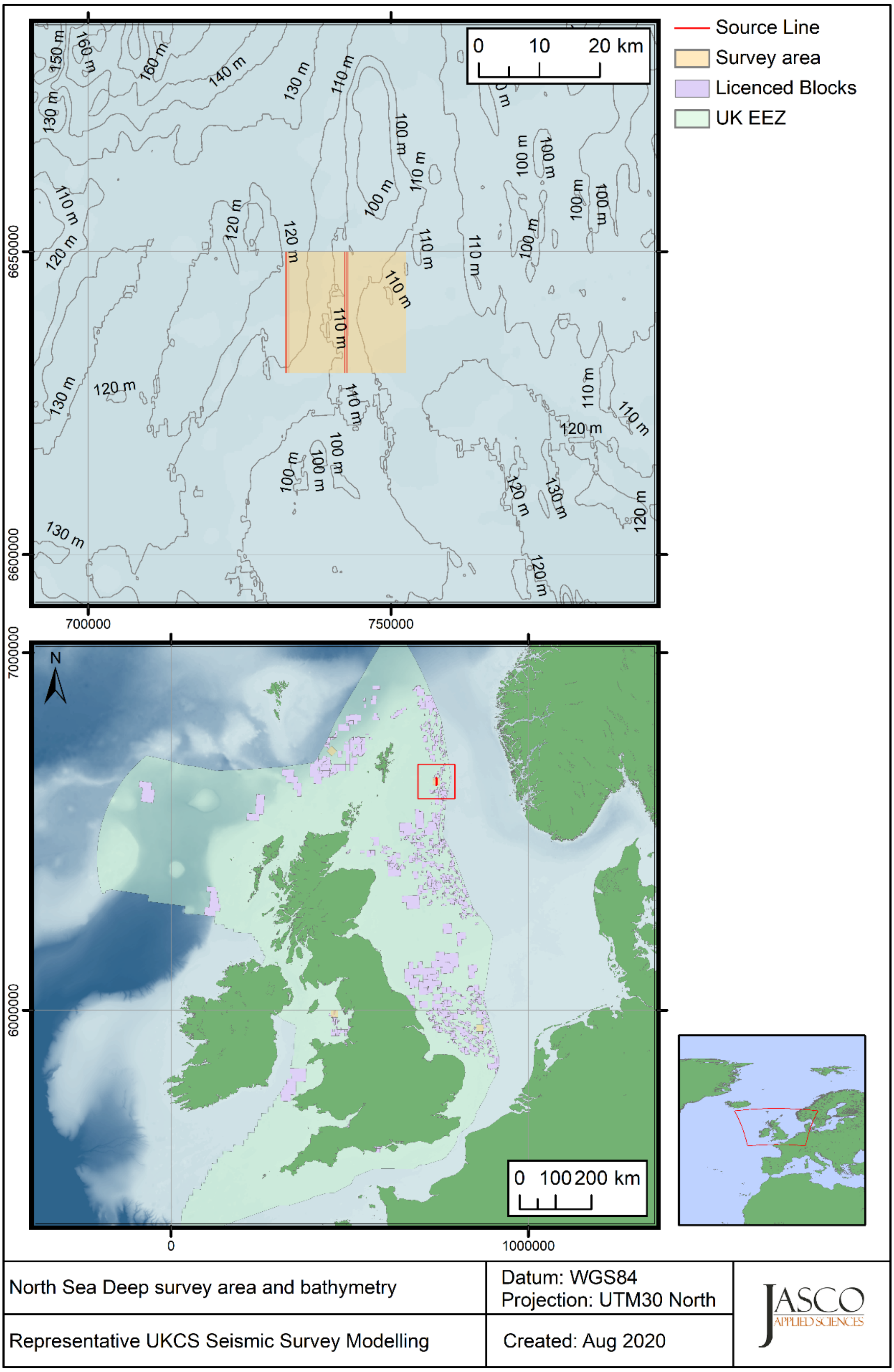

Figure 17. Bathymetry and modelled survey area for the North Sea Deep region.

5.1.4. Faroe-Shetland Channel

The Faroe-Shetland Channel region fulfils the requirements for Scenario 6. The depths in the region range considerably due to the slope of the channel. The bathymetry for the area is shown in Figure 19.

Based on the preliminary modelling study, the monthly sound speed profile that generated the greatest propagation was December; the sound speed profile is shown in Figure 18. The surficial sediment is typically gravelly muddy sand and consequently is treated as very coarse sand. Geoacoustic properties are calculated according to Ainslie using a grain size of -0.5ϕ; these are presented in Table 12.

Table 12. Geoacoustic properties for the Faroe-Shetland Channel modelling region.

Depth below seafloor (m)	Material	Density (g/cm³)	P-wave speed (m/s)	P-wave attenuation (dB/λ)	S-wave speed (m/s)	S-wave attenuation (dB/λ)
0+	Very coarse sand	2.476	1908.2	0.89	300.0	3.65

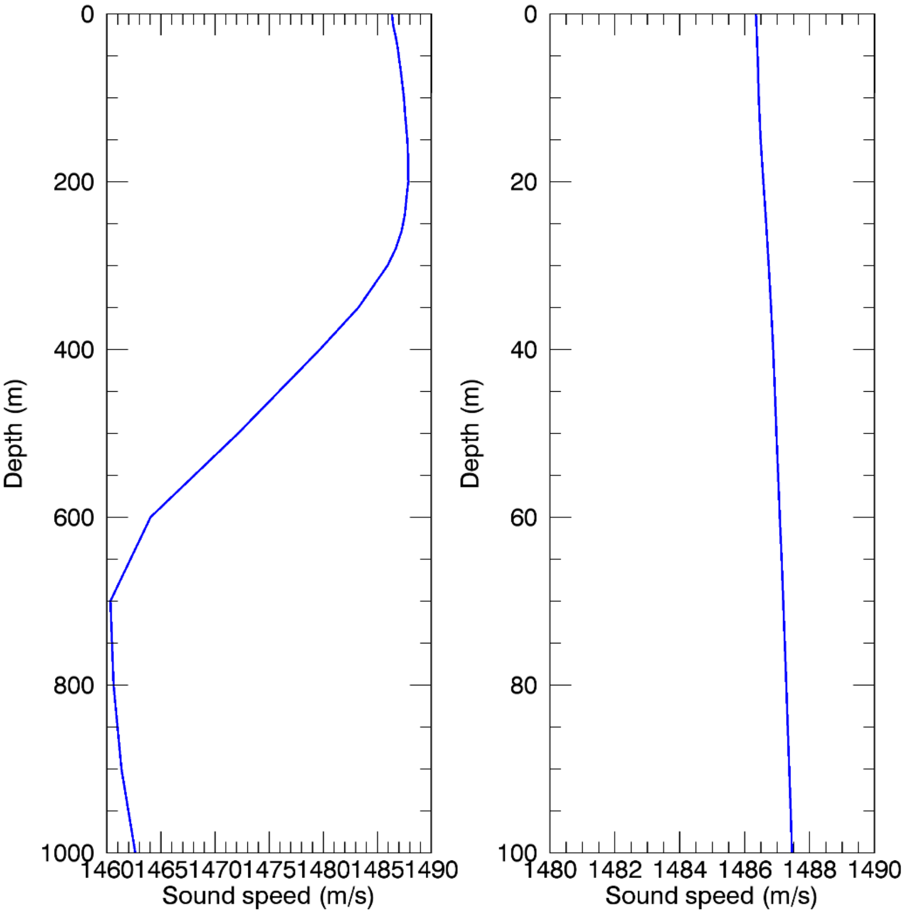

Figure 18. The sound speed profile for the Faroe-Shetland Channel region for December.

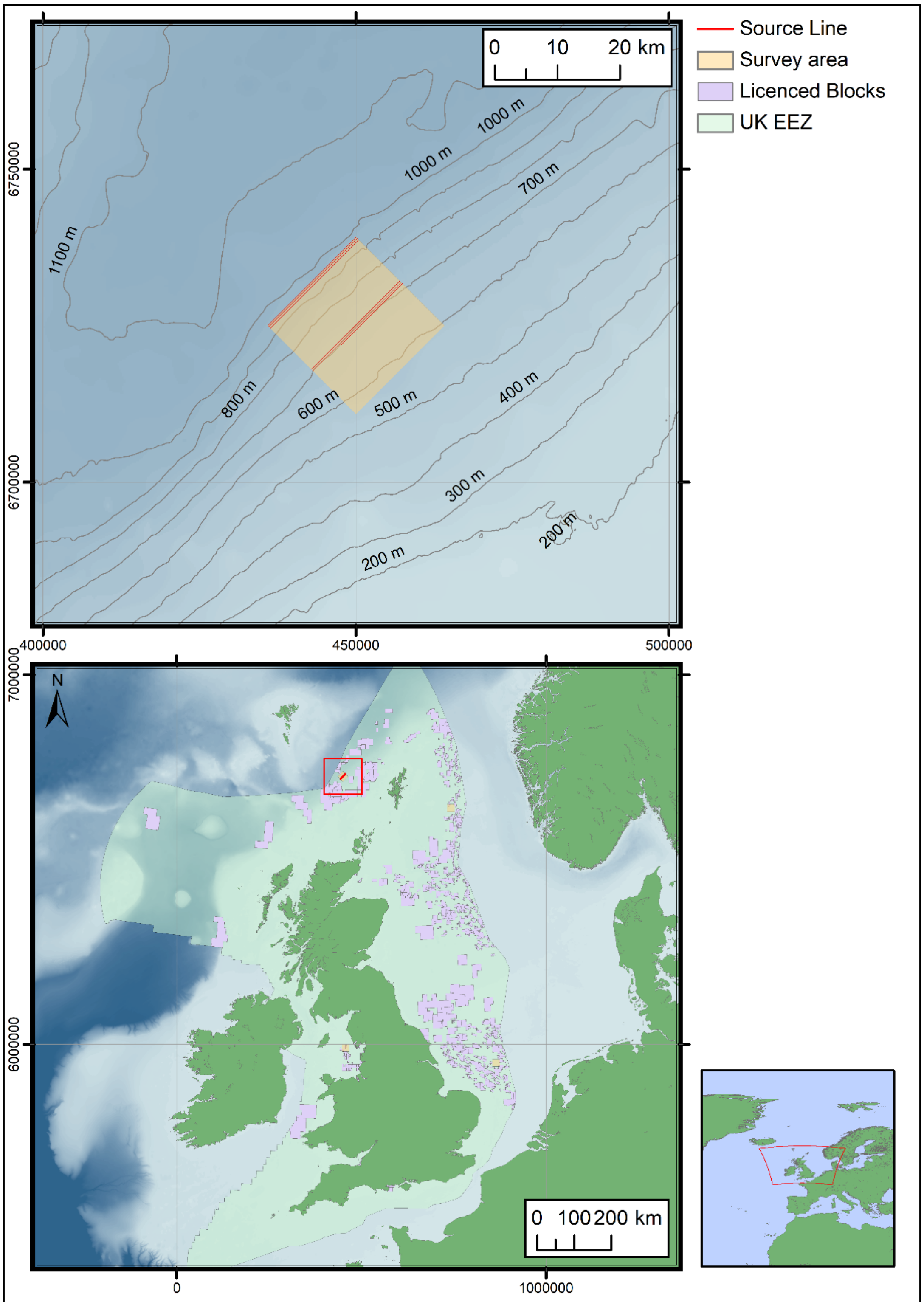

Faroe-Shetland Channel survey area and bathymetry	Datum: WGS84 Projection: UTM30 North	JASCO APPLIED SCIENCES
Representative UKCS Seismic Survey Modelling	Created: Aug 2020	

Figure 19. Bathymetry and modelled survey area for the Faroe-Shetland Channel region.

5.2. Environment Summary

The modelled environments are summarised below in Table 13, and geoacoustic properties in Table 14. The geoacoustic properties were assumed to be constant across each region for the purposes of the modelling. The numeric values of the sound speed profiles are shown in Appendix D.

Table 13. Summary of environments for all regions.

Environment	Water depth	Sediment type	Grain size	Time of year
Irish Sea	25-35 m	Coarse/medium Silt	+5.0 ϕ	December
North Sea Shallow	20-30 m	Medium sand	+1.5 ϕ	January
North Sea Deep	100-120 m	Medium sand	+1.5 ϕ	January
Faroe-Shetland Channel	600-900 m	Very coarse sand	-0.5 ϕ	December

Table 14. Geoacoustic properties for all regions.

Region	Material	Density (g/cm^3)	P-wave speed (m/s)	P-wave attenuation (dB/λ)	S-wave speed (m/s)	S-wave attenuation (dB/λ)
Irish Sea	Coarse/medium Silt	1.693	1577.4	0.71	200.0	3.65
North Sea Shallow	Medium sand	2.143	1766.0	0.88	300.0	3.65
North Sea Deep	Medium sand	2.145	1773.7	0.88	300.0	3.65
Faroe-Shetland Channel	Very coarse sand	2.476	1908.2	0.89	300.0	3.65

6. Cumulative Assessment Considerations

6.1. Soft-start Procedures

The soft-start procedures employed for each array type in Phase 2 are detailed below in Tables 15 to 17 and are based on the Joint Nature Conservation Committee (JNCC) guidelines (2017). In each case the procedure duration is the minimum recommended and all assume a constant operating pressure of 2000 lb/in^2 (2000 psi).

Table 15. Soft-start procedures for the site survey.

Step	Time (minutes)	Operating air guns	Total volume (in^3)	Time between pulses (s)
1	0	Air gun 1	40	12
2	3	Air gun 1	40	6
3	6	Air gun 1	40	3
4	9	Air guns 1 & 2	80	3
5	12	Air guns 1, 2, & 3	120	3
Full array	15	All air guns	160	3

Table 16. Soft-start procedures for the VSP survey.

Step	Time (minutes)	Operating air guns	Total volume (in^3)	Time between pulses (s)
1	0	Air gun 1	250	20
2	10	Air guns 1 & 2	500	20
Full array	20	All air guns	750	20

Table 17. Soft-start procedures for the regional survey (4130 in^3 array).

Step	Time (minutes)	Operating air guns	Total volume (in^3)	Time between pulses (s)
1	0	5	40	10
2	3	4, 5	100	10
3	6	3, 4, 5, 15	220	10
4	9	3, 4, 5, 6, 15, 16, 25, 26	500	10
5	12	3, 4, 5, 6, 7, 8, 9, 14, 15, 16, 24, 25, 26, 27	1030	10
6	16	1, 2, 3, 4, 5, 6, 7, 8, 9, 12, 13, 14, 15, 16, 17, 18, 19, 21, 24, 25, 26, 27	2080	10
Full array	20	All guns	4130	10

6.2. Implementation of the Soft-Start

Due to the sheer number of different configurations described in the previous section, steps were taken to reduce computational complexity, whilst still taking the effects of the soft-start into account. The sources were modelled for all steps within the soft-start sequence. From these results, a series of frequency weighting curves were generated. These weighting curves provide the azimuth- and frequency-dependent energy source level difference between the full array and the partial arrays in decidecade bands; no vertical directivity changes are considered. These were then applied to the modelling results of source points from the full array to simulate the soft-start.

Figure 20 shows the spectra of the different stages of the soft-start for the 4130 in³ array in the endfire and broadside directions. Figure 21 shows the weighting curves applied at each stage of the soft-start to simulate the reduction in total volume for the stage. Peak sound pressure levels and broadband single-pulse energy source levels for all arrays and steps of the soft-start are shown in Appendix E; energy source levels in decidecade bands for all arrays and steps of the soft-start are shown in Appendix F. Plots of acoustic pressure against time for all arrays and steps of the soft start are included in Appendix G.

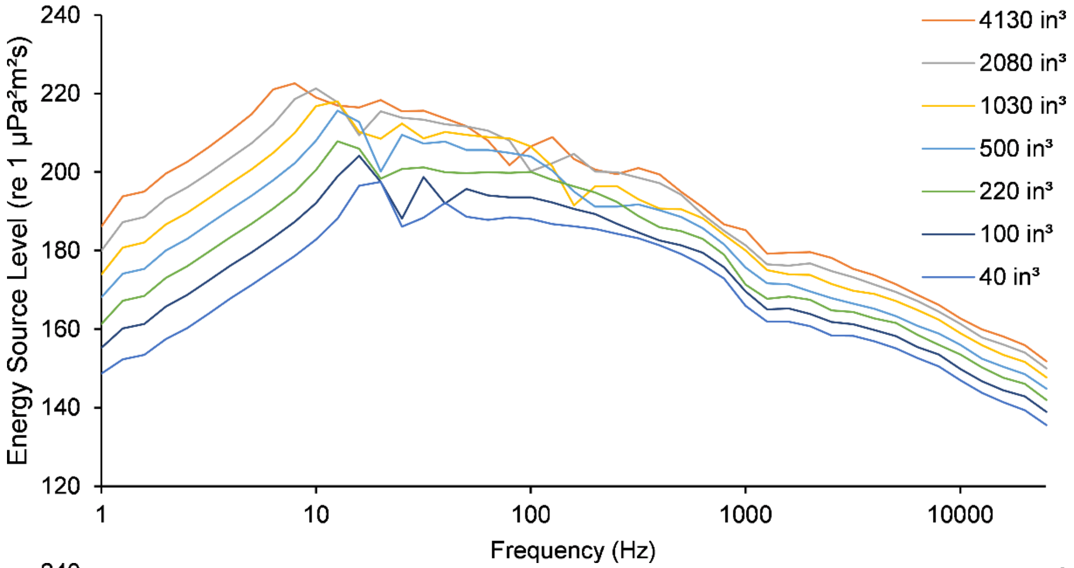

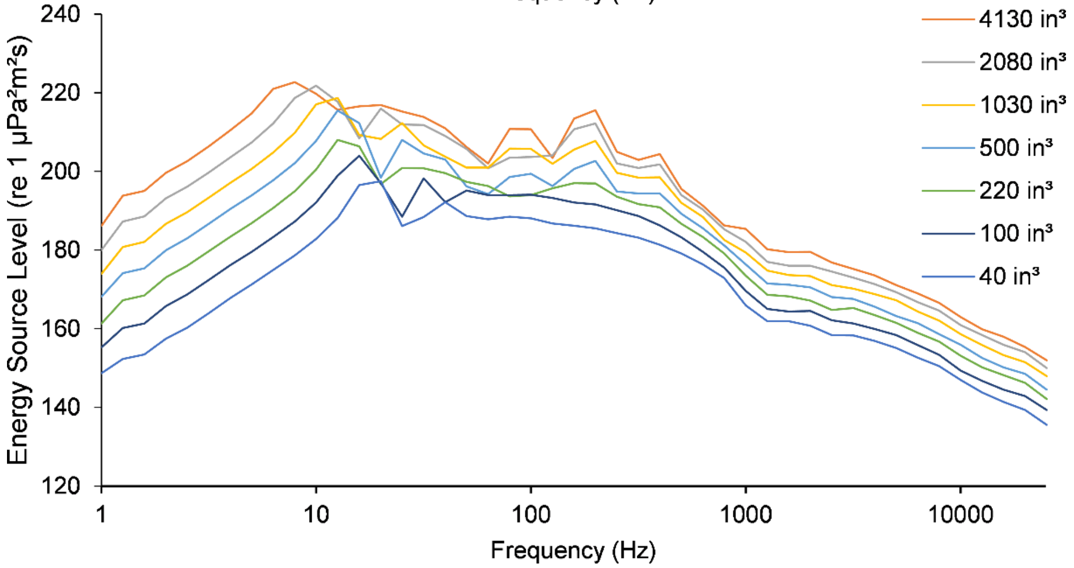

Figure 20. The spectra of the 4130 in³ array at all stages of the soft-start in the endfire (top) and broadside (bottom) directions up to 25 kHz.

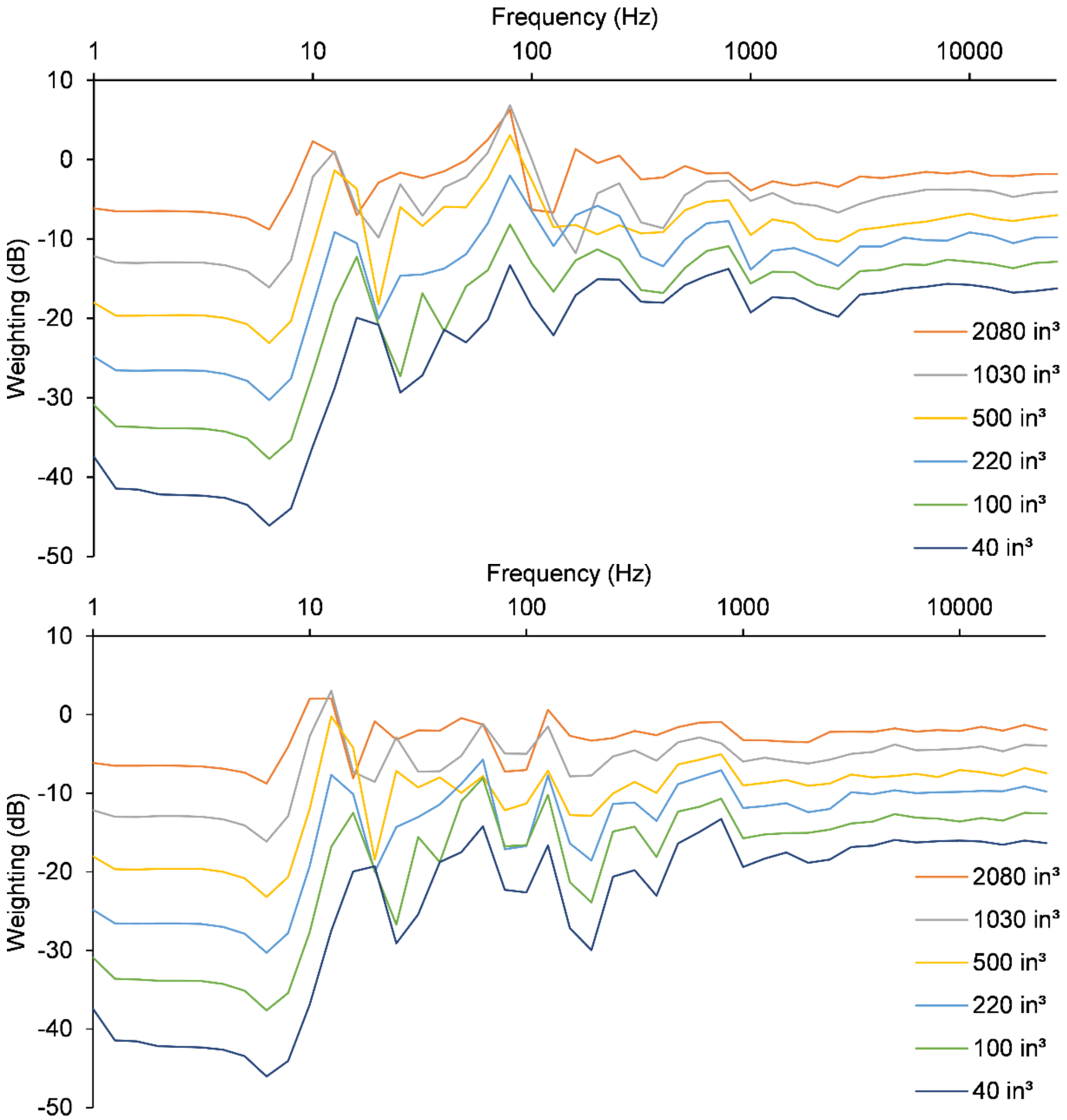

Figure 21. The frequency weighting curves applied to the full 4130 in³ array to reproduce the sound field generated by the different stages of the soft-start in the endfire (top) and broadside (bottom) directions up to 25 kHz.

6.3. Modelling Procedures

To determine the resulting sound fields for the initial baseline numerical modelling the following assumptions were made:

- For the calculation of peak and cumulative metrics, except where noted, levels were taken from results for a receiver at a depth of 10 m.
- All receivers were static.
- For the calculation of cumulative metrics, the calculated sound field(s) moved in accordance with the modelled source lines in Section 6.4; soft-start procedures were included as described in Section 6.1.
- Other modelling parameters relevant to the environment and source input files are listed in Appendix H.
- For the calculation of peak metrics, the source was assumed to be located at the centre of the defined survey block (Appendix C).

6.4. Modelled Source Points for Cumulative Assessment

6.4.1. Scenario 1 – Site Survey in the North Sea Deep environment

Scenario 1 of Phase 2 investigates the sound produced from a site survey. For the cumulative aspect of the survey, details of the sail lines were required that describe the path of the vessel and the source point locations. The initial study to determine the environment to use was performed using MONM-BELLHOP, which showed that the Scenario 5 environment (North Sea Deep) provided the greatest ranges to PTS onset levels (for LF cetaceans); consequently, it is this environment that was employed for Scenario 1.

A site survey area is typically significantly smaller than a regional type 3D survey and was therefore assumed to be over an area of 16 km² located at the centre of the North Sea Deep region modelled in Scenario 5.

The track lines were 4 km long with an assumed 50 m between adjacent lines, and 2 km between opposing tracks (and 1950 m on the return). The source point or pulse interval was 3 s, and the distance spacing between pulses was 6.25 m; this gave a vessel speed of 2.083 m/s (4.0497 knots) and 32 minutes for each line.

The soft-start process was set to take 15 min to reach full operating airgun array volume and features an increase in source-activation frequency, followed by an increase in number of operating airguns. The total distance covered by the vessel during the soft-start was 1875 m.

After each sail line, the vessel commenced a turn that involves a 1 km run-out section, a constant radius turn arc to orient itself to be on a path coincident with the next sail line, and a 1 km run-in section to bring any streamers in line with the following sail line. An increased vessel speed of 2.5 m/s is assumed between lines; consequently, a complete turn at each end took approximately 34 min. During the turn, the source was active at the full array operating volume and pressure in accordance with the details in Table 18; the source effort associated with the run-in started 400 s before the following survey line regardless of the time since the previous source point from the turn section.

Table 18. Source point interval between survey lines for the modelled site survey.

Activity	Duration (s)	Source point interval (s)
Run-out	400	200
Turn	N: 1257 S: 1225	180
Run-in	200	60
	100	30
	5	12
	5	6

Based on this, the site survey performed 22 complete lines in 24 hours; the vessel was partially through a turn at the point of reaching 24 hours. Assuming constant operation at this rate, the entire set of north-to-south survey lines would take almost four days to complete.

The activities within the first 24 hours of the survey are detailed in Table 19. A map showing the site survey source point lines is shown in Figure 22; the survey starts in the southwestern most corner.

Table 19. Timing of activities for the first 24 hours of the modelled site survey.

Activity	Duration	Activity end time
Soft-start	00:15:00	00:15:00
Line N 1	00:32:00	00:47:00
Turn N 1	00:34:17	01:21:17
Line S 1	00:32:00	01:53:17
Turn S 1	00:33:45	02:27:02
Line N 2	00:32:00	02:59:02
Turn N 2	00:34:17	03:33:19
Line S 2	00:32:00	04:05:19
Turn S 2	00:33:45	04:39:04
Line N 3	00:32:00	05:11:04
Turn N 3	00:34:17	05:45:21
Line S 3	00:32:00	06:17:21
Turn S 3	00:33:45	06:51:06
Line N 4	00:32:00	07:23:06
Turn N 4	00:34:17	07:57:23
Line S 4	00:32:00	08:29:23
Turn S 4	00:33:45	09:03:08
Line N 5	00:32:00	09:35:08
Turn N 5	00:34:17	10:09:25
Line S 5	00:32:00	10:41:25
Turn S 5	00:33:45	11:15:10
Line N 6	00:32:00	11:47:10
Turn N 6	00:34:17	12:21:27
Line S 6	00:32:00	12:53:27
Turn S 6	00:33:45	13:27:12
Line N 7	00:32:00	13:59:12
Turn N 7	00:34:17	14:33:29
Line S 7	00:32:00	15:05:29
Turn S 7	00:33:45	15:39:14
Line N 8	00:32:00	16:11:14
Turn N 8	00:34:17	16:45:31
Line S 8	00:32:00	17:17:31
Turn S 8	00:33:45	17:51:16
Line N 9	00:32:00	18:23:16
Turn N 9	00:34:17	18:57:33
Line S 9	00:32:00	19:29:33
Turn S 9	00:33:45	20:03:18
Line N 10	00:32:00	20:35:18
Turn N 10	00:34:17	21:09:35
Line S 10	00:32:00	21:41:35
Turn S 10	00:33:45	22:15:20
Line N 11	00:32:00	22:47:20
Turn N 11	00:34:17	23:21:37
Line S 11	00:32:00	23:53:37
Turn S 11	cut	24:00:00

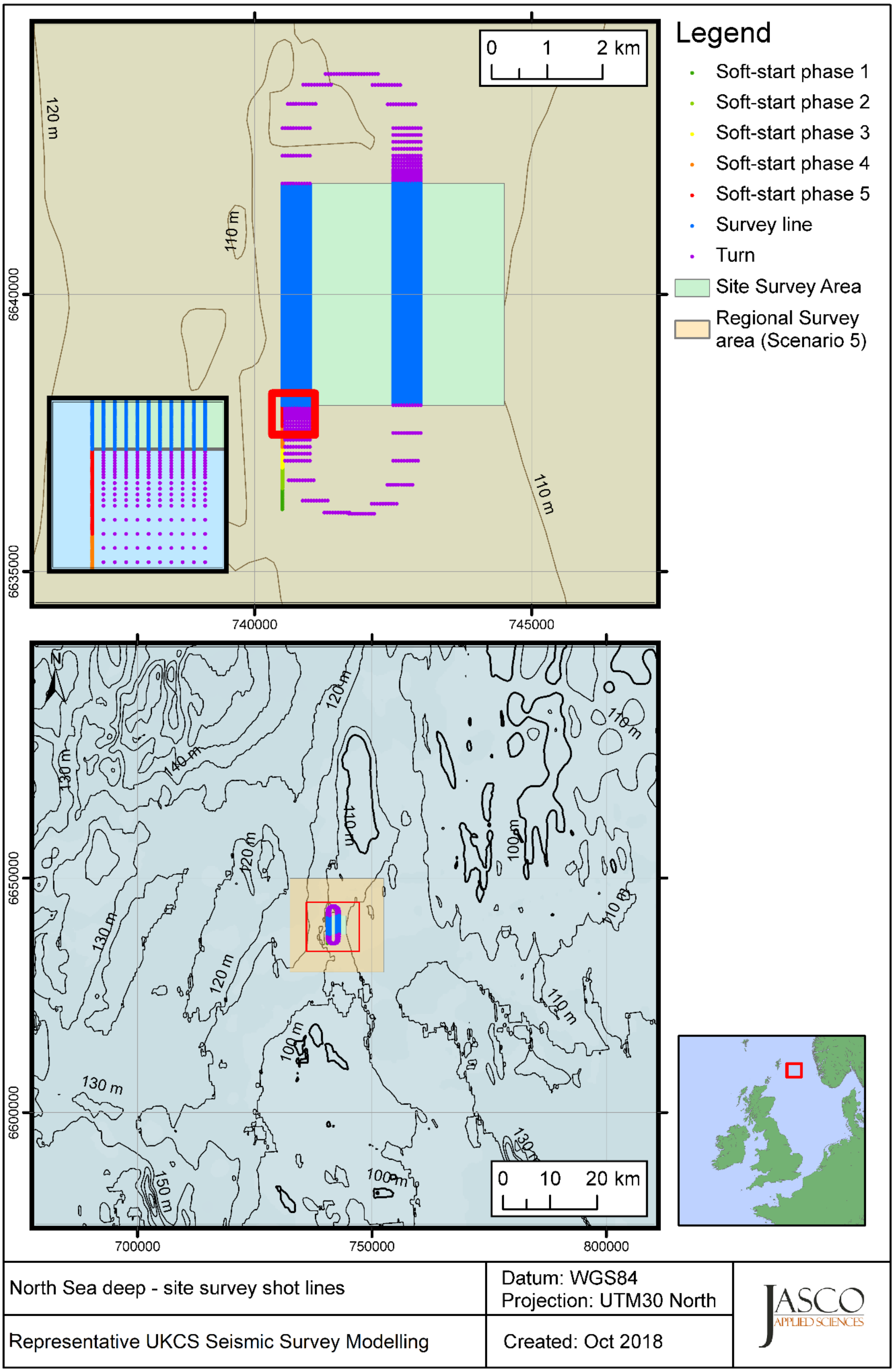

Figure 22. Modelled site survey lines.

6.4.2. Scenario 2 – VSP in the North Sea Deep environment

The VSP scenario involves a static source only. The cumulative assessment was performed assuming a soft-start period, as described in Table 16, followed by 1440 pulses at full power; this equates to 8 hours' worth of active operation with 20 s between pulses.

6.4.3. Scenarios 3-6 – Regional Survey in multiple environments

For the Phase 2 modelling, Scenarios 3 through 6 all followed the same racetrack survey design. The plan of the surveys is outlined in Figure 23, with the timings of each section over the 24-hour window shown in Table 20.

The modelled source lines for the first line from the point of full array volume are detailed in Table 21; subsequent lines locations are determined in accordance with the geometry in Figure 23. The vessel moved at a constant speed of 4.86 knots (2.5 m/s) and commenced with the soft-start procedure detailed in Section 6.1 to reach full volume at the start position listed in Table 21. Once at the full source array volume, the source array was activated with a source point spacing of 25 m (Scenarios 3–6). At the end of the source line, it is assumed that the source array was turned off. Due to the time for a turn taking longer than 40 min, a full 20-min soft-start was included immediately prior to each new line as based on JNCC guidelines (2017); it was assumed that the source restarts were performed in-line with the following survey line.

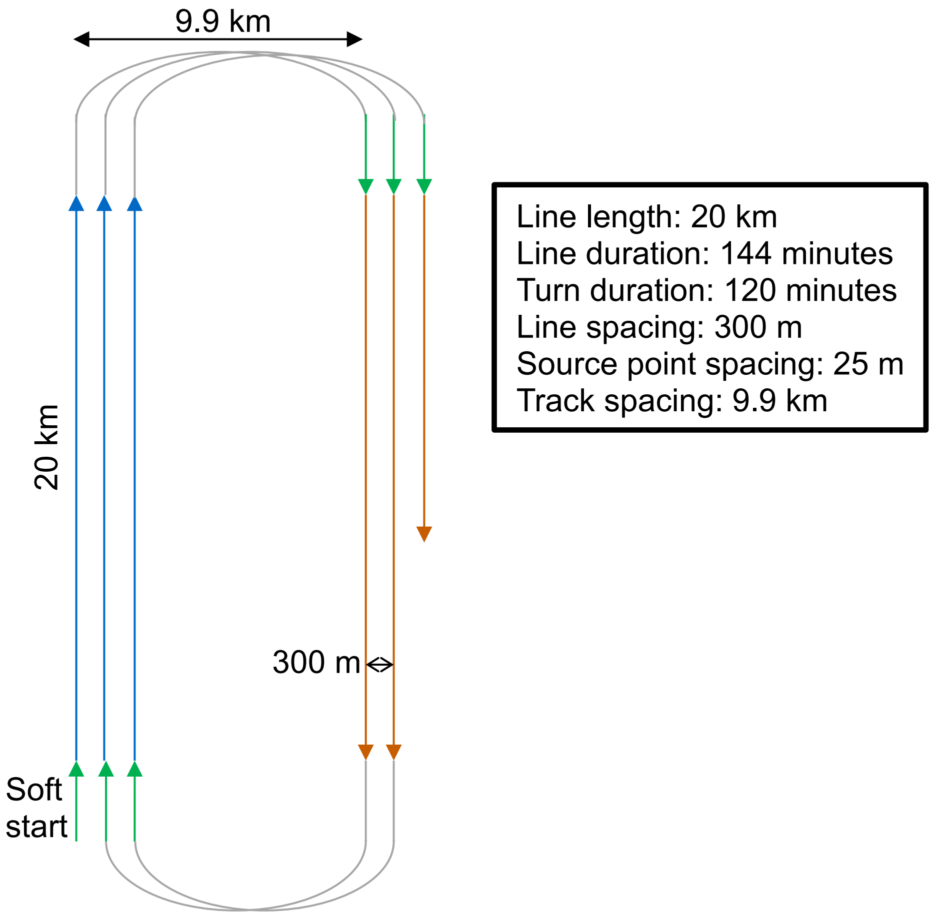

Figure 23. Survey racetrack design for all scenarios.

Table 20. Timings of activities within the survey over the first 24 hours.

Action	Duration (min)	Cumulative
Soft-start 1	20	0h20
Line 1	144	2h44
Turn 1	100	4h24
Soft-start 2	20	4h44
Line 2	144	7h08
Turn 2	100	8h48
Soft-start 3	20	9h08
Line 3	144	11h32
Turn 3	100	13h12
Soft-start 4	20	13h32
Line 4	144	15h56
Turn 4	100	17h36
Soft-start 5	20	17h56
Line 5	144	20h20
Turn 5	100	22h00
Soft-start 6	20	22h20
Line 6	100 (cut)	24h00

Table 21. First modelled source point lines for Scenarios 3 through 6. All Eastings and Northings are in UTM30 North.

Scenario	Region	Length	Ship heading (clockwise from North)	Start Easting (m)	Start Northing (m)	End Easting (m)	End Northing (m)
3	Irish Sea	20 km	0°	447500	5980000	447500	6000000
4	North Sea Shallow	20 km	0°	854000	5940000	854000	5960000
5	North Sea Deep	20 km	0°	732500	6630000	732500	6650000
6	Faroe-Shetland Channel	20 km	45°	435858	6725000	450000	6739142

6.5. Effect Distances

Effect distances were computed with species-specific impact thresholds (Section 3) for two metrics: frequency weighted SEL over a 24-hour period, and the single transmission peak sound pressure, $L_{p,\text{pk}}$. The R_{max} was chosen as the main estimate of effect distance for the entire study for comparisons across models and environments. For the SEL, the maximum range, R_{max}, was defined as the greatest distance from either the closest survey track line for Scenarios 1 and 3–6, or the VSP source location for Scenario 2 to the analysed sound level (Figure 24). The results for $L_{p,\text{pk}}$ are defined from only a single activation of the source, so ranges are calculated from that single source location. The SEL results for MONM also include the 95th percentile range over the calculated radials; this is detailed further in Section 7.3.1.2.

In some scenarios, the SEL_{24h} levels across the entire region between survey track lines exceeded the impact thresholds for some auditory groups. In those cases, where the maximum range to the given threshold was in this region, R_{max} was defined to a point on the line halfway between the inner survey tracks.

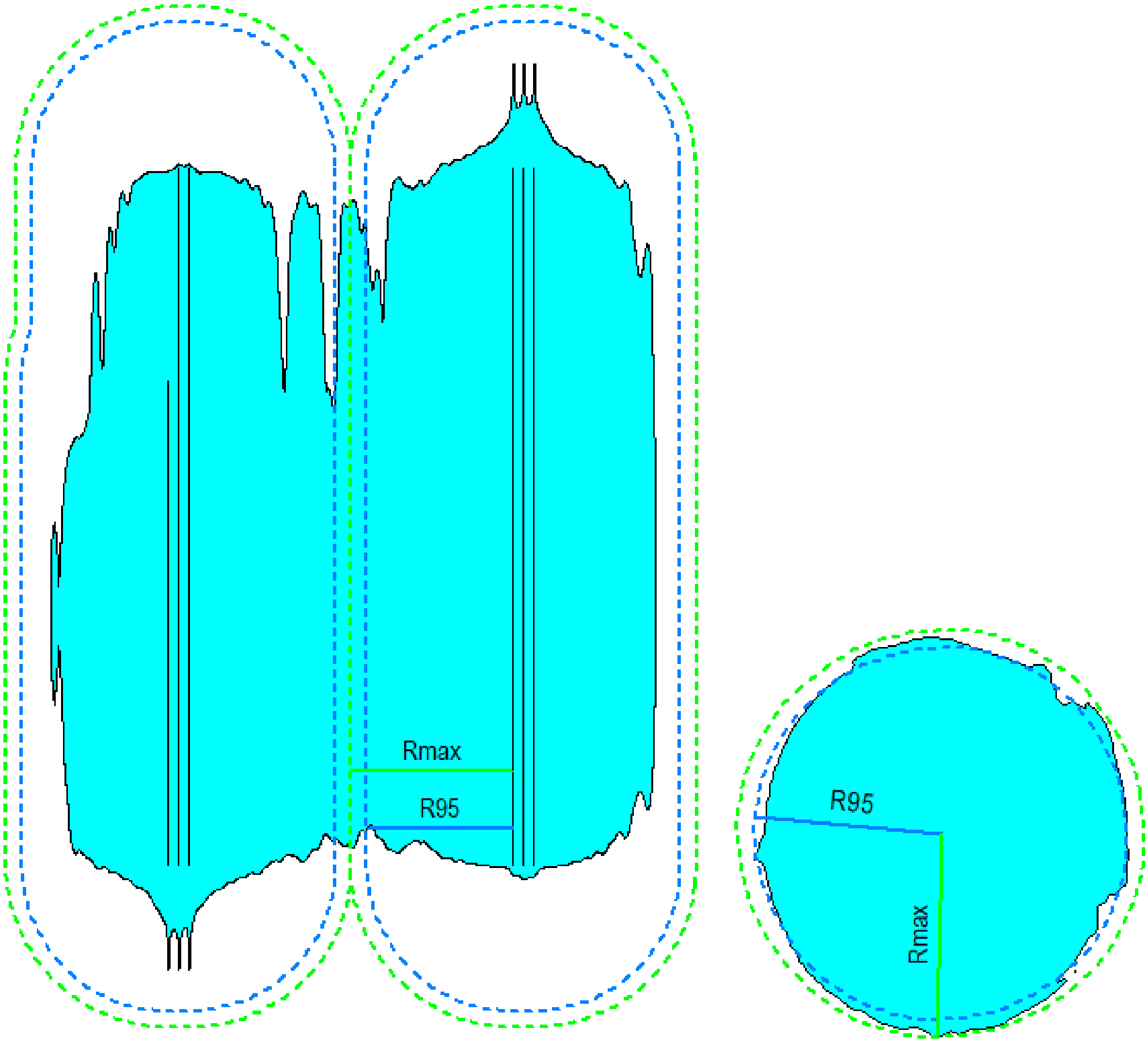

Figure 24. Determination of R_{max} and $R_{95\%}$ for the moving sources (left) and stationary or single shot sources (right).

7. Numerical Propagation Modelling

7.1. Modelling Process Overview

The radiation of sound through the environment was modelled by predicting the acoustic propagation loss—a measure of the decrease in sound level between a source and a receiver some distance away. Geometric spreading of acoustic waves is the predominant way by which transmission loss occurs. Radiation losses also occur when the sound is absorbed and scattered by the seawater, and absorbed, scattered (due to surface roughness caused by wind), and reflected at the water surface and within the seabed. The total propagation loss depends on the acoustic properties of the ocean and seabed and its value is strongly dependent on frequency.

If the acoustic energy source level ($L_{S,E}$), expressed in dB re 1 µPa²m²s, and propagation loss (PL), in units of dB re 1 m², at a given frequency are known, then the received sound exposure level (RL) at a receiver location can be calculated in dB re 1 µPa²s by RL = $L_{S,E}$ – PL. It is the PL that the underwater acoustic models discussed in this section calculate.

7.2. Underwater Acoustic Modelling

The propagation of sound, when considering standard linear acoustics, is fundamentally governed by what is known in physics as the wave equation; by solving the wave equation, given certain boundary conditions, one can characterise the sound field at all places and at all times. The equation relates the spatial variation of an acoustic parameter, typically pressure, to temporal variations in that same parameter. In its standard form, the equation is difficult to solve for general cases; there are techniques, however, that make the process easier.

Firstly, the signal in the time domain can be recast in what is known as the frequency domain by use of a Fourier transform (typically implemented as an FFT (fast Fourier transform)). This provides a decomposition of the signal into its individual frequency components. Similarly, a set of frequency components can be converted back into the time domain using an inverse Fourier transform.

Secondly, if one assumes the sound to be only at a single frequency, the time element can be removed from the wave equation; doing this provides a simpler function known as the Helmholtz equation that describes sound propagation at a specific frequency.

These two features of converting a signal to individual frequency components using an FFT and being able to solve the Helmholtz equation far more readily than the wave equation means that this is the most standard approach to sound propagation problems.

The acoustic models generally differ in how they go about solving the Helmholtz equation. These can include:

- Parabolic equation (PE) models;
- Ray- or beam-tracing models;
- Wavenumber integration models;
- Energy-flux models;
- Normal mode models.

A full discussion of how the models are derived is beyond the scope of this work but detailed descriptions can be found in literature.

Each model type has its strengths and weaknesses and it should be stressed that no single model works for every situation. Table 22 shows the list of model types, the specific project models that fall into each category, and their applicability to different acoustic problems from Etter (2012) . A summary of model capabilities and features is provided at the end of the section in Table 23.

Table 22. Domains of applicability of underwater acoustics propagation models reproduced from Etter (2012) with additions. Low frequency is <500 Hz, High frequency is >500 Hz; RI is range independent, RD is range dependent. Full circle denotes the approach is applicable and practical; half circle means there are limitations in accuracy or execution speed; empty circle indicates that the approach is neither applicable nor practical.

Model type	**Applications**							
	Shallow water				Deep water			
	Low frequency		High frequency		Low frequency		High frequency	
	RI	RD	RI	RD	RI	RD	RI	RD
Parabolic equation: MONM, FWRAM, dBSeaPE	◑	●	○	○	◑	●	◑	◑
Normal mode: Soprano – low frequencies	●	◑	●	◑	●	◑	◑	○
Wavenumber integration: VSTACK	●	◑	●	◑	●	◑	◑	◑
Ray tracing: BELLHOP, dBSeaRay	○	○	◑	●	◑	◑	●	●
Energy flux: Soprano - high frequencies	●	◑	●	◑	○	○	○	○

7.3. Project Underwater Acoustic Models

Below are the models used in the modelling for this report; each section provides a general description of each, and the particular model processes as applied to this project.

7.3.1. MONM-BELLHOP

7.3.1.1. Model description

Underwater sound propagation (i.e., transmission loss) was predicted with JASCO's Marine Operations Noise Model (MONM). This model computes sound propagation at lower frequencies via a wide-angle parabolic equation solution to the acoustic wave equation (Collins 1993) based on a version of the U.S. Naval Research Laboratory's Range-dependent Acoustic Model (RAM), which has been modified to account for a solid seabed (Zhang and Tindle 1995). MONM computes sound propagation at higher frequencies via the BELLHOP Gaussian beam acoustic ray-trace model (Porter and Liu 1994).

The parabolic equation method has been extensively benchmarked and is widely employed in the underwater acoustics community (Collins et al. 1996). MONM accounts for the attenuation due to reflection loss at the seabed resulting from partial conversion of incident compressional waves to shear waves at the seabed and sub-bottom interfaces where they exist, and it includes wave attenuations in all layers. Site-specific environmental properties incorporated are a bathymetric grid of the modelled area, underwater sound speed as a function of depth, and a geoacoustic profile based on the overall stratified composition of the seafloor.

MONM is a point source model, and as such, the source function from AASM is processed to allow for all acoustic energy to emanate from a single point whilst retaining horizontal directivity. MONM, however, does not include vertical directivity and so, for a given azimuth, energy source levels in the horizontal direction are used.

Acoustic fields are computed in three dimensions by modelling propagation loss within two-dimensional (2-D) vertical planes aligned along radials covering a 360° swath from the source, an approach commonly referred to as N×2-D. These vertical radial planes are separated by an angular step size of $\Delta\theta$, yielding $N = 360°/\Delta\theta$ number of planes (Figure 25).

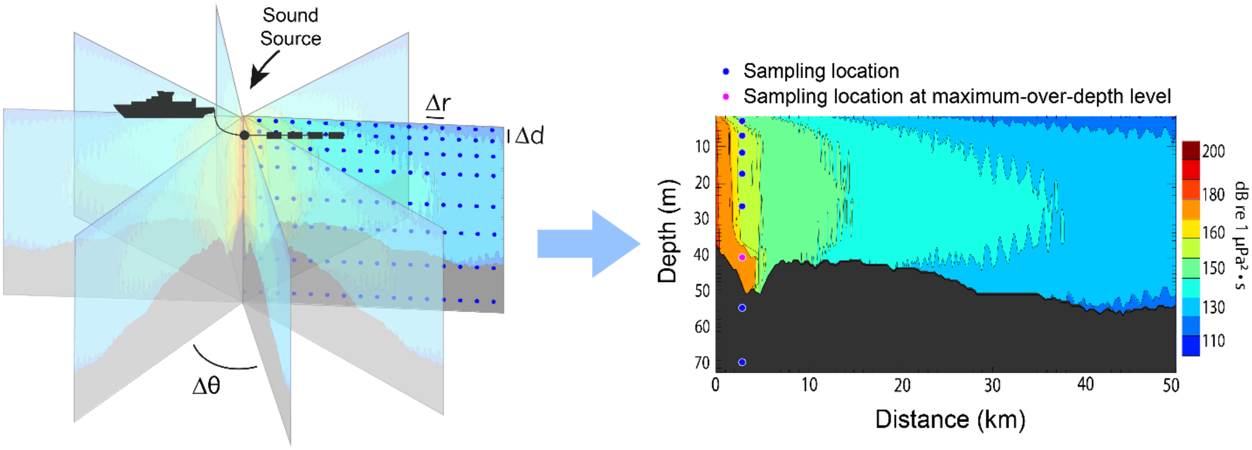

Figure 25. The N×2-D and maximum-over-depth modelling approach used by MONM.

Frequency dependence is addressed by computing acoustic propagation loss at the centre frequencies of decidecade bands. Sufficiently many decidecade bands, starting at 10 Hz, are modelled to include the majority of acoustic energy emitted by the source. At each centre frequency, the propagation loss is modelled within each of the N vertical planes as a function of depth and range from the source. The decidecade-band received per-pulse SELs are computed by subtracting the band propagation loss values from the directional source level in that frequency band. Composite broadband received SELs are then computed by summing the received decidecade-band levels.

The received per-pulse SEL sound field within each vertical radial plane is sampled at various ranges from the source with a fixed radial step size (Δr in Figure 25). At each sampling range along the surface, the sound field is sampled at various depths (Δd in Figure 25), with the step size between samples increasing with depth below the surface. The step sizes are chosen to provide increased coverage near the depth of the source and at depths of interest in terms of the sound speed profile.

MONM's predictions have been validated against experimental data from several underwater acoustic measurement programs conducted by JASCO (Hannay and Racca 2005, Aerts et al. 2008, Funk et al. 2008, Ireland et al. 2009, O'Neill et al. 2010, Warner et al. 2010, Racca et al. 2012a, Racca et al. 2012b, Martin et al. 2015).

7.3.1.2. Modelling process

For any given scenario, the modelling involved firstly generating the sound field for a single source point, and then transposing and summing this field in accordance with multiple source points along the survey sail lines. In the case of Scenario 6, due to the large difference in water depths at the source point locations (951 m at the edge of the survey area, and 701 m at the centre), two sound fields were generated to inform the cumulative calculations. As predicted ranges to PTS threshold values are typically short and, other than the example for Scenario 6, the bathymetries are generally similar in the region this is a valid approach. Where greater ranges are anticipated, for lower threshold values such as TTS, generating more modelled sound fields would be desirable.

The single pulse sound fields were calculated at a single frequency (the band centre frequency) for each individual decidecade band from 10 Hz to 800 Hz using MONM, and 1 kHz to 25 kHz using

BELLHOP. Scenarios 1 and 2 were calculated over 100 km × 100 km domains, whilst Scenarios 3 through 6 were calculated over 200 km × 200 km domains. Above 5 kHz, radials were limited to a maximum range of 15 km for Scenario 6. The calculations were performed over 144 transects (uniformly spaced 2.5° apart) with a radial step of 10 m, and a depth step that varied with frequency (between 2 m to 0.5 m). The BELLHOP calculation comprised 10000 beams within the angles ±89° from the horizontal, and used the semi-coherent summation process described in Jensen et al. (2011).

The post-processing steps recast the modelled radials onto a cartesian grid, with a grid resolution of 25 m. The inclusion of the azimuth- and frequency-dependent source level and the frequency weightings were applied at this point to generate received levels specific to the animal hearing groups for the single source pulse. Levels calculated in post-processing were generated only for a receiver at 10 m depth.

The cumulative calculation was performed by transposing the single-pulse sound field for each source point defined and summing on a universal grid. Maximum ranges are calculated as the largest distance from any point at which sound levels decreases to below the impact threshold to its closest location along the survey lines; typically, this is perpendicular to the sail lines.

For the MONM-BELLHOP results, two distances relative to the source are reported for each sound level: 1) R_{max}, the maximum range to the given sound level over all azimuths, and 2) $R_{95\%}$, the range to the given sound level after the 5% farthest points were excluded (see examples in Figure 26).

The $R_{95\%}$ is provided because sound field footprints are often irregular in shape. In some cases, a sound level contour might have small protrusions or anomalous isolated fringes. This is demonstrated in the image in Figure 26(a). In cases such as this, where relatively few points are excluded in any given direction, R_{max} can misrepresent the area of the region where a specific sound level may occur, and $R_{95\%}$ is considered more representative. In strongly asymmetric cases such as shown in Figure 26(b), on the other hand, $R_{95\%}$ neglects to account for significant protrusions in the footprint. In such cases R_{max} might better represent the region where a specific sound level may occur in specific directions. Cases such as this are usually associated with bathymetric features affecting propagation. The difference between R_{max} and $R_{95\%}$ depends on the source directivity and the non-uniformity of the acoustic environment. It is only available where the full 3D sound fields have been calculated, i.e., only for SEL.

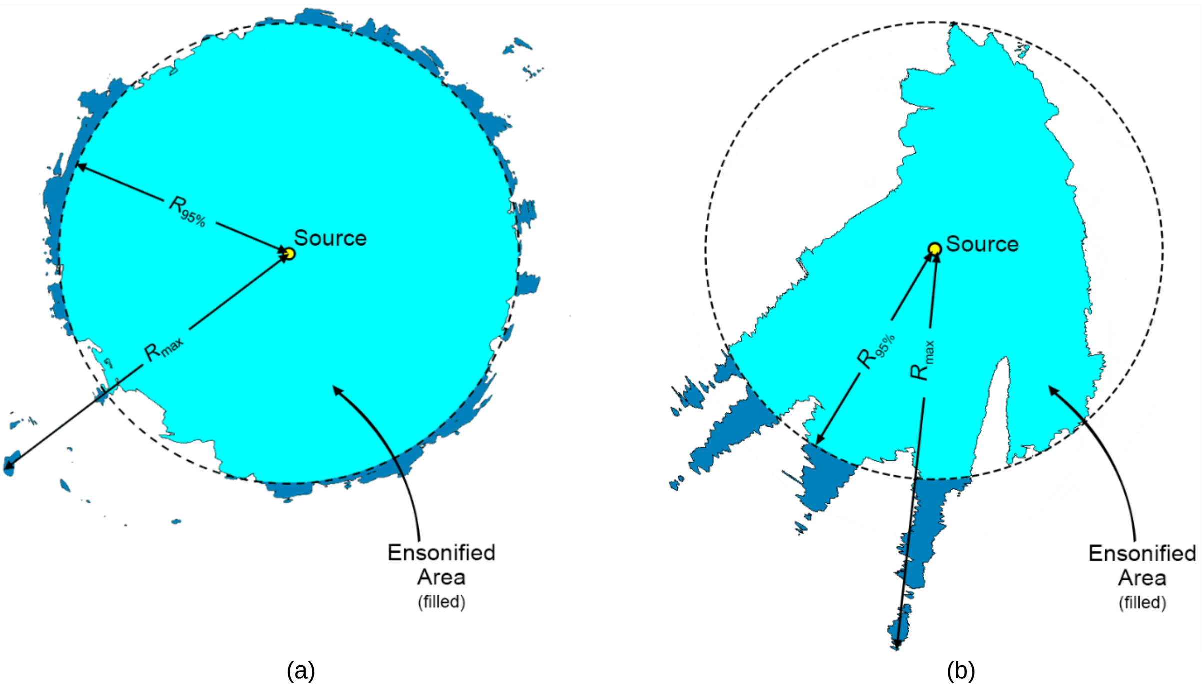

Figure 26. Sample areas ensonified to an arbitrary sound level with R_{max} and $R_{95\%}$ ranges shown for two different scenarios. (a) Largely symmetric sound level contour with small protrusions. (b) Strongly asymmetric sound level contour with long protrusions. Light blue indicates the ensonified areas bounded by $R_{95\%}$; darker blue indicates the areas outside this boundary which determine R_{max}.

7.3.2. VSTACK

7.3.2.1. Model description

Peak sound pressure levels were modelled using JASCO's VSTACK (Vertical Stacking Model) wavenumber integration model. Synthetic pressure waveforms are computed versus depth and range for arbitrarily layered, range-independent, acoustic environments using the wavenumber integration approach to solving the exact (range-independent) acoustic wave equation. This model is valid over the full angular range of the wave equation and can fully account for the shear wave properties of the sub-bottom. Wavenumber integration methods are extensively used in the fields of underwater acoustics and seismology where they are often referred to as reflectivity methods or discrete wavenumber methods.

Sound propagation is computed in arbitrarily stratified water and seabed layers by decomposing the outgoing field into a continuum of outward-propagating plane cylindrical waves. Seabed reflectivity in the model is dependent on the seabed layer properties: compressional and shear wave speeds, attenuation coefficients, and layer densities.

Steep-angle propagation is predicted in the proximity of the source but is computationally slow at predicting sound pressures at large distances due to the need for smaller wavenumber steps with increasing distance. Additionally, VSTACK assumes range-invariant bathymetry with a horizontally stratified medium (i.e., a range-independent environment) that is azimuthally symmetric about the source. VSTACK is thus best suited to modelling the sound field in close proximity to the source.

7.3.2.2. Modelling process

VSTACK is used in this project to provide values for the maximum range to identified peak sound pressure levels. As stated, this is suitable for modelling in close proximity to the source and thus is better suited to providing ranges to the higher levels. Given VSTACK's capability to accurately model shear wave transmission in the sediment, it is also used to provide short-range SEL results where sub-bottom layering effects with shear waves are investigated (Section 10.5.2).

Modelling was performed in a single transect, in the broadside direction of the airgun array up to a maximum range of 1.0 km. The output range step was 10 m, and values are generated for a receiver at a depth of 10 m. The frequency range modelled was 5 Hz to 1024 Hz.

7.3.3. FWRAM

7.3.3.1. Model description

For this study, synthetic pressure waveforms to calculate the peak sound pressure level were also computed using FWRAM (Full Waveform Range-dependent Acoustic Model), which is a time-domain acoustic model based on the same wide-angle parabolic equation (PE) algorithm as MONM. Synthetic pressure waveforms are computed versus range and depth for range-varying marine acoustic environments, and it takes the same environmental inputs as MONM (bathymetry, water sound speed profile, and seabed geoacoustic profile). Unlike MONM, FWRAM computes pressure waveforms via Fourier synthesis of the modelled acoustic transfer function in closely spaced frequency bands. An array starter method that generates the vertical directivity pattern from a distributed source to seed the field calculation is used to accurately model sound propagation (MacGillivray and Chapman 2012) rather than be limited to a point source assumption.

7.3.3.2. Modelling process

Synthetic pressure waveforms were modelled over the frequency range 10–1000 Hz, inside a 0.5 s window for all scenarios. The modelling was performed in endfire and broadside directions as these generate the greatest levels; this provided a total of four transects per scenario. The synthetic pressure waveforms were post-processed, after applying a travel time correction, to calculate the peak sound pressure metrics versus range from the source at a depth of 10 m. The model resolution was dependent on the frequency; the range step varied from 50 to 10 m, and the depth step ranged from 2.0 to 0.125 m. Results are presented for the largest range from the four calculated transects.

7.3.4. Soprano and Aquarius

7.3.4.1. Model description

SOPRANO is a hybrid approach for shallow waveguides. To achieve this, the method relies on two separate computationally efficient approximations for the propagation loss that are appropriate for low frequencies and high frequencies, and assumes no sound speed gradient is present (Macpherson and Daintith 1967, Weston 1971, Ainslie et al. 2014, Sertlek and Ainslie 2014). This combined model approach has been verified against several state-of-the-art propagation models (Sertlek et al. 2018). Calculations were performed using an adapted implementation of the model (Aquarius), developed at TNO (Jansen and de Jong 2017).

The model takes as input a description of the source spectrum in the form of an energy source levels in units of dB re 1 $\mu Pa^2 m^2 s$. The energy source level as a function of radial (in steps of 2.5°) was derived from the computed source waveforms (Section 4.3). The energy source level was then combined with the propagation loss computed with Aquarius to result in sound exposure level as a function of location and depth.

7.3.4.2. Modelling process

The energy source levels were taken from AASM for a frequency range from 10 Hz to 20 kHz and then propagated to obtain single source point SEL maps on a 20 x 20 km^2, and in some cases a 30 x 30 km^2 grid, with 20 m resolution in (x,y), this larger grid being used when necessary because of large ranges over which effects such as sound levels being above relevant threshold values were predicted. The model considered a single sound-speed for the water column, a single water depth and a single description of the seabed acoustic properties. It did not attempt to predict effects that might arise because of in-water refraction of sound. To manage the uncertainty that this represents in received level, it is considered good practice to put the receiver in a location that will ‘err on the side of caution’ in terms of potential impacts. The sound field was therefore computed at 1 m from the seafloor, considered to be representative of the maximum level over the water depth at that location. Broadband, and frequency-weighted sound exposure level maps were then generated (Figure 27; see Appendix J.2 for all scenarios), which were then used to compute stand-off distances for species-specific thresholds. Since the model has been developed for shallow-water large distance propagation, this approach was used to compute Scenarios 1–5, but did not consider the deep-water scenario, Scenario 6.

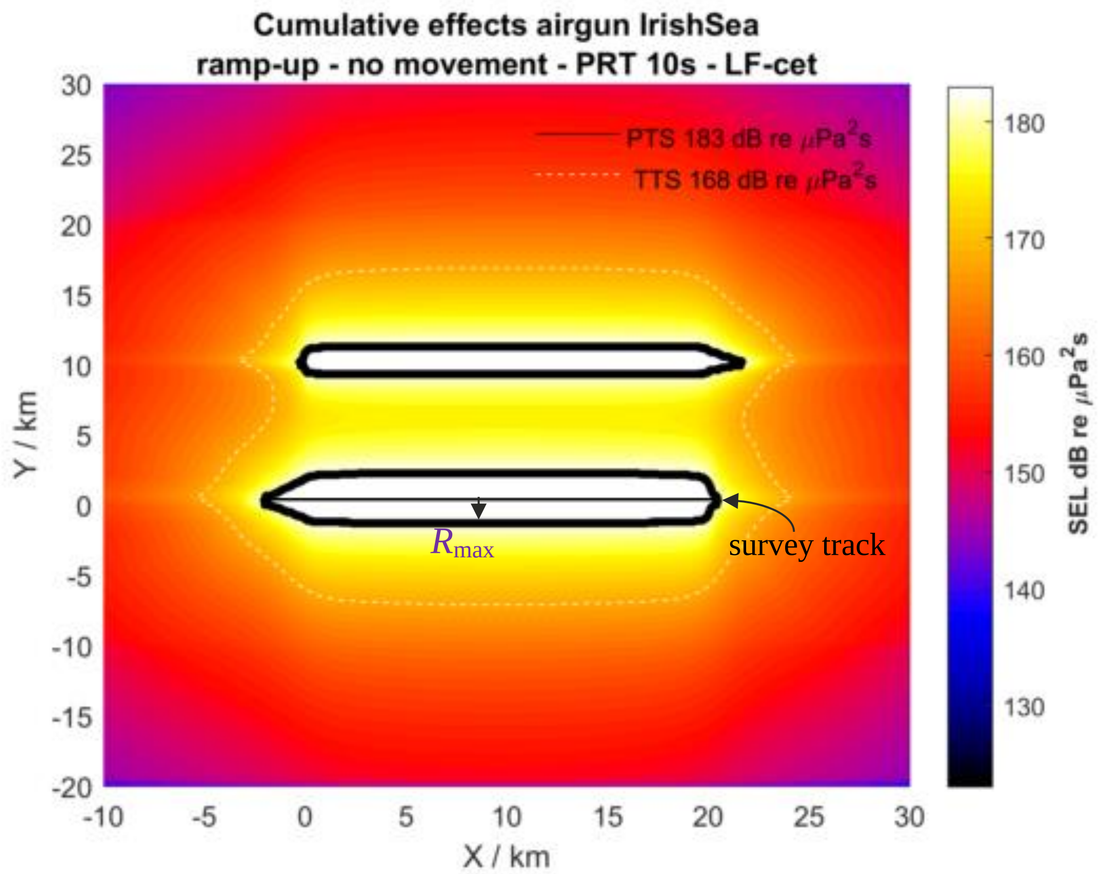

Figure 27. Example of isoclines for PTS (black solid lines) and TTS (white dashed line) thresholds (NMFS 2018), and maximum effect distance R_{max} for a stationary receiver. This example considers the LF-cetacean group, with cumulative SEL (colour-coded) for multiple lines within 24 hours, the Irish Sea environment (Scenario 3). The SEL_{cum} around the bottom tracks is higher because these involved three lines, whereas the upper track involved only two lines within a 24-hour period.

Peak sound pressure level, $L_{p,pk}$ maps were generated using single-source-point peak sound pressures, estimated by taking the single source point SEL_{ss}, $L_{p,E,ss}$, as computed using the Aquarius model and applying the empirical Galinda-Romero et al. (2015) relationships for airguns

$$L_{p,pk} = A \cdot L_{p,E,ss} + B,$$

with A = 1.21 dB re 1 µPa/dB re 1 µPa²s, and B = -20.1 dB re 1 µPa.

The cumulative sound exposure for different marine mammal species was computed using the method presented in von Benda-Beckmann et al. (2014), which has been extended to use propagation loss predictions using Aquarius and to incorporate the air gun soft-start schemes. For the Phase 2 computations, the animals were assumed to be stationary. Species-specific sound exposure maps were computed by summing the contributions from each source point over a 24-hour exposure period. The contribution from each source point location within a single line was based on the propagation loss for a single location with representative bottom depth, but accounted for increase in energy source level during the soft-start and transposed to account for the location and direction of the array.

For Scenarios 1 and 2, the contribution from all source points was computed, using source point locations adopted from supplied data. To speed up the computations, for Scenarios 3–5, first the single line cumulative sound exposure was computed which included the different stages of the soft-start, followed by a 20 km track, with the source moving at 4.5 knots, and a source point interval of 10 s. The SEL over a single survey line for a stationary animal was accumulated into a multi-track (ca. 24-hour) exposure. This was achieved by adding the single-track sound exposure from five tracks (the last partial survey line was omitted), with the tracks re-oriented using the race-track (Section 6.4). The race-track geometry was the same as described in Section 6.4.3. For all scenarios, from these multi-line cumulative exposure maps, the cross-track effect distances R_{max} were computed for the relevant thresholds as the greatest distance between the sound level isopleth to the associated closest point on the closest survey line.

7.3.5. dBSea

7.3.5.1. Model description

The dBSea software typically operates using 1/3-octave bands[3] (EN ISO 266). Band levels are either specified as SPL or as SEL. For the propagation calculation, the band energy is split across each band according to a chosen oversampling rate.

For peak levels ($L_{p,\mathrm{pk}}$) of impulsive sources, such as air guns, dBSea uses time-series of the pressure signature of the source (equivalent monopole). For all scenarios, the broadside direction (starboard or port for arrays, for VSP only 1 signature was given) of maximal energy ($\mathrm{SEL_{ss}}$) was chosen as source level, as dBSea only supports radially uniform or omni-directional sources. This means that we expect slightly larger ranges (all else being equal). The maximal broadside peak level ($L_{p,\mathrm{pk}}$) for the regional array was 249.5 dB re 1 µPa²s which was marginally lower than the endfire (aft) level (249.6 dB re 1 µPa²s). For the site survey this was 238.2 dB re 1 µPa²s broadside and 235.8 dB re 1 µPa²s endfire (Table 7). The VSP was horizontally omnidirectional. The time-series was then propagated using a ray-tracing algorithm, taking into account arrival times, reflections, and self-interference to calculate the resulting time-pressure-signature at all result-grid positions in the scenario. The result is presented as 1/3-octave bands and as $L_{p,\mathrm{pk}}$.

For SEL levels the source band levels specified in Sections 4 and 6.2 were used and propagated using a combination of dBSeaPE and dBSeaRay (with decidecade and 1/3-octave bands used interchangeably).

Weightings (e.g. NOAA/NMFS marine mammal weightings) were applied to the 1/3-octave-band levels to give weighted levels.

Sources that move were modelled as a series of point sources, each representing one or multiple activations of a given impulsive sound. For the multi-line models, when calculating received SEL, each point represented multiple shots pulses to keep the modelling load reasonable for long range scenarios (i.e., >1000 m from array). This means that, for example, if a source is activated ten times over 225 m and the range to the PTS threshold level is 1000 m, then the received energy level at 1000 m range from the source line will be approximately equal to a scenario with one point source in the middle of that line with the combined energy from the 10 pulses (Figure 28). In highly variable, shallow, or short range environments (relative to the source activation interval range) this can mean small changes to the received level at range.

[3] 1/3-octave-band centre frequencies differ slightly from decidecade bands centre frequencies (<1 %).

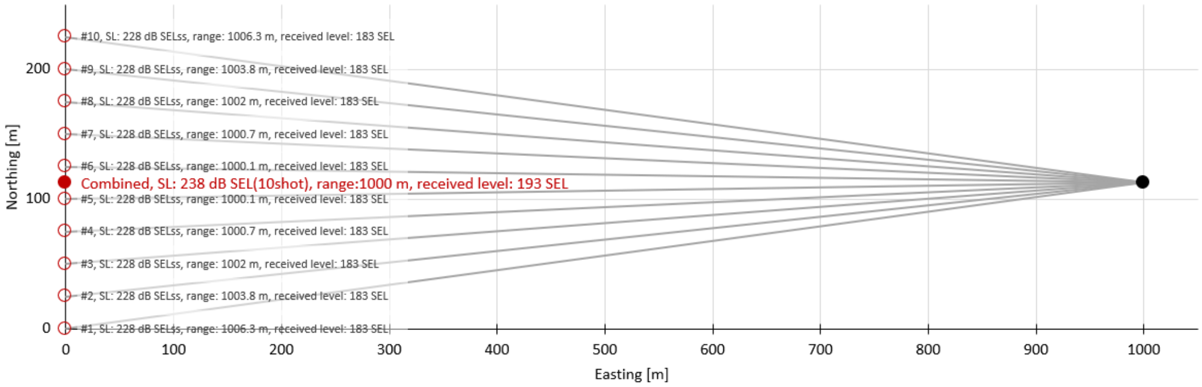

Figure 28. Example of combining source points for dBSea. The total energy of the 10 shots of 228 dB re 1 µPa²s is 238 dB re 1 µPa²s. With received total level of 192.98 dB re 1 µPa²s from the 10 points sources, and 193.00 dB re 1 µPa²s from the single "Combined source". Only valid for relatively uniform environments (compared to source point spacing).

dBSeaPE

Based on the theory laid out in Jensen et al. (2011) for wide angle PE models, and validated against multiple standard test cases against RAM, Kraken and BELLHOP (dBSea 2019). dBSeaPE was used for frequencies lower than 800 Hz. We used 5 Padé terms[4] in the shallow scenarios (Scenarios 3 and 4), and 10 terms in the deeper scenarios (Scenarios 5 and 6), to get high phase accuracy to angles over 70 degrees and an attenuation layer thickness under the lowest sediment layer of 10 times the relevant wavelength (attenuation is infinite at the bottom of this). A normal modes starter was used to generate the starting field.

Limitations: dBSeaPE is omnidirectional (no directivity) and does not support shear waves

dBSeaRay

Like dBSeaPE, this is based on the theory from Jensen et. al. 2011, and is used both for time-series propagation and high-frequency propagation loss calculation for SEL. At the sediment boundary, a complex reflection coefficient is calculated that is representative of underlying layer(s) (Jensen et al. 2011).

For peak sound pressure calculations, the model calculates a list of arrival times and propagation losses at each grid point in the scenario. This information is used to calculate the effective time-series at all grid locations, from which SEL and peak levels can be calculated.

Limitations: dBSeaRay is horizontally omnidirectional (but has vertical directionality), does not penetrate the sediment, but rather uses a reflection coefficient.

As with dBSeaPE, dBSeaRay has been tested across multiple standard cases against RAM, Kraken and BELLHOP (dBSea 2019). For detailed descriptions of the models see Jensen et al. (2011).

All propagation models in dBSea consider full range-dependency (where given) for sound speed profile, temperature, pH, salinity, current, depth and sediment composition.

7.3.5.2. Modelling process

For peak sound pressure calculations, the maximal broadside time series signature of the array was used as input into dBSeaRay. Where we were interested in the maximal range of impact, postprocessing was done to ensure that levels decrease monotonically as distance from the source increases at the relevant depth for the scenario (or max level over all depths if specified). This served

[4] Padé terms are used to decrease the phase error when using a wide-angle PE model, see Jensen et al. (2011) sec. 6.2 p. 468-469.

as a conservative measure but did not change the limit range significantly (for peak sound pressure levels), rather it made the interpretation of result easier.

For SEL calculations, dBSeaPE and dBSeaRay was used, with dBSeaPE calculating propagation losses for lower frequencies (<800 Hz) and dBSeaRay for higher frequencies. The single pulse SEL as band levels was used as source level in the model. For the stationary VSP, the source was omnidirectional, while a choice was made to use the louder of the two broadside source levels for the regional survey and site survey sources (Sections 4 and 4.5 for overview).

For moving sources each source point had propagation losses along a number of radials calculated. These results were interpolated into a results grid and, depending on evaluation metric, the results grid either accumulated energy or stored the maximal or average level (Figure 29).

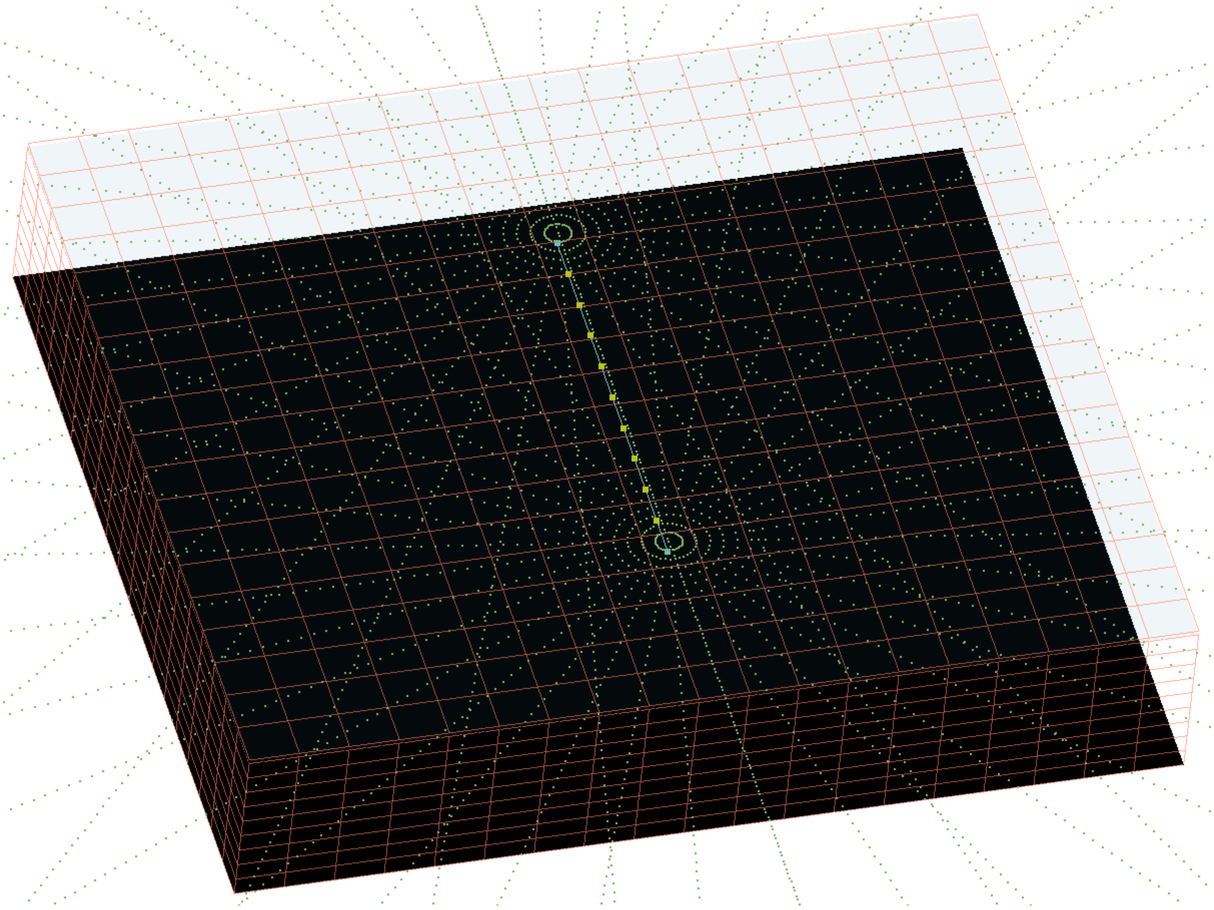

Figure 29. Schematic overview of the dBSea source/receiver paradigm. A moving source with 10 calculation points (2 waypoints (cyan) and 9 intermediate points (yellow)). Propagation loss is calculated from each calculation point to each point in each radial at each depth (only 1 depth layer shown, radials only shown for waypoints). Results are stored in the intersections of the results grid (red grid). For cumulative scenarios (SEL_{24h}) energy is accumulated in the results grid. This is a simplified example, the model had much higher resolution (Section 7.4)

Results are extracted from a 3D point grid with a depth resolution/step of 10 metres and a north-south / east-west resolution of 100 metres. This means a lower limit on ranges, R_{max}, of "<0.1 km". Where sampling did not coincide with grid-points, values were linearly interpolated from the 8 nearest points (corners of cube containing receiver point).

After applying weightings, the group-specific R_{max} is the maximal range, orthogonal to the survey line, to a position where the associated limit is not exceeded for the depth specified. Note that this range is measured from the nearest survey line and never across a survey line.

Moving receivers (modelled as a series of points) "absorb" energy from the eight nearest points in the result grid (inverse distance interpolation) at the time they are at a given position (relative to moving sources and sound speed), depending on their sensitivity (weighting) and time spent at the point (for SEL and SPL calculations).

7.4. Model Summary

A summary of key points of the models used in the project and selectable parameters is shown in Table 23.

Table 23. Summary of acoustic propagation models.

Model	MONM	BELLHOP	FWRAM	VSTACK	SOPRANO	dBSeaPE	dBSeaRay
Type	Parabolic equation	Ray tracing	Parabolic equation	Wavenumber integration	Normal mode/Energy flux	Parabolic equation	Ray tracing
Used for SEL calculations	Yes	Yes	No	No	Yes	Yes	Yes
Used for PK calculations	No	No	Yes	Yes	Yes†	No	Yes
Range-dependent bathymetry	Yes	Yes	Yes	No	No	Yes	Yes
Depth-dependent SSP	Yes	Yes	Yes	No	No	Yes	Yes
Layered geoacoustic capability	Yes	No	Yes	Yes	No	Yes	(Yes)*
Sediment shear wave capability	Partial	Partial	Partial	Yes	Partial	No	No
Sea surface roughness	No	Yes	No	No	Yes	No	No
Minimum modelled frequency (Hz)	10	1000	10	5	1	12.5	1 (PK) 1000 (SEL)
Maximum modelled frequency (Hz)	794.3	25119	1000	1024	25119	800	17678 (PK) 25000 (SEL)
Frequency spacing (Hz)	Bandwidth	Bandwidth	2 Hz	1 Hz	Bandwidth	Bandwidth	Bandwidth
Calculated transects per Scenario.	144	144	4	1	144	496-5024	496-5024
Includes source horizontal directivity	Yes	Yes	Yes	Yes	Yes	No	No

Model	MONM	BELLHOP	FWRAM	VSTACK	SOPRANO	dBSeaPE	dBSeaRay
Includes source vertical directivity	No	No	Yes	Yes	No	No	Yes
Number of modelled source locations	1 per Scenario 1-5 2 for Scenario 6		1 per Scenario 1-5 2 for Scenario 6		1	VSP: 1 Surveys: 62-628	VSP: 1 Surveys: 62-628
Maximum range (km)	141	141 (<5000 Hz) 15 (>5000 Hz)	25	1	28 or 42 (for cases with larger impact ranges)	141	141
Output range resolution	10	10‡	10	10	100	100	100
Range step (m)	10	10‡	10-50	10	100	25-150	1 at source then dependent on depth spacing
Depth step (m)	0.5 – 2.0	0.5 – 2.0‡	0.125-2.0	Calculated at single depth	Calculated at single depth	1-5	1-5
Number of rays	NA	10000 (constant with frequency)	NA	NA	NA	NA	500-1000
Receiver depth	10 m	10 m	10 m	10 m	1 m from seafloor	10 m	10 m

† SOPRANO predictions of sound-exposure were converted to estimates of peak sound pressure using an empirical relationship by Galinda-Romero et al. (2015).
‡ The resolution of the BELLHOP runs is determined according to frequency with results recast onto same grid as for MONM.
* dBSeaRay calculates a complex reflection coefficient based on the underlying layers, but does not propagate into them.

As previously stated, the different model types typically lend themselves to different applications. Furthermore, within a model type category, there are differences between the models that exist that affect the propagation loss results. For many of the aspects of modelling listed in Table 23 it is clear how modelling results might be affected; for example, range-dependent bathymetry is more important for environments featuring large changes in bathymetry but can be an overcomplication where the bathymetry is essentially flat; similarly, a depth-dependent SSP is often not required for shallow water due to there being very little difference in sound speed across the water column. There are factors, however, where their contribution is less obvious, and some of these are briefly discussed here.

The advantage of increased geoacoustic capabilities in models, such as layered geoacoustics and elastic seabed capabilities, are harder to quantify and can often be only as useful as the data used to generate any sub-bottom acoustic properties. In the case of high-frequency propagation, it is often only the top layer of sediment that is relevant due to absorption in the sediment layers making deeper layer information redundant. It is reasonably common to take shear wave properties into account as an additional energy loss term for waves incident on the sediment as is the case for MONM and SOPRANO for example.

Sea surface scattering and absorption are phenomena that affect higher frequency energy (i.e., above 1 kHz) significantly more than lower frequencies and so is typically omitted from models designed for low frequency sources. It does become increasingly important, however, for higher frequencies and higher wind speeds.

The choice of frequencies can have a large bearing on the resulting output. The minimum modelled frequency is often not a contentious point due to there being high propagation losses at the lowest frequencies and frequency-weighting curves having substantial roll-off towards lower frequencies. It is, however, much more significant for SEL calculations where higher-frequency weighting curves are being considered; taking the HF weighting curve into account (Figure A-1), the dominant frequencies for an airgun source can be pushed towards 5 to 10 kHz – these higher frequencies have to be modelled in order for the full frequency range of the signal to be considered in range calculations. The frequency spacing is either narrow-band or fractional-band (i.e., decidecade band or 1/3-octave bands). The advantage of modelling narrow-bands (i.e., 1 Hz or 2 Hz frequency spacing) is that the results can be converted into a pressure signal in time from which peak sound pressure levels can be calculated. The advantage of modelling, say, decidecade bands is that typically only the centre frequency is modelled and so uses a fraction of the computational resources.

The range and depth steps for the modelling are parameters whose effect depend on the type of model used. For parabolic equation models, the range and depth resolution can greatly affect the quality and the speed of the modelling run. The ideal values for each vary with modelled frequency so there are often compromises involved to allow for a wide frequency range to be modelled.

The previous sections have shown that the models can differ in how the sound source itself is treated. The ideal process would include directivity in both vertical and horizontal planes. In the case of point source models, other than ray-tracing methods, it is often difficult to include vertical directivity of a source. Directivity can be included in parabolic equation models by calculating the starting sound field including the directivity pattern and then propagated out normally thereafter. Another alternative that is applicable to airgun modelling is to model each source individually and to sum the resulting sound fields whilst considering the interactions from phase differences between array elements.

8. Baseline Numerical Modelling Outputs

This section includes the tabulated modelled maximum ranges to the identified NMFS 2018 PTS impact threshold levels for all scenarios; tabulated results for TTS and Southall 2007 criteria can be found in Appendix I. Graphical representations are included in Appendix J. A description of the $R_{95\%}$ metric can be found in Section 7.3.1.2. Receivers are assumed to be stationary for the range calculations and located at:

- 10 m depth for dBSea, MONM, FWRAM, and VSTACK results;
- 1 m from the sea floor for Soprano.

8.1. Tabulated Results

8.1.1. Scenario 1 – Site survey in North Sea Deep environment

Table 24. Scenario 1: Maximum ranges to the frequency weighted SEL_{24h} threshold values defined by the NMFS 2018 criteria.

Type of animal	Effect	$SEL_{24h,Weighted}$ (dB re 1 µPa²s)	Soprano	dBSea	MONM	
			R_{max} (km)	R_{max} (km)	R_{max} (km)	$R_{95\%}$ (km)
Low-frequency cetaceans	PTS	183	4.45	2.9	1.73	1.4
Mid-frequency cetaceans	PTS	185	0	<0.1	0	0
High-frequency cetaceans	PTS	155	0	<0.1	0	0
Phocid pinnipeds in water	PTS	185	0	0.2	0	0

Table 25. Scenario 1: Maximum ranges to the peak sound pressure level threshold values defined by the NMFS 2018 criteria.

Type of animal	Effect	$L_{p,pk}$ (dB re 1 µPa)	Soprano	dBSea	FWRAM	VSTACK
			R_{max} (km)	R_{max} (km)	R_{max} (km)	R_{max} (km)
Low-frequency cetaceans	PTS	219	0	<0.1	<0.01	<0.01
Mid-frequency cetaceans	PTS	230	0	<0.1	<0.01	0
High-frequency cetaceans	PTS	202	0	<0.1	0.04	0.05
Phocid pinnipeds in water	PTS	218	0	<0.1	<0.01	<0.01

8.1.2. Scenario 2 – VSP in North Sea Deep environment

Table 26. Scenario 2: Maximum ranges to the frequency weighted SEL_{24h} threshold values defined by the NMFS 2018 criteria.

Type of animal	Effect	$SEL_{24h,Weighted}$ (dB re 1 µPa²s)	Soprano	dBSea	MONM	
			R_{max} (km)	R_{max} (km)	R_{max} (km)	$R_{95\%}$ (km)
Low-frequency cetaceans	PTS	183	1.7	1.8	1.18	1.08
Mid-frequency cetaceans	PTS	185	0	<0.1	0	0
High-frequency cetaceans	PTS	155	0	0.2	0.06	0.06
Phocid pinnipeds in water	PTS	185	0	0.2	0.06	0.06

Table 27. Scenario 2: Maximum ranges to the peak sound pressure level threshold values defined by the NMFS 2018 criteria.

Type of animal	Effect	$L_{p,pk}$ (dB re 1 µPa)	Soprano	dBSea	FWRAM	VSTACK
			R_{max} (km)	R_{max} (km)	R_{max} (km)	R_{max} (km)
Low-frequency cetaceans	PTS	219	0	<0.1	0.01	0.01
Mid-frequency cetaceans	PTS	230	0	<0.1	<0.01	0
High-frequency cetaceans	PTS	202	0	0.1	0.05	0.06
Phocid pinnipeds in water	PTS	218	0	<0.1	0.01	0.01

8.1.3. Scenario 3 – Regional survey in Irish Sea environment

Table 28. Scenario 3: Maximum ranges to the frequency weighted SEL_{24h} threshold values defined by the NMFS 2018 criteria.

Type of animal	Effect	$SEL_{24h,Weighted}$ (dB re 1 μPa²s)	Soprano	dBSea	MONM	
			R_{max} (km)	R_{max} (km)	R_{max} (km)	$R_{95\%}$ (km)
Low-frequency cetaceans	PTS	183	1.68	5.5	1.6	1.4
Mid-frequency cetaceans	PTS	185	0	<0.1	0	0
High-frequency cetaceans	PTS	155	0	0.3	0	0
Phocid pinnipeds in water	PTS	185	0	0.6	0	0

Table 29. Scenario 3: Maximum ranges to the peak sound pressure level threshold values defined by the NMFS 2018 criteria.

Type of animal	Effect	$L_{p,pk}$ (dB re 1 μPa)	Soprano	dBSea	FWRAM	VSTACK
			R_{max} (km)	R_{max} (km)	R_{max} (km)	R_{max} (km)
Low-frequency cetaceans	PTS	219	0	<0.1	0.04	0.03
Mid-frequency cetaceans	PTS	230	0	<0.1	<0.01	<0.01
High-frequency cetaceans	PTS	202	0.09	0.2	0.32	0.34
Phocid pinnipeds in water	PTS	218	0	<0.1	0.04	0.03

8.1.4. Scenario 4 – Regional survey in North Sea Shallow environment

Table 30. Scenario 4: Maximum ranges to the frequency weighted SEL_{24h} threshold values defined by the NMFS 2018 criteria.

Type of animal	Effect	$SEL_{24h,Weighted}$ (dB re 1 μPa²s)	Soprano	dBSea	MONM	
			R_{max} (km)	R_{max} (km)	R_{max} (km)	$R_{95\%}$ (km)
Low-frequency cetaceans	PTS	183	5.4	5.3	4.66	4.1
Mid-frequency cetaceans	PTS	185	0	<0.1	0	0
High-frequency cetaceans	PTS	155	0.04	0.5	0	0
Phocid pinnipeds in water	PTS	185	0	1.3	0	0

Table 31. Scenario 4: Maximum ranges to the peak sound pressure level threshold values defined by the NMFS 2018 criteria.

Type of animal	Effect	$L_{p,pk}$ (dB re 1 μPa)	Soprano	dBSea	FWRAM	VSTACK
			R_{max} (km)	R_{max} (km)	R_{max} (km)	R_{max} (km)
Low-frequency cetaceans	PTS	219	0	<0.1	0.04	0.03
Mid-frequency cetaceans	PTS	230	0	<0.1	<0.01	<0.01
High-frequency cetaceans	PTS	202	0.2	0.2	0.54	0.34
Phocid pinnipeds in water	PTS	218	0	<0.1	0.04	0.03

8.1.5. Scenario 5 – Regional survey in North Sea Deep environment

Table 32. Scenario 5: Maximum ranges to the frequency weighted SEL_{24h} threshold values defined by the NMFS 2018 criteria.

Type of animal	Effect	$SEL_{24h,Weighted}$ (dB re 1 µPa²s)	Soprano	dBSea	MONM	
			R_{max} (km)	R_{max} (km)	R_{max} (km)	$R_{95\%}$ (km)
Low-frequency cetaceans	PTS	183	9.93	7.8	4.66	4.2
Mid-frequency cetaceans	PTS	185	0	<0.1	0	0
High-frequency cetaceans	PTS	155	0	0.1	0	0
Phocid pinnipeds in water	PTS	185	0	0.1	0	0

Table 33. Scenario 5: Maximum ranges to the peak sound pressure level threshold values defined by the NMFS 2018 criteria.

Type of animal	Effect	$L_{p,pk}$ (dB re 1 µPa)	Soprano	dBSea	FWRAM	VSTACK
			R_{max} (km)	R_{max} (km)	R_{max} (km)	R_{max} (km)
Low-frequency cetaceans	PTS	219	0	<0.1	0.04	0.03
Mid-frequency cetaceans	PTS	230	0	<0.1	<0.01	<0.01
High-frequency cetaceans	PTS	202	0.09	0.15	0.13	0.14
Phocid pinnipeds in water	PTS	218	0	<0.1	0.04	0.03

8.1.6. Scenario 6 – Regional survey in Faroe Shetland Channel

Note that, as discussed in Section 7.3.4, Soprano is unsuitable for deep-water propagation and so results are not presented for this scenario.

Table 34. Scenario 6: Maximum ranges to the frequency weighted SEL_{24h} threshold values defined by the NMFS 2018 criteria.

Type of animal	Effect	$SEL_{24h,Weighted}$ (dB re 1 μPa²s)	dBSea	MONM	
			R_{max} (km)	R_{max} (km)	$R_{95\%}$ (km)
Low-frequency cetaceans	PTS	183	5.7	0.15	0.12
Mid-frequency cetaceans	PTS	185	<0.1	0	0
High-frequency cetaceans	PTS	155	<0.1	0	0
Phocid pinnipeds in water	PTS	185	<0.1	<0.01	0

Table 35. Scenario 6: Maximum ranges to the peak sound pressure level threshold values defined by the NMFS 2018 criteria.

Type of animal	Effect	$L_{p,pk}$ (dB re 1 μPa)	dBSea	FWRAM	VSTACK
			R_{max} (km)	R_{max} (km)	R_{max} (km)
Low-frequency cetaceans	PTS	219	<0.1	0.04	0.03
Mid-frequency cetaceans	PTS	230	<0.1	<0.01	<0.01
High-frequency cetaceans	PTS	202	0.15	0.13	0.15
Phocid pinnipeds in water	PTS	218	<0.1	0.04	0.03

8.2. NMFS PTS Results Summary

This section provides a summary of the maximum ranges to the NMFS 2018 PTS thresholds across the models. Listed are the minimum and maximum results for the SEL_{24h} metrics (Table 36) and the $L_{p,pk}$ metrics (Table 37).

Table 36. Range of ranges to NMFS SEL_{24h} PTS thresholds for all scenarios.

Scenario	LF Cetacean		MF Cetacean		HF Cetacean		Phocid Pinniped	
	min (km)	max (km)	min (km)	max (km)	min (km)	max (km)	min (km)	max (km)
1	1.73	4.45	0	<0.1	0	<0.1	0	0.2
2	1.18	1.8	0	<0.1	0	0.2	0	0.2
3	1.6	5.5	0	<0.1	0	0.3	0	0.6
4	4.66	5.4	0	<0.1	0	0.5	0	1.3
5	4.66	9.93	0	<0.1	0	0.1	0	0.1
6	0.15	5.7	0	<0.1	0	<0.1	<0.01	<0.1
ALL	0.15	9.93	0	<0.1	0	0.5	0	1.3

Table 37. Range of ranges to NMFS $L_{p,pk}$ PTS thresholds for all scenarios.

Scenario	LF Cetacean		MF Cetacean		HF Cetacean		Phocid Pinniped	
	min (km)	max (km)	min (km)	max (km)	min (km)	max (km)	min (km)	max (km)
1	0	<0.1	0	<0.1	0	<0.1	0	<0.1
2	0	<0.1	0	<0.1	0	0.10	0	<0.1
3	0	<0.1	0	<0.1	0.09	0.34	0	<0.1
4	0	<0.1	0	<0.1	0.2	0.54	0	<0.1
5	0	<0.1	0	<0.1	0.09	0.15	0	<0.1
6	0.03	<0.1	<0.01	<0.1	0.13	0.15	0.03	<0.1
ALL	0	<0.1	0	<0.1	0	0.54	0	<0.1

The maximum range to PTS onset due to SEL_{24h} for LF cetaceans, $L_{p,pk}$ for HF cetaceans, and SEL_{24h} for phocid pinnipeds across models and scenarios are shown graphically in Figures 30 to 32; note the different Y-axis scale used for each hearing group.

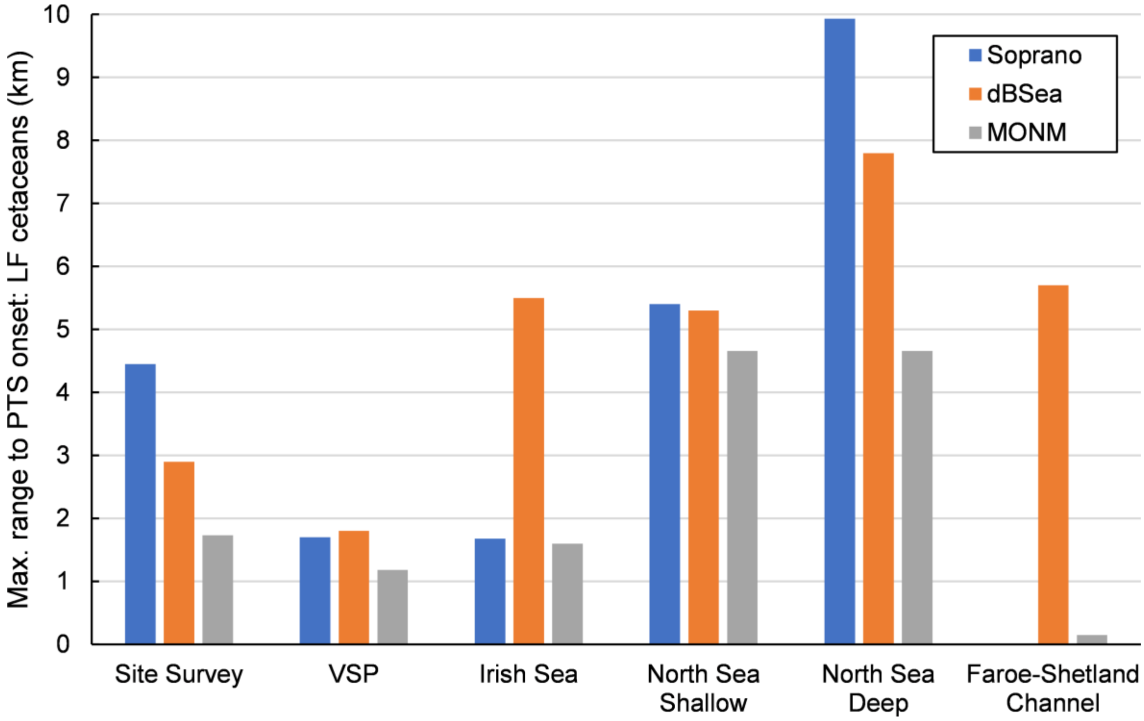

Figure 30. Maximum ranges to PTS onset (SEL_{24h}) for LF cetaceans across all models and scenarios.

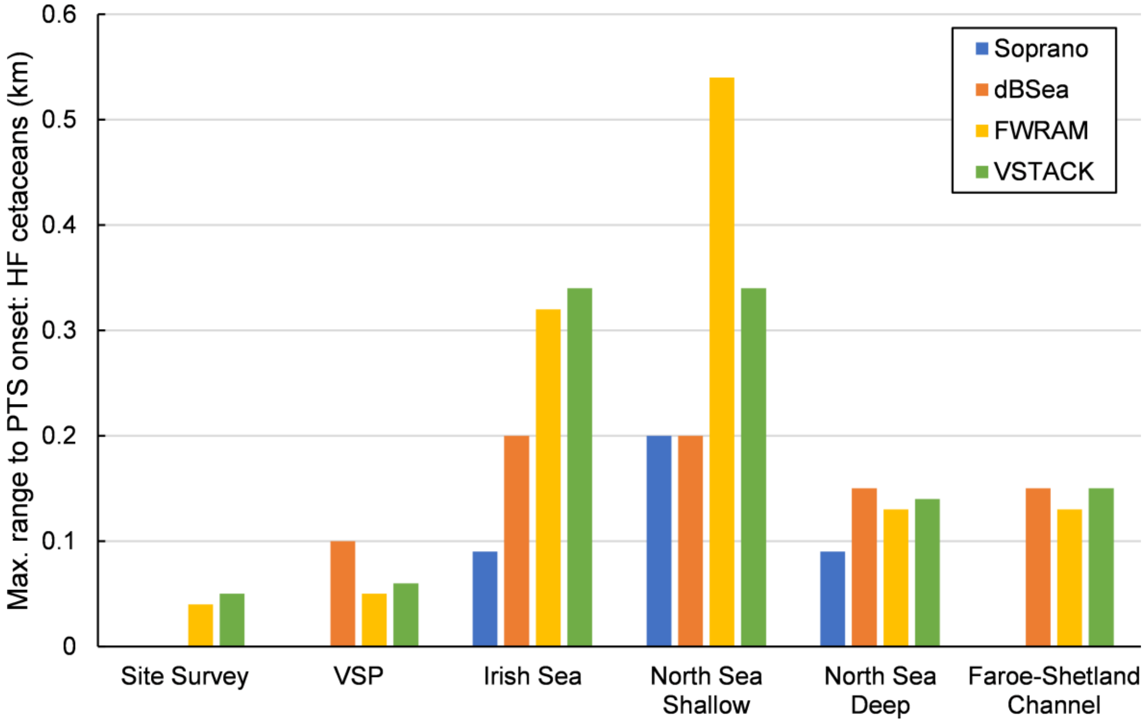

Figure 31. Maximum ranges to PTS onset ($L_{p,\mathrm{pk}}$) for HF cetaceans across all models and scenarios.

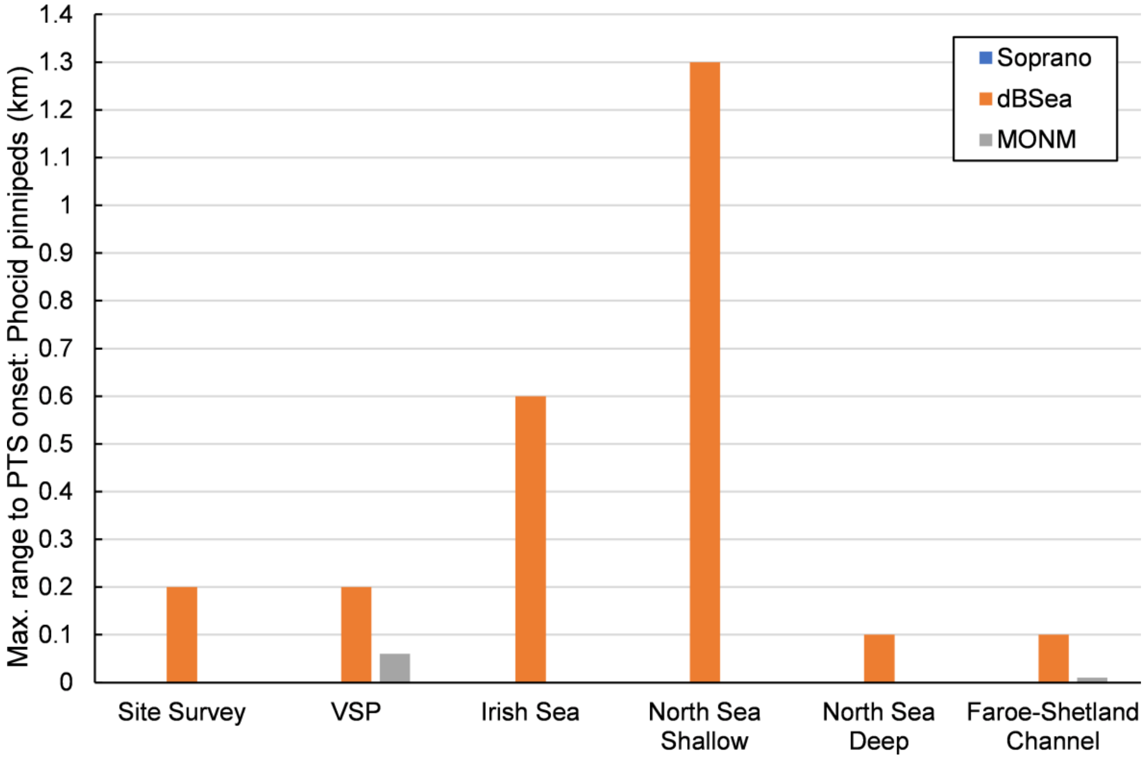

Figure 32. Maximum ranges to PTS onset (SEL_{24h}) for phocid pinnipeds across all models and scenarios.

8.3. Baseline Numerical Results Discussion

This section describes the baseline results summary seen in Tables 36 and 37 for the range of distances modelled to the impact thresholds defined by NMFS for PTS for the selected auditory groups.

8.3.1. Sound exposure level results

Table 36 presents the minimum and maximum ranges generated for Scenarios 1 to 6 for all models to the NMFS PTS threshold for SEL_{cum}. In terms of species, the ranges listed for LF cetaceans far exceed those of the other groups, with ranges typically measured in kilometres rather than hundreds of metres. For phocid pinnipeds and HF cetaceans, the maximum modelled ranges to SEL PTS thresholds were 1.3 km and 500 m respectively. In the case of the MF cetaceans, regardless of environment, the weighted received sound level decayed to less than the PTS threshold within one resolution step; as a resolution step of 100 m for dBSea was the largest, ranges in Tables 36 and 37 are listed as ‘less than 100 m’. Model predictions generally agreed on the order of effect distances with the exception of two cases (phocid pinnipeds, Tables 28 and 30; and LF cetaceans in deep water, Table 34).

Scenarios 1 and 2 represent sound field results from the smaller sources. Results show that in environments that support effective sound propagation, the predicted impact ranges for the Site and VSP surveys are of comparable order of magnitude, i.e., kms (albeit smaller) to those generated by the regional array. The source level of the VSP is greater than that of the site survey array; while the results show that in the case of HF cetacean impact, the VSP generates greater ranges to the PTS impact threshold, the result for LF cetaceans is that the maximum ranges to identified thresholds are greater for the site survey. This is caused by the moving source, the difference in the number of source points, and the sound levels required to reach the cumulative impact threshold; in the case of LF cetacean impact, sound levels are significant in terms of the impact threshold at greater distances from the source than for HF cetaceans. The VSP, being static, reinforces the sound close to the source but is limited in number of source points contributing to the longer-range sound field. The site survey comprised many more source points, but in different locations in time; consequently, points farther from the source received more sound energy, and those locations close to the source only accrued the energy from when the survey passed them. A further difference between the VSP and site survey array is that the VSP is made up of larger volume sources, which tend to produce their acoustic energy at lower frequencies (Figures 4 and 7). While the airgun source model predicted similar spectral levels at high frequencies (~1 kHz; Figures 4 and 7), high frequency content predicted may be subject to source model uncertainties, which is addressed further in Section 10.1.

Scenario 5 shows results for the regional survey in the same environment as for Scenarios 1 and 2. In all cases, the ranges are generally greater due to the larger source array. Despite this, however, the ranges to the HF cetacean PTS impact threshold remain similar to that for the VSP for the same reason as before, i.e., due to the high rate of decay spatially exhibited by the HF-weighted sound fields the stationary source results in greater accumulation of sound energy within the vicinity of the source that is less significant when considering the moving source.

Across the four environments different factors come into play to produce different potential impact ranges. In the case of particularly shallow waters, as one moves from the source there is significant energy lost in repeated bounces and interaction with the sediment; close to the source, however, there is greater sound energy due to these early local reflections and the sound level is raised. As one moves into greater water depths, the level of interaction with the seabed is reduced and thus sound may typically travel further in a medium supportive of greater propagation; close to the source in this environment, however, and the energy from nearby reflections is reduced.

Such a phenomenon is seen in the results between Scenarios 4, 5 and 6. In the case of LF cetacean impact ranges, for Scenario 4, significant energy is lost into the sediment due to the water being relatively shallow. There is, however, enough sound energy that remains in the water column from boundary reflections bringing the maximum range up to between 4.66 km and 5.4 km. In Scenario 5, the water depth is deep enough such that a significant proportion of the energy remains in the water column rather than be absorbed into the seabed, but shallow enough such that early reflections can contribute to the sound field within a few kilometres from the source thus producing typically greater ranges of between 4.66 km and 9.93 km. Things change again for the deeper-water scenario in the Faroe Shetland Channel; here we see a large difference between the results for dBSea and MONM. The MONM results are influenced by the early reflections from the seabed being too low in level to appreciably augment the levels from the direct sound and the sound channel not being strong enough to make a large difference over short ranges; consequently, it reports lower ranges to PTS onset levels. The results from dBSea, however, see a stronger refractive effect keeping energy in the sound channel with little attenuation and so produces greater ranges.

This effect is also strongly dependent on the geoacoustic characteristics of the seabed material, which are increasingly important for shallower water depths. The environments for Scenarios 3 and 4 are similar except for the different sediment types: the modelled Irish Sea seabed sediment is mud, while that for the North Sea is sand. Due to the greater difference in sound speed between the water and sediment, the sand is typically a better reflector of sound while the mud tends to absorb it better; because of this, impact ranges are greater for Scenario 4.

Another factor to consider is the frequency content of the source and how the energy at each frequency propagates. In this regard, it is important to note the presence of the pressure-release boundary of the water-air interface common to all underwater acoustic propagation models. For an ideal pressure-release boundary the sound pressure on the interface remains zero. The frequency at which a quarter wavelength is 10 m (assuming water sound speed of ≅1500 m/s) is 37.5 Hz; for a receiver at 10 m water depth, sound energy at lower frequencies than this are influenced by the pressure-release boundary that serve to reduce sound levels. Consequently, we would anticipate some significant sensitivity close to the surface in the receiver depth to be investigated in later sections. More generally, at low frequencies, the propagation of sound is mostly influenced by the water depth and the sediment, whereas at higher frequencies the sound speed profile and the surface roughness become more important.

8.3.2. Peak sound pressure results

Table 37 presents results of maximum ranges to the $L_{p,\text{pk}}$ thresholds for the identified animal groups. The comparison is made simpler in this case due to the absence of any frequency weighting component to account for species hearing sensitivity. Due to having the lowest injury threshold of all hearing groups, the ranges to the HF cetaceans impact thresholds are always the greatest. The metric is determined by the single greatest sound pressure level. Predicted PTS effect distances for LF, MF and PP groups were negligible and were up to 0.54 km for HF cetaceans (Table 36). Effect distances based on peak sound pressure risk criteria led to lower, and in some cases similar, PTS effect distances than those using the SEL_{24h} metric (Tables 36 and 37).

There is agreement across the models that the North Sea Shallow environment provides the greatest ranges in terms of $L_{p,\mathrm{pk}}$. In this environment, as discussed before, the sand serves as a more effective reflector of sound than the mud of the Irish Sea. Additionally, due to the shallow depths, the earliest reflections arrive in time to contribute to the initial pulse received at 10 m depth. Once one moves past a critical water depth, the early reflections no longer contribute to the peak level and thus ranges are reduced. As the water depth is increased further, however, no further reduction in range is seen.

The influence of the environment, however, generally has less effect on the peak sound pressure level than the sound exposure level; this is particularly the case for deeper waters. This is a consequence of risk thresholds being reached at typically small distances for peak sound pressure, and peak sound pressure dropping off faster with distance than cumulative SEL_{24h}.

8.3.3. Model differences

Tables 36 and 37 show the results across the different models employed, and indicates that the choice of model, or assumptions going into the model, affects the ranges to impact thresholds. MONM-BELLHOP and dBSea operate using very similar propagation models in that propagation loss for lower frequencies are calculated using a parabolic equation model, and at higher frequencies a beam- or ray-tracing model is used. They do, however, differ in the treatment of the source: MONM allows for variation of source levels in the horizontal plane, whereas dBSea operates assuming omnidirectional sources and a single value is used for all horizontal angles. The ray-tracing portion of dBSea, however, takes into account the vertical directivity of the source, whereas this is considered constant in MONM. Closer to the source, where there is a rapid change in propagation loss, changes in how the source is considered can lead to significant changes in the resulting impact ranges. The difference in Scenario 5 for LF-cetaceans is probably in part due to this difference; MONM does not have increased levels directed downwards that may contribute to sound levels closer to the source, whilst dBSea has no horizontal directivity, and therefore any reduced levels in bearings away from the principal lobes. Additionally, dBSea models the sediment as a viscous fluid, and does not support shear waves; MONM incorporates shear wave information as an additional energy loss mechanism for sound incident on the seabed. This may lead to differences in impact ranges particularly in the shallower scenarios due to increased interaction with the seafloor.

Soprano, the model used by TNO and implemented in Aquarius, provides an alternative approach to the modelling. It is more akin to a normal mode model where only the principal modes are calculated; additional contributing modes are then approximated using an integral over a continuum. This allows it to perform propagation loss calculations more rapidly than a complete normal mode solution. The model, however, assumes an isovelocity water column, hence its applicability only in shallower waters; this may contribute to the results between models digressing for the deep North-sea environment (see first row of Table 39) than for the shallow North-sea environment (see first row of Table 32). The model’s tendency towards a conservative estimate results in it predicting a slightly greater range than the other modelling approaches in the deep environment.

9. Use of Empirical Spreading Formulae

In environmental impact assessments, it is common to make simplifying assumptions using empirical "$X \log R$" spreading formulas in conjunction with a source level derived from commercial source modelling packages. It is a concern for regulators that such approaches may lead to erroneous estimation of the effect distances. Several common assumptions using empirical approaches are considered here, which provide insight into how these compare to more complex modelling (Sections 7 and 8). Although approaches reported in EIAs may differ by contractor, they tend to share the following assumptions:

For the source level, the downward radiated sound field (as predicted using industry-standard airgun far field signature modelling packages, which typically includes a contribution from the surface-reflected "ghost") is often used in conjunction with an "$X \log R$" function to estimate the trend with range. These packages were originally developed to serve as input for seismic data processing, in which the downward radiated far field signature is the signal of interest but are currently also being applied in environmental impact assessments. Common assumptions for X range from 20 (spherical spreading), to 15 dB (fall-off in a mode-stripping environment), or somewhere in between (i.e., based on trend-fits). When predicting peak sound pressure, often the peak of the surface downward radiated surface-affected waveform (output from conventional airgun processing tools) is considered. When estimating the SEL, often the SEL of that waveform is used as a proxy for the energy source level.

To quantify the variability in estimates that simplified empirical modelling methods have for various source and propagation sound level assumptions and to allow for a direct comparison to the numerical modelling results, we follow a generic analytical approach based on the following assumptions:

$L_{p,\mathrm{pk}}$: To predict peak sound pressure level, both vertical and horizontal (broadside) source waveforms were used. This was done for all 3 arrays (site survey, VSP, and area survey). Here, we take the peak sound pressure of the surface-affected source waveform as typically generated by commercial source models (Table 7) and then subtract a nominal value for the horizontal propagation. For the horizontal propagation three nominal trends with range were assumed of X being 20, 18, and 15. Additionally, three corrections for the off-axis reduction in source level, which are sometimes applied, were considered here: 0, -12 and -20 dB relative to the downward radiated source waveform.

SEL: To predict the SEL_{24h} we took the generated decidecade band levels for the downward radiated beams from the initial airgun array modelling source signature (Appendix F); these source levels were used as a starting point for the empirical extrapolation. For the horizontal propagation three nominal dependencies on range were assumed, again with values of X of 20, 18, and 15. The SEL_{24h} were computed for the area survey only to provide the maximum effect distances. Two corrections for the off-axis reduction in source level were considered: 0, and -12 dB relative to the downward radiated source waveform. Absorption was also accounted for by applying a frequency dependent absorption term (Thorp's equation) in each decidecade band. SEL_{24h} was predicted on a 30 km × 30 km grid with 20 m resolution. In some instances, the application of this empirical extrapolation procedure leads to SEL_{24h} values above threshold values at distances much greater than the 30 km × 30 km grid; in such cases, the effect distance was estimated by adding the contributions from all source points assuming the source was at a single location (i.e., neglecting the offset from the separate lines, which is a reasonable approximation for large distances).

The results of ranges to thresholds are in the tables as follows:

Scenario and metric	NMFS Criteria
Scenario 1: $L_{p,pk}$	Table 38
Scenario 2: $L_{p,\mathrm{pk}}$	Table 39
Scenario 3–6: $L_{p,\mathrm{pk}}$	Table 40
Scenario 1: SEL_{24h}	Table 41
Scenario 2: SEL_{24h}	Table 42
Scenario 3–6: SEL_{24h}	Table 43

Additional results, including the ranges to TTS thresholds from NMFS (2018) and Southall (2007) can be found in Appendix K.

9.1. Empirical Model Results – $L_{p,\mathrm{pk}}$

9.1.1. Scenario 1 – Site survey

Table 38. Scenario 1: Maximum ranges at 10 m depth to the peak sound pressure level PTS threshold value defined by the NMFS 2018 criteria using "$X \log R$". Empirical approach with X = (20, 18, and 15) and different nominal source level reductions relative to the vertical beam.

Type of animal	$20 \log R$			$18 \log R$			$15 \log R$		
	vert. beam (0 dB)	horiz. beam (-12 dB)	horiz. beam (-20 dB)	vert. beam (0 dB)	horiz. beam (-12 dB)	horiz. beam (-20 dB)	vert. beam (0 dB)	horiz. beam (-12 dB)	horiz. beam (-20 dB)
	R_{max} (km)	R_{max} (km)	R_{max} (km)	R_{max} (km)	R_{max} (km)	R_{max} (km)	R_{max} (km)	R_{max} (km)	R_{max} (km)
Low-frequency cetaceans	0.01	0.00	0.00	0.01	0.00	0.00	0.02	0.00	0.00
Mid-frequency cetaceans	0.00	0.00	0.00	0.00	0.00	0.00	0.00	0.00	0.00
High-frequency cetaceans	0.07	0.02	0.00	0.11	0.02	0.00	0.27	0.04	0.01
Phocid pinnipeds in water	0.01	0.00	0.00	0.01	0.00	0.00	0.02	0.00	0.00

9.1.2. Scenario 2 – VSP

Table 39. Scenario 2: Maximum ranges at 10 m depth to the peak sound pressure level PTS threshold value defined by the NMFS 2018 criteria using "$X \log R$". Empirical approach, with X = (20, 18, and 15) and different nominal source level reductions relative to the vertical beam.

Type of animal	$20 \log R$			$18 \log R$			$15 \log R$		
	vert. beam (0 dB)	horiz. beam (-12 dB)	horiz. beam (-20 dB)	vert. beam (0 dB)	horiz. beam (-12 dB)	horiz. beam (-20 dB)	vert. beam (0 dB)	horiz. beam (-12 dB)	horiz. beam (-20 dB)
	R_{max} (km)	R_{max} (km)	R_{max} (km)	R_{max} (km)	R_{max} (km)	R_{max} (km)	R_{max} (km)	R_{max} (km)	R_{max} (km)
Low-frequency cetaceans	0.01	0.00	0.00	0.01	0.00	0.00	0.02	0.00	0.00
Mid-frequency cetaceans	0.00	0.00	0.00	0.00	0.00	0.00	0.00	0.00	0.00
High-frequency cetaceans	0.08	0.02	0.01	0.12	0.03	0.01	0.32	0.05	0.02
Phocid pinnipeds in water	0.01	0.00	0.00	0.02	0.00	0.00	0.03	0.00	0.00

9.1.3. Scenarios 3 to 6 – Regional survey

Table 40. Scenario 3-6: Maximum ranges to the peak sound pressure level PTS threshold value defined by the NMFS 2018 criteria using “$X \log R$”. Empirical approach, with X = (20, 18, and 15) and different nominal source level reductions relative to the vertical beam.

Type of animal	20 log R			18 log R			15 log R		
	vert. beam (0 dB)	horiz. beam (-12 dB)	horiz. beam (-20 dB)	vert. beam (0 dB)	horiz. beam (-12 dB)	horiz. beam (-20 dB)	vert. beam (0 dB)	horiz. beam (-12 dB)	horiz. beam (-20 dB)
	R_{max} (km)	R_{max} (km)	R_{max} (km)	R_{max} (km)	R_{max} (km)	R_{max} (km)	R_{max} (km)	R_{max} (km)	R_{max} (km)
Low-frequency cetaceans	0.09	0.02	0.01	0.15	0.03	0.01	0.42	0.07	0.02
Mid-frequency cetaceans	0.03	0.01	0.00	0.04	0.01	0.00	0.08	0.01	0.00
High-frequency cetaceans	0.65	0.16	0.07	1.35	0.29	0.10	5.68	0.90	0.26
Phocid pinnipeds in water	0.10	0.03	0.01	0.17	0.04	0.02	0.49	0.08	0.02

9.2. Empirical Model Results - SEL_{24h}

9.2.1. Scenario 1 – Site survey

Table 41. Scenario 1: Maximum ranges at 10 m depth to the frequency-weighted SEL_{24h} PTS threshold value defined by NMFS (2018) using “$X \log R$”. All sound exposure levels are frequency-weighted. Model predictions are based on accumulation over all shots points, using empirical approach for propagation loss, with X = (20, 18, and 15) and nominal vertical beam corrections of 0 dB (downward) and -12 dB (horizontal).

Type of animal	Effect	$SEL_{24h,Weighted}$	20 log R		18 log R		15 log R	
		(dB re 1 µPa²s)	*0 dB*	*-12 dB*	*0 dB*	*-12 dB*	*0 dB*	*-12 dB*
			R_{max} (km)	R_{max} (km)	R_{max} (km)	R_{max} (km)	R_{max} (km)	R_{max} (km)
Low-frequency cetaceans	PTS	183	0.79	0.04	3.0	0.09	10.0	2.3
Mid-frequency cetaceans	PTS	185	0.04	0.04	0.04	0.04	0.04	0.04
High-frequency cetaceans	PTS	155	0.06	0.04	0.54	0.04	5.8	0.124
Phocid pinnipeds in water	PTS	185	0.04	0.04	0.04	0.04	0.80	0.04

9.2.2. Scenario 2 – VSP

Table 42. Scenario 2: Maximum ranges at 10 m depth to the frequency-weighted SEL_{24h} PTS threshold value defined by NMFS (2018) using "$X \log R$". All sound exposure levels are frequency-weighted. Model predictions are based on accumulation over all shots points, using empirical approach for propagation loss, with X = (20, 18, and 15) and nominal vertical beam corrections of 0 dB (downward) and -12 dB (horizontal).

Type of animal	Effect	$SEL_{24h,Weighted}$ (dB re 1 µPa²s)	$20 \log R$		$18 \log R$		$15 \log R$	
			0 dB	*-12 dB*	*0 dB*	*-12 dB*	*0 dB*	*-12 dB*
			R_{max} (km)	R_{max} (km)	R_{max} (km)	R_{max} (km)	R_{max} (km)	R_{max} (km)
Low-frequency cetaceans	PTS	183	0.63	0.16	1.3	0.3	5.3	0.85
Mid-frequency cetaceans	PTS	185	0.0	0.0	0.0	0.0	0.0	0.0
High-frequency cetaceans	PTS	155	0.14	0.04	0.23	0.05	0.70	0.11
Phocid pinnipeds in water	PTS	185	0.08	0.0	0.12	0.03	0.32	0.05

9.2.3. Scenarios 3 to 6 – Regional survey

Table 43. Scenario 3-6: Maximum ranges at 10 m depth to the frequency-weighted SEL_{24h} PTS threshold value defined by NMFS (2018) using "$X \log R$". All sound exposure levels are frequency-weighted. Model predictions are based on accumulation over all shots points, using empirical approach for propagation loss, with X = (20, 18, and 15) and nominal vertical beam corrections of 0 dB (downward) and -12 dB (horizontal).

Type of animal	Effect	$SEL_{24h,Weighted}$ (dB re 1 µPa²s)	$20 \log R$		$18 \log R$		$15 \log R$	
			0 dB	*-12 dB*	*0 dB*	*-12 dB*	*0 dB*	*-12 dB*
			R_{max} (km)	R_{max} (km)	R_{max} (km)	R_{max} (km)	R_{max} (km)	R_{max} (km)
Low-frequency cetaceans	PTS	183	10.0	1.19	26.2	5.3	178	31.6
Mid-frequency cetaceans	PTS	185	0.01	0.0	0.01	0.0	0.01	0.0
High-frequency cetaceans	PTS	155	2.6	0.12	8.9	0.60	23	9.5
Phocid pinnipeds in water	PTS	185	0.29	0.02	2.2	0.04	15.4	1.4

9.3. Empirical Modelling Results Discussion

In this section, model approaches that simplify the sound propagation using empirical "$X \log R$" spreading formulas in conjunction with a source level derived from commercial source modelling package, were considered. The minimum and maximum effect distances predicted by these approaches for Scenarios 1-6 are summarized in Table 44. Modelled effect distances vary strongly with assumed relation. For example, the LF cetaceans minimum and maximum effect distances ranged between 1.9 km to 178 km for the SEL_{24h} based criterion. Effect distances for MF cetacean groups were predicted to be small, regardless of the adopted spreading formula.

Comparing this variability in predictions to that obtained from the more complex modelling from Section 8 (Tables 36 and 37), it can be seen that empirical transmission loss approaches have the potential to severely underpredict or overpredict the effect distances, even when other modelling assumptions (e.g. stationary animals) are the same.

Several causes can be identified for the mismatch of these empirical approaches with the complex modelling.

Although "$X \log R$" approaches can be useful to characterize transmission loss (i.e. extrapolating between measurements of the same quantity at two different distances) they are not suitable to be used as *propagation loss* in conjunction with a source level term in most cases (when $X \neq 20$). In Ainslie et al. (2014), it has been shown that the appropriate way to model this analytically is to adopt $A + B \log R$, with the terms A and B chosen according to the source type, the environment, and the distance to the source. Ignoring the A term can lead to biases in the predicted levels, which depend on the bottom depth and range. A second issue is that in general, these terms also change with distance, as the sound propagation transits between different regimes (spherical spreading, cylindrical spreading, mode-stripping, single mode propagation), depending on the frequency and water depth considered. In other words, both A and B are themselves functions of range R. Hence, a single choice for X often fails to cover a wide range of species and environments.

A second cause for the mismatch is that the appropriate source term needs to be used in conjunction with the empirical propagation loss factor. The commonly used method to convert the surface-affected waveform (vertical source waveform including ghost), reflects a dipole source, rather than a monopole source for low frequencies. For dipole sources, different choices for X are applicable (Ainslie et al. 2014).

Finally, much of the acoustic energy contained in the airgun signal is at wavelength large compared to the water depth. This energy does not propagate effectively, thus reducing the effect distance. Although occasionally a combination of inappropriate or incorrect assumptions may cancel out and lead to similar predicted effect distances, this comparison demonstrates that an oversimplified approach typically leads to inaccurate estimates of effect distances.

Analytical approaches (as discussed in Ainslie et al. 2014) can be useful for fast estimates, as long as distance, frequency-specific choices in the A and B terms are considered, and the source term is appropriately used. Their greatest value is in providing insights into the sensitivity of propagation loss to environmental parameters (e.g., water depth, bottom reflection loss). These insights facilitate assessment of the applicability of results from one specific scenario to other similar scenarios with small differences in, say, water depth or seabed parameters.

Table 44. Range of minimum and maximum effect ranges to NMFS SEL_{24h} PTS thresholds for all scenarios predicted using simplified "$X \log R$" rules.

Scenario	Metric	LF Cetacean		MF Cetacean		HF Cetacean		Phocid Pinniped	
		min (km)	max (km)	min (km)	max (km)	min (km)	max (km)	min (km)	max (km)
1 (Site)	$L_{p,\mathrm{pk}}$	0.00	0.01	0.00	0.00	0.00	0.27	0.00	0.02
2 (VSP)	$L_{p,\mathrm{pk}}$	0.00	0.02	0.00	0.00	0.01	0.32	0.00	0.03
3–6 (Regional)	$L_{p,\mathrm{pk}}$	0.01	0.42	0.00	0.08	0.07	5.68	0.01	0.49
1 (Site)	SEL_{24h}	0.04	10.0	0.04	0.04	0.04	5.8	0.04	0.80
2 (VSP)	SEL_{24h}	0.16	5.3	0.00	0.00	0.04	0.70	0.00	0.32
3–6 (Regional)	SEL_{24h}	1.9	178	0.00	0.01	0.12	23	0.02	15.4

10. Numerical Modelling Variants

To investigate the effect of variability in the modelling results, further studies were devised that each focus on a particular aspect of the modelling. These were:

- the high-frequency energy in the source;
- seasonal variation in the sound speed profile;
- choice of target depth;
- surface loss due to waves;
- differences in the geoacoustic properties of the environment.

In addition to these, studies were performed using moving receivers using both prescribed motion and movement dictated by behavioural models.

10.1. Inter-model Source Energy Difference

Multiple air gun array models exist for the prediction of the source levels. A collection of these were compared for a meeting in order to determine the range of outputs these models provide (Ainslie et al. 2016). The workshop included contributions from AASM, Gundalf, Cagam, and Agora for a specified 3333 in³ array and provides a single example of variations in output spectra between different source function models.

One principal find was that, although at low frequencies there was good agreement between the models, above 1 kHz the inter-model differences exceeded 30 dB. The comparison of spectra is shown in Figure 33; the modelling in this project has been performed using AASM. The variation in energy at higher frequencies (i.e., above 1 kHz) affects the impact ranges for mid- and high-frequency cetaceans where they are most sensitive.

To allow for the difference in high-frequency energy between the two source models, the results from Figure 33 were used to generate a difference curve that was used directly with the results from AASM to serve as a proxy for Gundalf results. Assuming the high frequency differences are also present in the spectra of individual airguns, it is anticipated that the spectrum differences generated between AASM and Gundalf are likely to be similar regardless of the size of array (as the decibel difference value represents a ratio of sound energies).

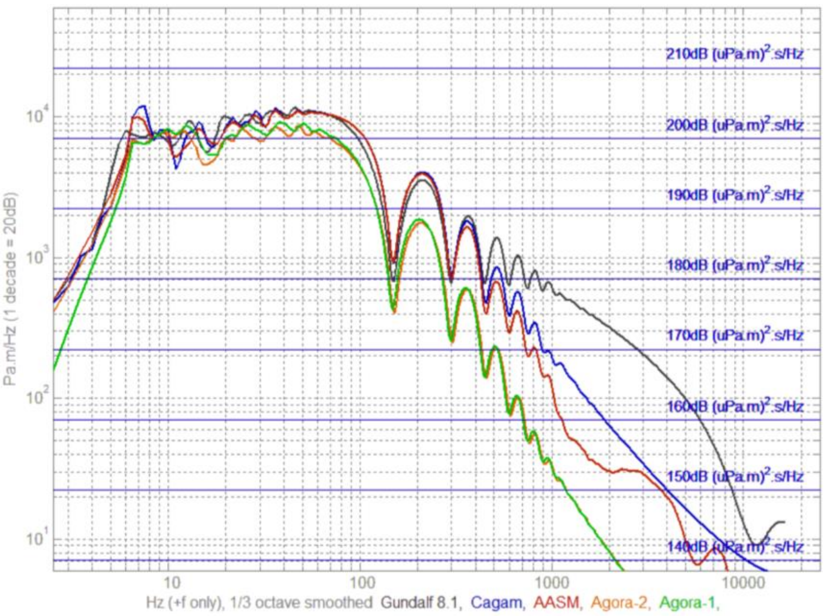

Figure 33. Comparison of spectra from multiple airgun array models. Reproduced from Ainslie et al.(2016).

The difference in energy source level at the centre frequency of each decidecade band is shown in Figure 34 and tabulated in Table 45; below 500 Hz, the differences between the two spectra are negligible for this exercise and so levels at these frequencies are left unaltered. Figures L-1 to L-7 in Appendix L show the maximum high-frequency cetacean weighted horizontal source level over all azimuths in decidecade bands for the seven steps involved in the ramp up of the 4130 in³ airgun array.

Figures L-8 to L-10 show the maximum horizontal source level over all azimuths in decidecade bands for no weighting, low-frequency cetacean weighting, and mid-frequency cetacean weighting respectively. The figures suggest that the effect of increased high frequency energy in the source affect the calculated ranges to mid- and high-frequency cetacean thresholds more than the low-frequency cetacean threshold ranges. The decidecade bands centred on 5 and 6.3 kHz are likely to have the greatest effect on high- and mid-frequency cetaceans before propagation losses are taken into account. As the propagation loss for these frequencies is higher than for lower frequencies, there is likely to be a shift in principal energy frequency band towards lower frequencies at greater ranges.

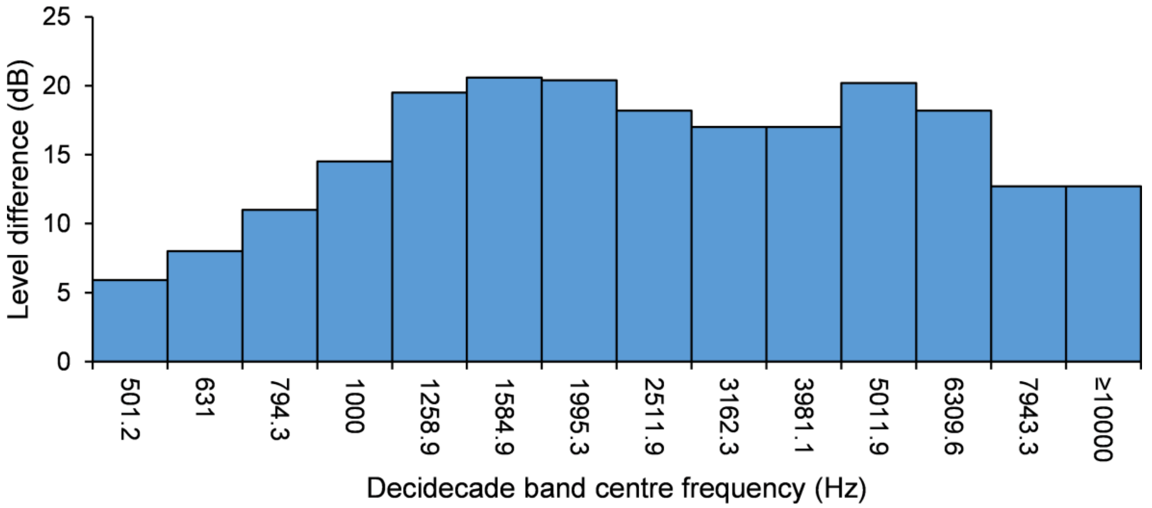

Figure 34. Difference between surface affected source levels from AASM and Gundalf 8.1.

Table 45. Difference between surface affected source levels from AASM and Gundalf 8.1 for decidecade bands 500 Hz and above.

Decidecade band centre frequency (Hz)	Difference in source level (dB)	Decidecade band centre frequency (Hz)	Difference in source level (dB)
501.2	5.9	2511.9	18.2
631.0	8.0	3162.3	17.0
794.3	11.0	3981.1	17.0
1000.0	14.5	5011.9	20.2
1258.9	19.5	6309.6	18.2
1584.9	20.6	7943.3	12.7
1995.3	20.4	≥10000	12.7

To investigate the effects the increased high-frequency energy would have, the new source was implemented in a re-run of Scenario 4: North Sea Shallow; in the baseline studies, this scenario had the greatest ranges associated with SEL over 24 hours for mid- and high-frequency cetaceans. All environmental parameters were kept the same as for the baseline study. The predicted ranges to PTS onset for mid- and high-frequency cetaceans for both original and high-frequency shifted source are shown in Table 46 and Figure 35; graphical results of the sound fields are shown in Appendix M

Table 46. Scenario 4: Maximum ranges to the frequency-weighted SEL_{24h} threshold values defined by the NMFS 2018 criteria.

Auditory Group	**$SEL_{24h,Weighted}$** (dB re 1 µPa²s)	**AASM source**				**AASM source + HF Shift**			
		Soprano	dBSea	MONM		Soprano	dBSea	MONM	
		R_{max} (km)	R_{max} (km)	R_{max} (km)	$R_{95\%}$ (km)	R_{max} (km)	R_{max} (km)	R_{max} (km)	$R_{95\%}$ (km)
Mid-frequency cetaceans	185	0	<0.1	0	0	0	<0.1	0	0
High-frequency cetaceans	155	0.04	0.5	0	0	5.5	3.3	5.98	4.65

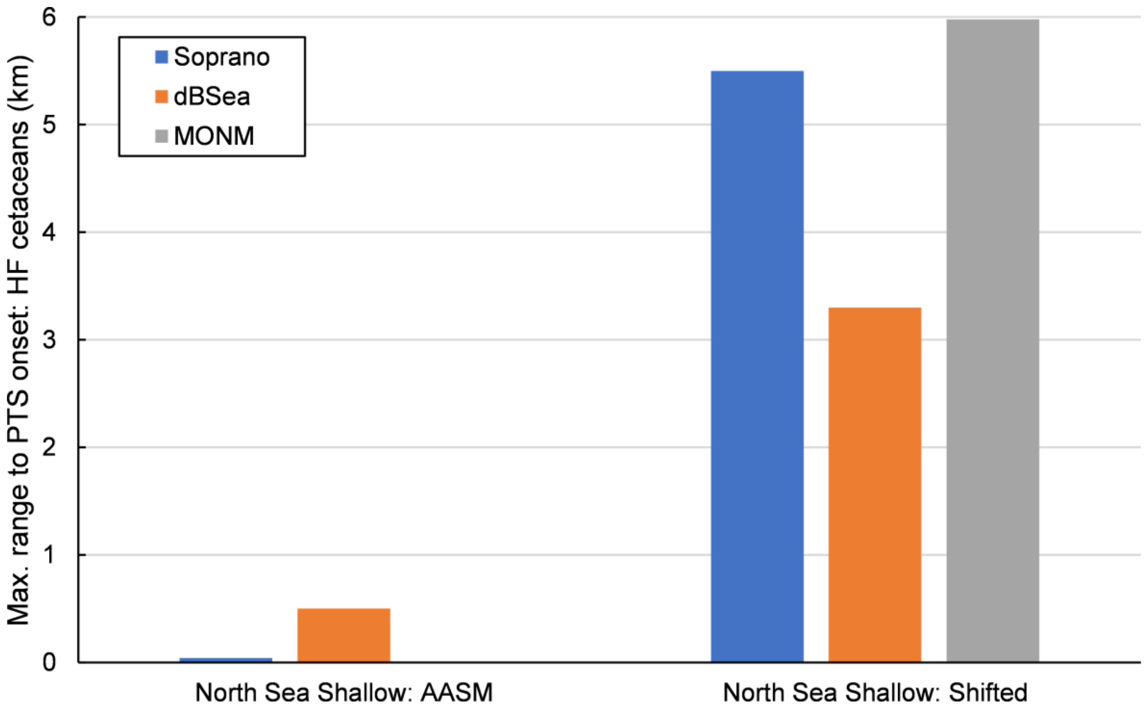

Figure 35. Maximum ranges to SEL_{24h} PTS onset thresholds for HF cetaceans for the original sound source function and the source including the inter-model high-frequency energy difference.

The difference between the two sources has a large impact on the results with ranges to PTS onset increasing significantly for high-frequency cetaceans from 0 to 500 m with the original source to 3.3 to 6 km with the alternate source. For mid-frequency cetaceans, however, the threshold for PTS onset is not exceeded beyond the first modelled resolution step even with the alternate source.

For all models, runs were performed neglecting sea surface roughness; consequently, these results are not indicative of real-world values and are considered conservative as high-frequency sound propagates less well the higher the wind speed and therefore higher sea surface roughness. For seismic survey modelling, however, it is not uncommon to ignore these effects for a source considered to be ‘low-frequency’ such as an airgun. As all results in this section, ranges are generated assuming static receivers throughout the 24-hour survey operation.

10.2. Seasonal Variation in the Sound Speed Profile

The original baseline modelling was generated using sound speed profiles representative of one month only (December for Irish Sea and Faroe Shetland Channel, January for North Sea Shallow and

North Sea Deep) chosen based on a quick preliminary study which identified these as the months with conditions that generated the greatest propagation (Appendix B).

In the shallow water scenarios, it is unlikely that the sound speed profile has any significant effect on the sound propagation. For the deeper cases, however, where sound channels and half channels can be supported, the sound speed profile has more influence on propagation. Typical summer profiles were selected for Scenarios 5 and 6; these are shown in Figure 36 and tabulated in Appendix N.

The North Sea Deep sound speed profile (left pane of Figure 36) changes from a slightly upwardly-refracting profile to one that is downwardly-refracting over the entire water column; an upwardly-refracting profile at the top of the water column allows for a surface duct to exist that can trap energy and result in efficient propagation within it; the downward refraction, in this case, directs the sound energy into the seabed resulting in more reflection losses, and reduced propagation, over greater distances. The sound speed profile for the Faroe Shetland Channel environment (centre and right panes of Figure 36) shows that changes here are most significant in the shallowest 300 m where the upwardly-refracting becomes downwardly-refracting; as evident in the range of sound speeds, however, this change is more slight than for the North Sea Deep environment.

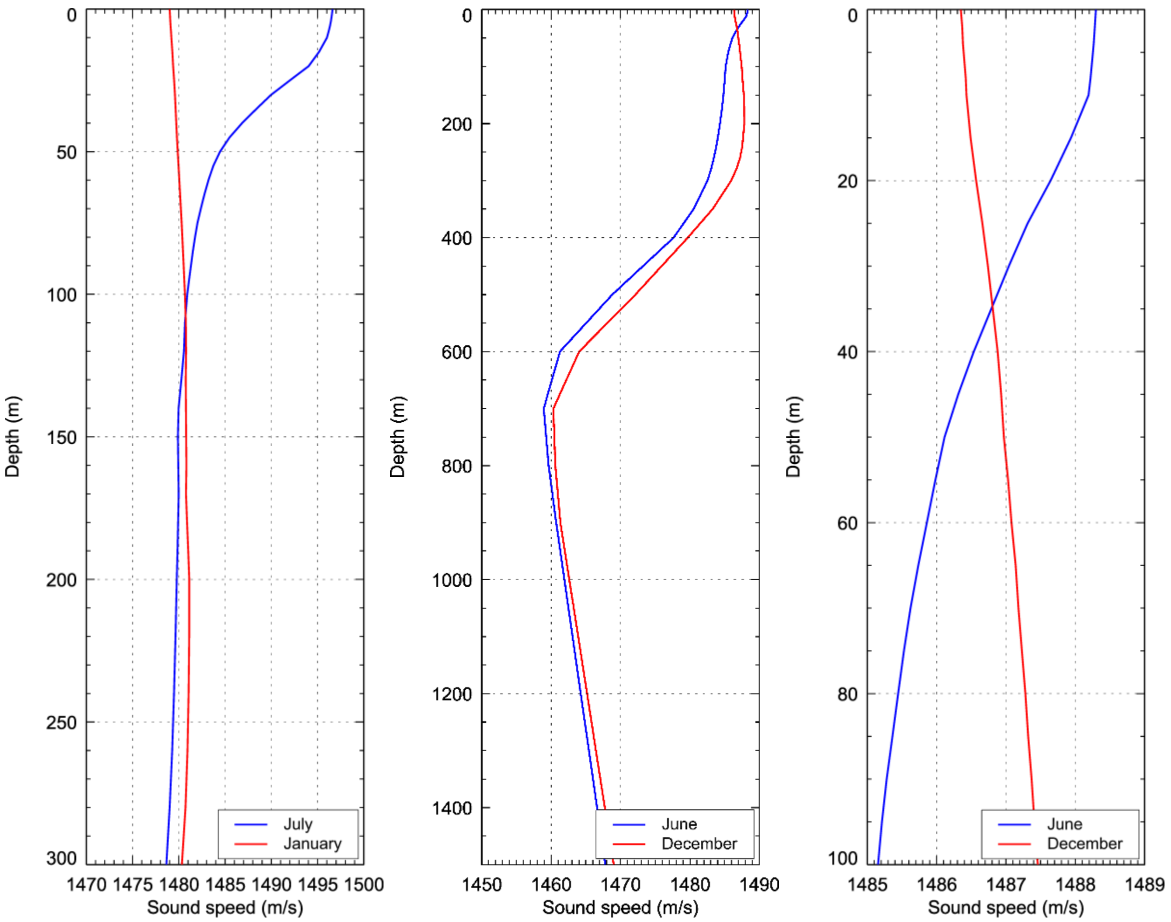

Figure 36. Sound speed profiles for North Sea Shallow (left) and Faroe Shetland Channel (centre, right) showing the winter (baseline) and summer profiles.

As the change only affects deep water modelling, results were generated only for MONM and dBSea. The predicted ranges to PTS onset for the summer SSP for low-frequency cetaceans for Scenarios 5 and 6 are shown in Tables 47 and 48 respectively and in Figure 37. Ranges to TTS thresholds are also included in the tables to illustrate the influence the SSP has at greater distances from the source. The associated sound field maps are shown in Appendix O.

Table 47. Scenario 5: North Sea Deep environment: Maximum ranges to the frequency-weighted SEL_{24h} threshold values defined by the NMFS 2018 criteria for low-frequency cetaceans for winter and summer environments.

Type of animal	Effect	$SEL_{24h,Weighted}$ (dB re 1 µPa²s)	Winter SSP			Summer SSP		
			dBSea	MONM		dBSea	MONM	
			R_{max} (km)	R_{max} (km)	$R_{95\%}$ (km)	R_{max} (km)	R_{max} (km)	$R_{95\%}$ (km)
Low-frequency cetaceans	PTS	183	7.8	4.66	4.2	7.9	4.65	4.18
	TTS	168	30.4	56.1	42.75	28.4	27.0	22.7

Table 48. Scenario 6: Faroe-Shetland Channel environment: Maximum ranges to the frequency-weighted SEL_{24h} threshold values defined by the NMFS 2018 criteria for low-frequency cetaceans for winter and summer environments

Type of animal	Effect	$SEL_{24h,Weighted}$ (dB re 1 µPa²s)	Winter SSP			Summer SSP		
			dBSea	MONM		dBSea	MONM	
			R_{max} (km)	R_{max} (km)	$R_{95\%}$ (km)	R_{max} (km)	R_{max} (km)	$R_{95\%}$ (km)
Low-frequency cetaceans	PTS	183	5.7	0.15	0.12	7.6	0.15	0.12
	TTS	168	63.7	77.8	67.6	48.3	77.9	66.4

Table 47 shows the difference in modelled distances at which sound levels decrease to below PTS and TTS threshold values between summer and winter sound speed profiles for the North Sea Deep environment. The water depths seen round the survey site are typically between 100 and 120 m. In terms of the PTS ranges, there is little change for either model between the two seasons; although the energy is being refracted down towards the seabed, the relatively high reflectivity of the seabed reflects much of the energy back into the water column. At greater ranges, for the distance to the TTS threshold, the compound effects of increased bottom bounces takes more energy from the water column and thus ranges to TTS onset levels reduce for this environment; this reduction is significantly more pronounced for MONM than for dBSea.

In Table 48, the equivalent result for the North Sea Deep environment, we see different phenomena. The maximum predicted range to the LF-cetacean PTS impact threshold value for dBSea has increased. This is potentially due to the refraction of energy in the water column and by having a receiver specifically at 10 m depth. The results for MONM show no change; this is caused by the very low initial ranges, and the little influence of refraction over this distance.

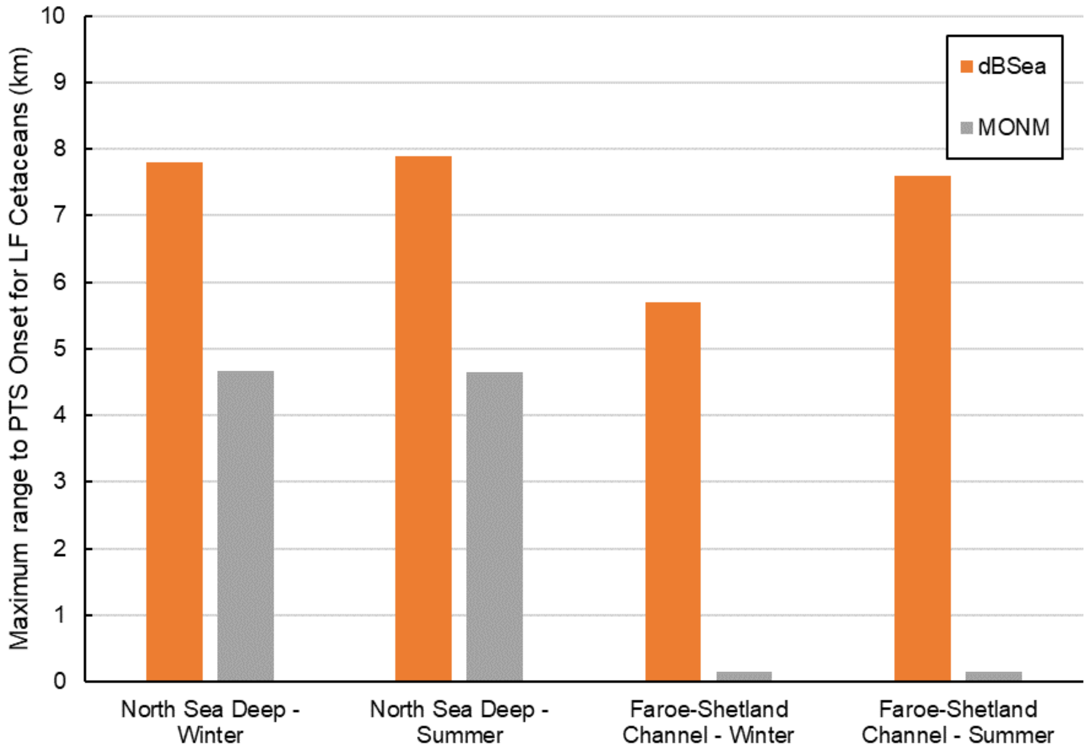

Figure 37. Maximum modelled ranges to SEL_{24h} PTS thresholds for LF cetaceans for Scenarios 5 and 6 using summer and winter sound speed profiles.

In the case of the TTS threshold ranges the result for dBSea is that ranges are reduced by 25% whereas there is practically no change in the maximum range from MONM results. There is, however, a reduction in range from the MONM results as shown in Figure O-2 towards the shallower waters in the southeast. The two models show a difference in how the refraction occurs, with MONM being less sensitive and dBSea being more sensitive to the ducting effects. The effect of the summer sound speed profile is not as pronounced at higher latitudes as the summer heating effect (in this case, of approximately 4°C) is insufficient to generate a large degree of downward refraction; the heating effect creates a weak thermocline down to approximately 90 m.

10.3. Maximum Sound Levels Over Depth

The baseline modelling from dBSea and MONM considers a single target depth of 10 m for the calculation of potential impact ranges. A more conservative approach is to use the maximum sound level over the entire water column for a given location.

It should be noted that the above does not apply to the results produced using the SOPRANO model. This model did not include the effects of changing sound-speed in the water and produces a conservative estimate (in the sense of minimising probability of underestimating exposure) by setting the receiver depth to be 1 m above the seabed. In this way, SOPRANO attempts to achieve, in a single model run, the conservative approach that it presented here for the other modelling approaches.

Modelling results for Scenarios 5 and 6 were reprocessed to generate the ranges to the PTS and TTS threshold levels for low-frequency cetaceans; the results are shown in Tables 49 and 50 and in Figure 38; sound field maps are shown as Figures P-1 to P-3 in Appendix P.

Table 49. Scenario 5: North Sea Deep environment: Maximum ranges at 10 m depth and maximum level over all depths to the frequency-weighted SEL_{24h} threshold values defined by the NMFS 2018 criteria for low-frequency cetaceans.

Type of animal	Effect	$SEL_{24h,Weighted}$ (dB re 1 µPa²s)	Target depth: 10 m			Maximum over all depths		
			dBSea	MONM		dBSea	MONM	
			R_{max} (km)	R_{max} (km)	$R_{95\%}$ (km)	R_{max} (km)	R_{max} (km)	$R_{95\%}$ (km)
Low-frequency cetaceans	PTS	183	7.8	4.66	4.2	9.1	6.48	5.33
	TTS	168	30.4	56.1	42.75	41.2	84.8	64.4

Table 50. Scenario 6: Faroe-Shetland Channel environment: Maximum ranges at 10 m depth and maximum level over all depths to the frequency-weighted SEL_{24h} threshold values defined by the NMFS 2018 criteria for low-frequency cetaceans.

Type of animal	Effect	$SEL_{24h,Weighted}$ (dB re 1 µPa²s)	Target depth: 10 m			Maximum over all depths		
			dBSea	MONM		dBSea	MONM	
			R_{max} (km)	R_{max} (km)	$R_{95\%}$ (km)	R_{max} (km)	R_{max} (km)	$R_{95\%}$ (km)
Low-frequency cetaceans	PTS	183	5.7	0.15	0.12	6.4	2.13	1.68
	TTS	168	63.7	77.8	67.6	64.4	84.9	73.6

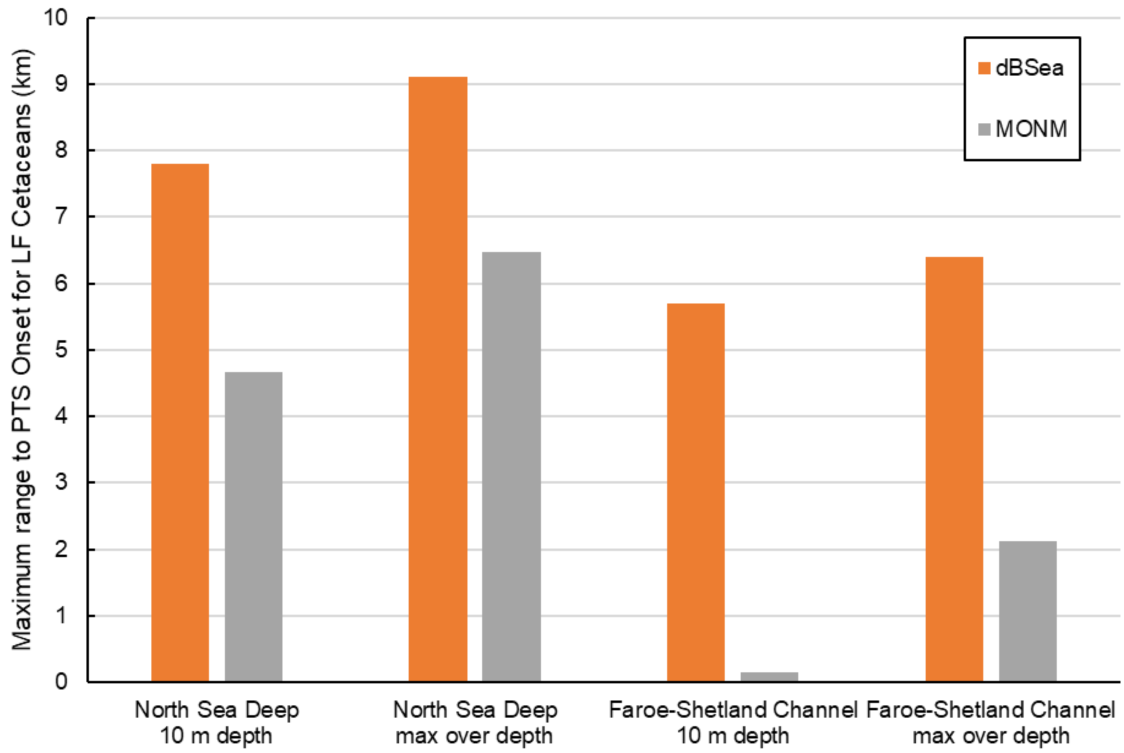

Figure 38. Maximum modelled ranges to SEL_{24h} PTS thresholds for LF cetaceans for Scenarios 5 and 6 assuming a receiver at 10 m depth and taking the maximum level over all depths.

The modelling results show that, for most cases, the use of the maximum level over depth can lead to an appreciable increase in the predicted ranges to impact threshold values (corresponding to roughly a 3 to 5 dB level difference). The results for the North Sea Deep environment in Tables 49 suggest that the levels at 10 m depth are typically somewhat lower than those seen deeper within the water column, with some large increases in ranges to impact thresholds; in terms of a decibel difference, however, this difference corresponds only to a modest increase. As shown in Figure 38, for maximum ranges to modelled PTS onset levels, the two models exhibit similar increases when considering the maximum level over depth.

For the Faroe Shetland Channel environment, the water depth extends to up to 1100 m. Consequently, reflections from the seabed are less influential than in shallower scenarios and, considering the directionality of the air gun array, initially the greater ranges are likely to be found at greater depths. However, the environment also exhibits a low gradient surface duct; this is likely to trap energy and thus, over greater distances, the greatest sound levels are likely to be found within the top hundreds of metres. These phenomena are evident in Table 50; the distance for the PTS threshold increased significantly for MONM, which predicted PTS ranges close to the source, whereas for dBSea there was a smaller increase due to predicting ranges some kilometres out. In terms of the TTS thresholds, there was practically no increase for the dBSea results, suggesting that the greatest levels were firmly within the surface duct. The MONM results showed a more substantial increase in range and is indicative of the surface duct being less influential in these modelling results.

10.4. High-frequency Energy Loss due to Surface Roughness

Results from Section 10.1 indicate a great increase in maximum ranges to PTS onset levels for high-frequency cetaceans when using the source with conservative inter-model differences applied. The baseline modelling presented in Section 10.1, however, does not consider the effects of high-frequency energy loss due to interactions with a rough sea surface.

The median monthly windspeed for the North Sea Shallow location was 19.0 knots from the QuikSCAT Monthly Ocean Vector Wind Data (Ricciardulli et al. 2011). Modelling results were generated using this and 9.5 knots to illustrate the effect of the surface roughness on the impact ranges for high-frequency cetaceans using the sound field results from MONM. The resulting ranges are shown in Table 51 and Figure 39 with sound field maps shown in Figures Q-1 and Q-2 for the 9.5 and 19.0 knot wind speed cases respectively (Appendix Q).

Table 51. Scenario 4: North Sea Shallow environment: Maximum ranges at 10 m depth to the frequency-weighted SEL_{24h} threshold values defined by the NMFS 2018 criteria.

Type of animal	Effect	$SEL_{24h,Weighted}$ (dB re 1 µPa²s)	AASM source		AASM source + HF Shift 0 knots		AASM source + HF Shift 9.5 knots		AASM source + HF Shift 19.0 knots	
			MONM		MONM		MONM		MONM	
			R_{max} (km)	$R_{95\%}$ (km)	R_{max} (km)	$R_{95\%}$ (km)	R_{max} (km)	$R_{95\%}$ (km)	R_{max} (km)	$R_{95\%}$ (km)
High-frequency cetaceans	PTS	155	0	0	5.98	4.65	3.33	2.60	0.43	0.38

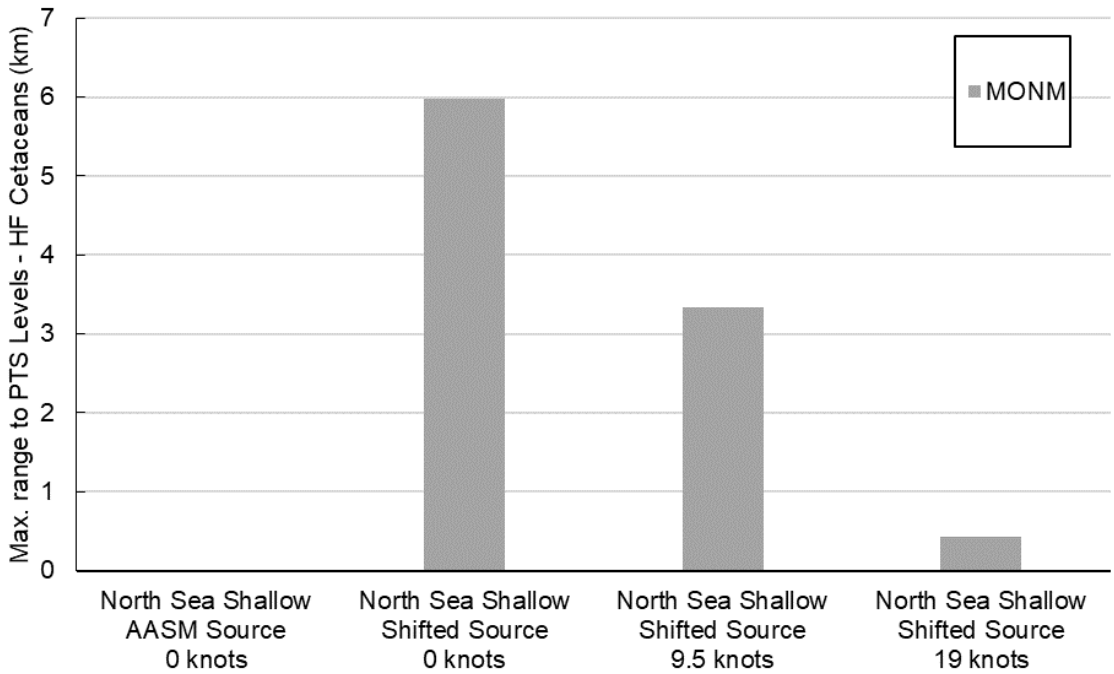

Figure 39. Maximum modelled ranges to SEL_{24h} PTS thresholds for HF cetaceans for Scenario 4 using source with inter-model difference and different wind speeds.

As shown, the inclusion of the surface roughness can serve to drastically reduce the sound propagation where high-frequency energy is governing the impact ranges. It should be noted that because the surface roughness has less effect on lower frequencies, the inclusion of surface roughness would not have a large effect on the base case modelling (i.e., those using the original AASM source). Where there is high-frequency energy, however, its propagation is going to be strongly dependent on the weather for which an accurate forecast is typically not available at the time of impact assessment but instead a range of predictions should be provided.

10.5. Change in Geoacoustic Properties

The Phase 2 modelling used a basic set of geoacoustic properties that comprised values that did not vary with depth but were instead based on the grain size of the prevalent surface sediment type. Available marine deposits data shows that in the waters around the UK there exists a rockier sub-layer within 100 mbsf (metres below sea floor) that may influence the sound propagation at the selected sites.

10.5.1. Irish Sea – Mudstone sub-layer

Data from the British Geological Survey show that in the region associated with the Irish Sea environment defined for Phase 2, there is a range of Quaternary deposit thicknesses from 20 m to greater than 50 m (Figure 40). Data for bedrock lithologies (Figure 41) indicates the substrate to be mudstone.

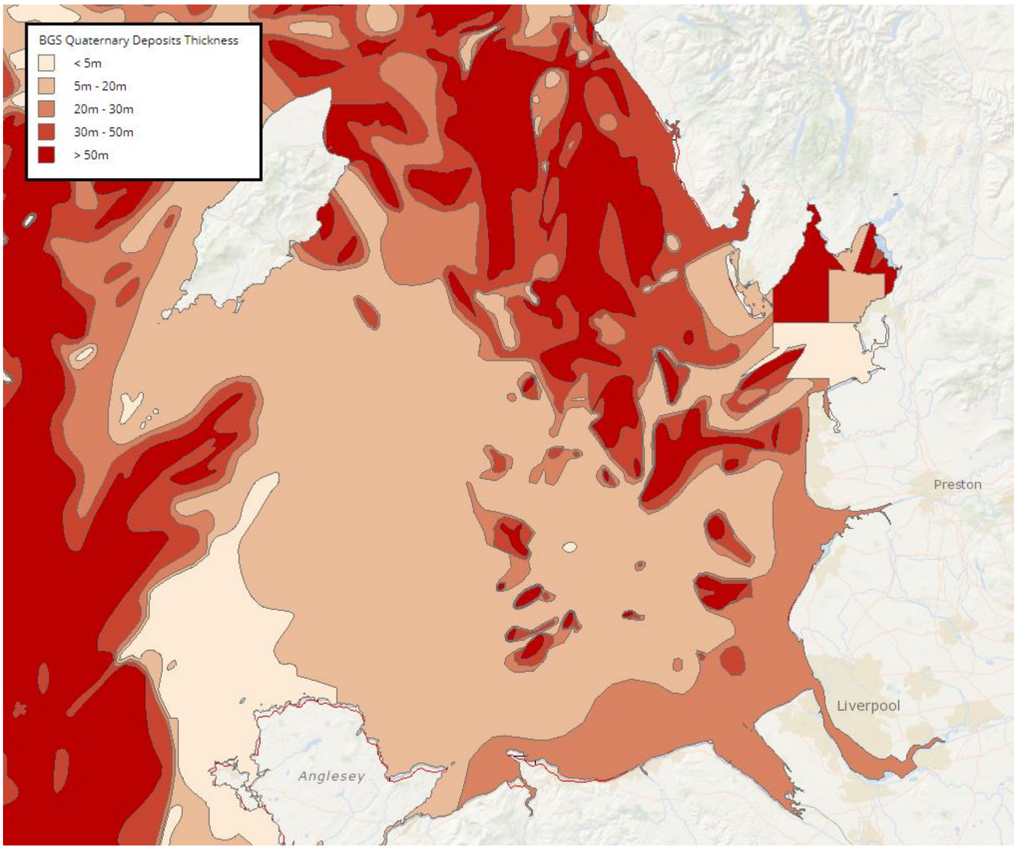

Figure 40. Quaternary deposit thicknesses for the Irish Sea; the sediment thickness is typically 20 m to greater than 50 m

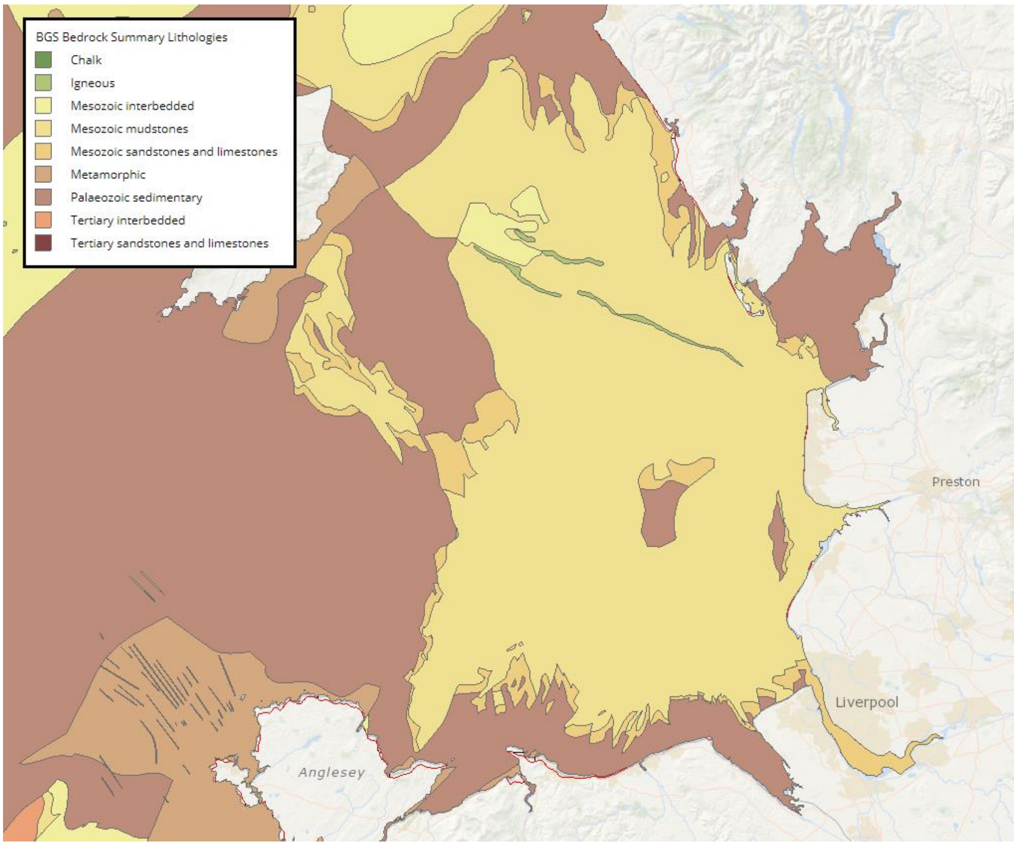

Figure 41. Bedrock lithologies for the Irish Sea; in the modelled location the bedrock is principally mudstones.

The geoacoustic profiles used for the modelling, assuming 20 and 50 m sediment layers, are shown in Table 52; properties for mudstone are taken from Ainslie (2010).

Table 52. Geoacoustic profiles including a sublayer for the Irish Sea modelling region.

Depth (mbsf)	Material	Density (g/cm^3)	P-wave speed (m/s)	P-wave attenuation (dB/λ)	S-wave speed (m/s)	S-wave attenuation (dB/λ)
0-20 / 0-50	Coarse/medium Silt	1.693	1577.4	0.71	200.0	3.65
20+ / 50+	Mudstone	1.5	2050	0.15	600.0†	0.4†

† Note that dBSea does not include shear wave properties, and MONM includes shear wave properties only for the water-sediment interface, and as such, these values were not used.

The modelling runs, with a 20 m sediment layer and with a 50 m sediment layer, were performed with MONM and dBSea with results shown in Table 53.

Table 53. Scenario 3: Irish Sea environment: Maximum ranges at 10 m depth for different substrate properties to the frequency-weighted SEL_{24h} threshold values defined by the NMFS 2018 criteria for low-frequency cetaceans.

Type of animal	Effect	$SEL_{24h,Weighted}$ (dB re 1 μPa²s)	Baseline: no sublayer			Sublayer depth: 50 m			Sublayer depth: 20 m		
			dBSea	MONM		dBSea	MONM		dBSea	MONM	
			R_{max} (km)	R_{max} (km)	$R_{95\%}$ (km)	R_{max} (km)	R_{max} (km)	$R_{95\%}$ (km)	R_{max} (km)	R_{max} (km)	$R_{95\%}$ (km)
Low-frequency cetaceans	PTS	183	5.5	1.6	1.4	3.1	1.6	1.4	3.1	1.7	1.4

The results for the two different models display different effects. In the case of MONM, there is very little difference between modelling run using constant sediment properties and those using the mudstone sediment; there is a slight increase in the PTS impact range where the sublayer is only 20 m below the sediment-water interface.

In the case of dBSea, the inclusion of the sublayers reduces the impact ranges. This behaviour, however, was not recreated when running dBSeaModes nor for dBSeaPE in similar environments; consequently, it is considered to be a modelling artefact for these specific inputs. The issue highlights the sensitivity of predicted ranges to sound levels where there is a received level that reduces slowly with range; in the dBSea example, it is estimated that the reduction from 5.5 to 3.1 km can be the result of a 2 to 4 dB difference in predicted level at range.

10.5.2. North Sea Deep – Sandstone sub-layer

A supplemental model run was performed to highlight potential differences that may occur due to the presence of a rocky sublayer in the modelled environment. Results are calculated and presented for a single pulse only due to the modelling methods employed.

This study is performed using the North Sea Deep environment to provide a large enough water depth such that low frequency energy is not 'cut-off'. According to BGS bedrock lithological data, the substrate is dominated by sandstone. The acoustical properties of sandstone can vary greatly depending on its composition and structure. Three geoacoustic profiles were generated that considers 'clean' sandstone, consolidated sandstone, and weakly cemented sandstone with properties taken from Marion (1990); these are presented in Table 54. The shear wave speed is determined from the compressional wave speed using a formula by Pickett (1963) for use with sandstone. For the modelling runs, although the quaternary deposit thickness layer is greater than 50 m, a thin sediment layer of 20 m was used to accentuate any effect caused by the sublayer.

Table 54. Acoustic properties of sandstone based on level of cementation; these are used as the investigated substrate properties for the North Sea Deep modelling region.

Material	Density (g/cm^3)	P-wave speed (m/s)	P-wave attenuation (dB/λ)	S-wave speed (m/s)	S-wave attenuation (dB/λ)
Clean sandstone	2.46	5000	0.10	3170	0.25
Consolidated sandstone	2.40	3800	0.15	2131	0.33
Weakly cemented sandstone	2.28	2500	0.20	1005	0.50

In this hypothetical example, we also consider the shear wave properties of the sediment in the formulation of the reflection coefficient at the sediment-water interface. It is common for shear wave properties to either be included in the model as an additional loss term at the seafloor simulating the conversion of energy into coupled shear waves at the sediment-water interface (such as in MONM) or disregarded entirely. It has been shown, however, that the shear wave effects can be important for sound propagation (Hughes et al. 1991, Tollefsen 1998, Ainslie 2003).

The only program employed in this report that has full functionality for sublayer shear wave calculation is VSTACK. Consequently, the environment comprises a flat bathymetry with a constant sound speed profile; modelling extends to a maximum distance of 1 km and a maximum frequency of 1024 Hz. Only a single pulse is considered here for illustrative purposes.

The modelled cases were:

- Baseline: uniform sand sediment with no sublayer.
- 20 m sand layer above clean sandstone
- 20 m sand layer above consolidated sandstone
- 20 m sand layer above weakly cemented sandstone

Results are shown in Figure 42 for both the unweighted case and the LF-weighted case; results are for a receiver at 10 m water depth.

The inclusion of a sublayer provides a deep sound reflector that serves to increase the sound energy levels within the water column; without the sublayer, and for a constant speed geoacoustic profile, there is no mechanism by which the sound energy can travel up from within the sediment. This is shown in the results, where the levels for the sublayer model runs are generally higher than for the sediment only run.

The difference in wave speeds for the sediment result in different critical angles and favourable reflective angles; consequently, the ranges of the peaks and troughs in the received level are slightly different between sub-layers: the regions of constructive interference change with the sublayer.

The greatest variation in results occur at approximately 300 m from the source. It is approximately here that we see the first contribution of the seabed reflections reaching the sublayer and reflected back up.

The inclusion of sub-layers is only likely to affect sound exposure level results for LF-cetaceans; due to the frequency weighting curves, sound energy at the frequencies pertinent for MF and HF cetaceans has greater losses in the sediment and so sub-layer properties are typically inconsequential. In the case of LF cetaceans, however, there is potential for sound levels to be raised particularly closer to the source.

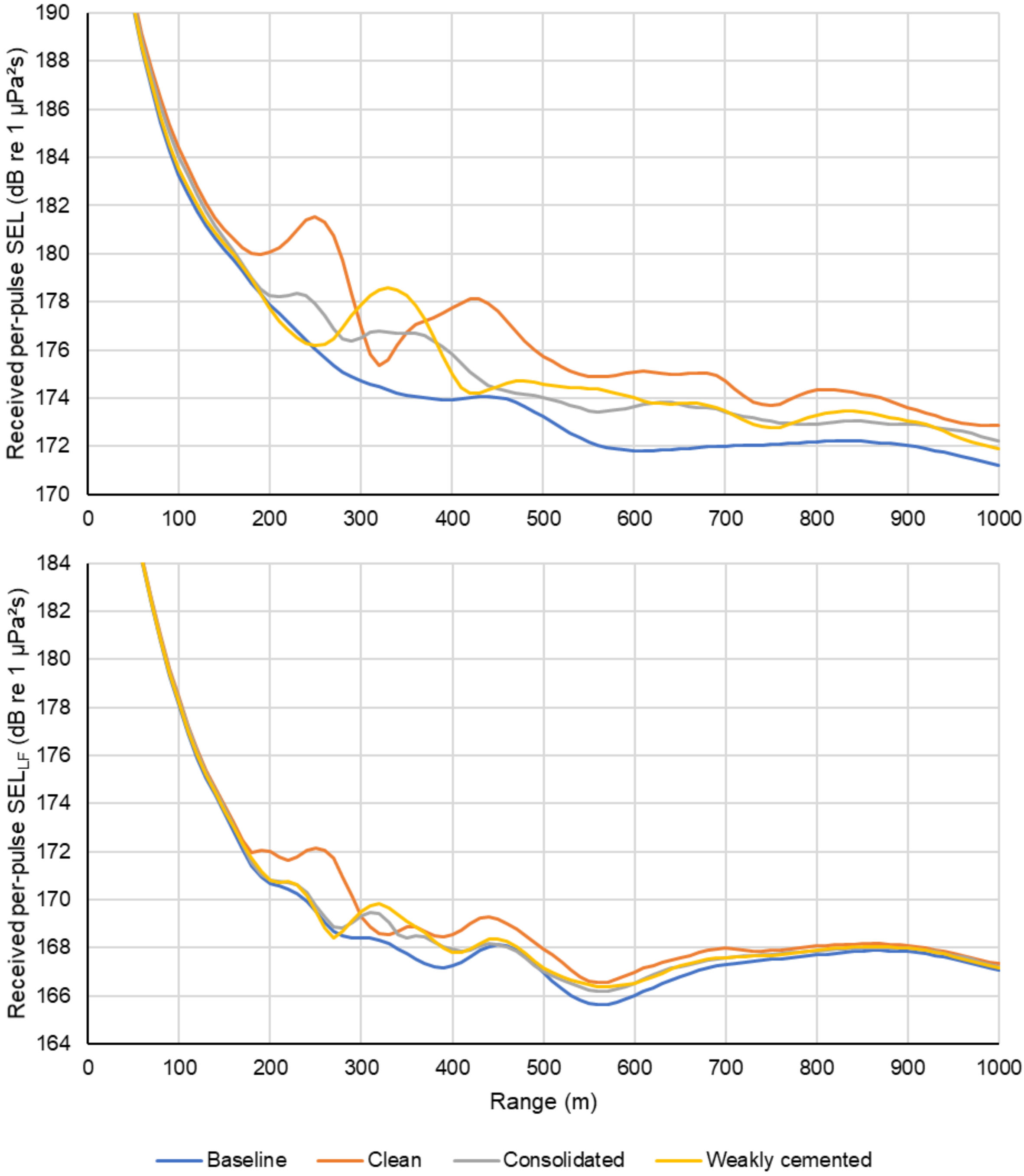

Figure 42. Received level at 10 m depth as a function range for the baseline and three sub-layer cases up to maximum frequency of 1024 Hz. Top plot shows unweighted levels, and bottom plot shows LF-weighted levels (NMFS 2018).

11. Mobile Receivers: Prescribed Motion

The results presented so far have considered impact ranges for static receivers. The following sections consider the effect that mobile receivers have on the modelled impact ranges. Two analyses are presented: receivers with prescribed motion perpendicular to the survey line using modelling results from dBSea, and animat modelling that considers the behavioural states of an animal using MONM- BELLHOP results in Section 12.

This section contains details of the analysis involving mobile receivers following prescribed motions performed using dBSea. The motion of the receivers, otherwise known in this case as animats, was prescribed to be perpendicular to the survey track, with the animats starting motion when the array was 500 m away (standard mitigation zone from the JNCC). Two additional animats started moving at ranges of 1000 and 3000 m.

11.1. Low-frequency Cetaceans – North Sea Deep Environment

11.1.1. Receiver locations

Eleven receivers were made to follow a path during a single line of the North Sea Deep Scenario with a sound source as specified by the Regional Survey setup (first line only) without the high-frequency shift. This involved six ramp-up/soft-start steps of increasing output and one full-power step. Receivers were made to sample sound levels along a track perpendicular to the survey line to establish the sound exposure of a sample of animats, with locations and paths as listed in Table 55 and shown in Figure 43. Nine of the animats started moving as soon as the survey vessel came within 500 m of their starting position, while two additional animats started moving when the survey vessel was 1000 m and 3000 m away respectively. Before movement onset, the animats were stationary at their starting position. Animats began accumulating sound exposure when the survey line started. The vessel moved directly north at 2.5 m/s with a source point every ten seconds or 25 m. Animats moved west at 1.5 m/s and all sound levels were taken at 10 m depth, as were the case in the baseline modelling results. Note that because of the relatively greater speed of the vessel, the minimal ranges from vessel to animat was 257 m, 772 m, and 1801 m for animats starting movement at ranges 500, 1000, 3000 m from the vessel.

Table 55. Prescribed movement of Animats in Scenario 5.All move at 1.5 m/s. All animats except “Animat 8_{1km}” and “Animat 8_{3km}” started moving when source was 500 m away, stationary before then. The two remaining animats started moving when source was 1 km and 3 km away. Total duration 9180 seconds (153 min). Positions are Eastings/Northings for zone UTM 30N.

Receiver name	Starting position		End position		Movement start time (s)	Source Point number
	Easting (m)	Northing (m)	Easting (m)	Northing (m)		
Animat 1	732500	6627525	718730	6627525	0	1
Animat 2	732500	6627975	719000	6627975	180	18
Animat 3	732500	6628425	719270	6628425	360	36
Animat 4	732500	6628875	719540	6628875	540	54
Animat 5	732500	6629325	719810	6629325	720	72
Animat 6	732500	6629925	720170	6629925	960	96
Animat 7	732500	6630525	720530	6630525	1200	120
Animat 8	732500	6640500	726515	6640500	5190	519
Animat 8_{1km}	732500	6641500	726515	6641500	5190	519
Animat 8_{3km}	732500	6643500	726515	6643500	5190	519
Animat 9	732500	6649975	732200	6649975	8980	898

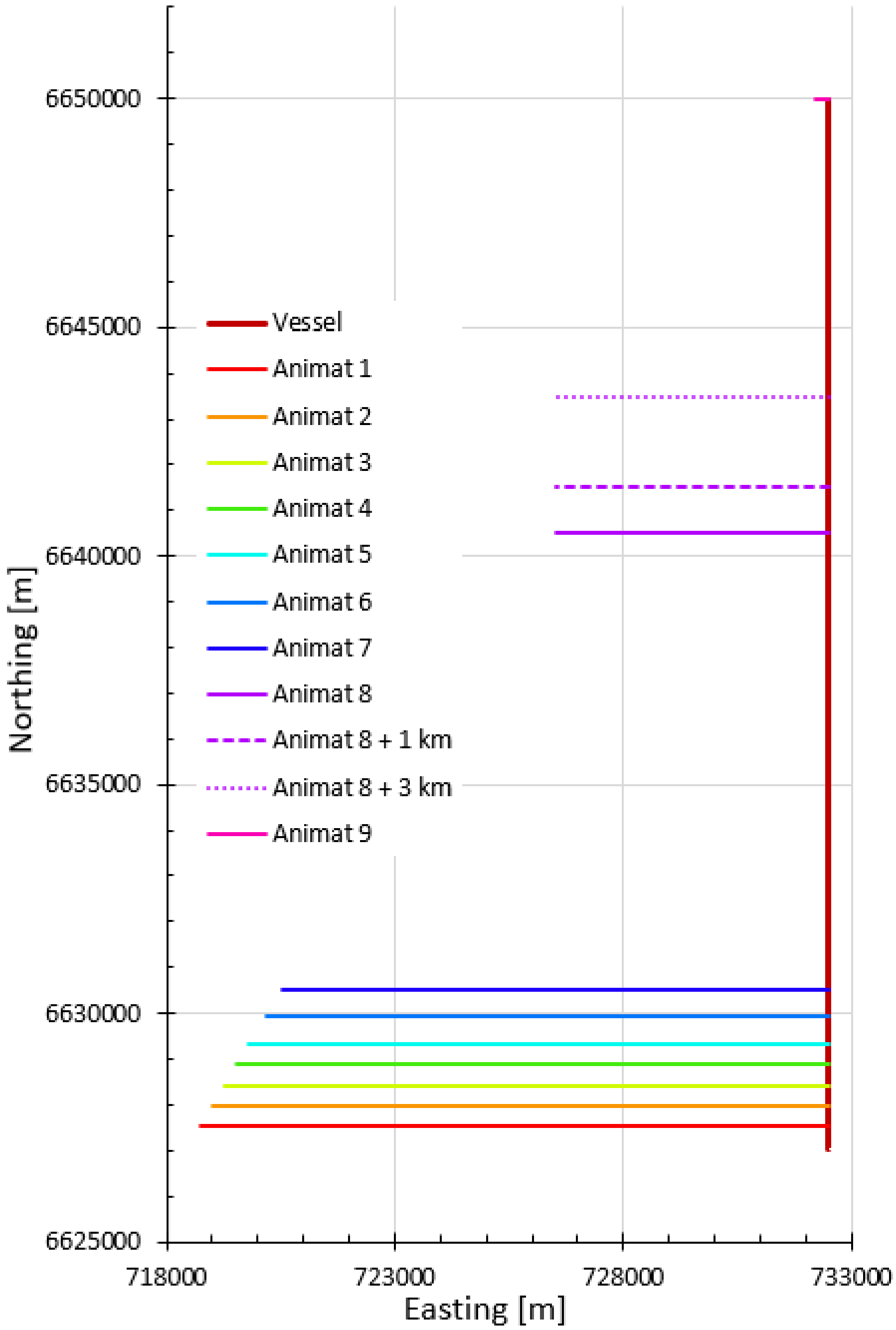

Figure 43. Vessel and animat tracks. Vessel speed 2.5 m/s, animat speed 1.5 m/s.

11.1.2. Results

The received levels are based on sampling the sound field from the activity every ten seconds; as the sound speed in water is finite, sampling the sound field once every ten seconds for the animats does not mean that the source pulse at that time step is captured. We have linearly interpolated between nearest values to estimate levels. Consequently, small irregularities will occur in the data when compared to a live, continuous model. The key sound metrics for the animats with prescribed motion are shown in Table 56. We can follow the received level for the animats at 10 second steps (Figure 44) and see the way the level changes over time with the relative movement of the vessel and the animats. The received level curves have been smoothed, so to be continuous and represent received SEL over every 10 second period. The accumulated sound energy results are shown in Figure 45.

Table 56. Key sound metrics for LF-weighted received levels for animats with prescribed motion.

Receiver Name	Sound exposure level (153 min) (dB re 1 µPa²s)	Max sound exposure level (10 s) (dB re 1 µPa²s)	Sound pressure level (dB re 1 µPa)	Limits exceeded after time (minutes)
Animat 1	180	161	150	TTS (5)
Animat 2	180	162	151	TTS (6)
Animat 3	183	165	153	TTS (7)
Animat 4	185	167	155	TTS (8) + PTS (23)
Animat 5	187	169	157	TTS (9) + PTS (17)
Animat 6	188	172	159	TTS (12) + PTS (18)
Animat 7	189	172	159	TTS (12) + PTS (21)
Animat 8	189	170	159	TTS (39) + PTS (79)
Animat 8_{1km}	187	169	157	TTS (39) + PTS (96)
Animat 8_{3km}	184	163	155	TTS (54) + PTS (116)
Animat 9	184	169	154	TTS (80) + PTS (152)

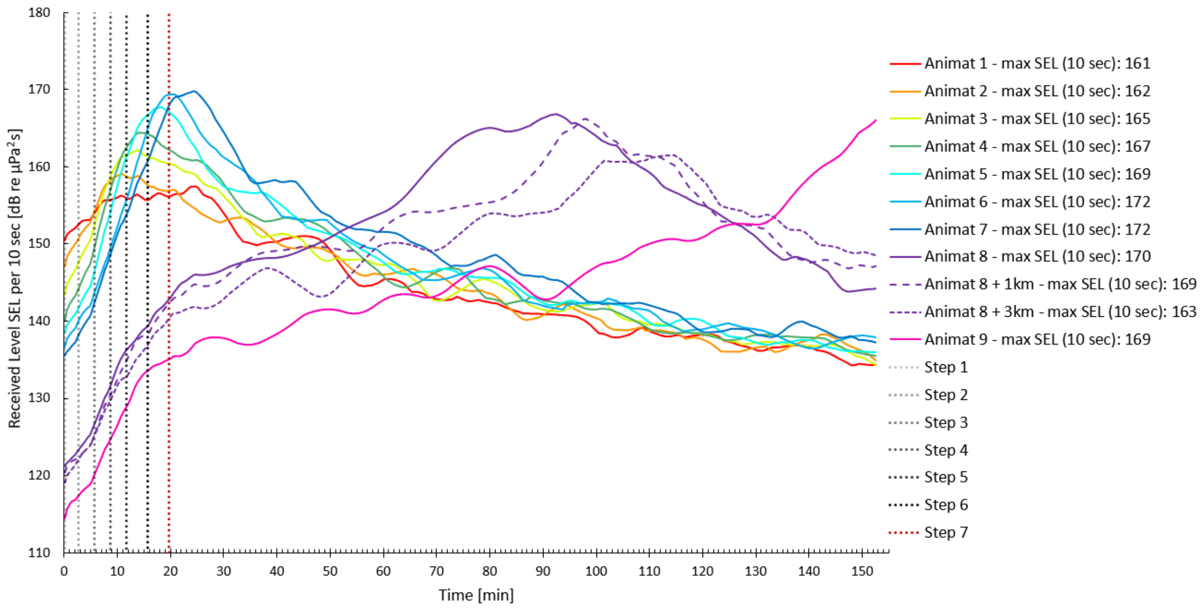

Figure 44. LF weighted received levels of animats. Levels presented as SEL per 10 second interval as this represents the rate of impulse repetition from the array. Lines have been smoothed to better show continuous change; consequently, the maximum SELs in Table 56 are not reflected in this plot.

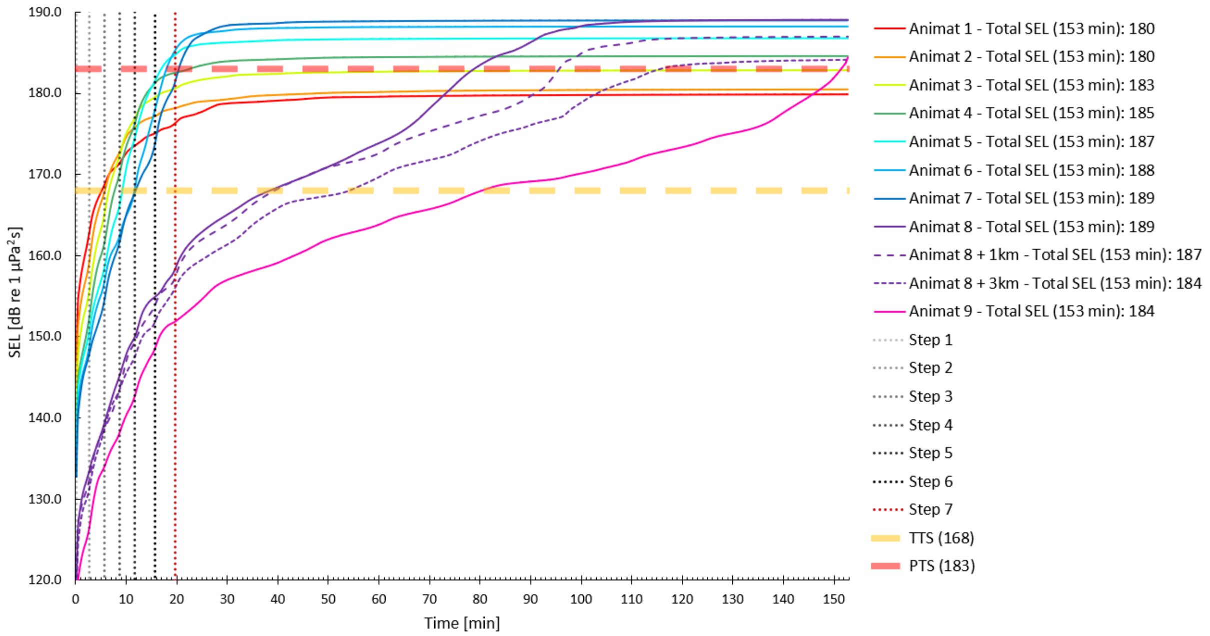

Figure 45. LF weighted cumulative exposure levels of animats. Levels presented as SEL over the duration of the first line. All animats exceed TTS limit for cumulative impulsive sound (168 dB re 1 µPa²s). Animats bar Animat 1, 2, and 3 exceed the PTS limit for cumulative impulsive sound (183 dB re 1 µPa²s).

11.2. High-frequency Cetaceans – North Sea Shallow Environment

11.2.1. Receiver locations

The paths and methods presented for the low-frequency auditory group are replicated here respective to the locations of the survey. The start and end locations of the receivers are shown in Table 57.

Table 57. Prescribed movement of Animats in Scenario 4. All move at 1.5 m/s. All animats except “Animat 8_{1km}” and “Animat 8_{3km}” started moving when source was 500 m away, stationary before then. The two remaining animats started moving when source was 1 km and 3 km away. Total duration 9180 seconds (153 min). Positions are Eastings/Northings for zone UTM 30.

Receiver name	Starting position		End position		Movement start time (s)	Shot number
	Easting (m)	Northing (m)	Easting (m)	Northing (m)		
Animat 1	854000	5937525	840230	5937525	0	1
Animat 2	854000	5937975	840500	5937975	180	18
Animat 3	854000	5938425	840770	5938425	360	36
Animat 4	854000	5938875	841040	5938875	540	54
Animat 5	854000	5939325	841310	5939325	720	72
Animat 6	854000	5939925	841670	5939925	960	96
Animat 7	854000	5940525	842030	5940525	1200	120
Animat 8	854000	5950500	848015	5950500	5190	519
Animat 8_{1km}	854000	5959975	853700	5959975	5190	519
Animat 8_{3km}	854000	5951500	848015	5951500	5190	519
Animat 9	854000	5953500	848015	5953500	8980	898

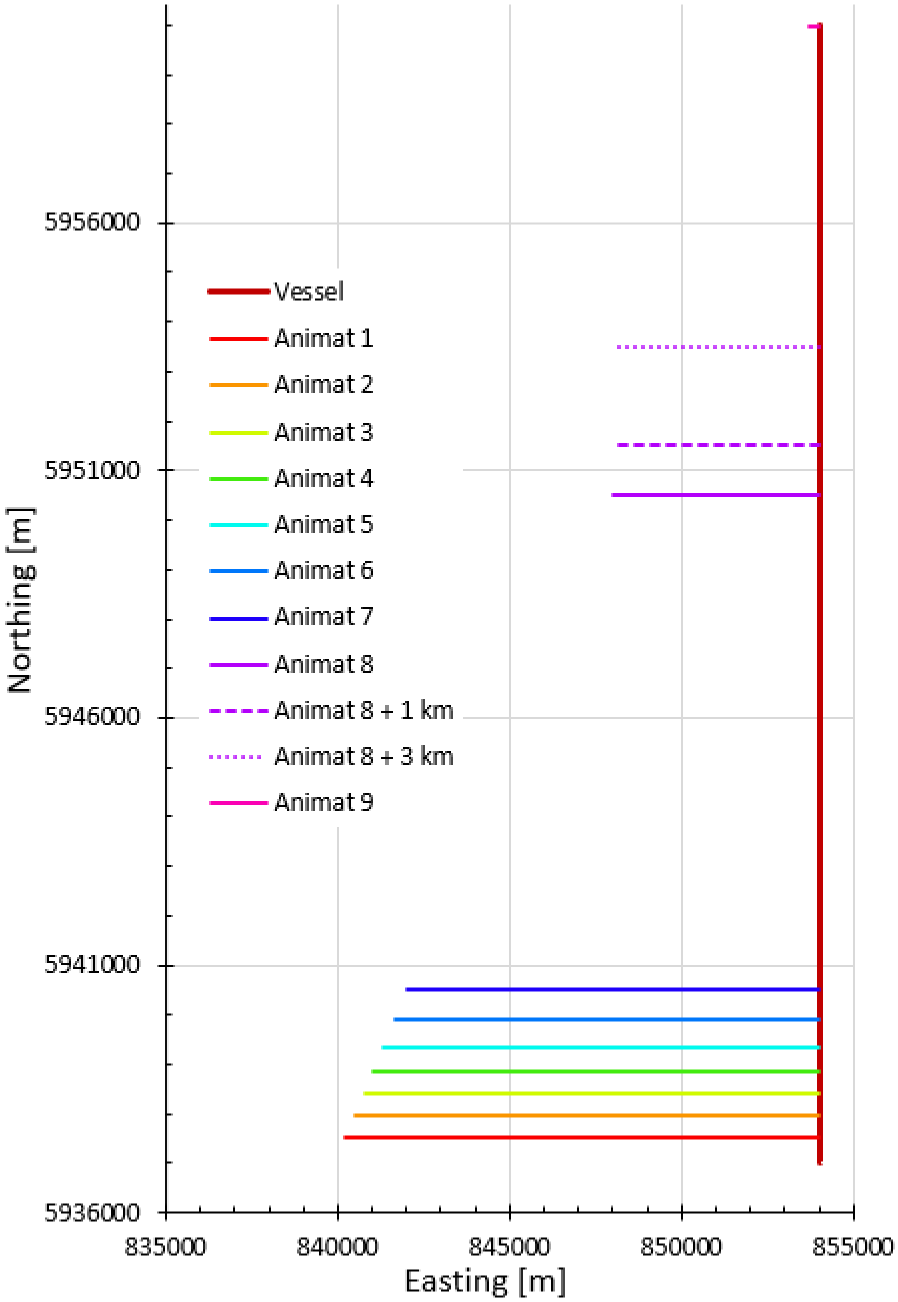

Figure 46. Vessel and animat tracks. Vessel speed 2.5 m/s, animat speed 1.5 m/s. Note that because of the greater speed of the vessel than the animats, the minimal ranges from the vessel to the animats were 257, 772, 1801 m for starting ranges 500, 1000, 3000 m.

11.2.2. Results

The key sound metrics for the animats with prescribed motion for the original source are shown in Table 58. We can follow the received level for the animats at 10 second steps (Figure 47) and see the way the level changes over time with the relative movement of the vessel and the animats. The received level curves have been smoothed, so to be continuous and represent received SEL over every 10 second period. The accumulated sound energy results are shown in Figure 48.

The results for the animats receiving levels from the high-frequency shifted source are shown in Table 59. The received per pulse SEL as a function of time over the first line is shown in Figure 49 with accumulated SEL shown in Figure 50.

11.2.2.1. Original Source

Received levels increase with proximity to a louder source, with Animats 1 to 8_{1km} exceeding the TTS threshold. No animats exceeded the PTS threshold level.

Table 58. Key sound metrics for HF-weighted received levels for animats with prescribed motion using the original source.

Receiver Name	Sound exposure level (153 min) (dB re 1 µPa²s)	Max sound exposure level (10 s) (dB re 1 µPa²s)	Sound pressure level (dB re 1 µPa)	Limits exceeded after time (minutes)
Animat 1	132	115	106	None exceeded
Animat 2	136	119	112	None exceeded
Animat 3	140	124	116	None exceeded
Animat 4	142	125	118	TTS (15)
Animat 5	146	130	122	TTS (14)
Animat 6	150	134	127	TTS (16)
Animat 7	148	132	125	TTS (20)
Animat 8	153	137	130	TTS (84)
Animat 8_{1km}	144	126	119	TTS (93)
Animat 8_{3km}	133	113	107	None exceeded
Animat 9	128	110	103	None exceeded

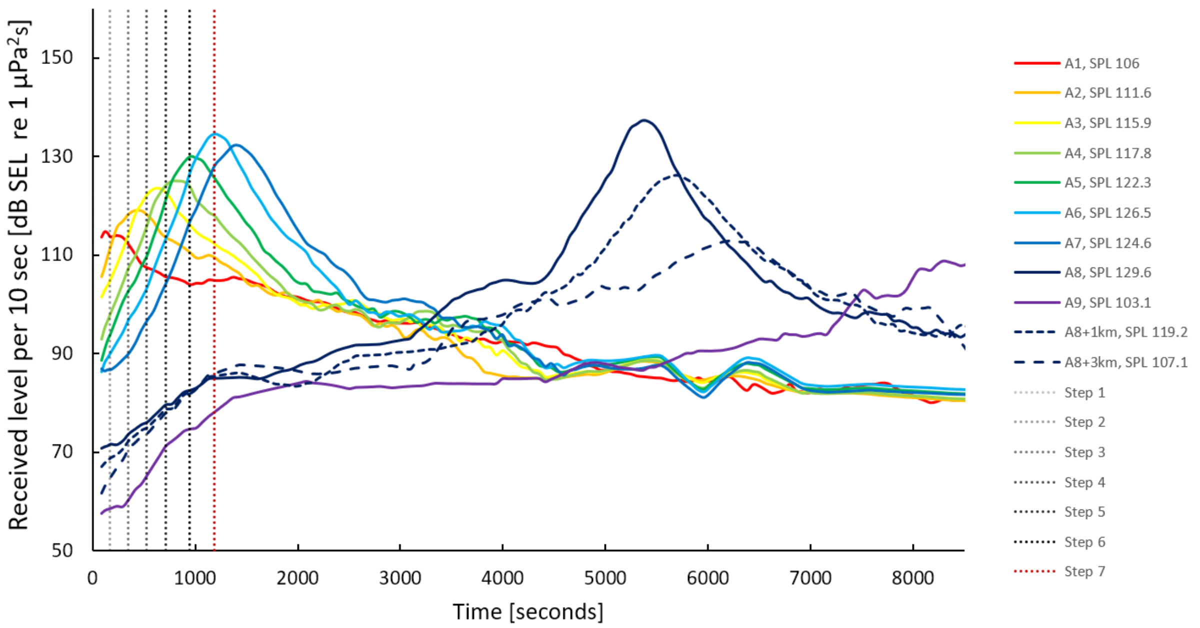

Figure 47. HF-weighted received levels of animats from the original source. Levels presented as SEL per 10 second interval as this represents the rate of impulse repetition from the array. Lines have been smoothed to better show continuous change.

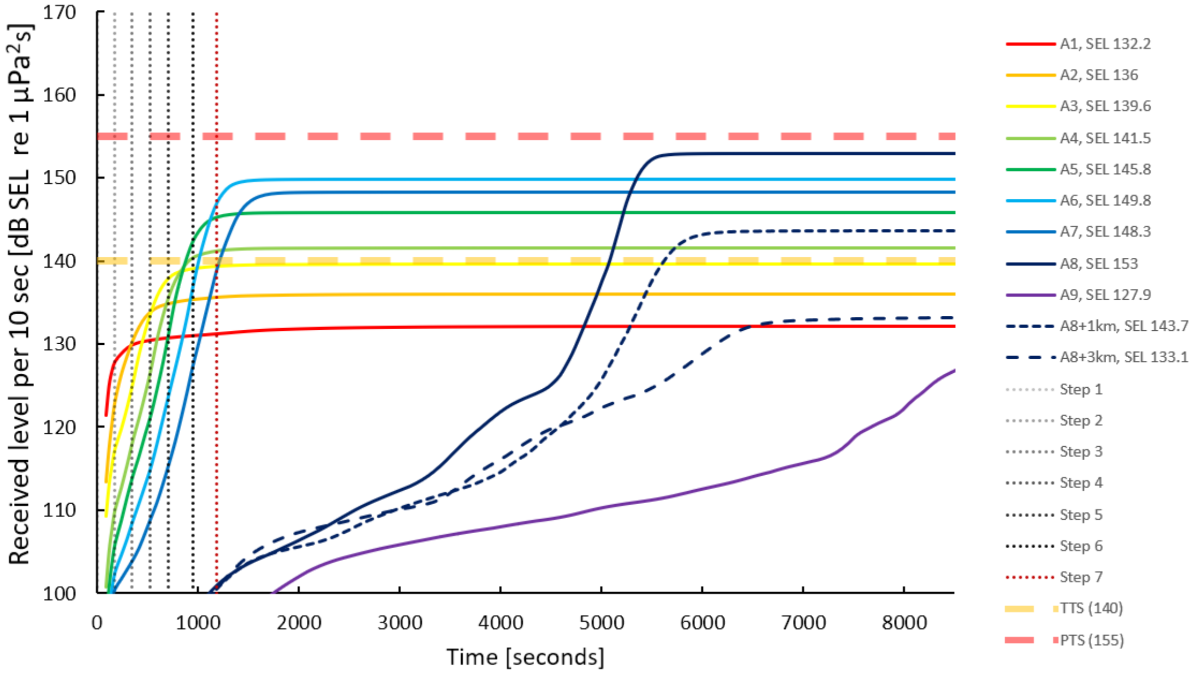

Figure 48. HF weighted cumulative exposure levels of animats from original source. Levels presented as SEL over the duration of the first line. Animats 4, 5, 6, 7, 8, and 8_{1km} exceed TTS limit for cumulative impulsive sound (140 dB re 1 µPa²s). No animats exceed the PTS limit for cumulative impulsive sound (155 dB re 1 µPa²s).

11.2.2.2. High Frequency-shifted Source

Table 59. Key sound level metrics for HF-weighted received levels for animats with prescribed motion using the high-frequency shifted source.

Receiver Name	Sound exposure level (153 min) (dB re 1 µPa²s)	Max sound exposure level (10 s) (dB re 1 µPa²s)	Sound pressure level (dB re 1 µPa)	Limits exceeded after time (minutes)
Animat 1	135	122	112	None exceeded
Animat 2	151	134	126	TTS (3)
Animat 3	154	138	130	TTS (5)
Animat 4	156	140	132	TTS (8) + PTS (16)
Animat 5	160	144	136	TTS (10) + PTS (15)
Animat 6	163	148	140	TTS (12) + PTS (17)
Animat 7	163	147	140	TTS (14) + PTS (20)
Animat 8	166	151	143	TTS (66) + PTS (85)
Animat 8_{1km}	160	142	135	TTS (73) + PTS (92)
Animat 8_{3km}	149	128	122	TTS (78)
Animat 9	146	127	120	TTS (124)

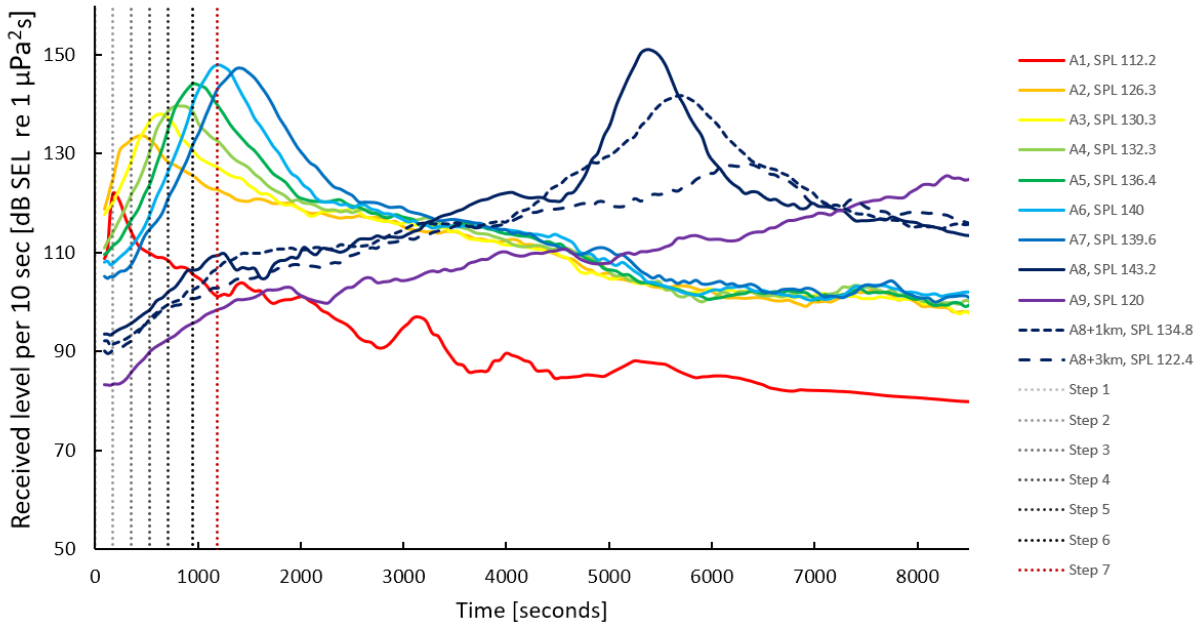

Figure 49. HF-weighted received levels of animats from HF-shifted source. Levels presented as SEL per 10 second interval as this represents the rate of impulse repetition from the array. Lines have been smoothed to better show continuous change. Note: Comment on Animat 1 in discussion, Section 11.3.2.2.

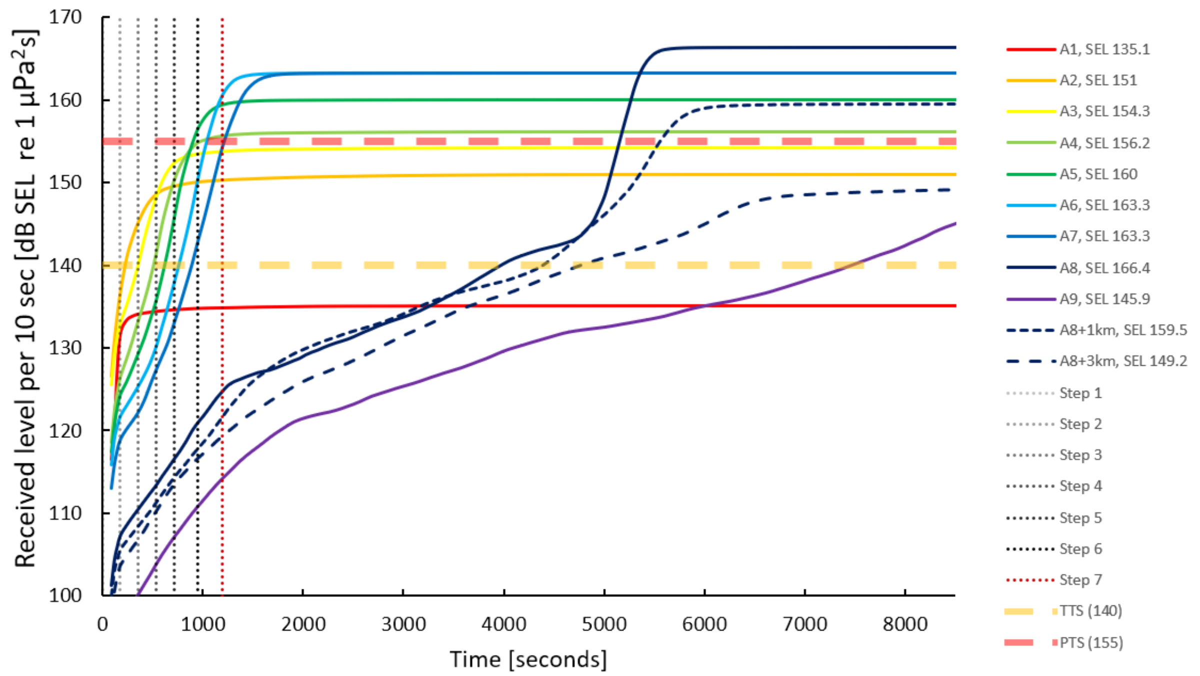

Figure 50. HF weighted cumulative exposure levels of animats from HF-shifted source. Levels presented as SEL over the duration of the first line (144 min). All animats except for Animat 1 exceed TTS limit for cumulative impulsive sound (140 dB re 1 μPa²s). Animats 4, 5, 6, 7, 8, and 8_{1km} exceed the PTS limit for cumulative impulsive sound (155 dB re 1 μPa²s).

Table 60. Increase in received level when using the source including the inter-source model difference.

Receiver Name	Sound exposure level (153 min) (dB)	Maximum sound exposure level (10 s) (dB)	Sound pressure level (dB)
Animat 1	3	7	6
Animat 2	15	15	14
Animat 3	14	14	14
Animat 4	14	15	14
Animat 5	14	14	14
Animat 6	13	14	13
Animat 7	15	15	15
Animat 8	13	14	13
Animat 8_{1km}	16	16	16
Animat 8_{3km}	16	15	15
Animat 9	18	17	17

11.3. Discussion

Based on these results, animats in the LF auditory group and most animats in the HF auditory group starting movement when 500 m from the source reached sound levels exceeding the TTS onset threshold; modelled exposures to PTS onset levels were limited to the LF group and to the HF group when the source including the inter-model difference was used. When animats started movement during the early ramp-up phase exposure was reduced markedly; none of Animats 1, 2, or 3 (i.e., 500 m away from the mitigation zone at the start of the soft-start) went on to accumulate enough energy to exceed the PTS threshold over the duration of the single survey line.

Also evident from the results is the consideration of high-frequency energy (i.e., above 1 kHz) on HF-weighted results similarly to results in Section 10.1. In this example, the introduction of the high-frequency energy shift resulted in modelled animats receiving levels above the PTS onset threshold, and a general increase in sound level of 14 dB (Table 60).

This form of assessment is strongly dependent on the speeds and travel directions of the source and receiver; in this example, an animat swimming at 1.5 m/s starting at 500 m in front of the vessel will be 257 m from the vessel at closest point, while the same animat swimming at 2.5 m/s will be 354 m from the vessel at closest point. A similar effect can be seen with regards to the direction an animal moves relative to a sound source, although this result is not as easily quantified as swimming speed variations. However, when the animat is slower than the vessel, we can assume that movement perpendicular to the vessel track is more effective than a simply moving directly away from the sound source, as more time will be spent with the vessel “catching” up to the animat.

11.3.1. The low-frequency group

In this study, as shown in Figure 45, the total received sound levels for Animats 1–3 do not reach PTS onset thresholds. From this information, we can estimate the range at which an LF animat in this scenario would reach PTS onset levels using the applied soft-start procedure. At the time of full array capacity (start of Step 7), Animat 3 was 2 km from the vessel (1.2 km from the survey line) and received a maximum per-pulse SEL of 165 dB re 1 µPa²s. Given a swimming speed of 1.5 m/s, 1.2 km from the survey line is travelled in 800 seconds (13.5 minutes); this corresponds to the range and time that, for the given modelling assumptions, the soft-start results in PTS level exceedance for an animat. Note that animats receive most of the energy from later ramp-up stages rather than the stage starting 500 m before them (Table 61).

Table 61. The stage of the seismic array causing most exposure (SEL) to the animats (see Figure 44).

Animat	Soft-start stage contributing most to cumulative levels
1	7
2	4
3	5
4	5
5	6
6	7
7	7
8	7
8_{1km}	7
8_{3km}	7
9	7

When compared to the HF group, the source level is relatively more important for the LF group in determining received level than the distance from the receiver. This is due to the higher sensitivity to lower frequencies of this group. Even though the two scenarios have different depths, this difference is thought to persist in most environments due to the frequencies involved.

Animat 8 has three starting ranges: 500 m, 1000 m, and 3000 m in front of the source, but only sees reduction in SEL from 189 dB re 1 µPa^{2}s (500 m) to 187 dB re 1 µPa^{2}s (1000 m) and to 184 dB re 1 µPa^{2}s (3000 m) over the duration of the line. This is due to the low propagation loss of the lower frequencies which the LF group is most sensitive to.

Given the modelling assumptions, ranges to PTS onset levels for LF groups can be reduced by the following:

- Limit energy at sensitive frequencies. The frequency weighting curve for LF cetaceans (Figure A-1) shows they are most sensitive to frequencies between 200 Hz and 10 kHz. Given the frequency-dependent propagation loss, a reduction of energy at the lower frequencies of this range would have the most influence in reducing ranges to identified threshold levels.
- Prolonging the soft-start. While this allows more time for the receiver to move away, it does not address the higher sound levels that animats far from the soft-start still receive when starting 500–3000 m from the sound source (Animats 8-9, 13-22 km from the soft-start).
- Slower survey speed relative to receivers. This would serve to maintain a greater distance between the source and receiver.
- Increased directivity of the source. The sound exposure is most influenced by energy travelling horizontally; reducing horizontal energy would reduce this exposure.

The long ranges to the PTS onset threshold mirror the results from Section 8, where PTS effects are predicted to ranges of 4.66-9.93 km from the survey line in Table 36 (stationary receivers).

11.3.2. The high-frequency group

11.3.2.1. Original source

Sound levels are predicted to be below the PTS onset threshold for all animats in the HF-group when using the original source, and above the TTS onset threshold for Animats 4, 5, 6, 7, 8, $8_{1\ km}$ (Table 58). As for the LF group we can make a cautious estimate of safe start distance from the survey line at full capacity, and as the animat paths are identical, we end up with the same ≈1.2 km as for the LF, but here to avoid TTS. This is equivalent to ≈800 seconds of fleeing time.

11.3.2.2. Source included inter-source model difference

The strong effect, approximately 14 dB increase in received level, from raising the higher-frequency (>1 kHz) energy content of the source (Figure 34) shows the importance keeping in mind the spectral variation in seismic sources. Received sound levels are below the TTS threshold value for Animat 1, and below the PTS threshold value for Animats 1, 2, 8_{3km} and 9 (Animat 9 likely only because the line ends). At the time of full array power (Step 7), Animat 2 is ≈2.5 km from the source, while Animat 8_{3km} is 1801 m from the source at the closest point. Animat 2, however, receives its greatest sound exposure from Step 3, approximately 450 seconds (7.5 min, range ~300 m) into the survey, and not from the full power stage in Step 7, suggesting that for these assumptions, ramp-up stages have sufficient energy to cause TTS.

Similarly, Animat 3 received greatest sound exposure during Step 4, Animat 4 during Step 5, and Animat 5 during Step 6; remaining animats received most energy from Step 7.

Recalling that all Animats except 8_{1km} and 8_{3km} are closest to the source 150 seconds (2.5 min) after they start moving, we see that proximity to the source, rather than only the source level, is important for predicting potential impact due to the rapid propagation loss for higher frequency energy. Compare this to the LF group (Figure 44) where animats receive most energy from comparably later stages than the HF group; in this case, the low rates of propagation loss mean that changes in source level have a greater effect on range predictions than for the HF group.

We note that Animat 1 under the HF-shifted source (Figure 49) has a received level trace over time that looks very different from the remaining traces. The received level of this animat decreases faster than for the remaining animats in the same scenario. We think this likely reflects a model artefact where the model resolution and the relative position of receiving point and the nearest radial have resulted in a lowered received level than should have been (received level are interpolated from nearest points, where there is no direct overlap with calculated levels, see Section 7.3.5.2).

11.3.3. Source directionality

It should be noted that dBSea assumes radially symmetrical sources, whereas the source directivity indicates that sound levels in the broadside directions are greater than in the endfire directions, particularly between 100 and 400 Hz (Figure 9) where LF weighting curves are near zero. However, for these modelling assumptions, we do not see the largest exposure when the receiver is on the survey line, rather we see it when the receiver has moved some way to port side, where the modelled source reflects the intended source level in that direction, indicating that broadside source level is a good estimate of the relevant source characteristics.

11.4. Conclusions

For the LF group, we can cautiously conclude that as Animat 3, being 2.01 km from the vessel when at Step 7, is predicted to receive cumulative levels not exceeding the PTS onset level, and Animat 8_{3km} is predicted to receive levels over the threshold and is closest at 1.80 km, an estimate of PTS range could lie in this interval (1801-2008 m). Given the modelling assumptions, the basic animal movement regime, and for a single studied survey line, the ramping up of the source sound level is a valid mitigation approach.

For the HF group there are two scenarios:

- The original source function where Animat 8_{1km} exceeds the TTS limit, but Animat 8_{3km} does not, suggesting a range for TTS onset levels in this example of 772–1801 m.
- The source including the inter-source-model difference for higher frequencies, where all animats bar Animat 1 receive total sound exposure exceeding the TTS onset level. Animat 8_{1km} receives

levels exceeding the PTS onset threshold, but Animat 8_{3km} does not, suggesting a range for PTS onset levels of 772–1801 m.

Animats 1-3 are all predicted to accumulate less energy than the PTS onset level over the duration of the first survey line, when starting movement 500 m from the array. This lends credibility to the 500 m exclusion zone suggested by the JNCC (2017), provided the received level from ramp-up stages are enough to elicit movement, and that the movement is comparable to what is used here.

Both animat groups receive most of their exposure in a relatively short time window (LF group: -10 dB width: 20–40 min. HF group: -10 dB width: 15–20 min[5]), compared to the line duration, and reducing the exposure during these windows would do much to reduce overall impact. For the HF group this can be achieved with lower high-frequency energy content in combination with relatively modest exclusion zones. For the LF group, the reduction in source level would have to be from ~100 Hz and up. This might not be feasible with current source types/levels as even starting receiver movement three kilometres from the source causes exceedance of the PTS limit. Larger exclusion zone might be hard to manage practically (though easier than for smaller cetaceans) and mitigation would therefore have to be related to changes in sound energy emitted radially from the source. Reducing the overall sound level, changing frequency content, or improving directivity (relatively more energy directed directly down) can all help to mitigate impacts.

[5] Excluding $A8_{3km}$ with a -10dB width of 90–120 min.

12. Mobile Receivers: Animat Modelling

The animat modelling and calculation of cumulated sound exposure was performed using the JASCO Animal Simulation Model Including Noise Exposure (JASMINE) with sound fields generated using MONM-BELLHOP; a description of JASMINE is provided in Appendix R. It should also be noted that the ranges presented in this section correspond to the minimum closest point of approach (CPA) distances to individual animats; here, the 95th percentile results are taken from all minimum CPAs of animats receiving levels exceeding the specified sound level threshold. This is different from R_{max} and $R_{95\%}$ ranges which are more suitable for static receivers.

12.1. Low-frequency Cetaceans – North Sea Deep Environment

In the baseline modelling, Scenario 5 - the North Sea Deep environment generated the greatest ranges to PTS onset levels for low-frequency cetaceans. To provide further insight into the possible sound exposure, modelling runs using JASMINE were performed using modelled sound field results for Scenario 5 for over 320,000 animat receivers. The receivers followed the behavioural guidelines defined for the minke whale (*Balaenoptera acutorostrata)* as this is the most common and widely distributed species of baleen whales within UK waters; the behavioural model inputs used in the modelling are provided in Table R-1. The modelling domain was limited to 39.25 km × 50.25 km centred on the survey tracks over the first 24 hours of the survey. Receivers were placed randomly within the domain, and neither interact with each other nor with the survey vessel and streamers. In this study, animat aversion was not used, i.e., animats do not flee at any point due to the sound. Results regarding PTS onset levels are provided in this section; supplemental results for TTS thresholds are included in Appendix S.

12.1.1. PTS exceedance

Of the modelled animats, 389 were subjected to sound levels above the PTS threshold level for low-frequency cetaceans. Of the animats exceeding the PTS threshold, the minimum slant distance (or closest point of approach (CPA) distance) between each animat and the acoustic centre of the airgun array ranged from 7 m to 805 m; the 95th percentile range was 426 m. Figure 51 shows the histogram of the minimum CPA ranges for all animats exceeding the PTS threshold; the count is dominated by animats that have a CPA distance of less than 250 m; a total of 9 animats had minimum CPA ranges of greater than 500 m.

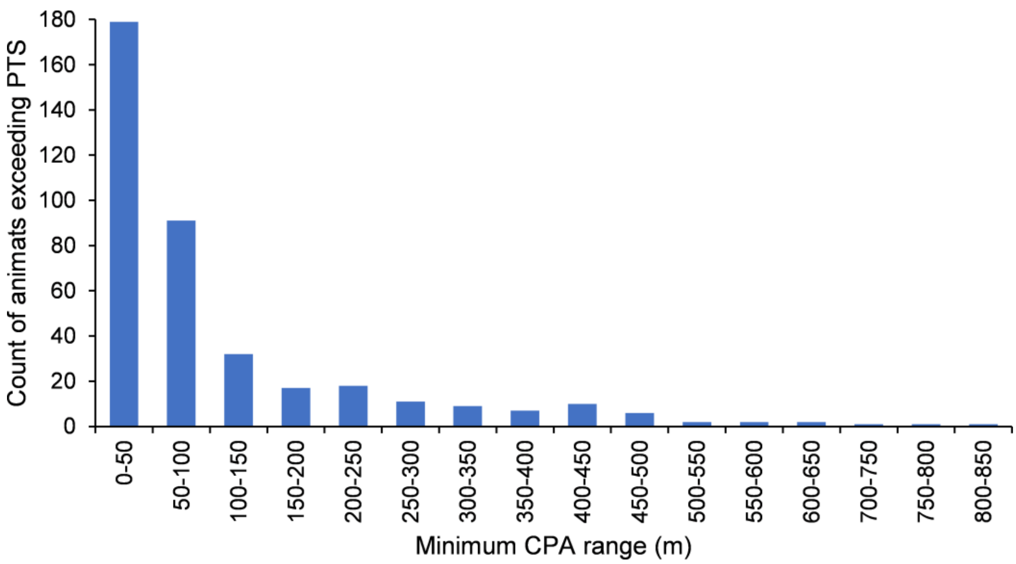

Figure 51. Minimum CPA distances of animats exceeding PTS threshold.

The histogram of the received levels of all animats experiencing levels greater than the PTS threshold is shown in Figure 52. Here, we see a drop off towards the higher levels. There is an exception at 200–201 dB re 1 µPa²s where there is an apparent spike in incidences (count of 14 animats); this artefact is due to the resolution of the sound fields around the source. The sound fields have a radial resolution of 20 m, and all animats in this bracket had a minimum CPA within 20 m. There is also a significant difference between the sound level at the surface (where the animat spends much of its time) and tens of metres down. The spike is caused by a single type of behaviour occurring within the 20 m exposing the animat to a level significantly greater than anything else experienced.

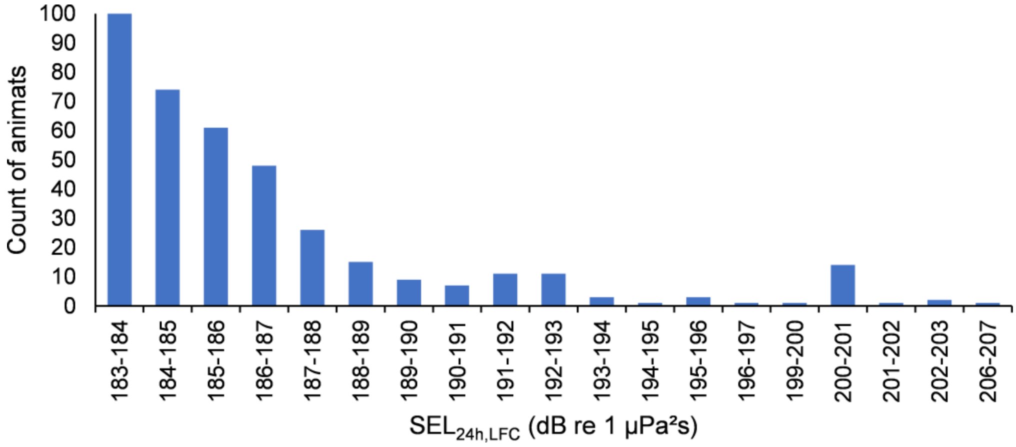

Figure 52. Distribution of received levels of animats exceeding the PTS threshold.

12.1.2. Levels within 500 m

In total, 3567 animats came within 500 m of the airgun array; the distribution of received levels is shown in Figure 53. Of the 3567 animats, 3494 were exposed to levels exceeding the TTS threshold (98%) and 380 were exposed to levels exceeding the PTS threshold (10.7%). The distribution has a modal value of 176–177 dB re 1 µPa²s; the spike at 200–201 dB re 1 µPa²s is the same as that discussed in the PTS exceedance section.

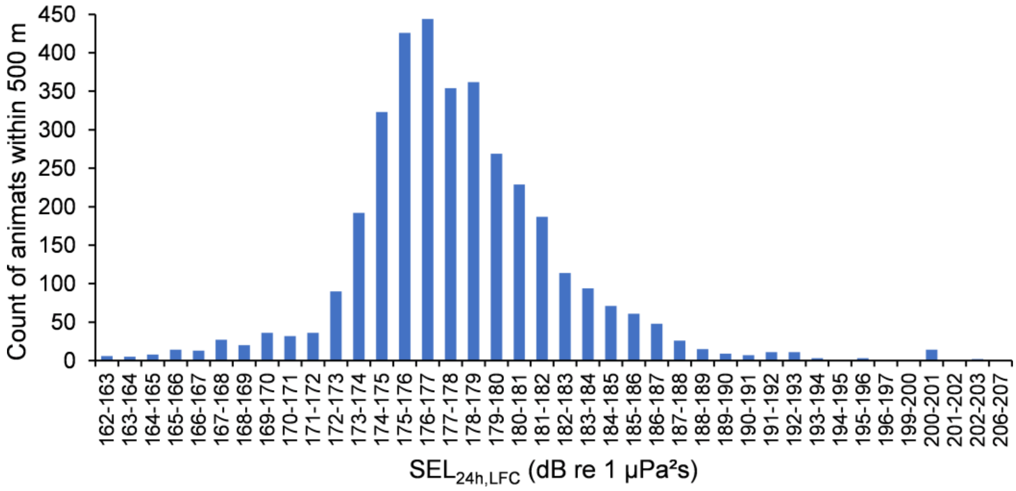

Figure 53. Distribution of received levels of animats with a CPA range within 500 m.

12.2. High-frequency Cetaceans – North Sea Shallow Environment

The results from Section 10.1 showed that ranges to PTS onset levels for high-frequency cetaceans can be highly dependent on the source model. Results in Section 10.4 show that including surface roughness can also greatly affect the impact ranges where the high-frequency energy of the source is significant.

Modelling runs using JASMINE were performed using modelled sound field results for Scenario 4 for 260,000 animat receivers. The receivers followed the behavioural guidelines defined for Harbour Porpoise (Table R-2), and the modelling domain was limited to 39.25 km × 50.25 km centred on the survey tracks over the first 24 hours of the survey. Receivers were placed randomly within the domain, and neither interact with each other nor with the survey vessel and streamers. In this study, animat aversion was not used, i.e., animats do not flee at any point due to the sound. The outputs are therefore likely to be conservative with respect to the harbour porpoise for example, which is known to actively avoid noisy areas.

This section presents the received sound exposure levels for animats for the cases:

- original source levels and no wind;
- source included inter-source-model difference and no wind;
- source included inter-source-model difference and 19.0 knots wind (mean monthly windspeed for area).

Supplemental results for TTS thresholds are included in Appendix S.

12.2.1. PTS exceedance

Of the 260 000 animats, in the case of the original source modelled using AASM, only two were subjected to levels that resulted in exceeding the cumulative threshold for high-frequency cetaceans; the minimum slant distance to the acoustic centre of the array were 5.2 and 6.0 m which would be within the geometry of the array.

Where the high-frequency shifted source was used with no surface reflection loss, the number of animats exceeding the PTS threshold for high-frequency cetaceans rose to 20,432. The maximum range at which an animat exceeded the PTS threshold was 5614 m and the 95th percentile range was 2959 m. The maximum level received by any animat was 169.9 dB re 1 µPa²s (weighted for high-frequency cetaceans). The distribution of received cumulative levels are shown in Figure 54, and the distribution of minimum CPA ranges in Figure 55.

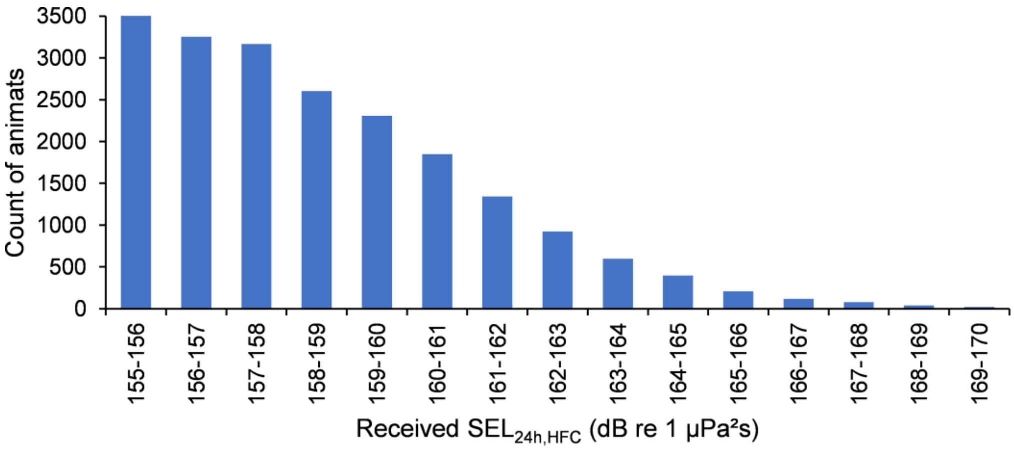

Figure 54. Distribution of received cumulative levels by animats for Scenario 4 using the source including the inter-model difference in source spectrum.

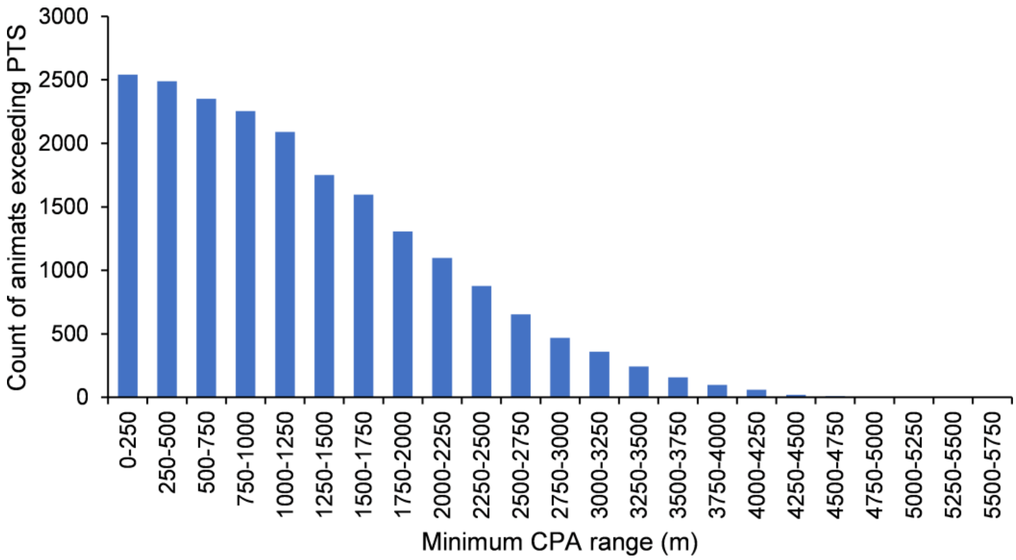

Figure 55. Distribution of minimum CPA ranges for all animats exceeding the PTS thresholds for the source including the inter-model difference for Scenario 4.

The inclusion of surface loss reduces the number of animats exceeding the PTS thresholds; for the median wind case of 19.0 knots, the number of animats exceeding the PTS threshold dropped to 1862. The maximum range at which the PTS threshold was exceeded was 455.0 m with a 95th percentile range being 250.7 m. The maximum level received by any animat was 167.3 dB re 1 µPa²s (weighted for high-frequency cetaceans). The distribution of received cumulative levels are shown in Figure 56, and the distribution of minimum CPA ranges in Figure 57.

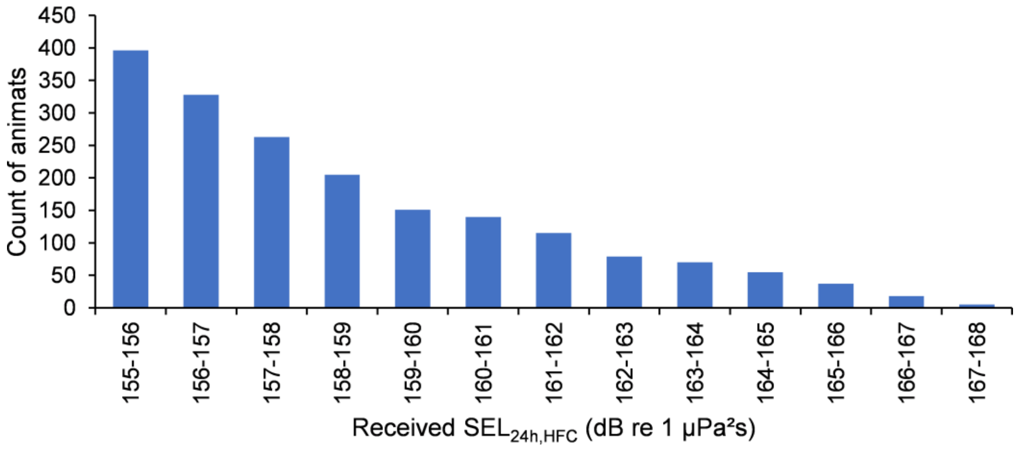

Figure 56. Distribution of received cumulative levels by animats for Scenario 4 using the source including the inter-model-difference in source spectrum and with the inclusion of surface roughness.

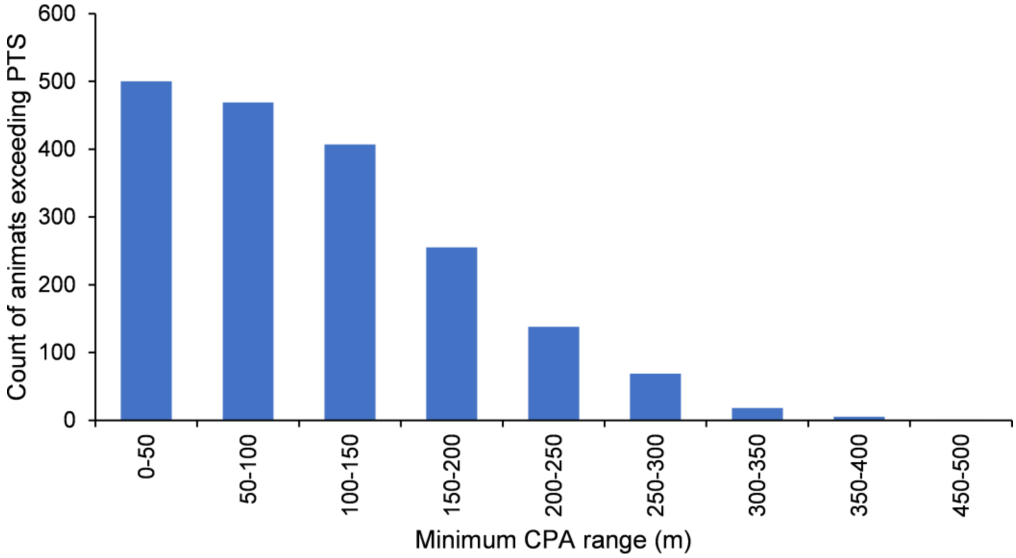

Figure 57. Distribution of minimum CPA ranges for all animats exceeding the PTS thresholds for the source including the inter-model difference for Scenario 4 with the inclusion of surface roughness.

12.2.2. Levels within 500 m

For the modelling runs generated, 5240 of the 260 000 animats came within 500 m of the source at some point during the 24-hour window. Table 62 shows the number of animats exceeding the TTS and PTS levels within 500 m for each of the high-frequency animat scenarios modelled.

Table 62. Number and proportion of animats within 500 m of the source exposed to TTS or PTS levels.

Threshold	Original source no wind	High-frequency shifted source no wind	High-frequency shifted source 19 knot wind
PTS	0 (0%)	5030 (96%)	1862 (36%)
TTS	4823 (92%)	5240 (100%)	5181 (99%)

Figures 58 to 60 show the distribution of received levels by all animats that come within 500 m of the source at any point during the study period for the three cases of the original source and no surface roughness, the high-frequency shifted source and no surface roughness, and the high-frequency shifted source including surface roughness.

Between Figures 58 and 59, the shape of the distribution is very similar with the principal difference being the absolute levels: the peak for the original source is at 144–145 dB re 1 µPa²s, and for the high-frequency shifted source is at 161–162 dB re 1 µPa²s. This is indicative of the propagation and shape of the spectrum being similar for the two cases, and essentially results in a broadband level difference.

The distribution changes when the surface roughness is included as shown in Figure 60; we see a larger distribution of sound levels and levels stretched from the peak towards higher sound levels. As discussed previously, the inclusion of surface roughness generates a compound effect with increasing potency with greater distances; consequently, close to the source, there are similarities to results shown in Figure 59, but as distances increase (along with lower received levels), the loss at the surface produces a cumulative effect and thus levels are reduced further. Comparatively, the peak appears at 152–153 dB re 1 µPa²s.

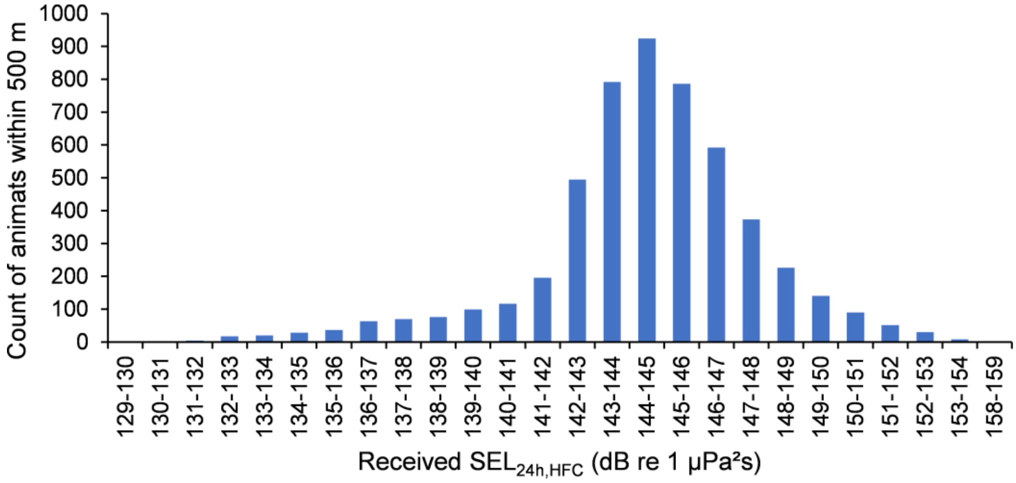

Figure 58. Histogram of received levels by animats (harbour porpoise) within 500 m. Results for original source with no surface roughness.

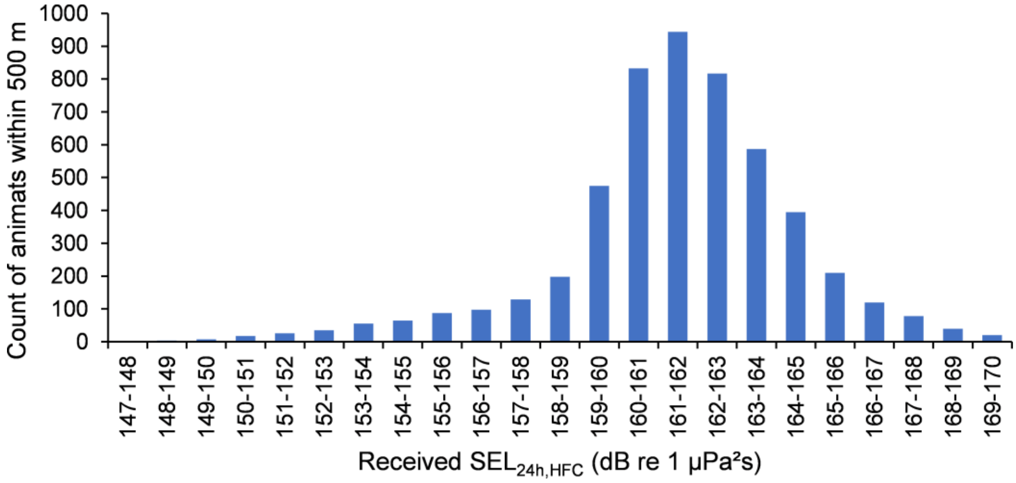

Figure 59. Histogram of received levels by animats (harbour porpoise) within 500 m. Results for source including the inter-model difference and no surface roughness.

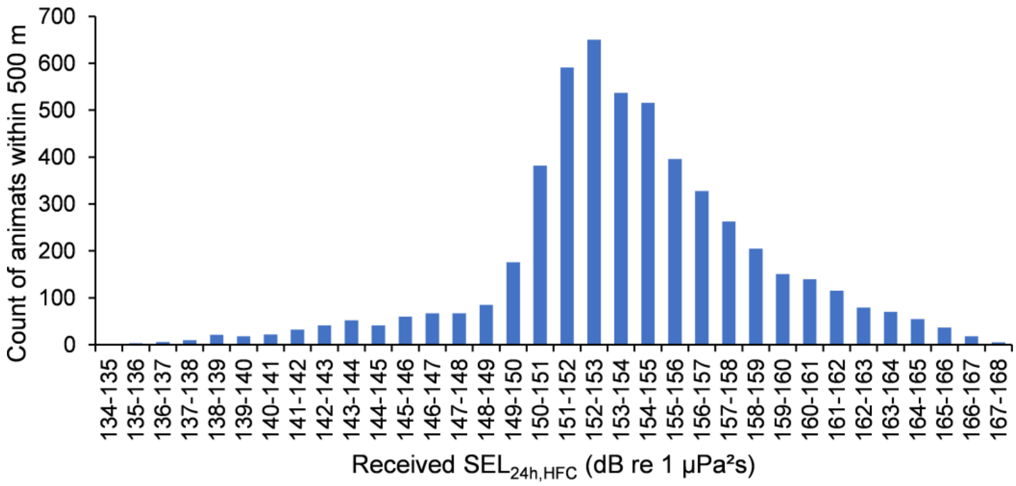

Figure 60. Histogram of received levels by animats (harbour porpoise) within 500 m. Results for source including the inter-model difference with 19.0 knots windspeed generating surface roughness.

12.2.3. Selected individual animats

Examples of the paths and accumulated SEL for three animats from a run including fewer animats are shown in Appendix T and Appendix U respectively; two were chosen that had a minimum CPA of 500 m from the source and the third to be one close to the source as detailed in Table 63. These demonstrate the behaviour of the animats in terms of path and dive profile; note that aversive behaviour is not included. Table 63 and Figure 61 show the maximum single pulse SEL and cumulative SEL experienced by each animat.

Figure U-1 shows the per-pulse SEL and the cumulative SEL over time for the animat coming within 7 m of the acoustic centre of the airgun array source. The point at which this happens is clearly identifiable as being approximately 11.5 hours into the operation. For most of the operation, the level difference between the original source and the HF-shifted source with no surface roughness is between 16–18 dB; however, at the CPA the level difference is only 3.4 dB. In each of the three model runs, the single loudest event has the greatest influence over the cumulative level; the cumulative level rises rapidly at the CPA and further received sound energy generates only a negligible contribution. The surface roughness causes additional high-frequency loss the further the sound travels; this is evident in the differences between the baseline (lower source level; lower propagation loss) and the HF-shifted source with surface roughness results (higher source level; higher propagation loss); for the first 5 hours, at distances far from the source, the baseline results show a higher received level than the HF-shifted source with surface roughness results; at closer ranges, the levels associated with the HF-shifted source are greater.

Figures U-2 and U-3 show the per-pulse SEL and the cumulative SEL over time for the two selected animats coming within approximately 500 m of the acoustic centre of the airgun array source. The main difference between the two sets of results is that Animat 5800 comes near the source just once (at approximately 9.5 hours), whereas Animat 1087 comes near the source twice, resulting in two peaks in the per-pulse SEL. Although, the minimum ranges were similar, the additional peak results in a 5 dB cumulative level increase for Animat 1087 over results for Animat 5800.

Table 63. Received SELs for the three selected animats showing results for the original source, the high-frequency shifted source with no surface roughness, and the high-frequency shifted source with surface roughness.

Animat	Minimum CPA (m)	Orig. source		HF-shifted source - no wind		HF-shifted source - median wind	
		max SEL_{ss}	SEL_{cum}	max SEL_{ss}	SEL_{cum}	max SEL_{ss}	SEL_{cum}
7765	6.8	158.1	158.6	161.5	166.8	161.5	164.4
1087	501.8	124.0	144.5	141.0	161.7	133.1	151.7
5800	501.6	121.9	139.5	138.7	156.7	130.5	146.9

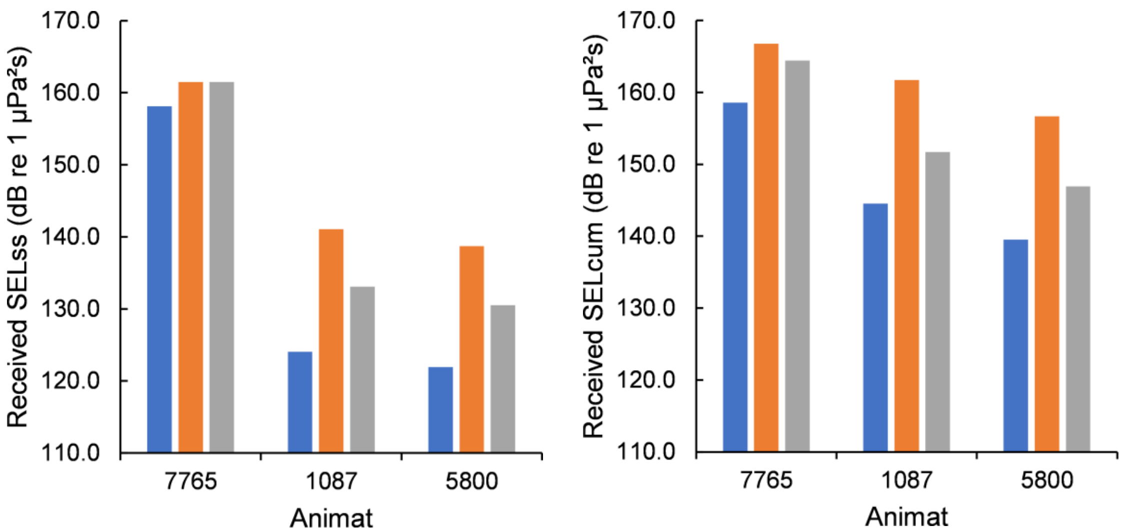

Figure 61. Received SEL (left: per-pulse; right: cumulative) for the three animats: blue: baseline conditions; orange: HF-shifted source with no surface roughness; grey: HF-shifted source with surface roughness.

12.3. Summary of animat modelling results

The work for Phase 3 animat modelling included looking at two scenarios: low-frequency cetaceans in the North Sea Deep environment, and high-frequency cetaceans in the North Sea Shallow environment. Further studies were performed for the high-frequency cetacean scenario to explore the effect of surface roughness on these results.

For the low-frequency cetaceans, the 95th percentile ranges to the thresholds resulting from the animat modelling were:

- PTS exceedance: 426 m (cf. 4.2 km from Phase 2 modelling)
- TTS exceedance: 7.7 km (cf. 42.75 km from Phase 2 modelling)

Within 500 m of the array:

- 10.7% of animats were exposed to levels greater than the PTS threshold
- 98.0% of animats were exposed to levels greater than the TTS threshold

For LF cetaceans, behavioural characteristics for minke whales were used. The results in Section 12.1 showed that the use of animats reduced the modelled impact ranges of the seismic survey compared to both the static receivers (Section 8) and the prescribed motion animats (Section 11.1) despite not including aversive behaviour; any introduction of aversive behaviour would lower the ranges further. The sound levels taken for the Phase 2 baseline modelling using MONM-BELLHOP were at a depth of 10 m, whereas the animats show dive behaviour similar to that in Figure 62; the significant reduction in ranges are due to the paths taken by the animats frequently reaching and remaining at the surface where sound levels, particularly for low-frequency cetaceans, are reduced due to the pressure-release surface at the sea-air interface. The sound exposure for LF cetaceans is more constant over a greater time period than for HF cetaceans due to the lower propagation losses at lower frequencies; due to the exposure being important over a longer period, time spent at the surface substantially reduces the overall exposure.

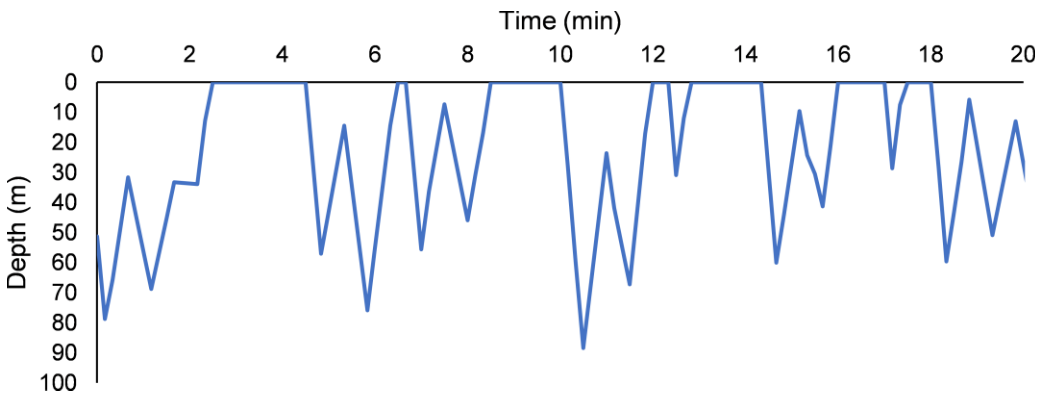

Figure 62. Representative dive behaviour of an example animat following behavioural characteristics for minke whales.

For the high-frequency cetacean group, the 95th percentile ranges to the thresholds resulting from the animat modelling are summarised in Table 64; the equivalent static receiver results are shown in Table 65.

Table 64. Scenario 4: North Sea Shallow environment: Maximum and 95th percentile ranges experienced by moving animats to the frequency weighted SEL_{24h} threshold values defined by the NMFS 2018 criteria.

	Original AASM source		**HF-shifted source - 0 knots wind speed**		**HF-shifted source - 19.0 knots wind speed**	
	R_{max} (km)	$R_{95\%}$ (km)	R_{max} (km)	$R_{95\%}$ (km)	R_{max} (km)	$R_{95\%}$ (km)
PTS (155 dB re 1 μPa²s)	0	0	5.61	2.96	0.46	0.25
TTS (140 dB re 1 μPa²s)	3.45	1.77	18.9	13.4	4.76	2.98

Table 65. Scenario 4: North Sea Shallow environment: Maximum ranges at 10 m depth to the frequency weighted SEL_{24h} threshold values for a static receiver. Results from the Phase 2 baseline modelling.

	Orig. source		**HF-shifted source - no wind**		**HF-shifted source - median wind**	
	R_{max} (km)	$R_{95\%}$ (km)	R_{max} (km)	$R_{95\%}$ (km)	R_{max} (km)	$R_{95\%}$ (km)
PTS (155 dB re 1 μPa²s)	0	0	5.98	4.65	0.43	0.38
TTS (140 dB re 1 μPa²s)	4.65	4.05	30.9	26.3	5.38	4.58

Within 500 m of the array:

- For the original airgun array source:
  - 0% of animats were exposed to levels greater than the PTS threshold
  - 92% of animats were exposed to levels greater than the TTS threshold
- For the HF-shifted source levels and no wind:
  - 96% of animats were exposed to levels greater than the PTS threshold
  - 100% of animats were exposed to levels greater than the TTS threshold
- For the HF-shifted source levels and 19.0 knots wind:
  - 36% of animats were exposed to levels greater than the PTS threshold
  - 99% of animats were exposed to levels greater than the TTS threshold

For HF cetaceans, the behavioural characteristics for harbour porpoise were used. Similarly to the LF cetacean case there was no aversive behaviour. Given that harbour porpoises are typically skittish and very likely to flee, the results presented are a conservative case. The impact ranges generated for the HF animats, while still being markedly lower, are relatively similar to those for the static receiver when compared to the LF cetacean results. This is likely due to the nature of the propagation as the rate of decay over distance is higher for HF-weighted sound than the LF-weighted sound. Consequently, the exposure is dominated by fewer nearby airgun pulses rather than accumulated over a wide area. Additionally, when diving, the animat is typically between 20 to 30 m water depth (Figure T-2) where the modelled sound levels do not vary largely and so the sound fields calculated for the static receiver case (i.e., at 10 m water depth) are relevant here.

The study again highlights the need for wind states to be considered if there is appreciable high-frequency energy in the source. For the source including the inter-model spectrum difference, the ranges are significantly reduced when there is surface roughness. This, however, is dependent on unpredictable weather states for the time of the survey. There would be little effect of surface roughness on the sound propagation for the original source due to the high-frequency energy already contributing little to the overall sound field.

13. Discussion and Conclusions

Several acoustic modelling approaches were compared to provide robust examples of typical scenarios of airgun operation and to gain insight into parameters affecting the resulting sound levels in the modelled domain. The focus in particular was determining distances at which sound levels associated with the use of airgun sound sources during geophysical surveys decrease to below threshold values associated with hearing impairment impacts on marine mammal species. The modelling considered different acoustic environments, covering a wide range of representative scenarios for seismic surveying around the UK continental shelf. Models varied in complexity, from more complex source and sound propagation models to simplistic transmission-loss type models ("$X \log R$"). We focused in particular on the question at what range PTS impacts were predicted by comparing predicted sound levels with available impact threshold criteria, and how these distances related to a nominal mitigation distances of 500 m from a seismic source (JNCC 2017). To understand the sensitivity of model predictions to various model assumptions and uncertainties, different sensitivity studies were carried out. The three main categories for model assumptions, detailed in the following sections, were sound source models, sound propagation models, and animal movement behaviour.

Effect of model assumptions and uncertainties on predicted impact distances

For the baseline model estimates, receivers (marine mammals) were assumed to remain stationary. Predictions between models generally agreed on the order of effect distances (small, comparable, or much larger than 500 m, Table 66) with the exception of two cases (phocid pinnipeds, Table 28, Table 32; and LF cetaceans in deep water, Table 34). However, substantial differences in estimated effect distances were present, resulting from differences in model assumptions. Effect distances based on the peak sound pressure level resulted in ranges to PTS impact thresholds of up to 0.54 km (HF cetaceans in Scenario 4); additionally, results between models were more consistent than for the SEL_{24h} predictions (Tables 36 and 37). Ranges calculated using the SEL_{24h} metric generated similar or greater ranges than equivalent $L_{p,\mathrm{pk}}$ results, and showed much greater variation between models. For this reason, further discussion of model uncertainties focuses on the SEL_{24h} based results.

Generally, the predicted effect distances were largest for the LF cetacean category. The models predicted a lower impact on LF cetaceans for the VSP survey (Scenario 2) than for the Site Survey (Scenario 1), even though the energy source level of the VSP was larger. This was a consequence of the accumulation over a larger number of airgun transmissions, and the lower frequency content in the VSP source array. Hence, the airgun array size is not necessarily a proxy for the effect distance. The largest effect distances were predicted for the Regional Surveys (Scenario 3–6), which were caused by the larger airgun array volume than the Site Survey, even though the Site Survey had a larger number of transmissions within the studied 24-hour window.

Table 66. Range of ranges to NMFS SEL_{24h} PTS thresholds for all scenarios, assuming no increased high frequency content (default scenario; same as Table 36).

Scenario	LF Cetacean		MF Cetacean		HF Cetacean		Phocid Pinniped	
	min (km)	max (km)	min (km)	max (km)	min (km)	max (km)	min (km)	max (km)
1	1.73	4.45	0	<0.1	0	<0.1	0	0.2
2	1.18	1.8	0	<0.1	0	0.2	0	0.2
3	1.6	5.5	0	<0.1	0	0.3	0	0.6
4	4.66	5.4	0	<0.1	0	0.5	0	1.3
5	4.66	9.93	0	<0.1	0	0.1	0	0.6
6	0.15	5.7	0	<0.1	0	<0.1	<0.01	<0.1
ALL	0.15	9.93	0	<0.1	0	0.5	0	1.3

The models, MONM and dBSea, are based on similar principles but in some cases generated large differences in ranges to thresholds. As discussed in Section 8.3, the source is treated very differently between the two models with dBSea having no azimuthal variation, and MONM having no vertical variation. A combination of the source treatment and the use of a single receiver depth at 10 m likely contributed to the large differences between the two models in the Scenario 6 environment; the difference in the predicted range to the PTS onset level was significantly reduced when considering the maximum level over depth as shown in Table 50. A receiver located at 10 m depth does not generate the most conservative estimate and consequently it is common to use a maximum-level-over depth or single deep receiver for estimating the effect distance as these are less influenced by the sea surface pressure release boundary.

The Soprano model differs from MONM and dBSea in that it is based on a normal mode approximation rather than the parabolic equation method; other differing factors are shown in Table 23. The model is not designed for large water depths and the results are less reliable in deeper waters. No range-dependent bathymetry was adopted in SOPRANO, but this is unlikely to affect results significantly as in the shallow water scenarios the bathymetry is slowly varying within the typical ranges of interest (i.e., those for PTS threshold levels). The effect of sound speed profile on the predicted effect distances was negligible for PTS distances (~1%) but can be significant (up to 200%) for TTS distances for LF cetaceans (i.e. especially relevant for large distances). The use of iso-velocity in the environments considered therefore is a reasonable assumption for predicting PTS effect distances where the effects of refraction are small.

The sensitivity study identified several parameters that influenced the predicted effect distances, which were species and environment specific.

Although air gun source models generally agree well for predicting low-frequency energy content (Ainslie et al. 2016), variability is high for energy content of the airgun sounds for frequencies above 1 kHz. In this study, the effect of this variability was investigated by increasing the high-frequency content in the airgun source model to match the highest levels predicted in the Ainslie et al. (2016) model comparison. The baseline results used AASM which, as shown in Figure 33, generated high-frequency energies that fell between the minimum and maximum of the source level predictions.

The increased high-frequency content in the airgun source model mostly affected the predicted effect distances for HF cetaceans. This adjustment increased the predicted PTS effect distances for HF cetaceans from approximately 500 m to 6.0 km (Table 46) depending on propagation model and assuming the receiving animal remains stationary. Additionally, it is currently not clear which source model best matches measurements at those higher frequencies, and more model and measurement comparisons are required to validate source models in that frequency regime.

The inclusion of surface loss due to rough sea surfaces caused by wind in the sound propagation model had a large effect on predicted PTS distances for HF cetaceans. In general, it is not known prior to the survey what weather will occur; however, seismic surveys are nominally limited during poor weather and high sea state conditions as these effect the quality of seismic data being collected by creating excessive unwanted signals. In this study we considered the range of 0 wind speed (flat sea surface, and no surface losses) to 19 knots, which corresponds roughly to the maximum wind speeds in which surveys can operate. The surface losses at the highest wind speeds (i.e., highest losses) were found to reduce high-frequency energy enough such that the ranges were more similar to those using the original airgun array source (Table 51). For intermediate wind speeds, the increased high-frequency energy loss compared to the flat-sea case did not entirely offset the increased high frequency content in the airgun source spectrum and so led to an increase in ranges to identified sound thresholds.

The geoacoustics can play a significant role on the range determination. From the baseline work, the main difference between the two shallow water environments is in the silt in Scenario 3, and the sand in Scenario 4. The sand has greater acoustic reflectivity than the silt and so ranges for this environment were generally increased. At some distance below the sediment layer the geology transitions to a stiffer, rockier sub-layer. The example presented for mudstone (Table 53) shows that in certain cases, it can have only little effect on the sound fields. There are other examples, however, that show that the geoacoustic properties of the sub-layer may contribute to the overall field (Figure 42). Inclusion of the sub-layer is only important for LF cetaceans at larger distances from the array. The higher frequency energy retained in the HF and MF frequency weighting curves is lost into the sediment, and the SEL will be dominated by nearby exposures during close encounters.

It is also important to consider that, due to potential low rates of decay in sound levels with distance, a slight change in sound level can equate to a large difference in range. For instance, for a fall-off of received level with range following "$X \log R$" and with X between 15 and 18, a 3 dB model difference would result in an effect distance of a factor approximately 1.5. This is more the case for LF cetaceans than MF or HF cetaceans due to the lower frequency content and lower rates of decay.

Section 9 investigated the use of frequently adopted simplified propagation loss expressions. These analytical formulas that consider empirical transmission loss with range (generally described in term of "$X \log R$", where X is a scaling factor and R is the distance) have the potential to either under or overpredict the potential effect distances, compared to more complex models with the similar assumptions (stationary animals). These models are not suitable to be used to calculate propagation loss in conjunction with a source level term in most cases.

Sections 11 and 12 introduced animal motion into the scenarios, with Section 11 providing results for receivers in prescribed motion travelling perpendicular to the sail lines, and Section 12 using behavioural models to mimic real-life behaviours. The effect of including animal movement was to reduce the predicted effect distances for LF cetaceans significantly for both models; for HF cetaceans, however, there were mixed results with the prescribed motion directly away from the source path reducing exceedances and behavioural algorithms showing little difference. For LF cetaceans, the baseline modelling had ranges to PTS onset levels of 7.8 and 4.66 km (dBSea and MONM respectively); the prescribed motion (using dBSea's sound fields) brought this down to 1.8–2.0 km and use of the behavioural algorithms (using MONM's sound fields) reduced it down to 426 m.

For the mobile HF cetacean results, the prescribed fleeing motion saw ranges to PTS onset levels reduced from 3.3 km to in the region of 0.77–1.8 km compared to the stationary receiver case. In the case of the behavioural motion results, the PTS effect distances predicted were less strongly affected, with a reduction of ~10%-50% in effect distance. The results for the HF and the LF cetaceans differed due to the nature of the radiated sound. The rate of decay of the HF-weighted sound is greater than for the LF-weighted sound due to increased absorption in the medium, greater losses from seabed reflections, and, where present, greater losses from surface roughness. Consequently, where impact levels for HF cetaceans are exceeded, they are typically caused by a few nearby shots as sound sources further away have less influence. In the case of low-frequency weighted sound, however, the lower rates of decay mean that sounds emanating from greater distances can contribute appreciably to the received level at a point. In terms of the animat modelling it means that impact levels for HF cetaceans are more likely to be exceeded due to fewer high level nearby acoustic events than for results from the entire 24-hour survey; in the case of the prescribed motion in Section 11, the more significant nearby events don't happen as the animal is already fleeing. For LF cetaceans, impact threshold exceedance in these examples resulted from accumulated levels over a longer period and at a greater range as the rate of sound drop off is less than for the HF-weighted; consequently, when taking certain behavioural models into account there is a marked reduction in impact ranges compared to the static receivers.

In the assessments in Section 12, aversive behaviour was not included such that any potential avoidance responses animals may have to the sound sources were neglected. Responses such as moving away from the sound source have been reported to occur for marine mammals (i.e., porpoises, and some baleen whale species, such as minke whales) in relation to seismic surveys or other sound sources (Stone and Tasker 2006, Pirotta et al. 2014, Sarnocińska et al. 2020); a direct fleeing response, that takes the receiver away from the survey line, would reduce the exposure levels and, therefore, the potential effect distances further.

It is worth noting, however, that the cases presented here are far from exhaustive and that there are situations where the fleeing response can lead to greater exposure. The work in Section 11 presumed that the receiver would flee perpendicular to the survey line; this particular assumption provides paths that are close to optimal, and any deviation from this will increase the overall received levels. A reported example is the case of a flee response directly away from the sound source that takes it in the same direction as the survey line (Ford et al. 2005, Kvadsheim et al. 2017); in this case, it is likely that there would be an increase in exposure levels over the stationary receiver case. Consequently, it would be prudent also to consider alternative receiver paths that are less than the ideal case.

Based on this study, general conclusions can be drawn on what the expected effect distances are for seismic surveys (summarized in Table 67). The predicted risk for animals outside the currently employed mitigation distance of 500 m depends strongly on the assumptions made in the models. The dominant model uncertainties affecting these outcomes are shown for each species are listed in Table 67. Trends are presented for pessimistic estimates (including factors such as static receivers and increased high frequency energy) and optimistic estimates (including animal movement for example).

Table 67. Summary of predicted risk of PTS within 500 m during seismic surveys for different species categories, and the dominant model uncertainties associated with these estimates.

Auditory Group	Predicted range to PTS >500 m	Pessimistic estimate of range to PTS (km)	Optimistic estimate of range to PTS (km)	Dominant uncertainties
LF cetaceans	Possible	10	<0.5	Propagation model, bottom parameters, animal movement
MF cetaceans	Unlikely	<0.1	—	
HF cetaceans	Possible	6.0	<0.5	High-frequency content, surface loss, animal movement
Phocid in water*	Possible	1.3	—	Propagation model, bottom parameters, animal movement

* effect of high frequency content in airgun source spectrum not considered for this auditory group in this study

The model comparison in this study shows that although the models generally agree in the order of effect predicted, they do differ quantitatively and that more model validation is required. From these uncertainties, whilst some are due to differences in model implementations and assumptions (e.g., inclusion of source directionality, sound speed profile, or depth at which the effect is estimated) others are inherently due to unknowns in the environments (e.g. bottom parameters, weather conditions), which may not be well known during the permitting process prior to the actual surveys, or due to variability in animal movement.

Based on this study, the following recommendations are given to further improve the realism of these assessments:

- Source models: compare source models with airgun measurements to evaluate whether the high frequency content is well predicted.
- Propagation models: carry out benchmarking (check for agreement of model implementation in conditions where the outcome is known), and model/data comparison for seismic surveys in shallow waters.
- We caution against the use of "$X \log R$" type model predictions except where:
  - proper motivation is provided for the validity of the slopes (X) for the environment and distances;
  - appropriate correction terms (A in "$A + B \log R$"), are used;
  - appropriate source levels are used, i.e., no extrapolated values based on an "$X \log R$" trend.
- Animal behaviour is useful to consider in the assessments to avoid over-conservative estimates of effect distances. It should be noted that if movement modelling is employed without aversive behaviour, there may be limited benefit for HF cetaceans due to exceedance typically being caused by fewer nearby shots.

Glossary

1/3-octave
One third of an octave. Note: A one-third octave is approximately equal to one decidecade (1/3 oct ≈ 1.003 ddec; ISO 2017).

1/3-octave-band
Frequency band whose bandwidth is one one-third octave. Note: The bandwidth of a one-third octave-band increases with increasing centre frequency.

absorption
The reduction of acoustic pressure amplitude due to acoustic particle motion energy converting to heat in the propagation medium.

acoustic impedance
The ratio of the sound pressure in a medium to the rate of alternating flow of the medium through a specified surface due to the sound wave.

attenuation
The gradual loss of acoustic energy from absorption and scattering as sound propagates through a medium.

audiogram
A graph of hearing threshold level (sound pressure levels) as a function of frequency, which describes the hearing sensitivity of an animal over its hearing range.

Auditory frequency weighting (auditory weighting function, frequency-weighting function)
The process of band-pass filtering sounds to reduce the importance of inaudible or less-audible frequencies for individual species or groups of species of aquatic mammals (ISO 2017). One example is M-weighting introduced by Southall et al. (2007) to describe "Generalized frequency weightings for various functional hearing groups of marine mammals, allowing for their functional bandwidths and appropriate in characterizing auditory effects of strong sounds".

azimuth
A horizontal angle relative to a reference direction, which is often magnetic north or the direction of travel. In navigation it is also called bearing.

bandwidth
The range of frequencies over which a sound occurs. Broadband refers to a source that produces sound over a broad range of frequencies (e.g., seismic airguns, vessels) whereas narrowband sources produce sounds over a narrow frequency range (e.g., sonar) (ANSI/ASA S1.13-2005 R2010).

bar
Unit of pressure equal to 100 kPa, which is approximately equal to the atmospheric pressure on Earth at sea level. 1 bar is equal to 10^5 Pa or 10^{11} µPa.

broadband sound level
The total sound pressure level measured over a specified frequency range. If the frequency range is unspecified, it refers to the entire measured frequency range.

broadside direction
Perpendicular to the travel direction of a source. Compare with endfire direction.

cetacean
Any animal in the order Cetacea. These are aquatic, mostly marine mammals and include whales, dolphins, and porpoises.

compressional wave
A mechanical vibration wave in which the direction of particle motion is parallel to the direction of propagation. Also called primary wave or P-wave.

continuous sound
A sound whose sound pressure level remains above ambient sound during the observation period (ANSI/ASA S1.13-2005 R2010). A sound that gradually varies in intensity with time, for example, sound from a marine vessel.

decade
Logarithmic frequency interval whose upper bound is ten times larger than its lower bound (ISO 2006).

decidecade
One tenth of a decade (ISO 2017). Note: An alternative name for decidecade (symbol ddec) is “one-tenth decade”. A decidecade is approximately equal to one third of an octave (1 ddec ≈ 0.3322 oct) and for this reason is sometimes referred to as a “one-third octave”.

decidecade band
Frequency band whose bandwidth is one decidecade. Note: The bandwidth of a decidecade band increases with increasing centre frequency.

decibel (dB)
One-tenth of a bel. Unit of level when the base of the logarithm is the tenth root of ten, and the quantities concerned are proportional to power (ANSI S1.1-1994 R2004).

delphinid
Family of oceanic dolphins, or Delphinidae, composed of approximately thirty extant species, including dolphins, porpoises, and killer whales.

endfire direction
Parallel to the travel direction of a source. See also broadside direction.

ensonified
Exposed to sound.

equal-loudness contour
A curve or curves that show, as a function of frequency, the sound pressure level required to cause a given loudness for a listener having normal hearing, listening to a specified kind of sound in a specified manner (ANSI S1.1-1994 R2004).

far-field
The zone where, to an observer, sound originating from an array of sources (or a spatially distributed source) appears t o radiate from a single point. The distance to the acoustic far-field increases with frequency.

frequency
The rate of oscillation of a periodic function measured in cycles-per-unit-time. The reciprocal of the period. Unit: hertz (Hz). Symbol: *f*. 1 Hz is equal to 1 cycle per second.

hearing group
Groups of marine mammal species with similar hearing ranges. Commonly defined functional hearing groups include low-, mid-, and high-frequency cetaceans, pinnipeds in water, and pinnipeds in air.

geoacoustic
Relating to the acoustic properties of the seabed.

ghost
The reflection of the acoustic source from the sea surface that typically interferes with the signal received directly from the source.

hertz (Hz)
A unit of frequency defined as one cycle per second.

high-frequency (HF) cetacean
The functional cetacean hearing group that represents those odontocetes (toothed whales) specialized for hearing high frequencies.

impulsive sound
Sound that is typically brief and intermittent with rapid (within a few seconds) rise time and decay back to ambient levels (NOAA 2013, ANSI S12.7-1986 R2006). For example, seismic airguns and impact pile driving.

lobe
Common feature of directivity patterns defining angles at which the radiated energy is a maximum.

low-frequency (LF) cetacean
The functional cetacean hearing group that represents mysticetes (baleen whales) specialized for hearing low frequencies.

median
The 50th percentile of a statistical distribution.

mid-frequency (MF) cetacean
The functional cetacean hearing group that represents those odontocetes (toothed whales) specialized for mid-frequency hearing.

Monte Carlo simulation
The method of investigating the distribution of a non-linear multi-variate function by random sampling of all of its input variable distributions.

mysticete
Mysticeti, a suborder of cetaceans, use their baleen plates, rather than teeth, to filter food from water. They are not known to echolocate, but they use sound for communication. Members of this group include rorquals (Balaenopteridae), right whales (Balaenidae), and grey whales (*Eschrichtius robustus*).

non-impulsive sound
Sound that is broadband, narrowband or tonal, brief or prolonged, continuous or intermittent, and typically does not have a high peak sound pressure with rapid rise time (typically only small fluctuations in decibel level) that impulsive signals have (ANSI/ASA S3.20-1995 R2008). For example, marine vessels, aircraft, machinery, construction, and vibratory pile driving (NIOSH 1998, NOAA 2015).

octave
The interval between a sound and another sound with double or half the frequency. For example, one octave above 200 Hz is 400 Hz, and one octave below 200 Hz is 100 Hz.

odontocete
The presence of teeth, rather than baleen, characterizes these whales. Members of the Odontoceti are a suborder of cetaceans, a group comprised of whales, dolphins, and porpoises. The skulls of toothed

whales are mostly asymmetric, an adaptation for their echolocation. This group includes sperm whales, killer whales, belugas, narwhals, dolphins, and porpoises.

parabolic equation method
A computationally efficient solution to the acoustic wave equation that is used to model transmission loss. The parabolic equation approximation omits effects of back-scattered sound, simplifying the computation of transmission loss. The effect of back-scattered sound is negligible for most ocean-acoustic propagation problems.

peak sound pressure level (PK)
The maximum sound pressure magnitude, expressed as a level, in a stated frequency band, within a stated period. Also called zero-to-peak sound pressure level. Unit: decibel (dB).

percentile level, exceedance
The sound level exceeded n% of the time during a measurement.

permanent threshold shift (PTS)
A permanent loss of hearing sensitivity caused by excessive noise exposure. PTS is considered auditory injury.

phocid
A common term used to describe all members of the family Phocidae. These true/earless seals are more adapted to in-water life than are otariids, which have more terrestrial adaptations. Phocids use their hind flippers to propel themselves. Phocids are one of the three main groups in the superfamily Pinnipedia; the other two groups are otariids and walrus.

phocid pinnipeds in water (PPW)
The functional pinniped hearing group that represents true/earless seals under water.

pinniped
A common term used to describe all three groups that form the superfamily Pinnipedia: phocids (true seals or earless seals), otariids (eared seals or fur seals and sea lions), and walrus.

point source
A source that radiates sound as if from a single point (ANSI S1.1-1994 R2004).

port throttling
The consideration of the cross-sectional area of the port in producing the bubble involved in airgun source generation.

power spectrum density
Generic term, formally defined as power in W/Hz, but sometimes loosely used to refer to the spectral density of other parameters such as square pressure or time-integrated square pressure.

pressure, acoustic
The deviation from the ambient hydrostatic pressure caused by a sound wave. Also called overpressure. Unit: pascal (Pa). Symbol: p.

propagation loss (PL)
The decibel (dB re m^2) reduction in sound level between an acoustic source and a receiver as a result of sound propagating away from the source subject to the influence of the surrounding environment. Compare with transmission loss.

received level (RL)
The sound level measured (or that would be measured) at a defined location.

reflection loss
The ratio of power between a reflected wave and the incident wave when sound hits a boundary.

rms
root-mean-square.

shear wave
A mechanical vibration wave in which the direction of particle motion is perpendicular to the direction of propagation. Also called secondary wave or S-wave. Shear waves propagate only in solid media, such as sediments or rock. Shear waves in the seabed can be converted to compressional waves in water at the water-seabed interface.

signature
Pressure signal generated by a source.

sound
A time-varying pressure disturbance generated by mechanical vibration waves travelling through a fluid medium such as air or water.

sound exposure
Time integral of squared, instantaneous frequency-weighted sound pressure over a stated time interval or event. Unit: pascal-squared second ($Pa^2 \cdot s$) (ANSI S1.1-1994 R2004).

sound exposure level (SEL)
A cumulative measure related to the sound energy in one or more pulses. Unit: dB re 1 $\mu Pa^2 \cdot s$. SEL is expressed over the summation period (e.g., per-pulse SEL [for airguns], single-strike SEL [for pile drivers], 24-hour SEL).

sound field
Region containing sound waves (ANSI S1.1-1994 R2004).

sound speed profile
The speed of sound in the water column as a function of depth below the water surface.

source level (SL)
The sound level measured in the far-field and scaled back to a standard reference distance of 1 metre from the acoustic centre of the source. Unit: dB re 1 $\mu Pa \cdot m$ (pressure level) or dB re 1 $\mu Pa^2 \cdot s \cdot m$ (exposure level).

spectrum
An acoustic signal represented in terms of its power, energy, mean-square sound pressure, or sound exposure distribution with frequency.

surface duct
The upper portion of a water column within which the sound speed profile gradient causes sound to refract upward and therefore reflect off the surface resulting in relatively long-range sound propagation with little loss.

temporary threshold shift (TTS)
Temporary loss of hearing sensitivity caused by excessive noise exposure.

thermocline
The depth interval near the ocean surface that experiences temperature gradients due to warming or cooling by heat conduction from the atmosphere and by warming from solar heating.

transmission loss (TL)
The decibel (dB re 1) reduction in sound level between two stated points that results from the radiation of sound subject to the influence of the surrounding environment. Compare with propagation loss.

wavelength
Distance over which a wave completes one cycle of oscillation. Unit: metre (m). Symbol: λ.

Bibliography

[BGS] British Geological Survey. 2018. *Marine Sediments 250k* (webpage). http://www.bgs.ac.uk/products/offshore/DigSBS250.html.

[ISO] International Organization for Standardization. 2006. *ISO 80000-3:2006 Quantities and units – Part 3: Space and time*. https://www.iso.org/standard/31888.html.

[ISO] International Organization for Standardization. 2017. *ISO 18405:2017. Underwater acoustics – Terminology*. Geneva. https://www.iso.org/standard/62406.html.

[JNCC] Joint Nature Conservation Committee. 2017. *JNCC guidelines for minimising the risk of injury to marine mammals from geophysical surveys*. Aberdeen, UK. 26 p. http://jncc.defra.gov.uk/pdf/jncc_guidelines_seismicsurvey_aug2017.pdf.

[NIOSH] National Institute for Occupational Safety and Health. 1998. *Criteria for a recommended standard: Occupational noise exposure. Revised Criteria*. Document Number 98-126. US Department of Health and Human Services, NIOSH, Cincinnati, OH, USA. 122 p. https://www.cdc.gov/niosh/docs/98-126/pdfs/98-126.pdf.

[NMFS] National Marine Fisheries Service (US). 2016. *Technical Guidance for Assessing the Effects of Anthropogenic Sound on Marine Mammal Hearing: Underwater Acoustic Thresholds for Onset of Permanent and Temporary Threshold Shifts*. US Department of Commerce, NOAA. NOAA Technical Memorandum NMFS-OPR-55. 178 p.

[NMFS] National Marine Fisheries Service (US). 2018. *2018 Revision to: Technical Guidance for Assessing the Effects of Anthropogenic Sound on Marine Mammal Hearing (Version 2.0): Underwater Thresholds for Onset of Permanent and Temporary Threshold Shifts*. US Department of Commerce, NOAA. NOAA Technical Memorandum NMFS-OPR-59. 167 p. https://www.fisheries.noaa.gov/webdam/download/75962998.

[NOAA] National Oceanic and Atmospheric Administration (US). 2013. *Draft guidance for assessing the effects of anthropogenic sound on marine mammals: Acoustic threshold levels for onset of permanent and temporary threshold shifts*. National Oceanic and Atmospheric Administration, US Department of Commerce, and NMFS Office of Protected Resources, Silver Spring, MD, USA. 76 p.

[NOAA] National Oceanic and Atmospheric Administration (US). 2015. *Draft guidance for assessing the effects of anthropogenic sound on marine mammal hearing: Underwater acoustic threshold levels for onset of permanent and temporary threshold shifts*. NMFS Office of Protected Resources, Silver Spring, MD, USA. 180 p.

Aerts, L.A.M., M. Blees, S.B. Blackwell, C.R. Greene, Jr., K.H. Kim, D.E. Hannay, and M.E. Austin. 2008. *Marine mammal monitoring and mitigation during BP Liberty OBC seismic survey in Foggy Island Bay, Beaufort Sea, July-August 2008: 90-day report*. Document Number P1011-1. Report by LGL Alaska Research Associates Inc., LGL Ltd., Greeneridge Sciences Inc., and JASCO Applied Sciences for BP Exploration Alaska. 199 p. ftp://ftp.library.noaa.gov/noaa_documents.lib/NMFS/Auke%20Bay/AukeBayScans/Removable%20Disk/P1011-1.pdf.

Ainslie, M.A. 2003. Conditions for the excitation of interface waves in a thin unconsolidated sediment layer. *Journal of Sound and Vibration* (268): 249-267.

Ainslie, M.A. 2010. *Principles of Sonar Performance Modeling*. Praxis Books. Springer, Berlin. https://doi.org/10.1007/978-3-540-87662-5.

Ainslie, M.A., P.H. Dahl, C.A.F. de Jong, and R.M. Laws. 2014. *Practical Spreading Laws: The Snakes and Ladders of Shallow Water Acoustics*. *UA2014 - 2nd International Conference and Exhibition on Underwater Acoustics*, 22-27 Jun 2014, Island of Rhodes, Greece, pp. 879-886.

Ainslie, M.A., M.B. Halvorsen, R.P.A. Dekeling, R.M. Laws, A.J. Duncan, A.S. Frankel, K.D. Heaney, E.T. Küsel, A.O. MacGillivray, et al. 2016. Verification of airgun sound field models for environmental impact assessment [abstract]. *Proceedings of Meetings on Acoustics* 27(1). https://doi.org/10.1121/2.0000339

Ainslie, M.A., C.A.F. de Jong, M.B. Halvorsen, and D.R. Ketten. 2018. *E&P Sound and Marine Life JIP Standard: Underwater Acoustics - Task 1: Terminology*. TNO 2016 R11076.

ANSI S12.7-1986. R2006. *American National Standard Methods for Measurements of Impulsive Noise*. American National Standards Institute, NY, USA.

ANSI S1.1-1994. R2004. *American National Standard Acoustical Terminology*. American National Standards Institute, NY, USA.

ANSI S1.20-1988. R2003. *American National Standard Procedures for Calibration of Underwater Electroacoustic Transducers*. American National Standards Institute, NY, USA.

ANSI/ASA S1.13-2005. R2010. *American National Standard Measurement of Sound Pressure Levels in Air*. American National Standards Institute and Acoustical Society of America, NY, USA.

ANSI/ASA S3.20-1995. R2008. *American National Standard Bioacoustical Terminology*. American National Standards Institute and Acoustical Society of America, NY, USA.

Blix, A.S. and L.P. Folkow. 1995. Daily energy expenditure in free living minke whales. *Acta Physiologica* 153(1): 61-66. https://doi.org/10.1111/j.1748-1716.1995.tb09834.x.

Collins, M.D. 1993. A split-step Padé solution for the parabolic equation method. *Journal of the Acoustical Society of America* 93(4): 1736-1742. https://doi.org/10.1121/1.406739.

Collins, M.D., R.J. Cederberg, D.B. King, and S. Chin-Bing. 1996. Comparison of algorithms for solving parabolic wave equations. *Journal of the Acoustical Society of America* 100(1): 178-182. https://doi.org/10.1121/1.415921.

Coppens, A.B. 1981. Simple equations for the speed of sound in Neptunian waters. *Journal of the Acoustical Society of America* 69(3): 862-863. https://doi.org/10.1121/1.382038.

Croll, D.A., A. Acevedo-Gutiérrez, B.R. Tershy, and J. Urbán-Ramírez. 2001. The diving behavior of blue and fin whales: Is dive duration shorter than expected based on oxygen stores? *Comparative Biochemistry and Physiology Part A* 129(4): 797-809. https://doi.org/10.1016/S1095-6433(01)00348-8.

dBSea. 2019. *Validation of dBSea* (webpage). dBSea. http://www.dbsea.co.uk/validation/.

Ellison, W.T., C.W. Clark, and G.C. Bishop. 1987. *Potential use of surface reverberation by bowhead whales, Balaena mysticetus, in under-ice navigation: Preliminary considerations*. Report of the International Whaling Commission. Volume 37. 329-332 p.

EMODnet Bathymetry Consortium. 2016. *EMODnet Digital Bathymetry (DTM)* (webpage). http://www.emodnet-bathymetry.eu/.

Etter, P.C. 2012. Advanced Applications for Underwater Acoustic Modeling. *Advances in Acoustics and Vibration* 2012: 1-28.

Finneran, J.J. 2015. *Auditory weighting functions and TTS/PTS exposure functions for cetaceans and marine carnivores*. Technical report by SSC Pacific, San Diego, CA, USA.

Finneran, J.J. 2016. *Auditory weighting functions and TTS/PTS exposure functions for marine mammals exposed to underwater noise*. Technical Report for Space and Naval Warfare Systems Center Pacific, San Diego, CA, USA. 49 p. https://apps.dtic.mil/dtic/tr/fulltext/u2/1026445.pdf.

Ford, J.K.B., G.M. Ellis, D.R. Matkin, K.C. Balcomb, D. Briggs, and A.B. Morton. 2005. Killer Whale Attacks on Minke Whales: Prey Capture and Antipredator Tactics. *Marine Mammal Science* 21(4): 603-618.

Frankel, A.S., W.T. Ellison, and J. Buchanan. 2002. Application of the acoustic integration model (AIM) to predict and minimize environmental impacts. *Oceans '02 MTS/IEEE*. 29-31 Oct 2002. IEEE, Biloxi, MI, USA. pp. 1438-1443. https://doi.org/10.1109/OCEANS.2002.1191849.

Funk, D.W., D.E. Hannay, D.S. Ireland, R. Rodrigues, and W.R. Koski. 2008. *Marine mammal monitoring and mitigation during open water seismic exploration by Shell Offshore Inc. in the Chukchi and Beaufort*

Seas, July–November 2007: 90-day report. LGL Report P969-1. Prepared by LGL Alaska Research Associates Inc., LGL Ltd., and JASCO Research Ltd. for Shell Offshore Inc., National Marine Fisheries Service (US), and US Fish and Wildlife Service. 218 p.

Galindo-Romero, M., T. Lippert, and A. Gavrilov. 2015. Empirical prediction of peak pressure levels in anthropogenic impulsive noise. Part I: Airgun arrays signals. *Journal of the Acoustical Society of America* 138(6): EL540-EL544. https://doi.org/10.1121/1.4938269.

Goldbogen, J.A., J. Calambokidis, R.E. Shadwick, E.M. Oleson, M.A. Mcdonald, and J.A. Hildebrand. 2006. Kinematics of foraging dives and lunge-feeding in fin whales. *Journal of Experimental Biology* 209(7): 1231-1244. https://jeb.biologists.org/content/209/7/1231.

Goldbogen, J.A., J. Calambokidis, E. Oleson, J. Potvin, N.D. Pyenson, G. Schorr, and R.E. Shadwick. 2011. Mechanics, hydrodynamics and energetics of blue whale lunge feeding: efficiency dependence on krill density. *Journal of Experimental Biology* 214: 131-146. http://jeb.biologists.org/content/jexbio/214/1/131.full.pdf.

Hannay, D.E. and R.G. Racca. 2005. *Acoustic Model Validation*. Document Number 0000-S-90-04-T-7006-00-E, Revision 02. Technical report for Sakhalin Energy Investment Company Ltd. by JASCO Research Ltd. 34 p.

Hooker, S.K., H. Whitehead, and S. Gowans. 1999. Marine protected area design and the spatial and temporal distribution of cetaceans in a submarine canyon. *Conservation Biology* 13(3): 592-602. https://doi.org/10.1046/j.1523-1739.1999.98099.x

Houser, D.S. and M.J. Cross. 1999. *Marine Mammal Movement and Behavior (3MB): A Component of the Effects of Sound on the Marine Environment (ESME) Distributed Model*. Version 8.08, by BIOMIMETICA.

Houser, D.S. 2006. A method for modeling marine mammal movement and behavior for environmental impact assessment. *IEEE Journal of Oceanic Engineering* 31(1): 76-81. https://doi.org/10.1109/JOE.2006.872204.

Hughes, S.J., D.M.F. Chapman, and N.R. Chapman. 1991. The effect of shear wave attenuation on acoustic bottom loss resonance in marine sediments. *In* Hovem, J.M., M.d. Richard, and R.D. Stoll (eds.). *Shear Waves in Marine Sediments*. Springer. pp. 439-446. https://doi.org/10.1007/978-94-011-3568-9_50.

Ireland, D.S., R. Rodrigues, D.W. Funk, W.R. Koski, and D.E. Hannay. 2009. *Marine mammal monitoring and mitigation during open water seismic exploration by Shell Offshore Inc. in the Chukchi and Beaufort Seas, July–October 2008: 90-Day Report*. Document Number P1049-1. 277 p.

Jansen, E. and C.A.F. de Jong. 2017. Experimental Assessment of Underwater Acoustic Source Levels of Different Ship Types. *IEEE Journal of Oceanic Engineering* 42(2): 439-448. https://doi.org/10.1109/JOE.2016.2644123.

Jensen, F.B., W.A. Kuperman, M.B. Porter, and H. Schmidt. 2011. *Computational Ocean Acoustics*. 2nd edition. AIP Series in Modern Acourics and Signal Processing. AIP Press - Springer, New York. 794 p. https://doi.org/10.1007/978-1-4419-8678-8.

Kraus, S.D., S. Leiter, K. Stone, B. Wikgren, C.A. Mayo, P. Hughes, R.D. Kenney, C.W. Clark, A.N. Rice, et al. 2016. *Northeast Large Pelagic Survey Collaborative Aerial and Acoustic Surveys for Large Whales and Sea Turtles*. US Department of the Interior, Bureau of Ocean Energy Management. OCS Study BOEM 2016-054, Sterling, Virginia. 117 + appendices p. https://www.boem.gov/RI-MA-Whales-Turtles/.

Kvadsheim, P.H., S. DeRuiter, L.D. Sivle, J. Goldbogen, R. Roland-Hansen, P.J.O. Miller, F.-P.A. Lam, J. Calambokidis, A. Friedlaender, et al. 2017. Avoidance responses of minke whales to 1–4kHz naval sonar. *Marine Pollution Bulletin* 121(1): 60-68. https://doi.org/10.1016/j.marpolbul.2017.05.037.

Lepper, P.A., J. Gordon, C. Booth, P.D. Theobald, S.P. Robinson, S.P. Northridge, and L.S. Wang. 2014. *Establishing the sensitivity of cetaceans and seals to acoustic deterrent devices in Scotland*. Report Number 517. Commissioned by Scottish Natural Heritage. 121 p.

Lucke, K., U. Siebert, P. Lepper, A., and M.-A. Blanchet. 2009. Temporary shift in masked hearing thresholds in a harbor porpoise (*Phocoena phocoena*) after exposure to seismic airgun stimuli. *Journal of the Acoustical Society of America* 125(6): 4060-4070. https://doi.org/10.1121/1.3117443.

Lurton, X. 2002. *An Introduction to Underwater Acoustics: Principles and Applications*. Springer, Chichester, UK. 347 p.

MacGillivray, A.O. 2006. *An Acoustic Modelling Study of Seismic Airgun Noise in Queen Charlotte Basin*. MSc Thesis. University of Victoria, Victoria, BC, Canada. 98 p.

MacGillivray, A.O. and N.R. Chapman. 2012. Modeling underwater sound propagation from an airgun array using the parabolic equation method. *Canadian Acoustics* 40(1): 19-25. https://jcaa.caa-aca.ca/index.php/jcaa/article/view/2502/2251.

MacGillivray, A.O. 2019. An Airgun Array Source Model Accounting for High-frequency Sound Emissions During Firing and Solutions to the IAMW Source Test Cases. *IEEE Journal of Oceanic Engineering* 44(3). https://doi.org/10.1109/JOE.2018.2853199.

Macpherson, J.D. and M.J. Daintith. 1967. Practical Model of Shallow-Water Acoustic Propagation. *The Journal of the Acoustical Society of America* 41(4A): 850-854.

Marion, D.P. 1990. *Acoustic, mechanical, and transport properties of sediments and granular materials*. PhD Thesis. Stanford University, Palo Alto, California.

Martin, B., K. Bröker, M.-N.R. Matthews, J.T. MacDonnell, and L. Bailey. 2015. Comparison of measured and modeled air-gun array sound levels in Baffin Bay, West Greenland. *OceanNoise 2015*. 11-15 May 2015, Barcelona, Spain.

Matthews, M.-N.R., D.S. Ireland, R. Brune, D.G. Zeddies, J. Christian, G.A. Warner, T.J. Deveau, H. Frouin-Mouy, S.L. Denes, et al. 2018. *Determining the Environmental Impact of Marine Vibrator Technology: Final Report*. Document Number 01542, Version 1.0. Technical report by JASCO Applied Sciences, LGL Ecological Research Associates Inc., and Robert Brune LLC for the IOGP Marine Sound and Life Joint Industry Programme. https://gisserver.intertek.com/JIP/DMS/ProjectReports/Cat1/JIP-Proj1.6.2_Mar%20Vib%20EA%20Phase%201%20-%20Final%20Report%20rev1.0.pdf.

Mattsson, A. and M. Jenkerson. 2008. Single Airgun and Cluster Measurement Project. *Joint Industry Programme (JIP) on Exploration and Production Sound and Marine Life Proramme Review*. 28-30 Oct 2008. International Association of Oil and Gas Producers, Houston, TX, USA.

Nedwell, J.R. and A.W. Turnpenny. 1998. The use of a generic frequency weighting scale in estimating environmental effect. *Workshop on Seismics and Marine Mammals*. 23–25 Jun 1998, London, UK.

Nedwell, J.R., A.W. Turnpenny, J. Lovell, S.J. Parvin, R. Workman, J.A.L. Spinks, and D. Howell. 2007. *A validation of the* dB_{ht} *as a measure of the behavioural and auditory effects of underwater noise*. Document Number 534R1231 Report prepared by Subacoustech Ltd. for Chevron Ltd, TotalFinaElf Exploration UK PLC, Department of Business, Enterprise and Regulatory Reform, Shell UK Exploration and Production Ltd, The Industry Technology Facilitator, Joint Nature Conservation Committee, and The UK Ministry of Defence. 74 p. https://tethys.pnnl.gov/sites/default/files/publications/Nedwell-et-al-2007.pdf.

O'Neill, C., D. Leary, and A. McCrodan. 2010. Sound Source Verification. (Chapter 3) *In* Blees, M.K., K.G. Hartin, D.S. Ireland, and D.E. Hannay (eds.). *Marine mammal monitoring and mitigation during open water seismic exploration by Statoil USA E&P Inc. in the Chukchi Sea, August-October 2010: 90-day report*. LGL Report P1119. Prepared by LGL Alaska Research Associates Inc., LGL Ltd., and JASCO Applied Sciences Ltd. for Statoil USA E&P Inc., National Marine Fisheries Service (US), and US Fish and Wildlife Service. pp. 1-34.

Osmek, S., J. Calambokidis, J. Laake, P. Gearin, R.A. Delong, J. Scordino, S. Jeffries, and R. Brown. 1996. *Assessment of the Status of Harbor Porpoise (Phocoena phocoena) in Oregon and Washington Waters*. U.S. Department of Commerce, NOAA Technical Memorandum NMFS-AFSC-76. 46 p. https://www.afsc.noaa.gov/Publications/AFSC-TM/NOAA-TM-AFSC-76.pdf.

Otani, S., Y. Naito, A. Kawamura, M. Kawasaki, S. Nishiwaki, and A. Kato. 1998. Diving behavior and performance of harbor porpoises, *Phocoena phocoena*, in Funka Bay, Hokkaido, Japan. *Marine Mammal Science* 14(2): 209-220. https://doi.org/10.1111/j.1748-7692.1998.tb00711.x.

Otani, S., Y. Naito, A. Kato, and A. Kawamura. 2000. Diving behavior and swimming speed of a free-ranging harbor porpoise, *Phocoena phocoena*. *Marine Mammal Science* 16(4): 811-814. http://dx.doi.org/10.1111/j.1748-7692.2000.tb00973.x.

Pickett, G.R. 1963. Acoustic Character Logs and Their Applications in Formation Evaluation. *Journal of Petroleum Technology* 15(06).

Pirotta, E., K.L. Brookes, I.M. Graham, and P.M. Thompson. 2014. Variation in harbour porpoise activity in response to seismic survey noise. *Biology Letters* 10(5): 20131090.

Porter, M.B. and Y.C. Liu. 1994. Finite-element ray tracing. *In*: Lee, D. and M.H. Schultz (eds.). *International Conference on Theoretical and Computational Acoustics*. Volume 2. World Scientific Publishing Co. pp. 947-956.

Racca, R.G., A.N. Rutenko, K. Bröker, and M.E. Austin. 2012a. A line in the water - design and enactment of a closed loop, model based sound level boundary estimation strategy for mitigation of behavioural impacts from a seismic survey. *11th European Conference on Underwater Acoustics*. Volume 34(3), Edinburgh, UK.

Racca, R.G., A.N. Rutenko, K. Bröker, and G. Gailey. 2012b. Model based sound level estimation and in-field adjustment for real-time mitigation of behavioural impacts from a seismic survey and post-event evaluation of sound exposure for individual whales. *In*: McMinn, T. (ed.). *Acoustics 2012*. Fremantle, Australia. http://www.acoustics.asn.au/conference_proceedings/AAS2012/papers/p92.pdf.

Ricciardulli, L., F.J. Wentz, and D.K. Smith. 2011. *Remote Sensing Systems QuikSCAT Ku-2011 Monthly Ocean Vector Winds on 0.25 deg grid, Version 4.* (webpage). Remote Sensing Systems. www.remss.com/missions/qscat. (Accessed 26 April 2016).

Sarnocińska, J., J. Teilmann, J.D. Balle, F.M. van Beest, M. Delefosse, and J. Tougaard. 2020. Harbor Porpoise (*Phocoena phocoena*) Reaction to a 3D Seismic Airgun Survey in the North Sea. *Frontiers in Marine Science* 6(824). https://doi.org/10.3389/fmars.2019.00824.

Sertlek, H.O. and M.A. Ainslie. 2014. A depth-dependent formula for shallow water propagation. *Journal of the Acoustical Society of America* 136(2): 573-82. https://www.ncbi.nlm.nih.gov/pubmed/25096092.

Sertlek, H.O., M.A. Ainslie, and K.D. Heaney. 2018. Analytical and Numerical Propagation Loss Predictions for Gradually Range-Dependent Isospeed Waveguides. *IEEE Journal of Oceanic Engineering*: 1-13.

Southall, B.L., A.E. Bowles, W.T. Ellison, J.J. Finneran, R.L. Gentry, C.R. Greene, Jr., D. Kastak, D.R. Ketten, J.H. Miller, et al. 2007. Marine Mammal Noise Exposure Criteria: Initial Scientific Recommendations. *Aquatic Mammals* 33(4): 411-521.

Southall, B.L., J.J. Finneran, C.J. Reichmuth, P.E. Nachtigall, D.R. Ketten, A.E. Bowles, W.T. Ellison, D.P. Nowacek, and P.L. Tyack. 2019. Marine Mammal Noise Exposure Criteria: Updated Scientific Recommendations for Residual Hearing Effects. *Aquatic Mammals* 45(2): 125-232. https://doi.org/10.1578/AM.45.2.2019.125.

Stockin, K.A., R.S. Fairbairns, E.C.M. Parsons, and D.W. Sims. 2001. Effects of diel and seasonal cycles on the dive duration of the minke whale (*Balaenoptera acutorostrata*). *Journal of the Marine Biological Association of the United Kingdom* 81(1): 189-190. https://doi.org/10.1017/S0025315401003630.

Stone, C.J. and M.L. Tasker. 2006. The effects of seismic airguns on cetaceans in UK waters. *Journal of Cetacean Research and Management* 8(3): 255-263.

Teague, W.J., M.J. Carron, and P.J. Hogan. 1990. A comparison between the Generalized Digital Environmental Model and Levitus climatologies. *Journal of Geophysical Research* 95(C5): 7167-7183. https://doi.org/10.1029/JC095iC05p07167.

Thomas L. Holzer, Michael J. Bennett, Thomas E. Noce, and John C. Tinsley. 2005. Shear-Wave Velocity of Surficial Geologic Sediments in Northern California: Statistical Distributions and Depth Dependence. *Earthquake Spectra* 21(1): 161-177.

Tollefsen, D. 1998. Thin-sediment shear-induced effects on low-frequency broadband acoustic propagation in a shallow continental sea. *Journal of the Acoustical Society of America* 104(5): 2718-2716.

Von Benda-Beckmann, A.M., P.J. Wensveen, P.H. Kvadsheim, F.P. Lam, P.J. Miller, P.L. Tyack, and M.A. Ainslie. 2014. Modeling effectiveness of gradual increases in source level to mitigate effects of sonar on marine mammals. *Conservation Biology* 28(1): 119-28. https://www.ncbi.nlm.nih.gov/pubmed/24471782.

Warner, G.A., C. Erbe, and D.E. Hannay. 2010. Underwater Sound Measurements. (Chapter 3) *In* Reiser, C.M., D. Funk, R. Rodrigues, and D.E. Hannay (eds.). *Marine Mammal Monitoring and Mitigation during Open Water Shallow Hazards and Site Clearance Surveys by Shell Offshore Inc. in the Alaskan Chukchi Sea, July-October 2009: 90-Day Report*. LGL Report P1112-1. Report by LGL Alaska Research Associates Inc. and JASCO Applied Sciences for Shell Offshore Inc., National Marine Fisheries Service (US), and Fish and Wildlife Service (US). pp. 1-54.

Watwood, S.L. and D.M. Buonantony. 2012. *Dive distribution and group size parameters for marine species occuring in Navy training and testing areas in the North Atlantic and North Pacifiic Oceans*. NUWC-NPT Technical Document 12,085. Naval Undersea Warfare Center Division, Newport, Rhode Island.

Westgate, A.J., A.J. Head, P. Berggren, H.N. Koopman, and D.E. Gaskin. 1995. Diving behaviour of harbour porpoises, *Phocoena phocoena*. *Canadian Journal of Fisheries and Aquatic Sciences* 52(5): 1064-1073. https://doi.org/10.1139/f95-104.

Weston, D.E. 1971. Intensity-range relations in oceanographic acoustics. *Journal of Sound and Vibration* 18(2): 271-287.

Zeddies, D.G., S. Denes, and C. Pyć. 2017. *Gulf of Mexico Acoustic Exposure Model Variable Analysis*. Document Number 01445. Technical report by JASCO Applied Sciences for International Association of Geophysical Contractors and the American Petroleum Institute. http://www.iagc.org/uploads/4/5/0/7/45074397/api_iagc_gom_analysis_v2.1.pdf.

Zhang, Z.Y. and C.T. Tindle. 1995. Improved equivalent fluid approximations for a low shear speed ocean bottom. *Journal of the Acoustical Society of America* 98(6): 3391-3396. https://doi.org/10.1121/1.413789.

Appendix A. Marine Mammal Auditory Frequency Weighting and Threshold Levels

The potential for noise to affect animals depends on how well the animals can hear it. Noises are less likely to disturb or injure an animal if they are at frequencies that the animal cannot hear well. An exception occurs when the sound pressure is so high that it can physically injure an animal by non-auditory means (i.e., barotrauma). For sound levels below such extremes, the importance of sound components at particular frequencies can be scaled by frequency weighting relevant to an animal's sensitivity to those frequencies (Nedwell and Turnpenny 1998, Nedwell et al. 2007).

A.1. NMFS Marine Mammal Frequency Weighting Functions

In 2015, a U.S. Navy technical report by Finneran (2015) recommended new auditory weighting functions. The auditory weighting functions for marine mammals are applied in a similar way as A-weighting for noise level assessments for humans. The frequency-weighting functions are expressed as:

$$G(f) = K + 10\log_{10}\left\{\frac{(f/f_1)^{2a}}{[1+(f/f_1)^2]^a[1+(f/f_2)^2]^b}\right\} \quad \text{(A-1)}$$

Finneran (2015) proposed five functional hearing groups for marine mammals in water: low-, mid- and high-frequency cetaceans (LF, MF, and HF cetaceans, respectively), phocid pinnipeds, and otariid pinnipeds. The parameters for these frequency-weighting functions were further modified the following year (Finneran 2016) and were adopted in NOAA's technical guidance that assesses noise impacts on marine mammals (NMFS 2018). Table A-1 lists the frequency-weighting parameters for each hearing group. Figure A-1 shows the resulting frequency-weighting curves.

Table A-1. Parameters for the auditory weighting functions recommended by NMFS (2018).

Functional hearing group	a	b	f_1 (Hz)	f_2 (Hz)	K (dB)
Low-frequency cetaceans	1.0	2	200	19,000	0.13
Mid-frequency cetaceans	1.6	2	8,800	110,000	1.20
High-frequency cetaceans	1.8	2	12,000	140,000	1.36
Phocid pinnipeds in water	1.0	2	1,900	30,000	0.75
Otariid pinnipeds in water	2.0	2	940	25,000	0.64

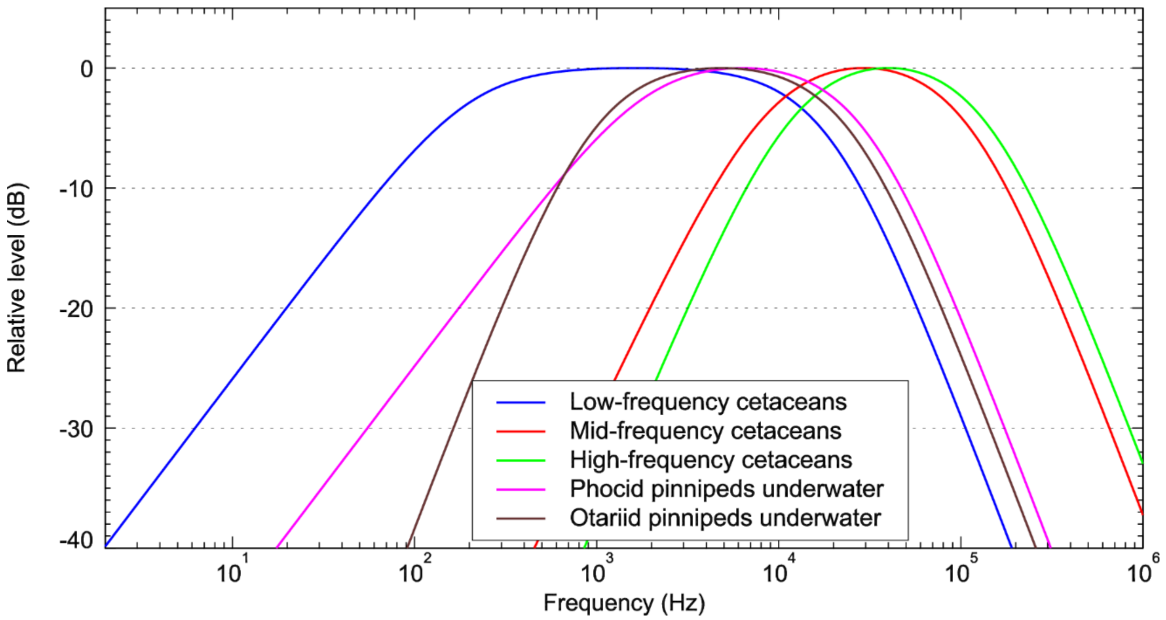

Figure A-1. Auditory weighting functions for the functional marine mammal hearing groups as recommended by NMFS (2018).

A.2. Southall Marine Mammal Frequency Weighting Functions

Auditory weighting functions for marine mammals—called M-weighting functions—were proposed by Southall et al. (2007). Functions were defined for five hearing groups of marine mammals:

- Low-frequency (LF) cetaceans—mysticetes (baleen whales)
- Mid-frequency (MF) cetaceans—some odontocetes (toothed whales)
- High-frequency (HF) cetaceans—odontocetes specialized for using high-frequencies
- Pinnipeds in water (Pw)—seals, sea lions, and walrus
- Pinnipeds in air (not addressed here)

The M-weighting functions have unity gain (0 dB) through the passband and their high and low frequency roll-offs are approximately –12 dB per octave. The amplitude response in the frequency domain of each M-weighting function is defined by:

$$G(f) = -20\log_{10}\left[\left(1+\frac{a^2}{f^2}\right)\left(1+\frac{f^2}{b^2}\right)\right] \quad \text{(A-2)}$$

where $G(f)$ is the weighting function amplitude (in dB) at the frequency f (in Hz), and a and b are the estimated lower and upper hearing limits, respectively, which control the roll-off and passband of the weighting function. The parameters a and b are defined uniquely for each hearing group (Table A-2). Figure A-2 shows the auditory weighting functions recommended by Southall et al. (2007).

Table A-2. Parameters for the auditory weighting functions recommended by Southall et al. (2007).

Functional hearing group	*a* (Hz)	*b* (Hz)
Low-frequency cetaceans	7	22,000
Mid-frequency cetaceans	150	160,000
High-frequency cetaceans	200	180,000
Pinnipeds in water	75	75,000

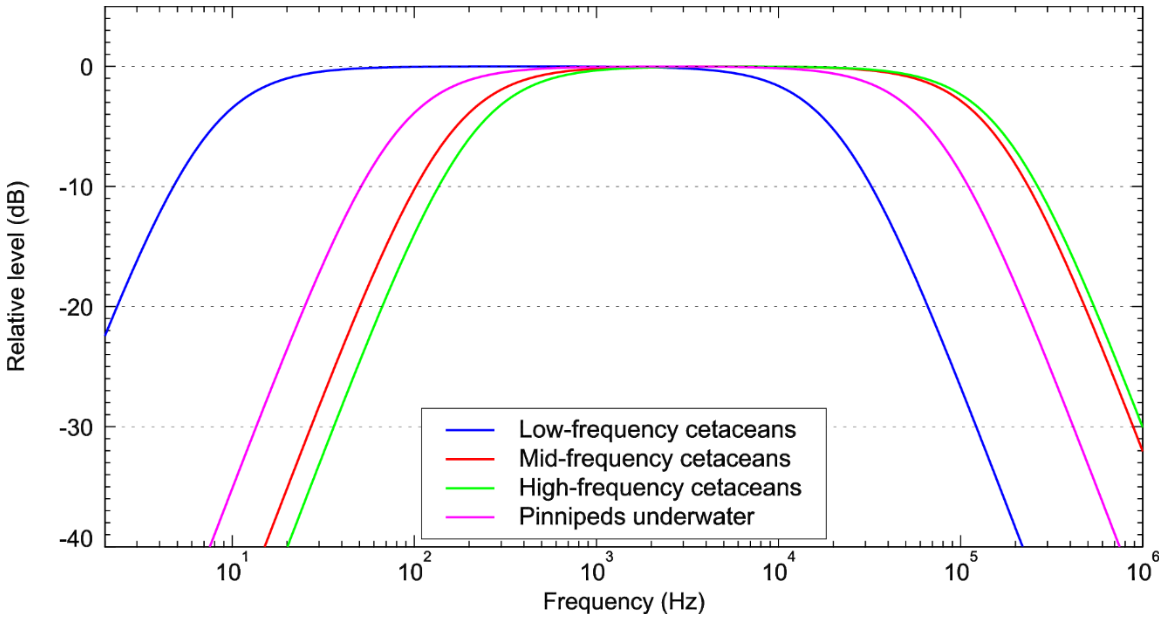

Figure A-2. Auditory weighting functions for the functional marine mammal hearing groups as recommended by Southall et al. (2007).

A.3. Acoustic Threshold Levels

Table A-3. PTS and TTS onset thresholds from NMFS (2018). Frequency-weighting is specified by NMFS (2018). The subscript “24h” indicates accumulation of sound exposure over 24 hours.

Marine mammal group	PTS		TTS	
	$L_{p,pk}$ dB re 1 µPa	M-weighted SEL_{24h} dB re 1 µPa²s	$L_{p,pk}$ dB re 1 µPa	M-weighted SEL_{24h} dB re 1 µPa²s
Low-frequency cetaceans	219	183	213	168
Mid-frequency cetaceans	230	185	224	170
High-frequency cetaceans	202	155	196	140
Phocid pinnipeds in water	218	185	212	170

Table A-4. PTS and TTS onset thresholds from Southall et al. (2007) and update for harbour porpoises in Lepper et al. (2014) (based on Lucke et al.(2009)). M-weighting is specified by Southall et al. (2007). The subscript “24h” indicates accumulation of sound exposure over 24 hours.

Marine mammal group	PTS		TTS	
	$L_{p,pk}$ dB re 1 µPa	M-weighted SEL_{24h} dB re 1 µPa²s	$L_{p,pk}$ dB re 1 µPa	M-weighted SEL_{24h} dB re 1 µPa²s
Low-frequency cetaceans	230	198	224	183
Mid-frequency cetaceans	230	198	224	183
High-frequency cetaceans	230	198	224	183
High-frequency cetaceans (post-Lucke et al. (2009))†	200	179	194	164
Phocid pinnipeds in water	218	186	212	171

†This threshold is not typically used in this context, nor is it typically frequency-weighted, but is included here to provide comparison with other works where this has been the case.

Appendix B. Preliminary Modelling Ranges by Month

The preliminary modelling study considered the 4130 in³ array using the geoacoustic parameters according to grain size and sound speed profiles for each month. Table B-1 presents the range for each region and each month to the 150 dB re 1 µPa²s single shot SEL threshold (value chosen arbitrarily to fit within modelled domain as a comparison). Modelling was performed over 24 radial transects up to a maximum frequency of 800 Hz in a region 50 km by 50 km with the source at the centre.

Table B-1. Maximum range to the 150 dB single shot SEL threshold.

Region	Jan	Feb	Mar	Apr	May	Jun	Jul	Aug	Sep	Oct	Nov	Dec
IS	8.80	8.90	8.70	8.30	6.90	6.50	6.60	6.90	7.40	7.50	7.60	8.90
NSS	13.30	13.30	13.30	13.10	12.70	12.40	12.20	12.50	12.70	12.80	12.90	13.20
NSD	16.00	16.00	16.00	15.80	14.90	14.00	12.70	11.80	12.90	14.30	15.00	15.90
FSC	19.66	19.30	19.30	19.38	19.73	19.94	20.29	20.15	20.79	21.07	20.51	21.92

Appendix C. Survey Areas

Region	North Sea Deep – Scenario 1			
Enclosed Area	16 km²			
Point ID	**Easting**	**Northing**	**Distance to next point**	**Heading**
1	740500	6642000	4 km	90°
2	744500	6642000	4 km	180°
3	744500	6638000	4 km	270°
4	740500	6638000	4 km	0°
5	740500	6642000	---	---
Centre	742500	6640000	NA	NA

Region	Irish Sea – Scenario 3			
Enclosed Area	400 km²			
Point ID	**Easting**	**Northing**	**Distance to next point**	**Heading**
1	447500	6000000	20 km	90°
2	467500	6000000	20 km	180°
3	467500	5980000	20 km	270°
4	447500	5980000	20 km	0°
5	447500	6000000	---	---
Centre	457500	5990000	NA	NA

Region	North Sea Shallow – Scenario 4			
Enclosed Area	400 km²			
Point ID	**Easting**	**Northing**	**Distance to next point**	**Heading**
1	854000	5960000	20 km	90°
2	874000	5960000	20 km	180°
3	874000	5940000	20 km	270°
4	854000	5940000	20 km	0°
5	854000	5960000	---	---
Centre	864000	5950000	NA	NA

Region	North Sea Deep – Scenario 5			
Enclosed Area	400 km²			
Point ID	**Easting**	**Northing**	**Distance to next point**	**Heading**
1	732500	6650000	20 km	90°
2	752500	6650000	20 km	180°
3	752500	6630000	20 km	270°
4	732500	6630000	20 km	0°
5	732500	6650000	---	---
Centre	742500	6640000	NA	NA

Region	Faroe-Shetland Channel – Scenario 6			
Enclosed Area	400 km²			
Point ID	**Easting**	**Northing**	**Distance to next point**	**Heading**
1	450000	6739142	20 km	135°
2	464142	6725000	20 km	225°
3	450000	6710858	20 km	315°
4	435858	6725000	20 km	45°
5	450000	6739142	---	---
Centre	450000	6725000	NA	NA

Appendix D. Tabulated Sound Speed Profiles

Water depth (m)	Irish Sea (m/s)	North Sea Shallow (m/s)	North Sea Deep (m/s)	Faroe-Shetland Channel (m/s)
0	1481.81	1473.99	1479.01	1486.35
2	1481.90	1473.99	1479.04	1486.37
4	1481.99	1473.99	1479.07	1486.38
6	1482.36	1474.00	1479.11	1486.40
8	1482.85	1474.02	1479.15	1486.42
10	1483.69	1474.04	1479.20	1486.43
15	1484.00	1474.10	1479.30	1486.49
20	1484.54	1474.17	1479.38	1486.57
25	1485.49	1474.25	1479.49	1486.66
30	1486.01	1474.33	1479.58	1486.74
35	1486.89	1474.33	1479.66	1486.81
40	1487.15	1474.10	1479.73	1486.88
45	1487.40	1474.18	1479.80	1486.93
50	1487.66		1479.88	1486.97
55	1487.92		1479.97	1487.03
60	1488.17		1480.06	1487.08
65			1480.14	1487.14
70			1480.22	1487.18
75			1480.31	1487.23
80			1480.38	1487.28
85			1480.45	1487.32
90			1480.52	1487.37
95			1480.59	1487.41
100			1480.66	1487.46
110			1480.76	1487.52
120			1480.79	1487.56
130			1480.75	1487.64
140			1480.77	1487.70
150			1480.79	1487.77
160			1480.82	1487.81
170			1480.78	1487.83
180				1487.83
190				1487.85
200				1487.86
220				1487.69
240				1487.54
260				1487.22

Water depth (m)	Irish Sea (m/s)	North Sea Shallow (m/s)	North Sea Deep (m/s)	Faroe-Shetland Channel (m/s)
280				1486.70
300				1485.95
350				1483.26
400				1479.70
500				1472.14
600				1464.04
700				1460.32
800				1460.61
900				1461.34
1000				1462.62
1100				1463.90
1200				1465.18

Appendix E. Soft-start Broadband Source Levels

Table E-1. Peak sound pressure levels and single-pulse sound exposure levels for all stages of the site survey soft-start.

Direction	$L_{S,pk}$ (dB re 1 µPa·m)				$L_{S,E}$ (dB re 1 µPa²·m²·s)			
	All guns	3 guns	2 guns	1 gun	All guns	3 guns	2 guns	1 gun
Broadside	238.2	236.0	232.7	226.9	213.6	211.6	208.6	203.4
Endfire	235.8	232.8	231.6	226.9	213.1	211.3	208.4	203.4
Vertical (no ghost)	238.6	236.3	232.7	226.9	213.7	211.6	208.6	203.4
Vertical (with ghost)	238.6	236.2	232.7	226.9	212.5	210.5	207.3	202.1

Table E-2. Peak sound pressure levels and single-shot sound exposure levels for all stages of the VSP soft-start.

Direction	$L_{S,pk}$ (dB re 1 µPa·m)			$L_{S,E}$ (dB re 1 µPa²·m²·s)		
	All guns	2 guns	1 gun	All guns	2 guns	1 gun
Horizontal in-plane	239.6	236.9	231.7	218.1	215.7	211.2
Horizontal out-of-plane	239.9	237.0	231.7	218.2	215.7	211.2
Vertical (no ghost)	239.5	236.7	231.7	218.1	215.6	211.2
Vertical (with ghost)	239.5	236.7	231.7	216.7	214.0	209.0

Table E-3. Peak sound pressure levels for all stages of the regional survey soft-start.

Direction	$L_{S,pk}$ (dB re 1 µPa·m)						
	All guns	22 guns	14 guns	8 guns	4 guns	2 guns	1 gun
Broadside	249.5	246.3	243.6	238.6	236.0	232.8	226.3
Endfire	246.6	245.0	243.5	240.6	236.8	231.0	226.3
Vertical (no ghost)	258.3	254.8	250.5	245.4	238.9	232.9	226.3
Vertical (with ghost)	258.3	254.8	250.5	245.4	238.9	232.9	226.3

Table E-4. Single-shot sound exposure levels for all stages of the regional survey soft-start.

Direction	$L_{S,E}$ (dB re 1 µPa²·m²·s)						
	All guns	22 guns	14 guns	8 guns	4 guns	2 guns	1 gun
Broadside	229.4	225.9	222.3	218.1	212.1	208.5	202.7
Endfire	228.7	226.4	223.2	220.0	213.3	208.3	202.7
Vertical (no ghost)	232.5	229.1	225.1	220.8	213.6	208.5	202.7
Vertical (with ghost)	234.1	230.6	226.4	222.2	215.2	210.1	204.7

Appendix F. Source Energy Levels in Decidecade-bands

F.1. Site Survey Source 160 in³

Decidecade-band centre frequency (Hz)	Fore $L_{S,E}$ (dB re 1 µPa²·m²·s)				Port $L_{S,E}$ (dB re 1 µPa²·m²·s)			
	All guns	3 guns	2 guns	1 gun	All guns	3 guns	2 guns	1 gun
1.00	161.4	159.2	155.8	151.0	161.4	159.2	155.8	151.0
1.26	168.5	165.7	162.1	155.7	168.5	165.7	162.1	155.7
1.58	169.8	167.0	163.3	156.9	169.8	167.0	163.3	156.9
2.00	174.5	171.6	168.0	161.3	174.5	171.6	168.0	161.3
2.51	177.4	174.6	171.0	164.2	177.4	174.6	171.0	164.2
3.16	181.1	178.2	174.6	167.9	181.1	178.2	174.6	167.9
3.98	184.7	181.9	178.3	171.7	184.7	181.9	178.3	171.7
5.01	188.3	185.4	181.8	175.1	188.3	185.4	181.8	175.1
6.31	192.4	189.4	185.7	178.9	192.4	189.4	185.7	178.9
7.94	197.3	194.0	190.3	183.1	197.4	194.0	190.3	183.1
10.00	204.6	200.5	196.4	188.3	204.6	200.5	196.4	188.3
12.6	208.7	207.3	204.2	196.9	208.8	207.3	204.2	196.9
15.8	197.1	199.8	198.4	198.4	197.3	199.6	198.4	198.4
20.0	197.0	190.0	185.8	187.1	197.0	190.1	185.8	187.1
25.1	204.1	202.4	199.0	188.5	204.3	202.2	199.0	188.5
31.6	198.2	194.5	192.9	193.3	198.2	194.4	192.9	193.3
39.8	200.1	199.6	196.7	189.2	200.4	199.4	196.7	189.2
50.1	199.6	197.6	194.6	188.8	200.0	197.6	194.6	188.8
63.1	199.0	196.3	193.5	189.2	199.4	196.5	193.6	189.2
79.4	197.8	196.1	192.9	188.8	198.4	196.5	193.0	188.8
100.0	197.0	195.0	192.8	187.4	197.8	195.7	192.8	187.4
125.9	196.1	194.1	192.0	187.2	197.2	195.3	192.2	187.2
158.5	194.9	192.9	191.3	186.6	196.9	195.0	191.6	186.6
199.5	193.7	191.6	190.8	186.0	196.8	194.9	191.1	186.0
251.2	191.6	189.2	189.7	185.1	196.3	194.3	190.2	185.1
316.2	187.3	185.2	187.6	183.5	193.8	192.1	188.2	183.5
398.1	185.2	183.5	185.5	181.8	191.1	189.7	185.9	181.8
501.2	186.4	183.6	184.0	180.0	189.1	187.6	184.2	180.0

Decidecade-band centre frequency (Hz)	Fore $L_{S,E}$ (dB re 1 µPa²·m²·s)				Port $L_{S,E}$ (dB re 1 µPa²·m²·s)			
	All guns	3 guns	2 guns	1 gun	All guns	3 guns	2 guns	1 gun
631.0	184.2	180.9	180.7	177.0	184.3	182.9	180.7	177.0
794.3	181.2	178.8	177.3	173.8	181.3	179.2	177.5	173.8
1000.0	172.4	171.9	168.5	166.3	173.6	171.0	169.2	166.3
1258.9	168.8	167.8	163.5	162.7	169.7	167.3	164.5	162.7
1584.9	168.4	167.0	165.0	162.8	168.6	166.6	164.9	162.8
1995.3	167.7	165.9	164.6	161.0	166.4	165.1	163.6	161.0
2511.9	163.6	163.0	162.1	158.3	163.1	162.6	162.1	158.3
3162.3	164.7	163.7	161.6	158.6	163.6	163.4	162.0	158.6
3981.1	163.2	161.9	161.2	157.3	162.9	162.4	161.1	157.3
5011.9	160.8	159.9	159.9	155.9	161.5	160.2	159.6	155.9
6309.6	159.4	157.8	157.1	153.6	158.4	158.3	157.0	153.6
7943.3	156.8	155.9	154.5	151.6	156.7	156.6	155.0	151.6
10000.0	153.1	152.5	151.2	148.0	152.7	151.8	150.6	148.0
12589.3	149.6	148.8	147.5	144.7	150.2	149.7	147.7	144.7
15848.9	148.2	146.8	145.6	142.5	147.9	147.2	145.7	142.5
19952.6	146.6	145.4	144.4	140.6	146.6	145.3	144.3	140.6
25118.9	142.8	141.5	140.9	137.0	142.7	142.0	140.7	137.0

F.2. VSP Source 750 in³

Decidecade-band centre frequency (Hz)	In-plane $L_{S,E}$ (dB re 1 µPa²·m²·s)			Perpendicular (out-of-plane) $L_{S,E}$ (dB re 1 µPa²·m²·s)		
	All guns	2 guns	1 gun	All guns	2 guns	1 gun
1.00	172.3	169.3	164.2	172.3	169.3	164.2
1.26	181.6	177.6	171.3	181.6	177.6	171.3
1.58	182.9	178.9	172.6	182.9	178.9	172.6
2.00	187.7	183.7	177.1	187.7	183.7	177.1
2.51	190.6	186.7	180.2	190.6	186.7	180.2
3.16	194.2	190.4	184.0	194.2	190.4	184.0
3.98	198.7	194.5	188.0	198.7	194.5	188.0
5.01	204.1	199.1	192.0	204.1	199.1	192.0
6.31	212.4	206.8	198.1	212.4	206.8	198.1
7.94	210.8	211.2	206.6	210.8	211.2	206.6
10.0	196.2	201.2	203.9	196.2	201.2	203.9
12.6	207.1	197.6	191.6	207.1	197.6	191.6
15.8	206.2	206.5	199.9	206.2	206.5	199.9
20.0	206.3	199.5	198.6	206.3	199.5	198.6
25.1	203.8	202.8	198.4	203.8	202.8	198.4
31.6	204.3	201.9	196.2	204.3	201.9	196.2
39.8	203.3	201.2	196.3	203.3	201.2	196.3
50.1	203.1	200.7	195.4	203.1	200.7	195.4
63.1	202.4	199.8	195.0	202.3	199.7	195.0
79.4	201.8	199.1	194.2	201.7	199.1	194.2
100.0	201.3	198.7	193.6	201.1	198.5	193.6
125.9	200.8	198.0	192.8	200.6	197.8	192.8
158.5	199.8	197.0	191.9	199.4	196.7	191.9
199.5	197.6	194.9	190.2	197.0	194.4	190.2
251.2	195.4	192.6	187.9	194.4	191.8	187.9
316.2	193.2	190.2	185.6	191.8	189.2	185.6
398.1	189.5	186.2	182.3	187.4	184.8	182.3
501.2	185.7	181.8	178.4	182.7	180.6	178.4
631.0	180.8	176.3	173.5	177.7	176.2	173.5
794.3	175.1	171.4	168.7	173.6	172.0	168.7

Decidecade-band centre frequency (Hz)	**In-plane $L_{S,E}$** (dB re 1 µPa²·m²·s)			**Perpendicular (out-of-plane) $L_{S,E}$** (dB re 1 µPa²·m²·s)		
	All guns	2 guns	1 gun	All guns	2 guns	1 gun
1000.0	174.8	173.5	169.8	175.4	173.2	169.8
1258.9	170.8	170.6	166.7	171.8	169.6	166.7
1584.9	170.6	169.8	166.1	170.5	169.7	166.1
1995.3	169.1	168.4	164.8	170.4	168.9	164.8
2511.9	165.6	164.4	160.4	165.7	164.4	160.4
3162.3	161.8	160.7	156.5	162.2	160.0	156.5
3981.1	160.0	158.8	155.0	160.0	158.1	155.0
5011.9	159.6	157.4	153.8	159.3	157.6	153.8
6309.6	157.3	155.7	152.1	156.6	156.0	152.1
7943.3	155.8	154.7	150.8	155.3	154.4	150.8
10000.0	152.2	151.0	148.3	152.0	151.4	148.3
12589.3	149.6	148.9	145.9	149.7	148.9	145.9
15848.9	147.5	146.3	143.7	147.5	145.9	143.7
19952.6	145.3	144.0	141.3	145.5	143.6	141.3
25118.9	141.2	139.0	137.0	140.8	139.5	137.0

F.3. Regional Survey 4130 in³

Decidecade-band centre frequency (Hz)	Fore $L_{S,E}$ (dB re 1 µPa²·m²·s)						
	All guns	22 guns	14 guns	8 guns	4 guns	2 guns	1 gun
1.00	186.1	180.0	174.0	168.1	161.3	155.2	148.7
1.26	193.8	187.3	180.8	174.1	167.2	160.1	152.3
1.58	195.1	188.5	182.0	175.4	168.5	161.4	153.5
2.00	199.6	193.1	186.7	180.0	173.0	165.8	157.4
2.51	202.6	196.1	189.6	183.0	176.0	168.7	160.3
3.16	206.3	199.7	193.3	186.7	179.7	172.4	164.0
3.98	210.4	203.5	197.1	190.5	183.4	176.2	167.8
5.01	214.7	207.3	200.7	193.9	186.8	179.6	171.2
6.31	221.0	212.2	204.9	197.9	190.7	183.3	174.9
7.94	222.6	218.6	209.9	202.3	195.0	187.3	178.6
10.00	219.0	221.3	216.8	208.0	200.5	192.1	182.8
12.6	217.0	217.8	218.0	215.6	207.8	198.9	188.1
15.8	216.4	209.4	210.2	212.7	205.9	204.2	196.5
20.0	218.3	215.4	208.5	200.1	198.3	197.5	197.5
25.1	215.4	213.8	212.3	209.4	200.8	188.1	186.1
31.6	215.6	213.3	208.5	207.2	201.1	198.8	188.4
39.8	213.7	212.2	210.2	207.7	199.9	192.0	192.2
50.1	211.7	211.6	209.5	205.6	199.7	195.7	188.6
63.1	208.0	210.5	208.9	205.6	200.0	194.1	187.8
79.4	201.7	208.0	208.6	204.8	199.8	193.5	188.4
100.0	206.5	200.2	206.5	203.9	200.0	193.5	188.1
125.9	208.9	202.2	201.4	200.4	198.0	192.3	186.8
158.5	203.3	204.6	191.5	195.1	196.3	190.6	186.2
199.5	200.6	200.2	196.4	191.2	194.8	189.3	185.5
251.2	199.4	199.9	196.4	191.2	192.4	186.8	184.3
316.2	201.0	198.5	193.1	191.7	188.8	184.6	183.1
398.1	199.4	197.1	190.7	190.3	185.9	182.6	181.3
501.2	195.0	194.2	190.5	188.6	184.9	181.3	179.1
631.0	191.0	189.2	188.2	185.7	182.9	179.5	176.4
794.3	186.7	185.0	184.0	181.6	178.9	175.8	172.9

Decidecade-band centre frequency (Hz)	Fore $L_{S,E}$ (dB re 1 µPa²·m²·s)						
	All guns	22 guns	14 guns	8 guns	4 guns	2 guns	1 gun
1000.0	185.2	181.3	180.0	175.7	171.3	169.6	165.9
1258.9	179.2	176.5	175.0	171.7	167.7	165.1	161.9
1584.9	179.5	176.2	174.0	171.4	168.3	165.3	161.9
1995.3	179.6	176.7	173.8	169.6	167.5	163.8	160.7
2511.9	178.2	174.7	171.5	167.8	164.8	161.8	158.3
3162.3	175.3	173.2	169.8	166.5	164.4	161.2	158.3
3981.1	173.7	171.4	168.9	165.1	162.7	159.8	156.9
5011.9	171.4	169.5	167.1	163.3	161.6	158.2	155.1
6309.6	168.7	167.1	164.9	160.8	158.5	155.4	152.6
7943.3	166.1	164.4	162.4	158.8	156.0	153.5	150.5
10000.0	162.7	161.3	158.9	156.0	153.6	149.9	146.9
12589.3	159.9	157.9	155.9	152.5	150.3	146.7	143.7
15848.9	158.1	156.0	153.4	150.4	147.6	144.5	141.4
19952.6	155.9	154.1	151.7	148.5	146.0	142.9	139.3
25118.9	151.8	150.0	147.7	144.8	142.0	138.9	135.6

Decidecade-band centre frequency (Hz)	Port $L_{S,E}$ (dB re 1 μPa²·m²·s)						
	All guns	22 guns	14 guns	8 guns	4 guns	2 guns	1 gun
1.00	186.1	180.0	174.0	168.1	161.3	155.2	148.7
1.26	193.8	187.3	180.8	174.1	167.2	160.1	152.3
1.58	195.0	188.5	182.0	175.3	168.4	161.4	153.5
2.00	199.6	193.1	186.7	180.0	173.0	165.8	157.4
2.51	202.6	196.1	189.7	183.0	176.0	168.7	160.3
3.16	206.3	199.7	193.3	186.7	179.7	172.4	164.0
3.98	210.4	203.5	197.1	190.4	183.4	176.1	167.8
5.01	214.7	207.3	200.6	193.9	186.8	179.5	171.2
6.31	220.9	212.2	204.8	197.8	190.7	183.3	174.9
7.94	222.7	218.6	209.8	202.1	194.9	187.3	178.6
10.00	219.7	221.7	217.0	207.7	200.5	192.1	182.8
12.6	215.6	217.7	218.7	215.4	208.0	198.8	188.1
15.8	216.5	208.4	209.2	212.3	206.4	204.0	196.5
20.0	216.8	216.0	208.3	198.4	196.8	197.0	197.5
25.1	215.2	212.0	212.3	208.0	200.9	188.4	186.1
31.6	213.8	211.8	206.6	204.5	200.8	198.3	188.4
39.8	211.0	208.9	203.8	203.0	199.5	192.2	192.2
50.1	206.2	205.7	200.9	196.2	197.3	195.1	188.6
63.1	202.0	200.8	200.9	194.2	196.3	194.0	187.8
79.4	210.7	203.5	205.8	198.6	193.6	194.0	188.4
100.0	210.7	203.6	205.7	199.3	193.9	194.1	188.1
125.9	203.4	204.0	201.9	196.3	195.7	193.2	186.8
158.5	213.4	210.7	205.5	200.6	197.0	192.1	186.2
199.5	215.5	212.2	207.8	202.6	196.9	191.6	185.5
251.2	204.9	202.0	199.6	194.9	193.6	190.1	184.3
316.2	202.9	200.8	198.4	194.3	191.7	188.6	183.1
398.1	204.4	201.7	198.5	194.4	190.8	186.2	181.3
501.2	195.5	194.0	192.0	189.2	186.7	183.2	179.1
631.0	191.3	190.3	188.4	185.5	183.3	179.6	176.4
794.3	186.2	185.3	182.6	181.2	179.2	175.5	172.9

Decidecade-band centre frequency (Hz)	Port $L_{S,E}$ (dB re 1 µPa²·m²·s)						
	All guns	22 guns	14 guns	8 guns	4 guns	2 guns	1 gun
1000.0	185.3	182.1	179.4	176.3	173.4	169.6	165.9
1258.9	180.2	177.0	174.7	171.5	168.6	165.0	161.9
1584.9	179.5	176.0	173.6	171.2	168.2	164.4	161.9
1995.3	179.5	176.0	173.3	170.5	167.1	164.5	160.7
2511.9	176.8	174.6	171.1	168.0	164.8	162.2	158.3
3162.3	175.2	173.0	170.2	167.5	165.3	161.3	158.3
3981.1	173.6	171.3	168.8	165.6	163.5	159.9	156.9
5011.9	171.1	169.3	167.3	163.2	161.4	158.4	155.1
6309.6	168.9	166.7	164.4	161.4	158.9	155.8	152.6
7943.3	166.6	164.6	162.1	158.6	156.7	153.4	150.5
10000.0	163.0	160.9	158.6	155.9	153.1	149.4	146.9
12589.3	159.9	158.3	155.8	152.5	150.2	146.7	143.7
15848.9	158.0	155.9	153.3	150.2	148.2	144.5	141.4
19952.6	155.3	154.0	151.5	148.5	146.2	142.9	139.3
25118.9	152.0	150.0	148.0	144.5	142.2	139.4	135.6

Appendix G. Soft-start Signatures and Spectra

G.1. Site Survey Source 160 in³

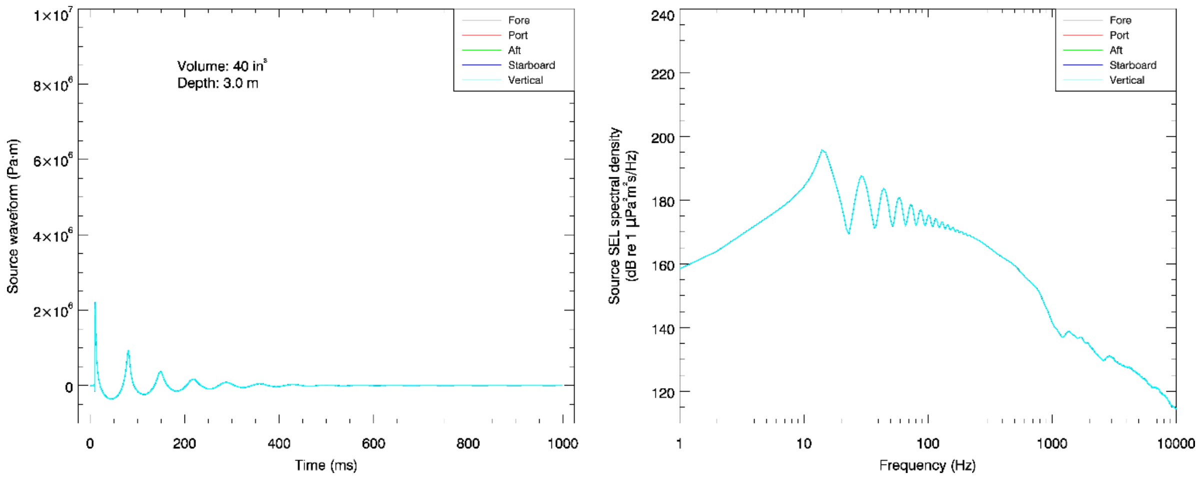

Figure G-1. Signatures and spectra from the site survey source operating a single gun.

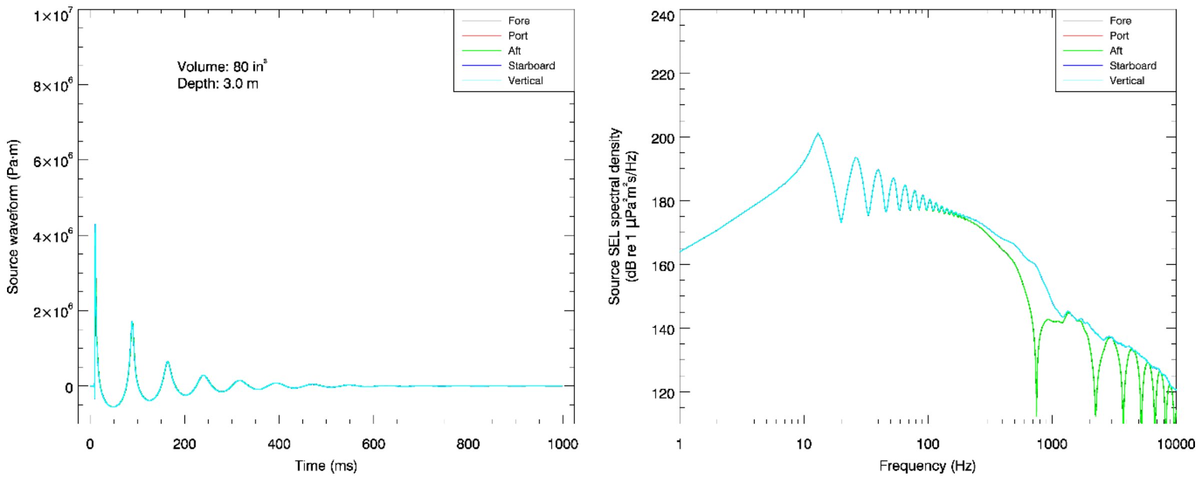

Figure G-2. Signatures and spectra from the site survey source operating two guns.

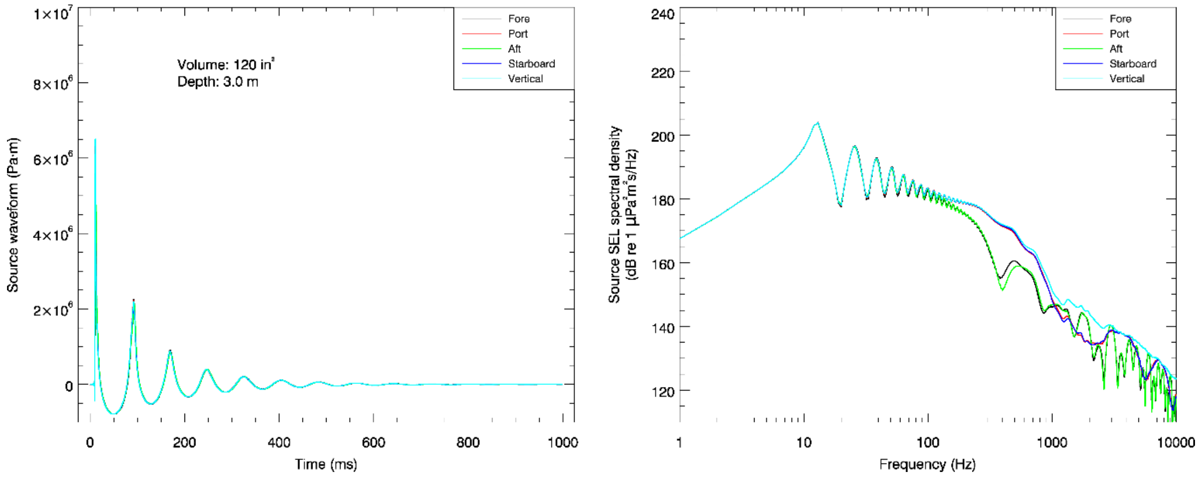

Figure G-3. Signatures and spectra from the site survey source operating three guns.

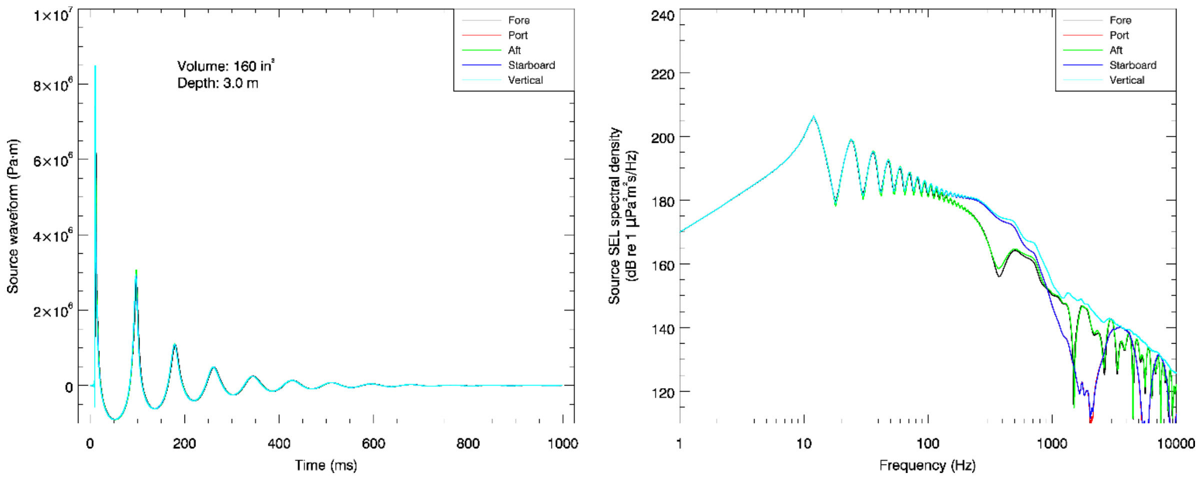

Figure G-4. Signatures and spectra from the site survey source operating with all guns.

G.2. VSP Source 750 in³

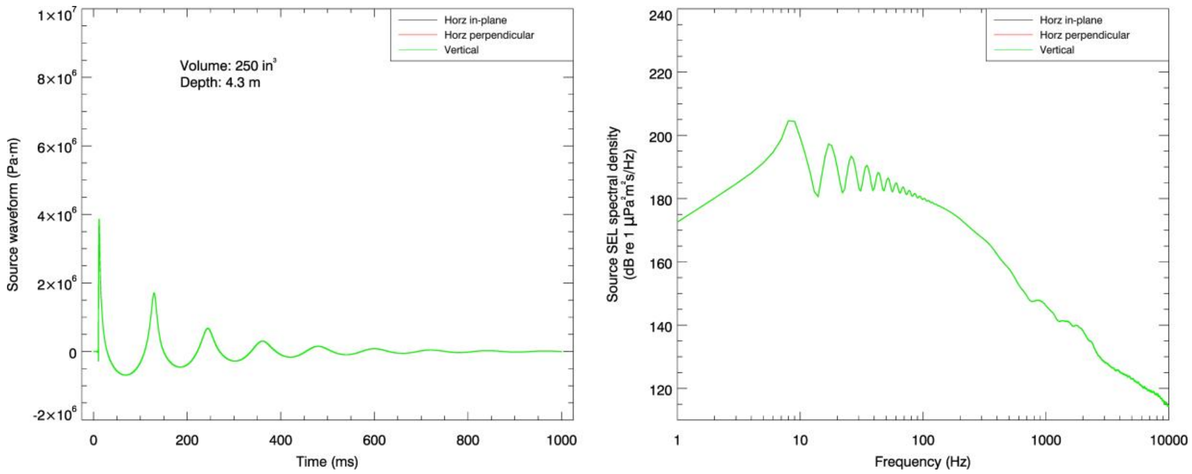

Figure G-5. Signatures and spectra from the VSP source operating a single gun.

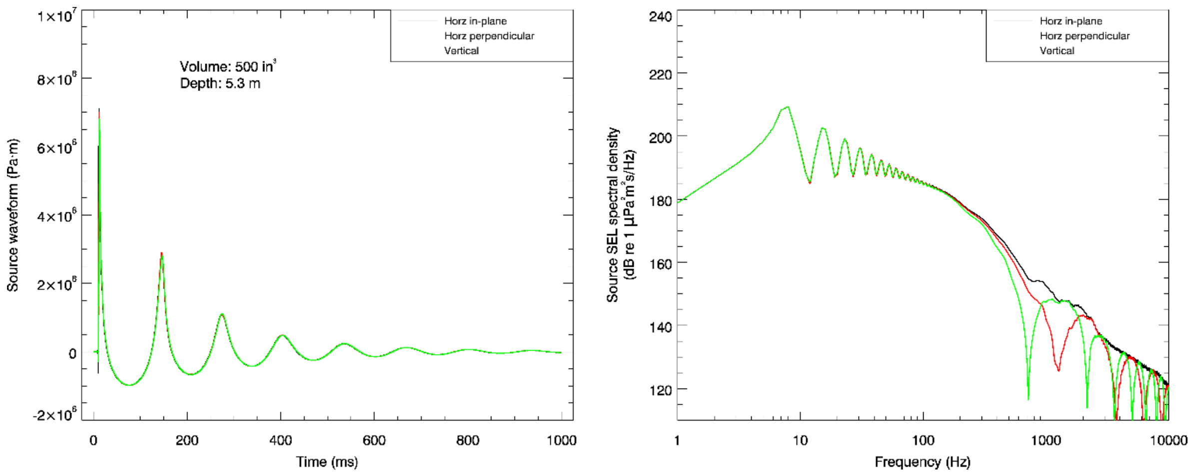

Figure G-6. Signatures and spectra from the VSP source operating two guns.

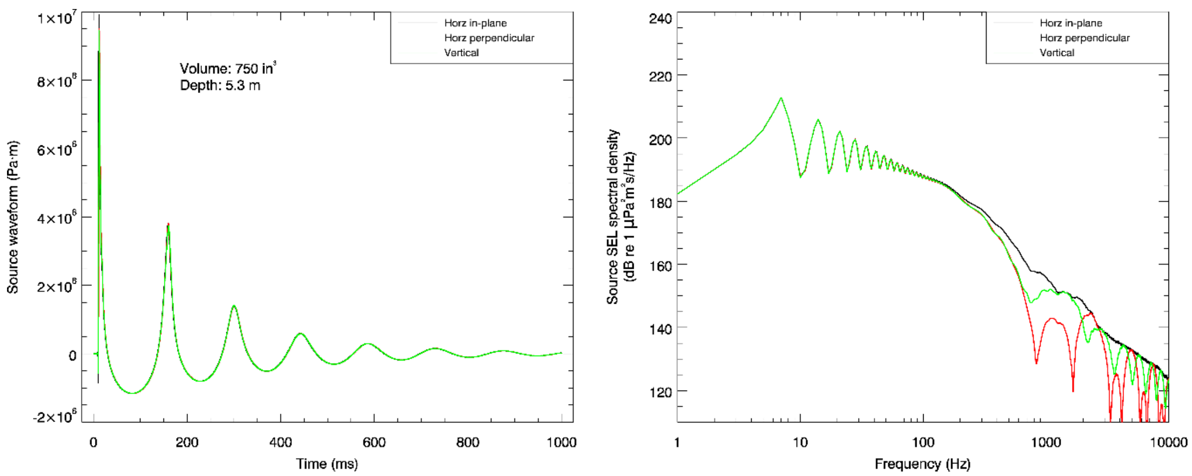

Figure G-7. Signatures and spectra from the VSP source operating with all guns.

G.3. Regional Survey 4130 in³

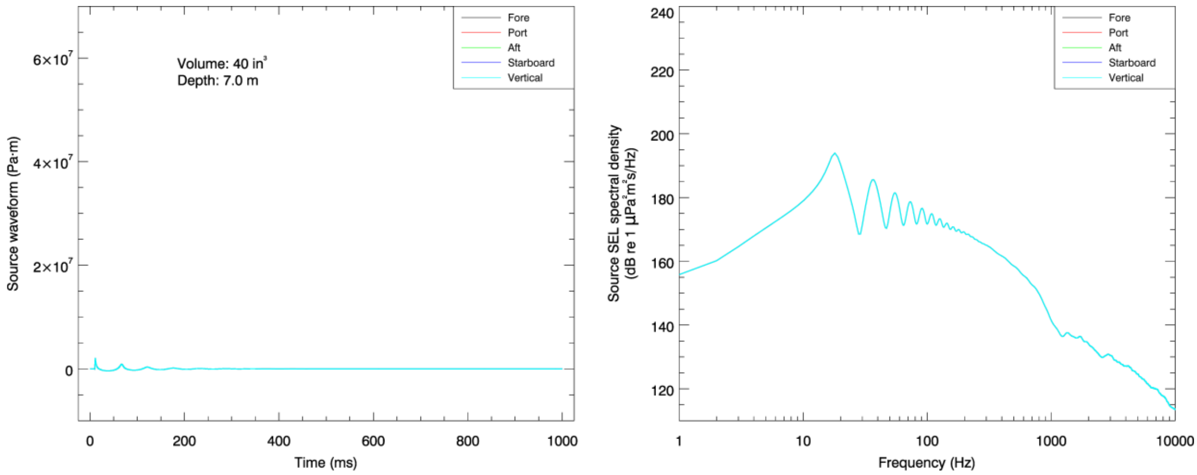

Figure G-8. Signatures and spectra from the regional survey source operating a single gun.

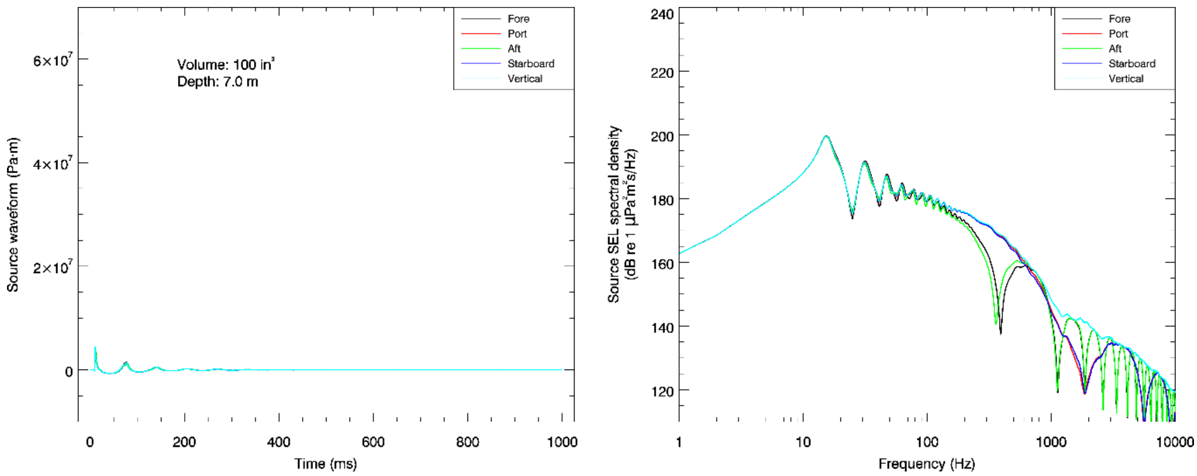

Figure G-9. Signatures and spectra from the regional survey source operating with guns totalling 100 in³.

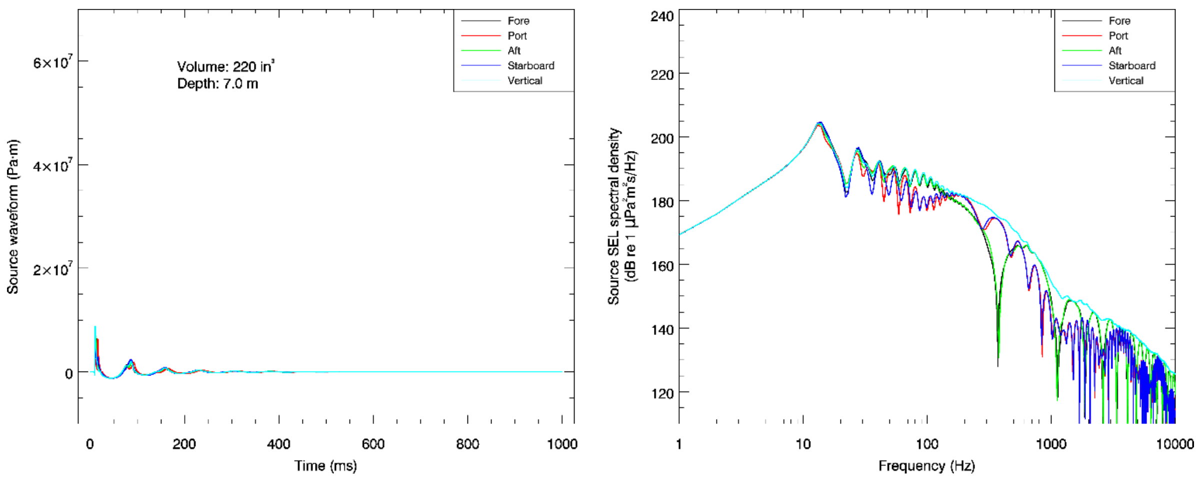

Figure G-10. Signatures and spectra from the regional survey source operating with guns totalling 220 in³.

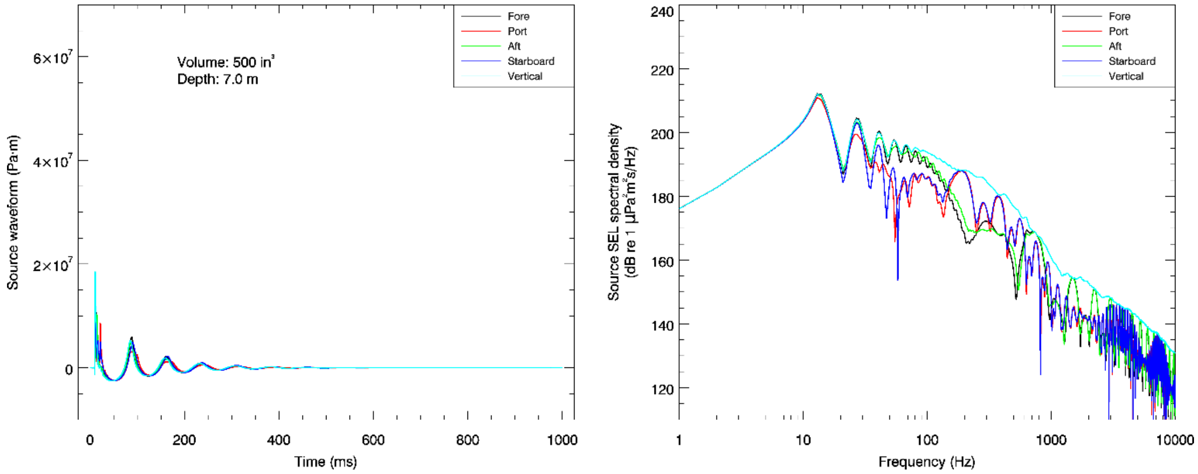

Figure G-11. Signatures and spectra from the regional survey source operating with guns totalling 500 in³.

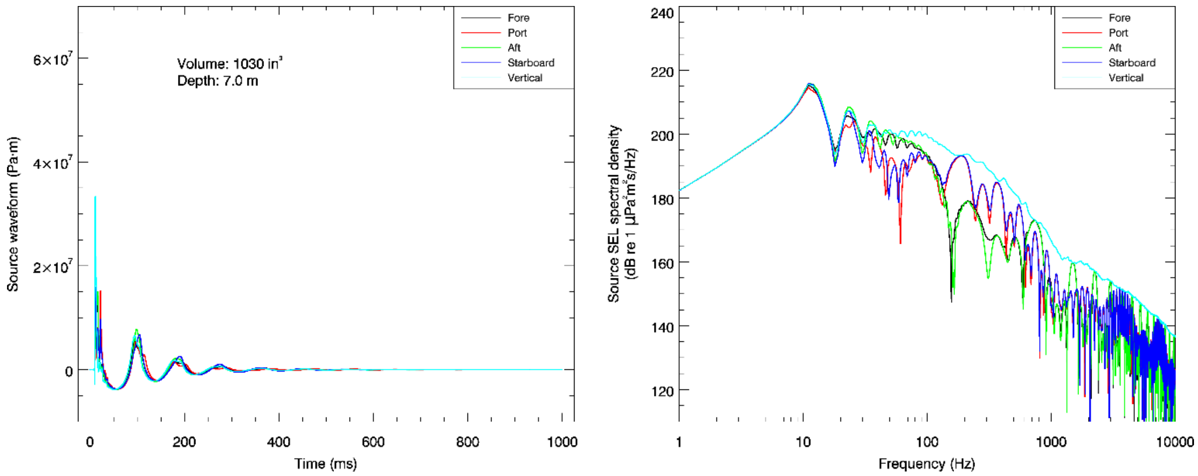

Figure G-12. Signatures and spectra from the regional survey source operating with guns totalling 1030 in³.

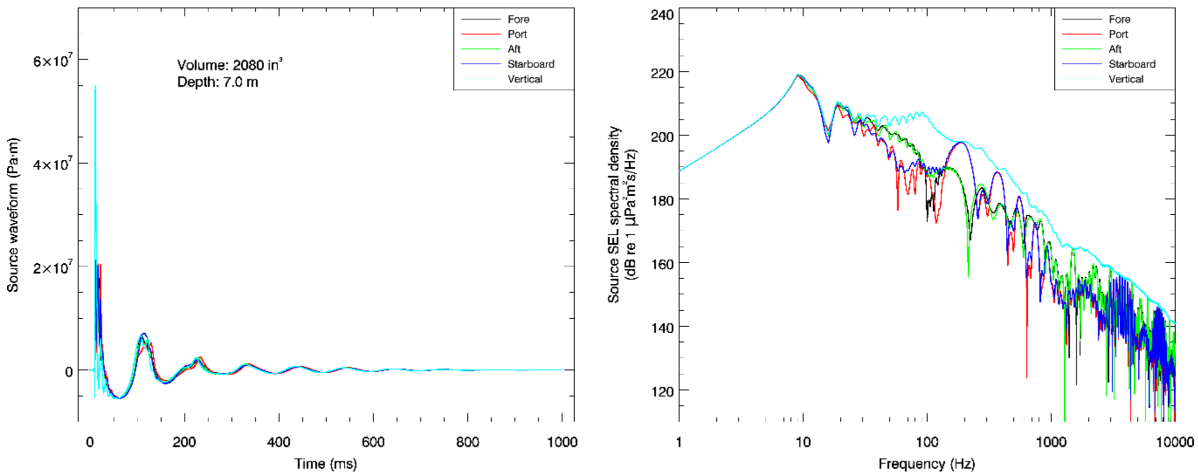

Figure G-13. Signatures and spectra from the regional survey source operating with guns totalling 2080 in³.

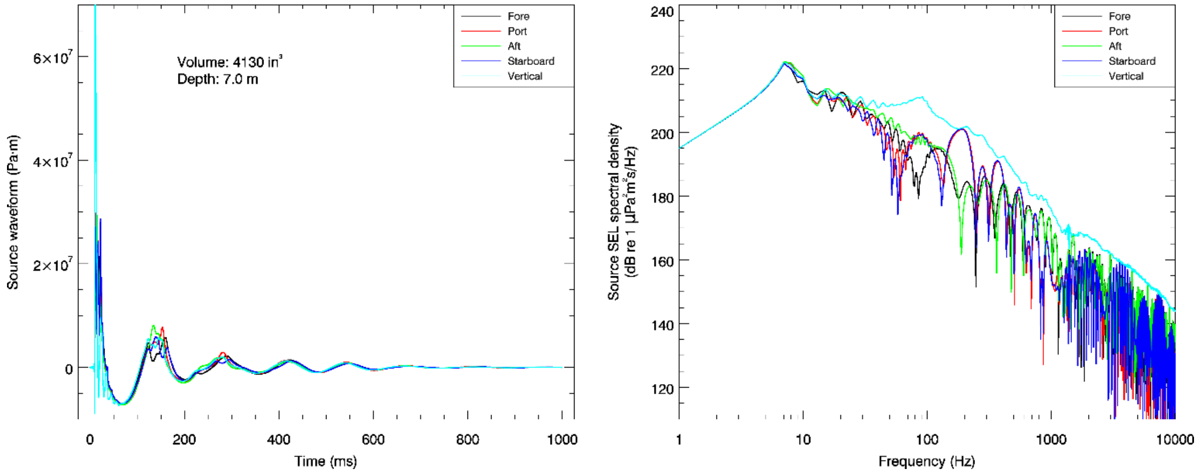

Figure G-14. Signatures and spectra from the regional survey source operating with all guns (4130 in³).

Appendix H. Modelling Parameters Descriptions

H.1. Environmental and Location Parameter Descriptions

Table H-1 provides an overview of the modelling parameters provided for the modelling studies in Phase 2.

Table H-1. Modelling parameters defined for each scenario.

Bathymetry	• A single file was provided for each scenario
	• ASCII file of the format:
	`X1, Y1, Z1`
	`X2, Y2, Z2`
	`. . .`
	`Xn, Yn, Zn`
	• The X and Y coordinates form a regular grid
	• All values in metres
	• X and Y correspond to Eastings and Northings projected using UTM30 North (Datum: WGS84)
	• Z indicates elevation (i.e., negative values correspond to underwater)
	• Data from EMODnet, and projected onto UTM grid

Geoacoustics	• For each scenario, a single value for each of the following was provided: o Density (g/cm^3) o Compressional wave speed (m/s) o Compressional wave attenuation (dB/λ) o Shear wave speed (m/s) o Shear wave attenuation (dB/λ) • No range nor depth dependence in the geoacoustics was included for Phase 2 • The properties were derived from a specified grain size, and the sound speed in water at a nominal depth • The sediment layer depth was chosen to effectively mimic a half-space (i.e., no discernible reflections from a sub-layer)
Sound speed profile	• A single sound speed profile for each scenario was extracted from GDEM comprising tabulated depth and sound speed pairs • The profile that resulted in the greatest sound propagation was used for Phase 2 • Data for the closest location to the nominal centre of the survey for each scenario was used (i.e., nearest neighbour – no interpolation scheme) • Where necessary, profile data was supplemented by data from nearby deeper waters to provide a profile extending to all water depths within the modelling domain
Surface roughness	• A smooth water-air interface was assumed for all scenarios in Phase 2
Scenario description	• Shot point file provided containing tabulated data of: o Time (in seconds) from start of survey o Easting (m) (UTM30N) o Northing (m) (UTM30N) o Soft-start stage

H.2. Airgun Array Source Level Files

Source levels for each step of the soft-start and for all arrays were generated in the following two formats:

- horizontal directional far-field energy source levels as a function of decidecade band centre frequencies;
- far-field pressure signatures in cardinal and vertical directions.

The energy source level files (*.lev) are in ASCII text format and have the following format:

```
NFREQ              NANG
FREQ(1) ANG(1) SL(1,1)
FREQ(1) ANG(2) SL(1,2)
FREQ(1) ANG(3) SL(1,3)
...
FREQ(1) ANG(NANG) SL(1,NANG)
FREQ(2) ANG(1) SL(2,1)
FREQ(2) ANG(2) SL(2,2)
FREQ(2) ANG(3) SL(2,3)

...
```

where:

- NFREQ is an integer indicating the number of band centre frequencies;
- NANG is an integer indicating the number of azimuths;
- FREQ is the frequency in hertz;
- ANG is the azimuthal angle in degrees;
- SL is the energy source level in dB re 1 µPa²m²s.

The soft-start difference files are of the same format except for the SL being the difference in source level at the specified frequency and azimuth.

The format of the signal (*.txt) files, taken in directions indicated by the file name, are in the following format:

```
T(1) P(1)
T(2) P(2)
T(3) P(3)
...
```

where:

- T = time in milliseconds;
- P = acoustic far-field monopole source pressure in pascals.

Appendix I. Full Tabulated Baseline Modelling Results

I.1. Scenario 1 – Site survey in North Sea Deep environment

Table I-1. Scenario 1: Maximum ranges at 10 m depth to the frequency weighted SEL_{24h} threshold values defined by the NMFS 2018 criteria.

Type of animal	Effect	$SEL_{24h,Weighted}$ (dB re 1 µPa²s)	Soprano	dBSea	MONM	
			R_{max} (km)	R_{max} (km)	R_{max} (km)	$R_{95\%}$ (km)
Low-frequency cetaceans	PTS	183	4.45	2.9	1.73	1.4
	TTS	168	>30	10.5	15.8	13.1
Mid-frequency cetaceans	PTS	185	0	<0.1	0	0
	TTS	170	0	<0.1	0	0
High-frequency cetaceans	PTS	155	0	<0.1	0	0
	TTS	140	2	3.4	1.7	1.4
Phocid pinnipeds in water	PTS	185	0	0.2	0	0
	TTS	170	3.1	2.1	1.4	1.13

Table I-2. Scenario 1: Maximum ranges at 10 m depth to the peak sound pressure level threshold values defined by the NMFS 2018 criteria.

Type of animal	Effect	$L_{p,pk}$ (dB re 1 µPa)	Soprano	dBSea	FWRAM	VSTACK
			R_{max} (km)	R_{max} (km)	R_{max} (km)	R_{max} (km)
Low-frequency cetaceans	PTS	219	0	<0.1	<0.01	<0.01
	TTS	213	0	<0.1	0.01	0.02
Mid-frequency cetaceans	PTS	230	0	<0.1	<0.01	0
	TTS	224	0	<0.1	<0.01	0
High-frequency cetaceans	PTS	202	0	<0.1	0.04	0.05
	TTS	196	0	0.1	0.07	0.08
Phocid pinnipeds in water	PTS	218	0	<0.1	<0.01	<0.01
	TTS	212	0	<0.1	0.01	0.02

Table I-3. Scenario 1: Maximum ranges at 10 m depth to the M-weighted SEL_{24h} threshold values defined by Southall (2007) and Lucke (2009). All sound exposure levels are M-weighted.

Type of animal	Effect	$SEL_{24h,Weighted}$ (dB re 1 µPa²s)	Soprano	dBSea	MONM	
			R_{max} (km)	R_{max} (km)	R_{max} (km)	$R_{95\%}$ (km)
Low-frequency cetaceans	PTS	198	0.4	0.9	3.15	2.65
	TTS	183	8.33	7.2	19.43	16.3
Mid-frequency cetaceans	PTS	198	0	0.2	0	0
	TTS	183	3.48	2.2	1.3	1.05
High-frequency cetaceans	PTS	198	0	0.2	0	0
	TTS	183	2.21	2.8	0.78	0.7
High-frequency cetaceans (based on Lucke)	PTS	179	5.09	2.9	2.43	2
	TTS	164	>30	10.2	22.1	16.6
Phocid pinnipeds in water	PTS	186	3.63	2.5	1.13	0.9
	TTS	171	>30	10.1	12.6	10.6

Table I-4. Scenario 1: Maximum ranges at 10 m depth to the peak sound pressure threshold values defined by Southall (2007) and Lucke (2009).

Type of animal	Effect	$L_{p,pk}$ (dB re 1 µPa)	Soprano	dBSea	FWRAM	VSTACK
			R_{max} (km)	R_{max} (km)	R_{max} (km)	R_{max} (km)
Low-frequency cetaceans	PTS	230	0	<0.1	<0.01	0
	TTS	224	0	<0.1	<0.01	0
Mid-frequency cetaceans	PTS	230	0	<0.1	<0.01	0
	TTS	224	0	<0.1	<0.01	0
High-frequency cetaceans	PTS	230	0	<0.1	<0.01	0
	TTS	224	0	<0.1	<0.01	0
High-frequency cetaceans (based on Lucke)	PTS	200	0	0.1	0.05	0.06
	TTS	194	0	0.1	0.07	0.09
Phocid pinnipeds in water	PTS	218	0	<0.1	<0.01	<0.01
	TTS	212	0	<0.1	0.01	0.02

I.2. Scenario 2 – VSP in North Sea Deep environment

Table I-5. Scenario 2: Maximum ranges at 10 m depth to the frequency weighted SEL_{24h} threshold values defined by the NMFS 2018 criteria.

Type of animal	Effect	$SEL_{24h,Weighted}$ (dB re 1 µPa²s)	Soprano	dBSea	MONM	
			R_{max} (km)	R_{max} (km)	R_{max} (km)	$R_{95\%}$ (km)
Low-frequency cetaceans	PTS	183	1.7	1.8	1.18	1.08
	TTS	168	11.7	10.4	9.6	7.93
Mid-frequency cetaceans	PTS	185	0	<0.1	0	0
	TTS	170	0	<0.1	<0.02	<0.02
High-frequency cetaceans	PTS	155	0	0.2	0.06	0.06
	TTS	140	0.5	1	0.5	0.48
Phocid pinnipeds in water	PTS	185	0	0.2	0.06	0.06
	TTS	170	0.98	1.2	0.64	0.56

Table I-6. Scenario 2: Maximum ranges at 10 m depth to the peak sound pressure level threshold values defined by the NMFS 2018 criteria.

Type of animal	Effect	$L_{p,pk}$ (dB re 1 µPa)	Soprano	dBSea	FWRAM	VSTACK
			R_{max} (km)	R_{max} (km)	R_{max} (km)	R_{max} (km)
Low-frequency cetaceans	PTS	219	0	<0.1	0.01	0.01
	TTS	213	0	<0.1	0.01	0.02
Mid-frequency cetaceans	PTS	230	0	<0.1	<0.01	0
	TTS	224	0	<0.1	<0.01	<0.01
High-frequency cetaceans	PTS	202	0	0.1	0.05	0.06
	TTS	196	0	0.1	0.08	0.09
Phocid pinnipeds in water	PTS	218	0	<0.1	0.01	0.01
	TTS	212	0	<0.1	0.02	0.02

Table I-7 Scenario 2: Maximum ranges at 10 m depth to the M-weighted SEL_{24h} threshold values defined by Southall (2007) and Lucke (2009). All sound exposure levels are M-weighted.

Type of animal	Effect	$SEL_{24h,Weighted}$ (dB re 1 μPa²s)	Soprano	dBSea	MONM	
			R_{max} (km)	R_{max} (km)	R_{max} (km)	$R_{95\%}$ (km)
Low-frequency cetaceans	PTS	198	0.29	0.9	0.11	0.11
	TTS	183	4.09	5	2.51	2.39
Mid-frequency cetaceans	PTS	198	0	0.2	0.06	0.06
	TTS	183	1.19	1.4	0.81	0.74
High-frequency cetaceans	PTS	198	0	0.2	0.06	0.06
	TTS	183	0.7	0.9	0.3	0.28
High-frequency cetaceans (based on Lucke)	PTS	179	1.59	1.7	1.2	1.05
	TTS	164	12.1	9.6	10.8	9.17
Phocid pinnipeds in water	PTS	186	1.49	1.8	0.99	0.95
	TTS	171	10.7	9.9	8.38	7.47

Table I-8Scenario 2: Maximum ranges at 10 m depth to the peak sound pressure threshold values defined by Southall (2007) and Lucke (2009).

Type of animal	Effect	$L_{p,pk}$ (dB re 1 μPa)	Soprano	dBSea	FWRAM	VSTACK
			R_{max} (km)	R_{max} (km)	R_{max} (km)	R_{max} (km)
Low-frequency cetaceans	PTS	230	0	<0.1	<0.01	0
	TTS	224	0	<0.1	<0.01	<0.01
Mid-frequency cetaceans	PTS	230	0	<0.1	<0.01	0
	TTS	224	0	<0.1	<0.01	<0.01
High-frequency cetaceans	PTS	230	0	<0.1	<0.01	0
	TTS	224	0	<0.1	<0.01	<0.01
High-frequency cetaceans (based on Lucke)	PTS	200	0	0.1	0.06	0.07
	TTS	194	0	0.2	0.1	0.10
Phocid pinnipeds in water	PTS	218	0	<0.1	0.01	0.01
	TTS	212	0	<0.1	0.02	0.02

I.3. Scenario 3 – Regional survey in Irish Sea environment

Table I-9. Scenario 3: Maximum ranges at 10 m depth to the frequency weighted SEL_{24h} threshold values defined by the NMFS 2018 criteria.

Type of animal	Effect	$SEL_{24h,Weighted}$ (dB re 1 µPa²s)	Soprano	dBSea	MONM	
			R_{max} (km)	R_{max} (km)	R_{max} (km)	$R_{95\%}$ (km)
Low-frequency cetaceans	PTS	183	1.68	5.5	1.6	1.4
	TTS	168	7.3	29.5	36	29.6
Mid-frequency cetaceans	PTS	185	0	<0.1	0	0
	TTS	170	0	0.3	0	0
High-frequency cetaceans	PTS	155	0	0.3	0	0
	TTS	140	4.38	3	2.73	2.18
Phocid pinnipeds in water	PTS	185	0	0.6	0	0
	TTS	170	10.5	6.4	1.55	1.3

Table I-10. Scenario 3: Maximum ranges at 10 m depth to the peak sound pressure level threshold values defined by the NMFS 2018 criteria.

Type of animal	Effect	$L_{p,pk}$ (dB re 1 µPa)	Soprano	dBSea	FWRAM	VSTACK
			R_{max} (km)	R_{max} (km)	R_{max} (km)	R_{max} (km)
Low-frequency cetaceans	PTS	219	0	<0.1	0.04	0.03
	TTS	213	0	<0.1	0.06	0.06
Mid-frequency cetaceans	PTS	230	0	<0.1	<0.01	<0.01
	TTS	224	0	<0.1	0.03	0.01
High-frequency cetaceans	PTS	202	0.09	0.2	0.32	0.34
	TTS	196	0.2	0.9	0.84	0.77
Phocid pinnipeds in water	PTS	218	0	<0.1	0.04	0.03
	TTS	212	0	<0.1	0.07	0.07

Table I-11. Scenario 3: Maximum ranges at 10 m depth to the M-weighted SEL_{24h} threshold values defined by Southall (2007) and Lucke (2009). All sound exposure levels are M-weighted.

Type of animal	Effect	$SEL_{24h,Weighted}$ (dB re 1 µPa²s)	Soprano	dBSea	MONM	
			R_{max} (km)	R_{max} (km)	R_{max} (km)	$R_{95\%}$ (km)
Low-frequency cetaceans	PTS	198	0.22	0.9	0.03	0.03
	TTS	183	2.54	6.8	3.23	2.63
Mid-frequency cetaceans	PTS	198	0	0.7	<0.01	<0.01
	TTS	183	8.89	5	1.3	1.1
High-frequency cetaceans	PTS	198	0	0.4	<0.01	<0.01
	TTS	183	10.2	4.6	0.7	0.55
High-frequency cetaceans (based on Lucke)	PTS	179	2.18	8.3	3	2.4
	TTS	164	8.6	36.1	57	45.8
Phocid pinnipeds in water	PTS	186	1.3	4.1	1.03	0.88
	TTS	171	10.42	24.1	25.7	21

Table I-12. Scenario 3: Maximum ranges at 10 m depth to the peak sound pressure threshold values defined by Southall (2007) and Lucke (2009).

Type of animal	Effect	$L_{p,pk}$ (dB re 1 µPa)	Soprano	dBSea	FWRAM	VSTACK
			R_{max} (km)	R_{max} (km)	R_{max} (km)	R_{max} (km)
Low-frequency cetaceans	PTS	230	0	<0.1	<0.01	<0.01
	TTS	224	0	<0.1	0.03	0.01
Mid-frequency cetaceans	PTS	230	0	<0.1	<0.01	<0.01
	TTS	224	0	<0.1	0.03	0.01
High-frequency cetaceans	PTS	230	0	<0.1	<0.01	<0.01
	TTS	224	0	<0.1	0.03	0.01
High-frequency cetaceans (based on Lucke)	PTS	200	0.1	0.3	0.46	0.42
	TTS	194	0.29	1.3	0.86	0.84
Phocid pinnipeds in water	PTS	218	0	<0.1	0.04	0.03
	TTS	212	0	<0.1	0.07	0.07

I.4. Scenario 4 – Regional survey in North Sea Shallow environment

Table I-13. Scenario 4: Maximum ranges at 10 m depth to the frequency weighted SEL_{24h} threshold values defined by the NMFS 2018 criteria.

Type of animal	Effect	$SEL_{24h,Weighted}$ (dB re 1 µPa²s)	Soprano	dBSea	MONM	
			R_{max} (km)	R_{max} (km)	R_{max} (km)	$R_{95\%}$ (km)
Low-frequency cetaceans	PTS	183	5.4	5.3	4.66	4.1
	TTS	168	19.7	15.3	21.7	18.2
Mid-frequency cetaceans	PTS	185	0	<0.1	0	0
	TTS	170	0	0.2	0	0
High-frequency cetaceans	PTS	155	0.04	0.5	0	0
	TTS	140	5.98	3.8	4.65	4.05
Phocid pinnipeds in water	PTS	185	0	1.3	0	0
	TTS	170	5.25	5.8	4.55	3.25

Table I-14. Scenario 4: Maximum ranges at 10 m depth to the peak sound pressure level threshold values defined by the NMFS 2018 criteria.

Type of animal	Effect	$L_{p,pk}$ (dB re 1 µPa)	Soprano	dBSea	FWRAM	VSTACK
			R_{max} (km)	R_{max} (km)	R_{max} (km)	R_{max} (km)
Low-frequency cetaceans	PTS	219	0	<0.1	0.04	0.03
	TTS	213	0	<0.1	0.08	0.07
Mid-frequency cetaceans	PTS	230	0	<0.1	<0.01	<0.01
	TTS	224	0	<0.1	0.03	0.01
High-frequency cetaceans	PTS	202	0.2	0.2	0.54	0.34
	TTS	196	0.5	1	0.96	0.96
Phocid pinnipeds in water	PTS	218	0	<0.1	0.04	0.03
	TTS	212	0	<0.1	0.08	0.08

Table I-15. Scenario 4: Maximum ranges at 10 m depth to the M-weighted SEL_{24h} threshold values defined by Southall (2007) and Lucke (2009). All sound exposure levels are M-weighted.

Type of animal	Effect	$SEL_{24h,Weighted}$ (dB re 1 μPa²s)	Soprano	dBSea	MONM	
			R_{max} (km)	R_{max} (km)	R_{max} (km)	$R_{95\%}$ (km)
Low-frequency cetaceans	PTS	198	1.3	1.3	0.15	0.15
	TTS	183	7.85	4.8	5.58	4.63
Mid-frequency cetaceans	PTS	198	0	1	<0.01	<0.01
	TTS	183	5.25	4.5	3.88	3.00
High-frequency cetaceans	PTS	198	0	0.8	<0.01	<0.01
	TTS	183	5.38	4	2.1	1.68
High-frequency cetaceans (based on Lucke)	PTS	179	6.19	5.8	4.65	4.28
	TTS	164	19.71	16.3	28	22.4
Phocid pinnipeds in water	PTS	186	5.25	3.8	3.1	2.45
	TTS	171	18.9	12.1	18	15.7

Table I-16. Scenario 4: Maximum ranges at 10 m depth to the peak sound pressure threshold values defined by Southall (2007) and Lucke (2009).

Type of animal	Effect	$L_{p,pk}$ (dB re 1 μPa)	Soprano	dBSea	FWRAM	VSTACK
			R_{max} (km)	R_{max} (km)	R_{max} (km)	R_{max} (km)
Low-frequency cetaceans	PTS	230	0	<0.1	<0.01	<0.01
	TTS	224	0	<0.1	0.03	0.01
Mid-frequency cetaceans	PTS	230	0	<0.1	<0.01	<0.01
	TTS	224	0	<0.1	0.03	0.01
High-frequency cetaceans	PTS	230	0	<0.1	<0.01	<0.01
	TTS	224	0	<0.1	0.03	0.01
High-frequency cetaceans (based on Lucke)	PTS	200	0.29	0.5	0.60	0.61
	TTS	194	0.69	1.3	1.20	1.03
Phocid pinnipeds in water	PTS	218	0	<0.1	0.04	0.03
	TTS	212	0	<0.1	0.08	0.08

I.5. Scenario 5 – Regional survey in North Sea Deep environment

Table I-17. Scenario 5: Maximum ranges at 10 m depth to the frequency weighted SEL_{24h} threshold values defined by the NMFS 2018 criteria.

Type of animal	Effect	$SEL_{24h,Weighted}$ (dB re 1 µPa²s)	Soprano	dBSea	MONM	
			R_{max} (km)	R_{max} (km)	R_{max} (km)	$R_{95\%}$ (km)
Low-frequency cetaceans	PTS	183	9.93	7.8	4.66	4.2
	TTS	168	>30	30.8	56.1	42.75
Mid-frequency cetaceans	PTS	185	0	<0.1	0	0
	TTS	170	0	0.3	0	0
High-frequency cetaceans	PTS	155	0	0.1	0	0
	TTS	140	5.25	4.4	3.1	2.4
Phocid pinnipeds in water	PTS	185	0	0.1	0	0
	TTS	170	6.26	6.6	2.08	1.6

Table I-18. Scenario 5: Maximum ranges at 10 m depth to the peak sound pressure level threshold values defined by the NMFS 2018 criteria.

Type of animal	Effect	$L_{p,pk}$ (dB re 1 µPa)	Soprano	dBSea	FWRAM	VSTACK
			R_{max} (km)	R_{max} (km)	R_{max} (km)	R_{max} (km)
Low-frequency cetaceans	PTS	219	0	<0.1	0.04	0.03
	TTS	213	0	<0.1	0.06	0.06
Mid-frequency cetaceans	PTS	230	0	<0.1	<0.01	<0.01
	TTS	224	0	<0.1	0.03	0.01
High-frequency cetaceans	PTS	202	0.09	0.15	0.13	0.14
	TTS	196	0.2	0.5	0.58	0.42
Phocid pinnipeds in water	PTS	218	0	<0.1	0.04	0.03
	TTS	212	0	<0.1	0.07	0.07

Table I-19. Scenario 5: Maximum ranges at 10 m depth to the M-weighted SEL_{24h} threshold values defined by Southall (2007) and Lucke (2009). All sound exposure levels are M-weighted.

Type of animal	Effect	$SEL_{24h,Weighted}$ (dB re 1 μPa²s)	Soprano	dBSea	MONM	
			R_{max} (km)	R_{max} (km)	R_{max} (km)	$R_{95\%}$ (km)
Low-frequency cetaceans	PTS	198	1.29	1.4	0.03	0.03
	TTS	183	15.73	9.9	8.73	7.38
Mid-frequency cetaceans	PTS	198	0	0.4	<0.01	<0.01
	TTS	183	7.79	6.9	4.63	3.18
High-frequency cetaceans	PTS	198	0	0.4	<0.01	<0.01
	TTS	183	5.25	6	0.18	0.15
High-frequency cetaceans (based on Lucke)	PTS	179	10.42	9.1	4.75	4.28
	TTS	164	20	36.6	63.5	49.3
Phocid pinnipeds in water	PTS	186	8.03	25.9	4.65	3.18
	TTS	171	>30	7.2	47.3	34.8

Table I-20. Scenario 5: Maximum ranges at 10 m depth to the peak sound pressure threshold values defined by Southall (2007) and Lucke (2009).

Type of animal	Effect	$L_{p,pk}$ (dB re 1 μPa)	Soprano	dBSea	FWRAM	VSTACK
			R_{max} (km)	R_{max} (km)	R_{max} (km)	R_{max} (km)
Low-frequency cetaceans	PTS	230	0	<0.1	<0.01	<0.01
	TTS	224	0	<0.1	0.03	0.01
Mid-frequency cetaceans	PTS	230	0	<0.1	<0.01	<0.01
	TTS	224	0	<0.1	0.03	0.01
High-frequency cetaceans	PTS	230	0	<0.1	<0.01	<0.01
	TTS	224	0	<0.1	0.03	0.01
High-frequency cetaceans (based on Lucke)	PTS	200	0.1	0.2	0.24	0.17
	TTS	194	0.3	0.5	0.68	0.76
Phocid pinnipeds in water	PTS	218	0	<0.1	0.04	0.03
	TTS	212	0	<0.1	0.07	0.07

I.6. Scenario 6 – Regional survey in Faroe Shetland Channel

Note that, as discussed in Section 7.3.4, Soprano is unsuitable for deep-water propagation and so results are not presented for this scenario.

Table I-21. Scenario 6: Maximum ranges at 10 m depth to the frequency weighted SEL_{24h} threshold values defined by the NMFS 2018 criteria.

Type of animal	Effect	$SEL_{24h,Weighted}$ (dB re 1 µPa²s)	dBSea	MONM	
			R_{max} (km)	R_{max} (km)	$R_{95\%}$ (km)
Low-frequency cetaceans	PTS	183	5.7	0.15	0.12
	TTS	168	52.3	77.8	67.6
Mid-frequency cetaceans	PTS	185	<0.1	0	0
	TTS	170	<0.1	0	0
High-frequency cetaceans	PTS	155	<0.1	0	0
	TTS	140	1.7	0.31	0.24
Phocid pinnipeds in water	PTS	185	<0.1	<0.01	0
	TTS	170	3.3	0.1	0.08

Table I-22. Scenario 6: Maximum ranges at 10 m depth to the peak sound pressure level threshold values defined by the NMFS 2018 criteria.

Type of animal	Effect	$L_{p,pk}$ (dB re 1 µPa)	dBSea	FWRAM	VSTACK
			R_{max} (km)	R_{max} (km)	R_{max} (km)
Low-frequency cetaceans	PTS	219	<0.1	0.04	0.03
	TTS	213	<0.1	0.06	0.06
Mid-frequency cetaceans	PTS	230	<0.1	<0.01	<0.01
	TTS	224	<0.1	0.03	0.01
High-frequency cetaceans	PTS	202	0.15	0.13	0.15
	TTS	196	0.5	0.19	0.21
Phocid pinnipeds in water	PTS	218	<0.1	0.04	0.03
	TTS	212	<0.1	0.07	0.07

Table I-23. Scenario 6: Maximum ranges at 10 m depth to the M-weighted SEL_{24h} threshold values defined by Southall (2007) and Lucke (2009). All sound exposure levels are M-weighted.

Type of animal	Effect	$SEL_{24h,Weighted}$ (dB re 1 μPa²s)	dBSea	MONM	
			R_{max} (km)	R_{max} (km)	$R_{95\%}$ (km)
Low-frequency cetaceans	PTS	198	2.7	0.03	0.03
	TTS	183	18.2	11.9	8.3
Mid-frequency cetaceans	PTS	198	0.2	<0.01	<0.01
	TTS	183	3.6	0.09	0.08
High-frequency cetaceans	PTS	198	0.2	0	0
	TTS	183	2.9	0.08	0.07
High-frequency cetaceans (based on Lucke)	PTS	179	7.5	0.15	0.13
	TTS	164	64.0	81.4	70.4
Phocid pinnipeds in water	PTS	186	4.8	0.11	0.08
	TTS	171	38.5	75.2	63.7

Table I-24. Scenario 6: Maximum ranges at 10 m depth to the peak sound pressure threshold values defined by Southall (2007) and Lucke (2009).

Type of animal	Effect	$L_{p,pk}$ (dB re 1 μPa)	dBSea	FWRAM	VSTACK
			R_{max} (km)	R_{max} (km)	R_{max} (km)
Low-frequency cetaceans	PTS	230	<0.1	<0.01	<0.01
	TTS	224	<0.1	0.03	0.01
Mid-frequency cetaceans	PTS	230	<0.1	<0.01	<0.01
	TTS	224	<0.1	0.03	0.01
High-frequency cetaceans	PTS	230	<0.1	<0.01	<0.01
	TTS	224	<0.1	0.03	0.01
High-frequency cetaceans (based on Lucke)	PTS	200	0.4	0.16	0.16
	TTS	194	0.8	0.22	0.23
Phocid pinnipeds in water	PTS	218	<0.1	0.04	0.03
	TTS	212	<0.1	0.07	0.07

Appendix J. Baseline Modelling Sound Field Maps

J.1. Results from ICC

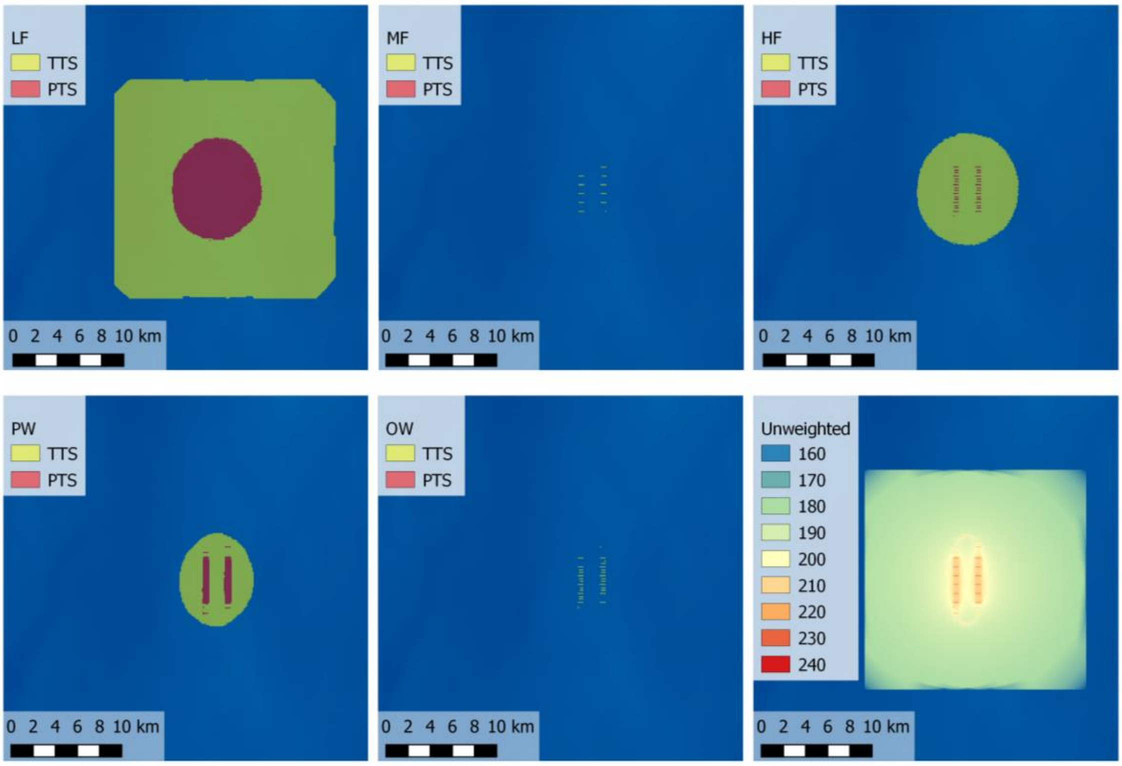

Figure J-1. Scenario 1: NMFS (2018) frequency-weighted results.

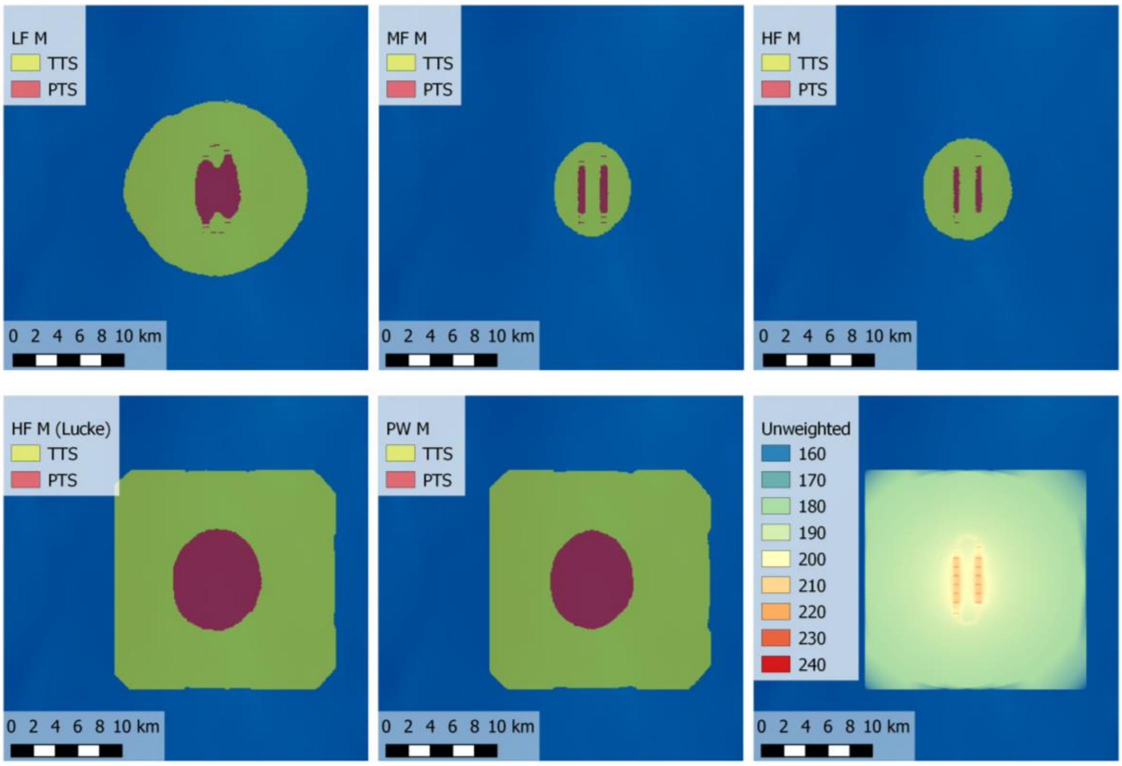

Figure J-2. Scenario 1: Southall (2007) M-weighted results.

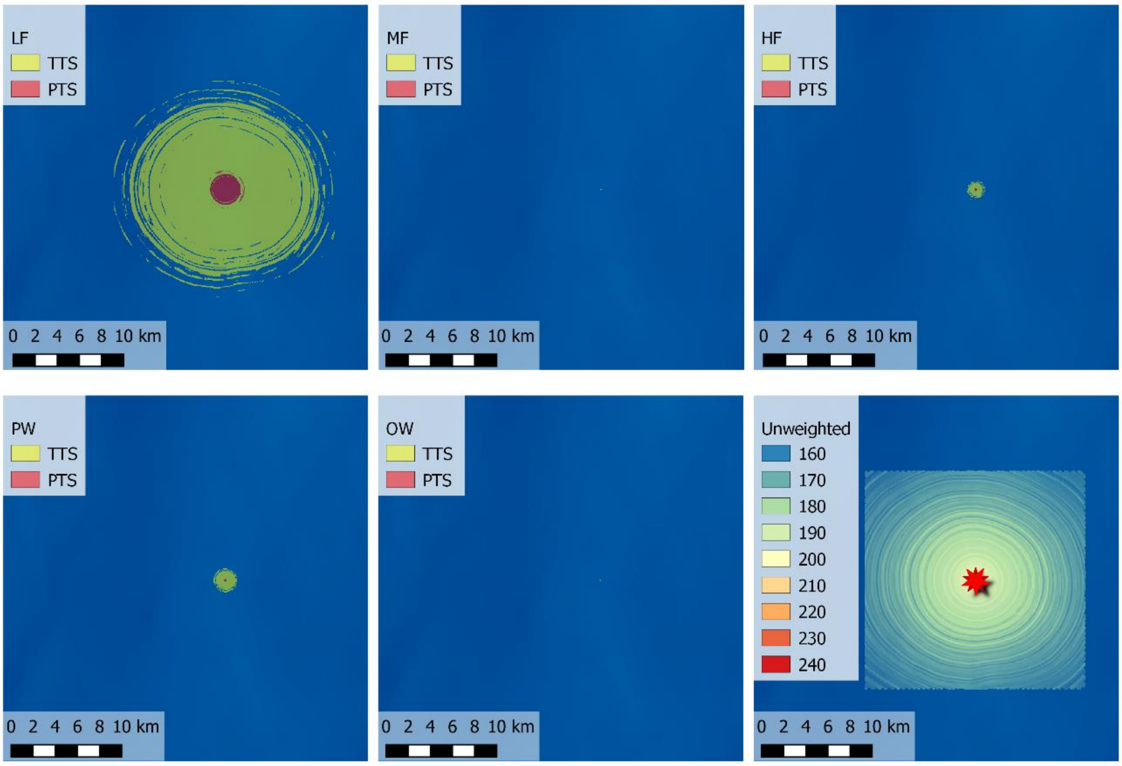

Figure J-3. Scenario 2: NMFS (2018) frequency-weighted results.

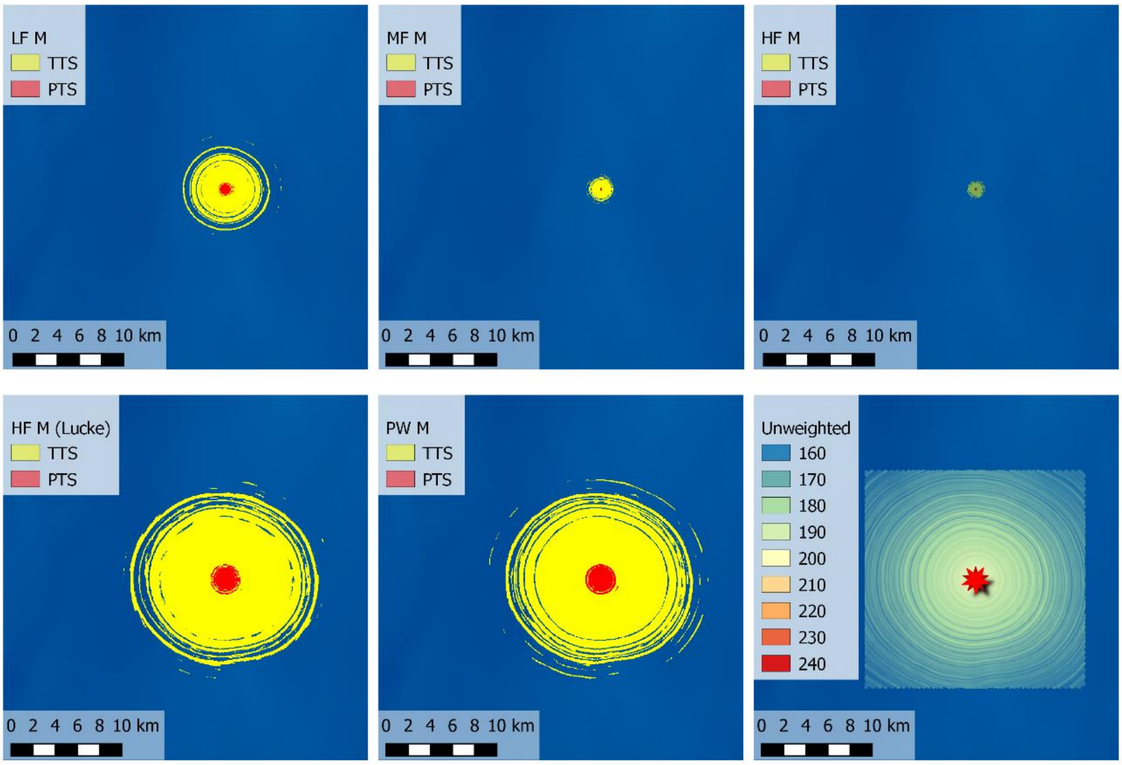

Figure J-4. Scenario 2: Southall (2007) M-weighted results.

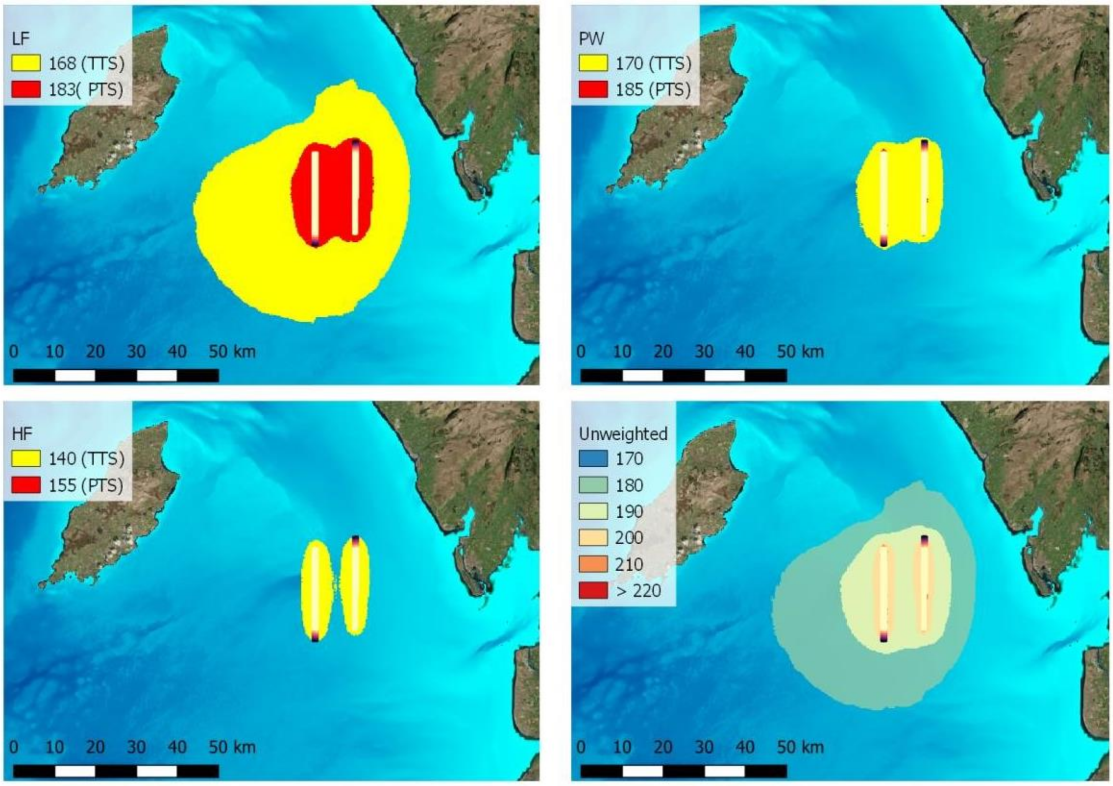

Figure J-5. Scenario 3: Overview of TTS and PTS (NMFS 2018) risk zones for a stationary receiver at 10 m depth. Groups “MF” and “OW” had risk zones too small to meaningfully show.

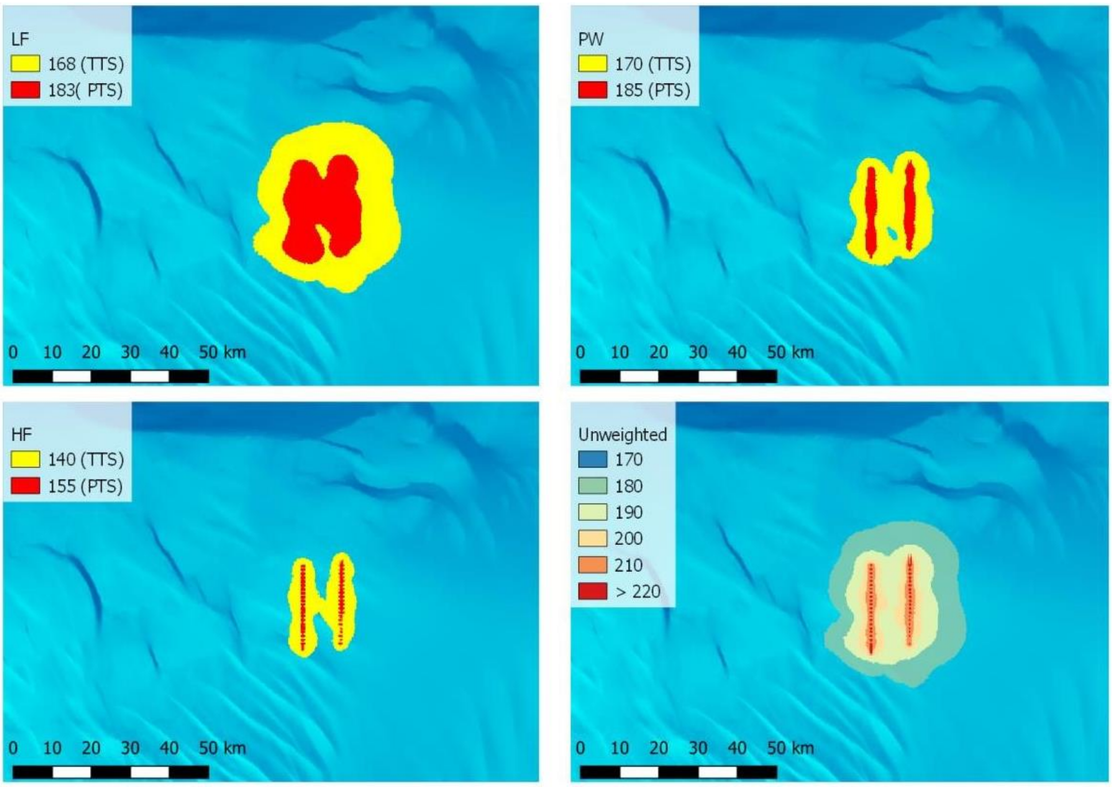

Figure J-6. Scenario 4: Overview of TTS and PTS (NMFS 2018) risk zones for a stationary receiver at 10 m depth. Groups “MF” and “OW” had risk zones too small to meaningfully show.

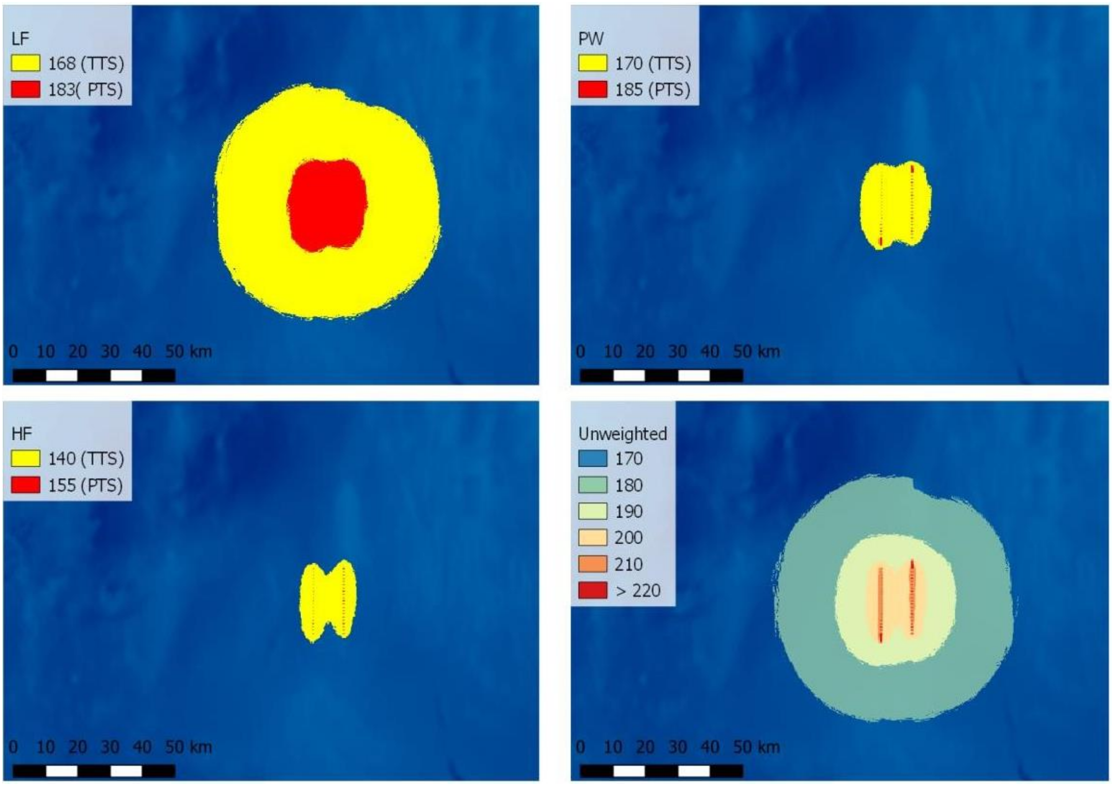

Figure J-7. Scenario 5: Overview of TTS and PTS (NMFS 2018) risk zones for a stationary receiver at 10 m depth. Groups “MF” and “OW” had risk zones too small to meaningfully show.

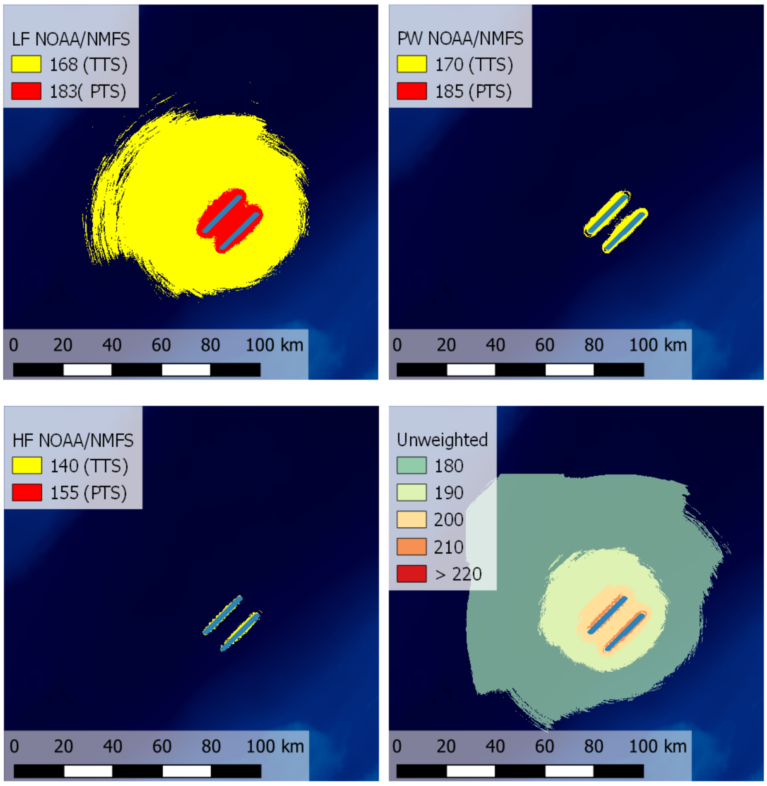

Figure J-8. Scenario 6: Overview of TTS and PTS risk zones for a stationary receiver at 10 m depth. Groups “MF” and “OW” had risk zones too small to meaningfully show.

J.2. Results from TNO

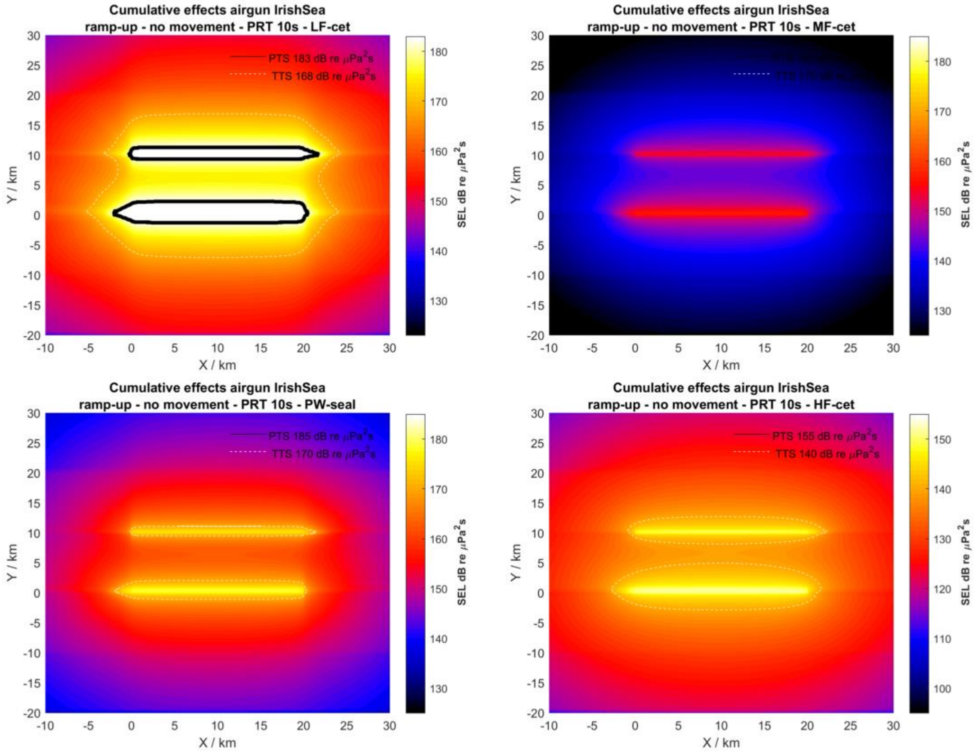

Figure J-9. Scenario 3 Cumulative SEL for multiple lines, assuming no animal movement, using different NMFS-2016 weighting functions for the Irish Sea environment.

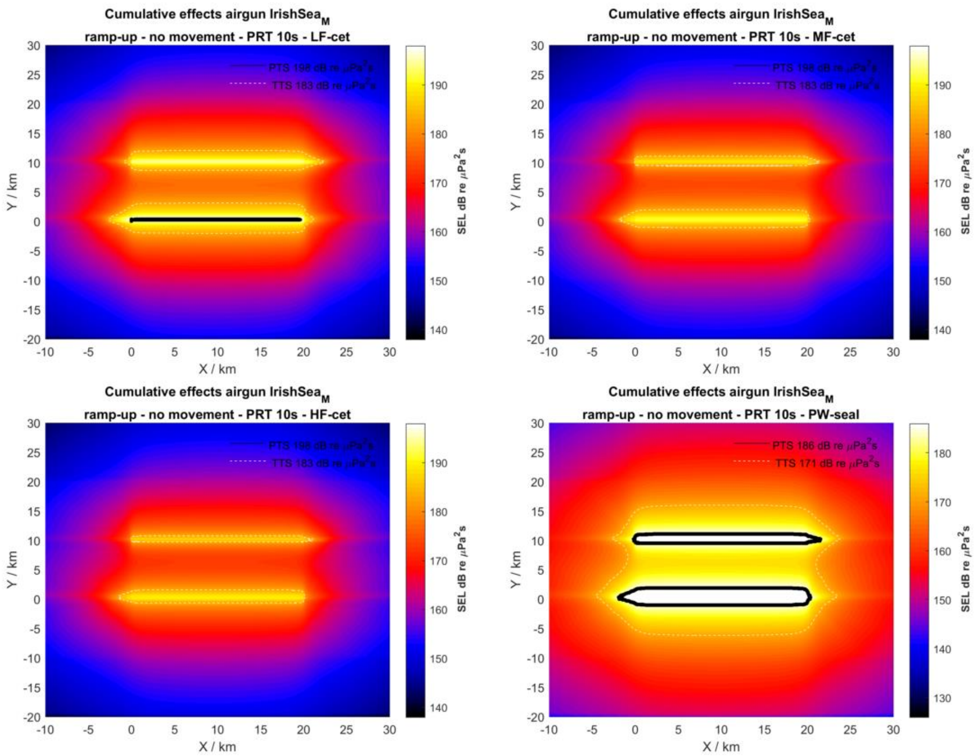

Figure J-10. Scenario 3: Cumulative SEL for multiple lines, assuming no animal movement, using different Southall et al. (2007) M-weighting functions for the Irish Sea scenario.

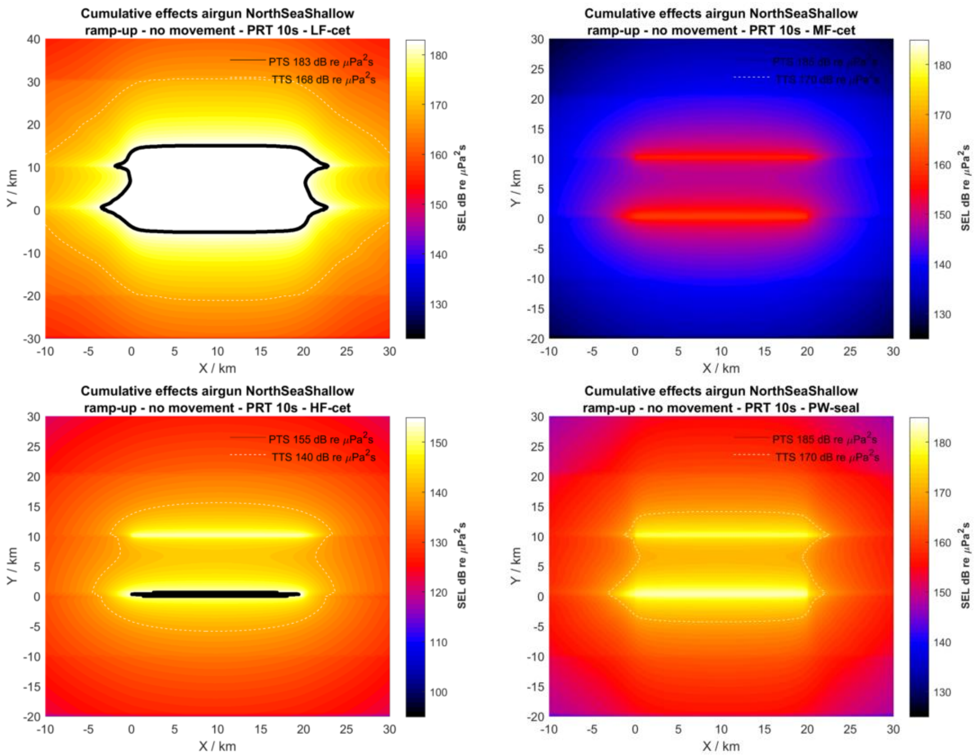

Figure J-11. Scenario 4: Cumulative SEL for multiple lines, assuming no animal movement, using different NMFS-2016 weighting functions for the North Sea Shallow environment.

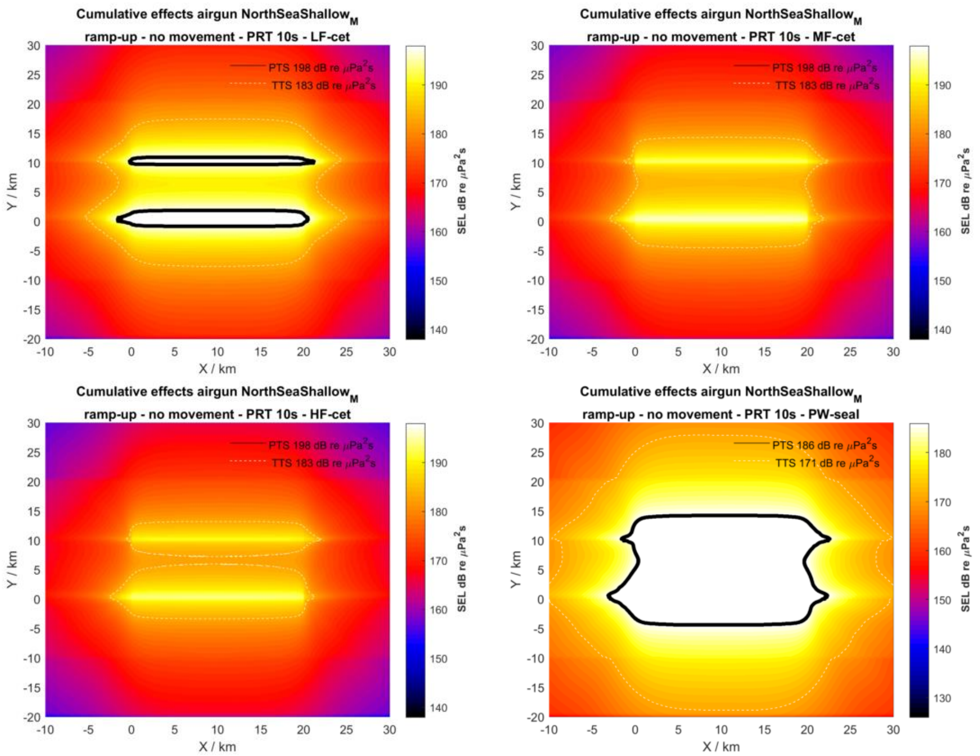

Figure J-12. Scenario 4: Cumulative SEL for multiple lines, assuming no animal movement, using different Southall et al. (2007) M-weighting functions for the North Sea-Shallow environment.

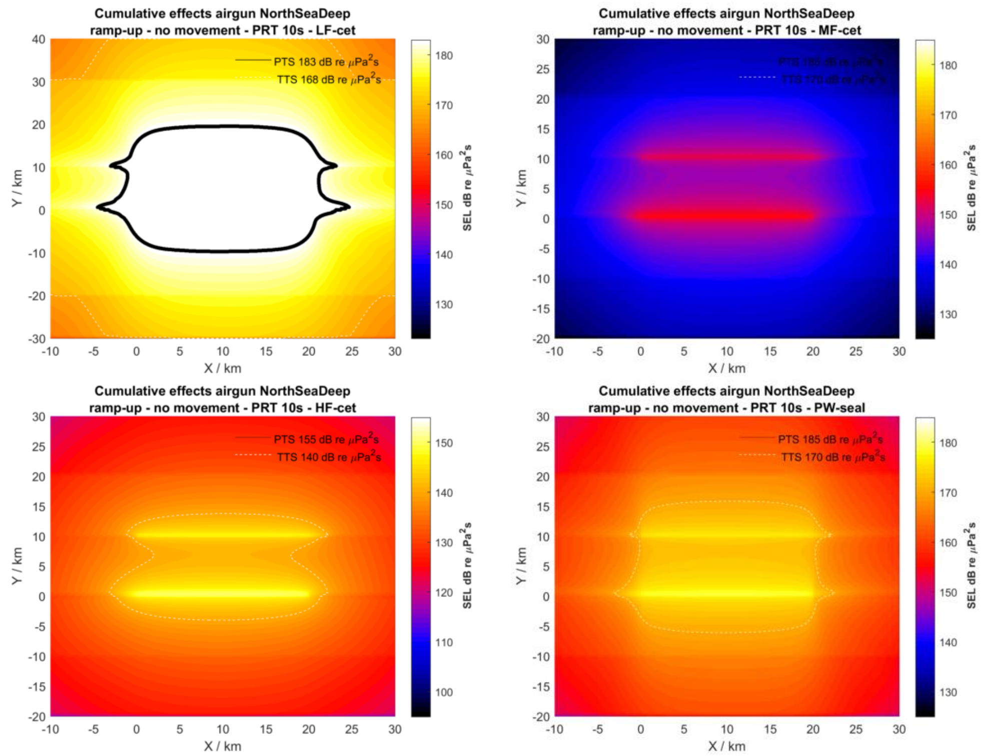

Figure J-13. Scenario 5: Cumulative SEL for multiple lines, assuming no animal movement, using different NMFS-2016 weighting functions for the North Sea Deep environment. Note that the TTS contours on the LF-cetacean (top left panel) were truncated due to the 30 km grid size used in the propagation loss modelling.

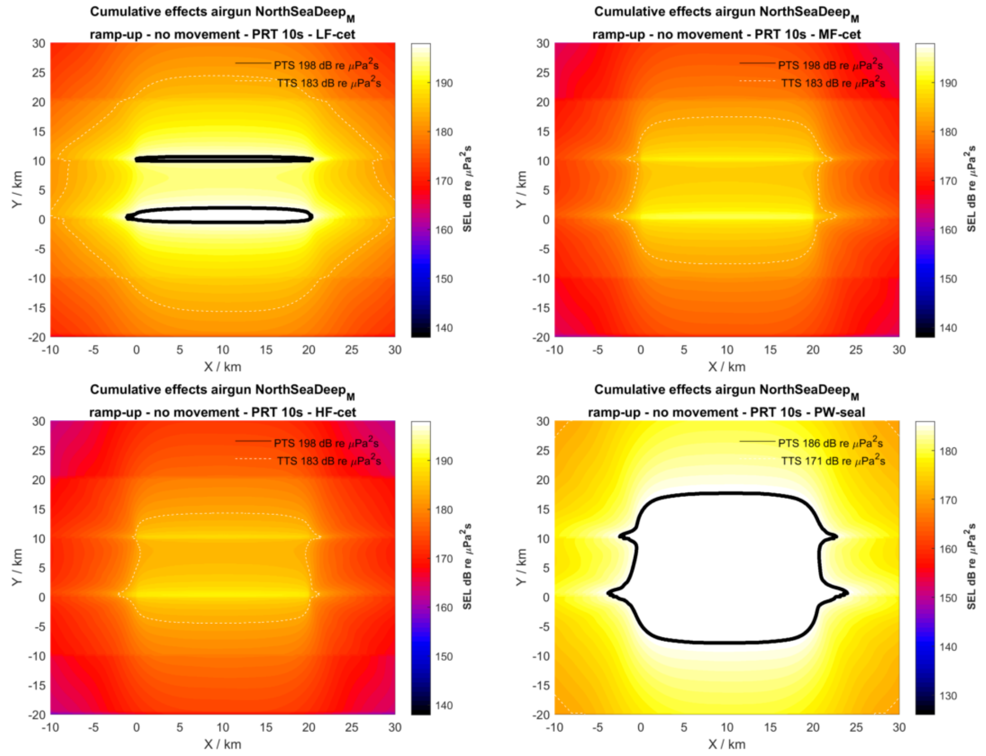

Figure J-14. Cumulative SEL for multiple lines, assuming no animal movement, using different Southall et al. (2007) M-weighting functions for the North Sea-Deep scenario. Note that the TTS contours on the PW-seal (bottom right panel) were truncated due to the 30 km grid size used in the propagation loss modelling.

J.3. Results from JASCO

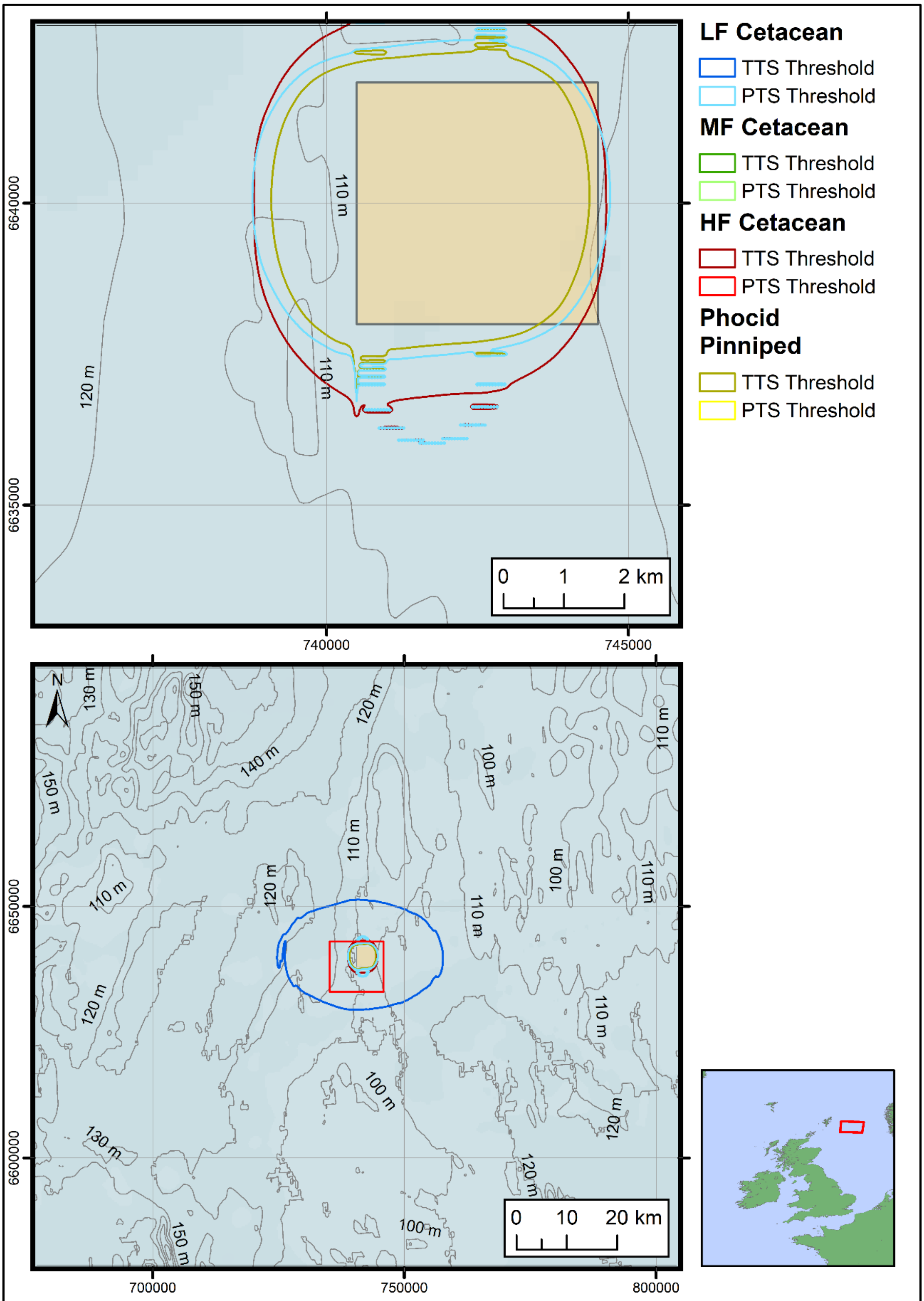

Scenario 1: Site Survey - North Sea Deep - NMFS frequency-weighted results	Datum: WGS84 Projection: UTM30 North	JASCO APPLIED SCIENCES
Representative UKCS Seismic Survey Modelling	Created: Aug 2020	

Figure J-15. Scenario 1: Isopleths to identified frequency-weighted sound impact thresholds.

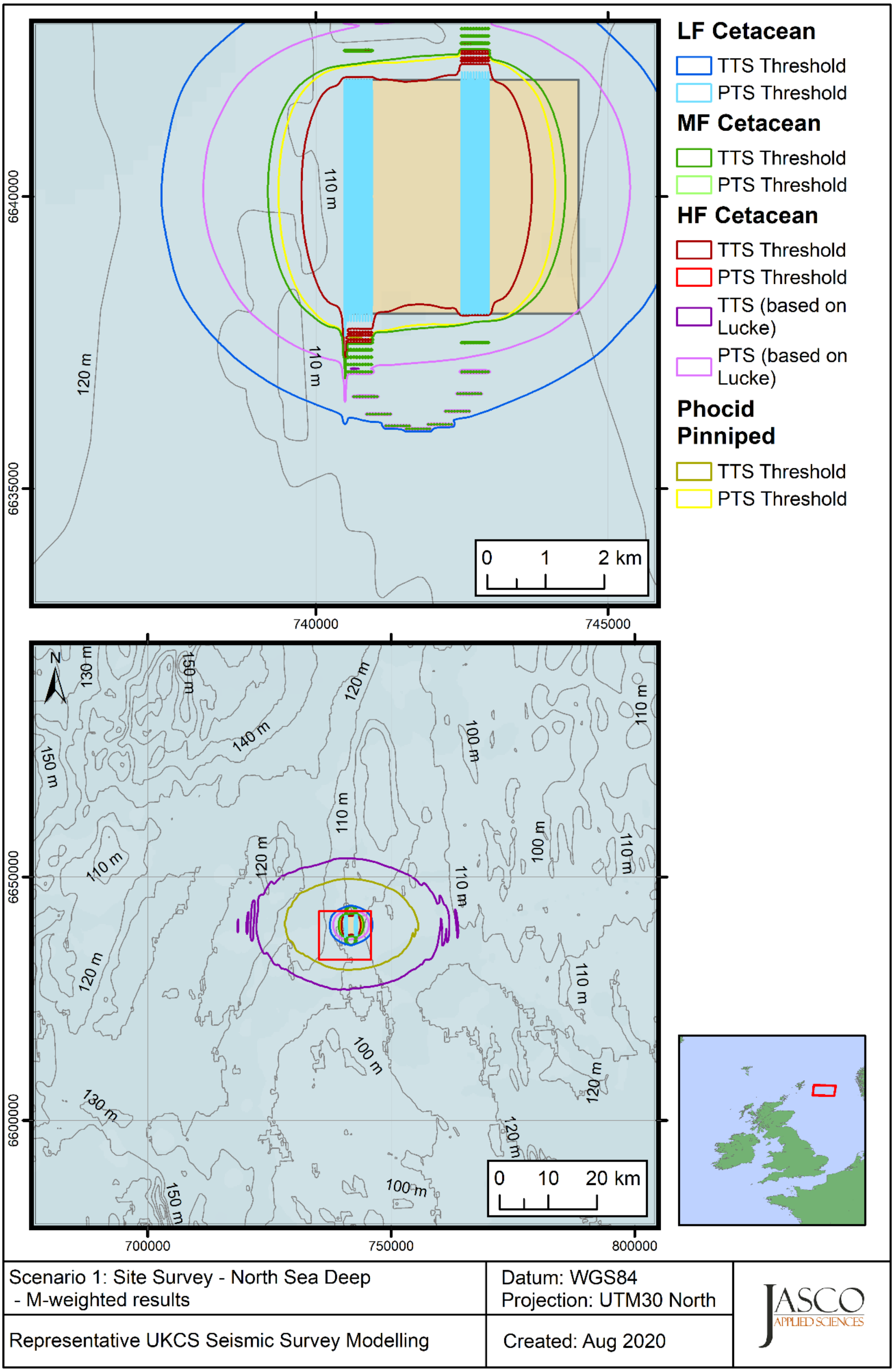

Figure J-16. Scenario 1: Isopleths to identified M-weighted sound impact thresholds.

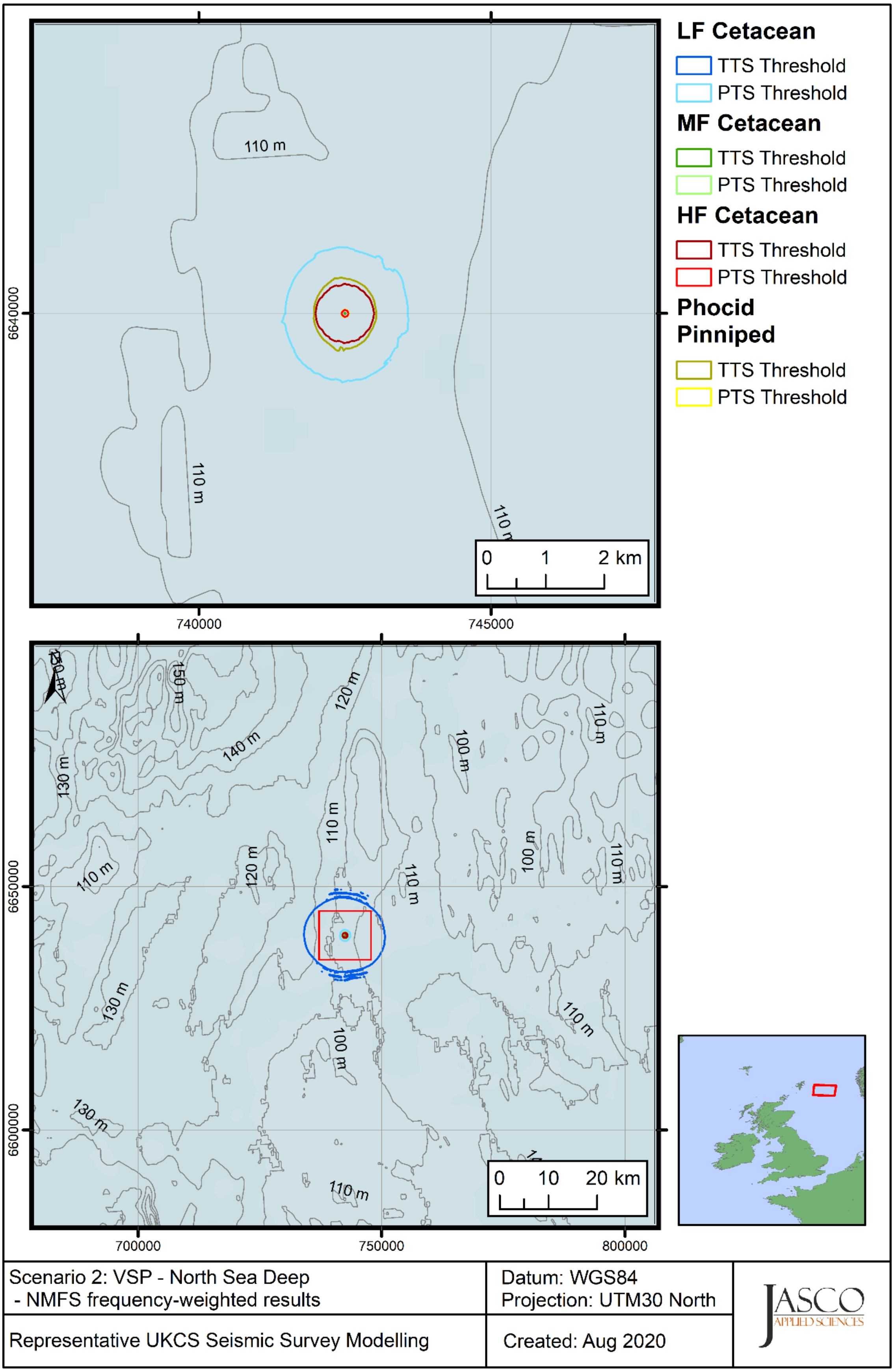

Figure J-17. Scenario 2: Isopleths to identified frequency-weighted sound impact thresholds.

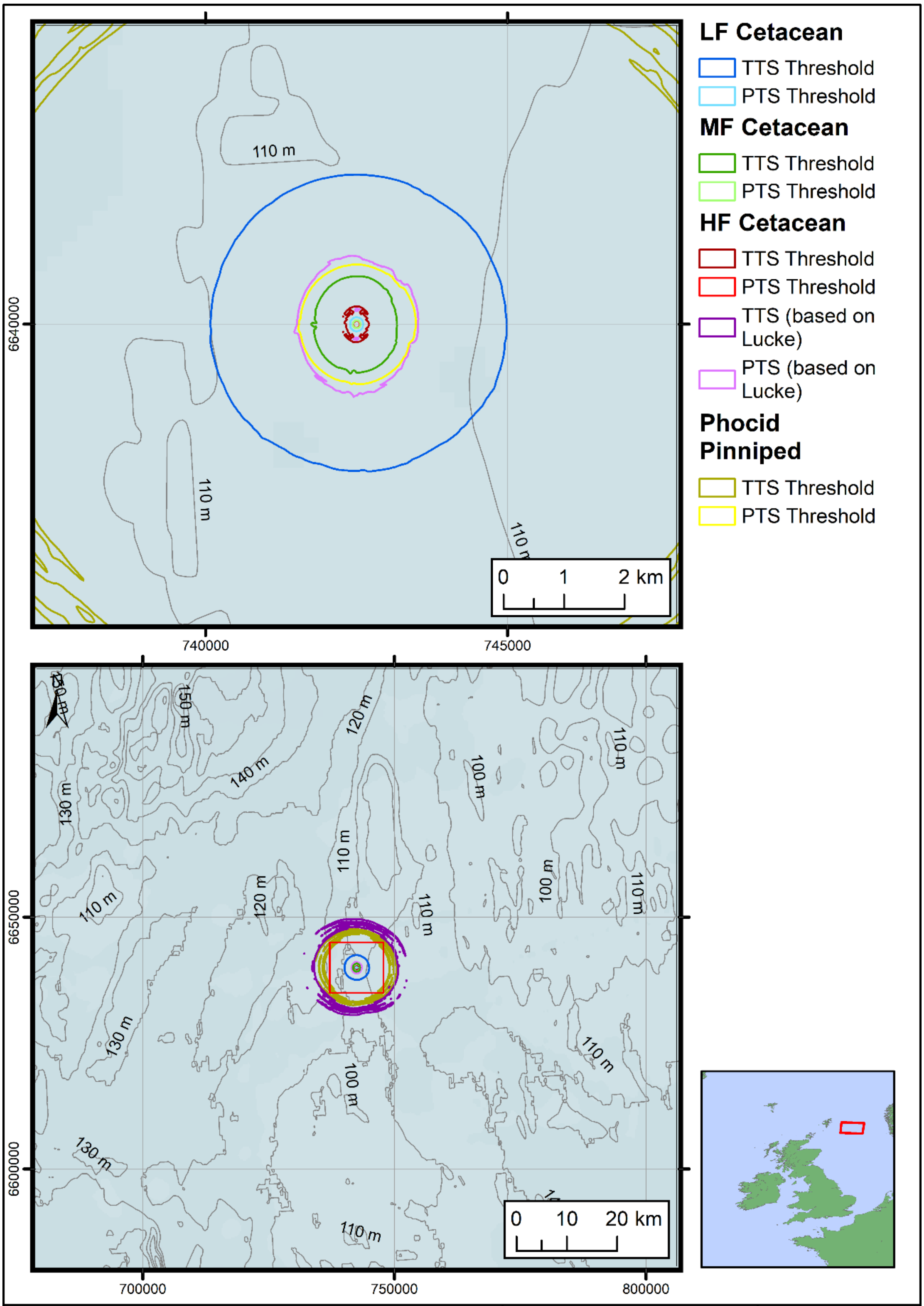

Scenario 2: VSP - North Sea Deep - M-weighted results	Datum: WGS84 Projection: UTM30 North	JASCO APPLIED SCIENCES
Representative UKCS Seismic Survey Modelling	Created: Aug 2020	

Figure J-18. Scenario 2: Isopleths to identified M-weighted sound impact thresholds.

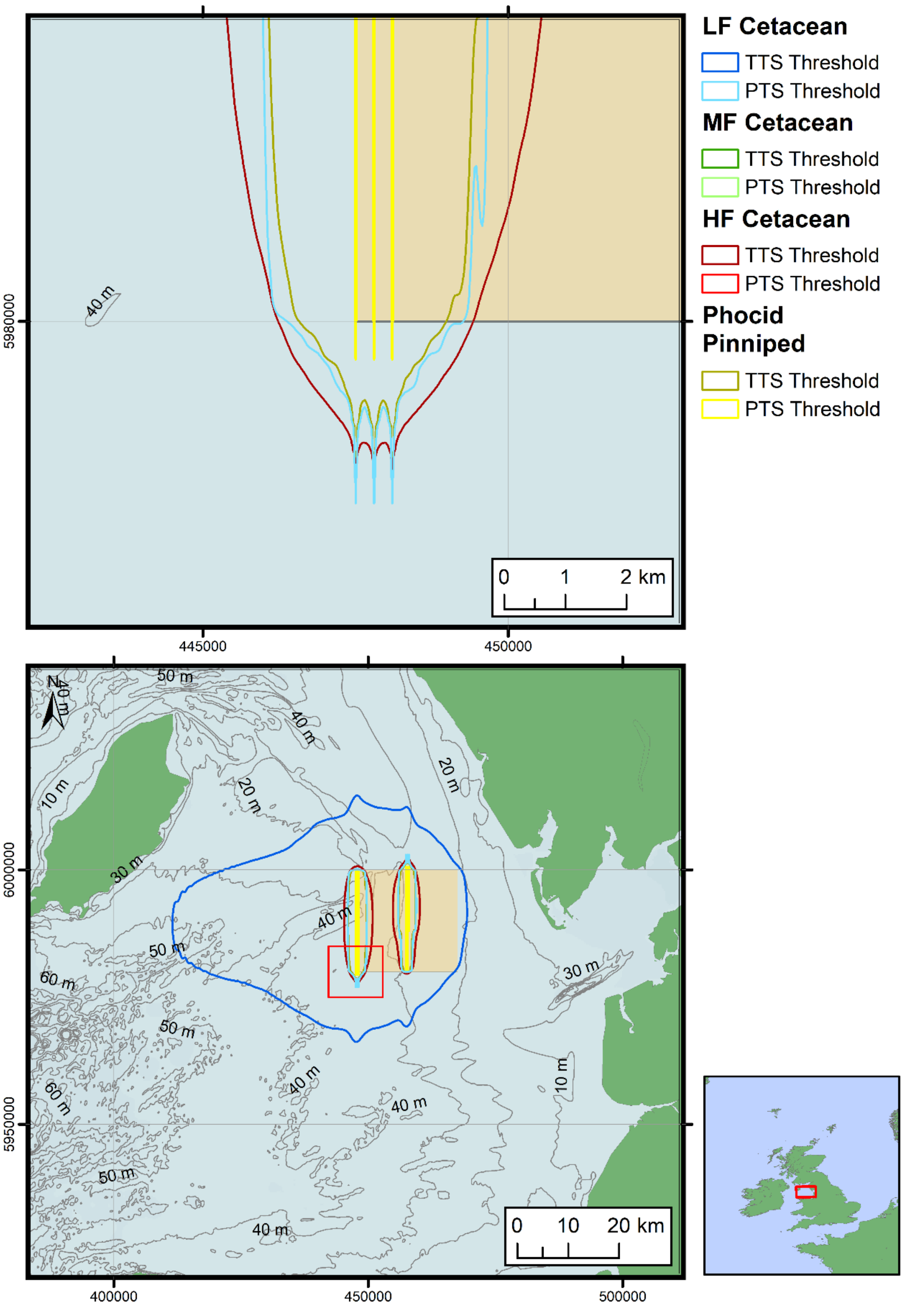

Scenario 3: Regional Survey - Irish Sea - NMFS frequency-weighted results	Datum: WGS84 Projection: UTM30 North	JASCO APPLIED SCIENCES
Representative UKCS Seismic Survey Modelling	Created: Aug 2020	

Figure J-19. Scenario 3: Isopleths to identified frequency-weighted sound impact thresholds.

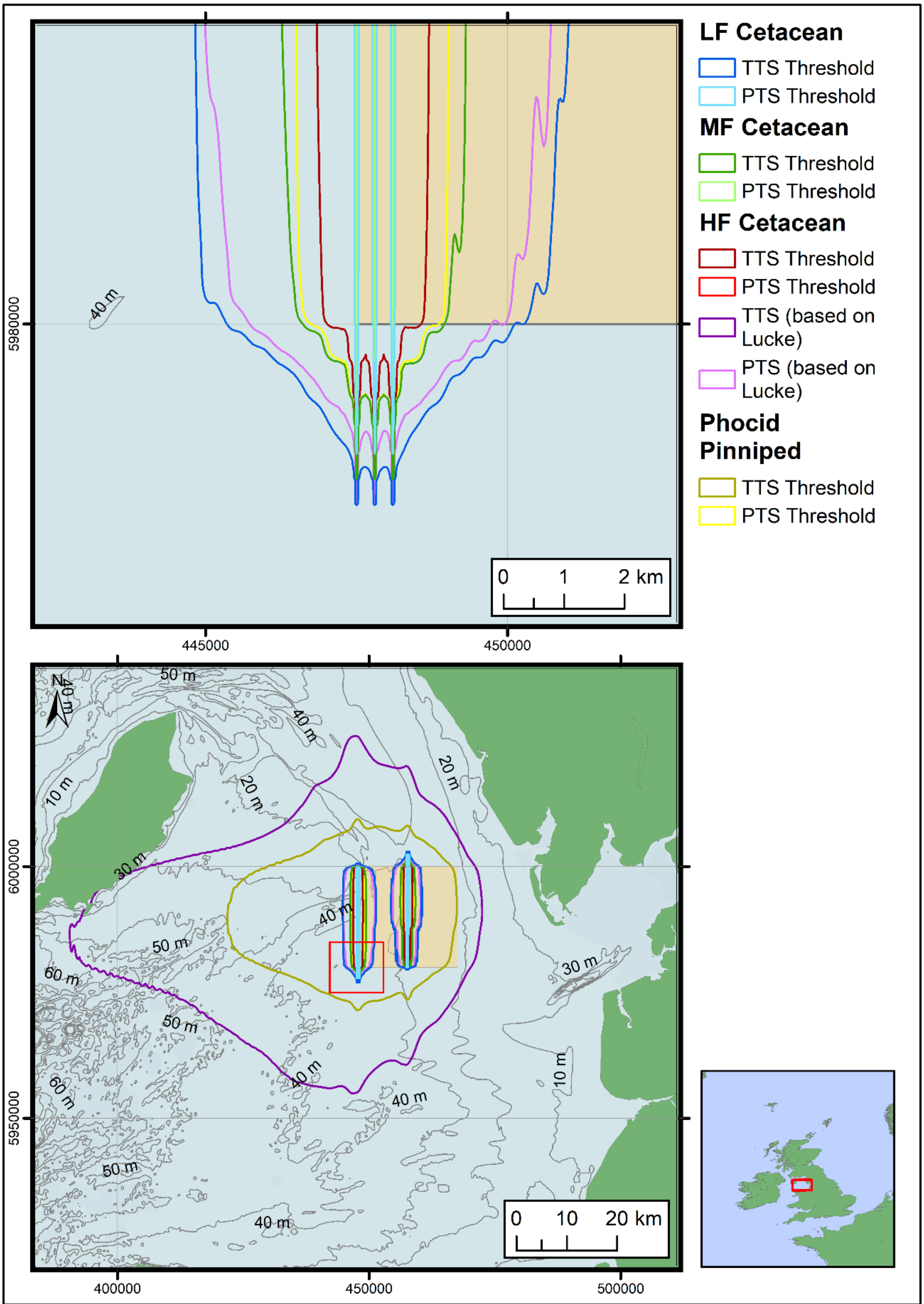

Scenario 3: Regional Survey - Irish Sea - M-weighted results	Datum: WGS84 Projection: UTM30 North
Representative UKCS Seismic Survey Modelling	Created: Aug 2020

Figure J-20. Scenario 3: Isopleths to identified M-weighted sound impact thresholds.

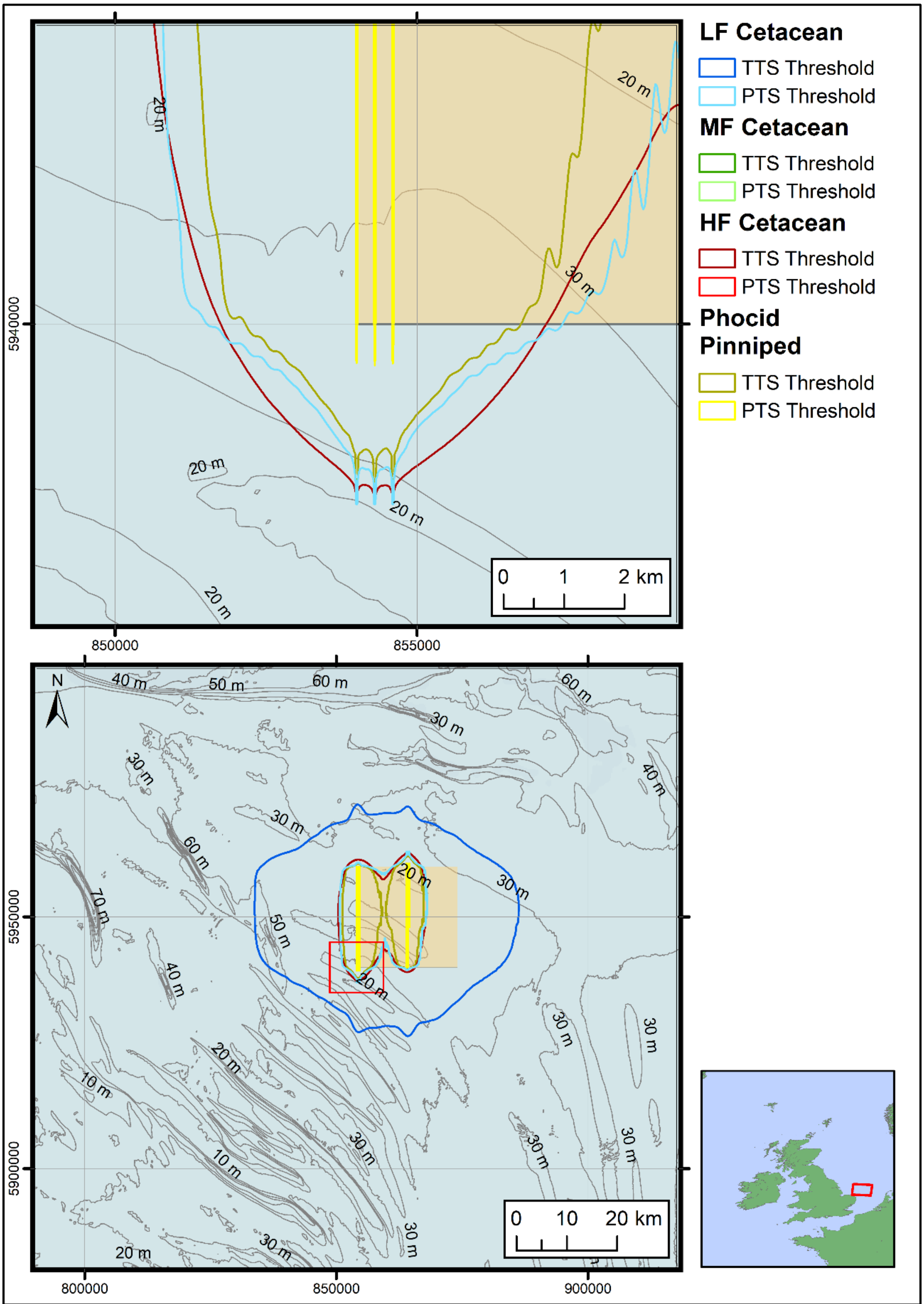

Scenario 4: Regional Survey - North Sea Shallow - NMFS frequency-weighted results	Datum: WGS84 Projection: UTM30 North	JASCO APPLIED SCIENCES
Representative UKCS Seismic Survey Modelling	Created: Aug 2020	

Figure J-21. Scenario 4: Isopleths to identified frequency-weighted sound impact thresholds.

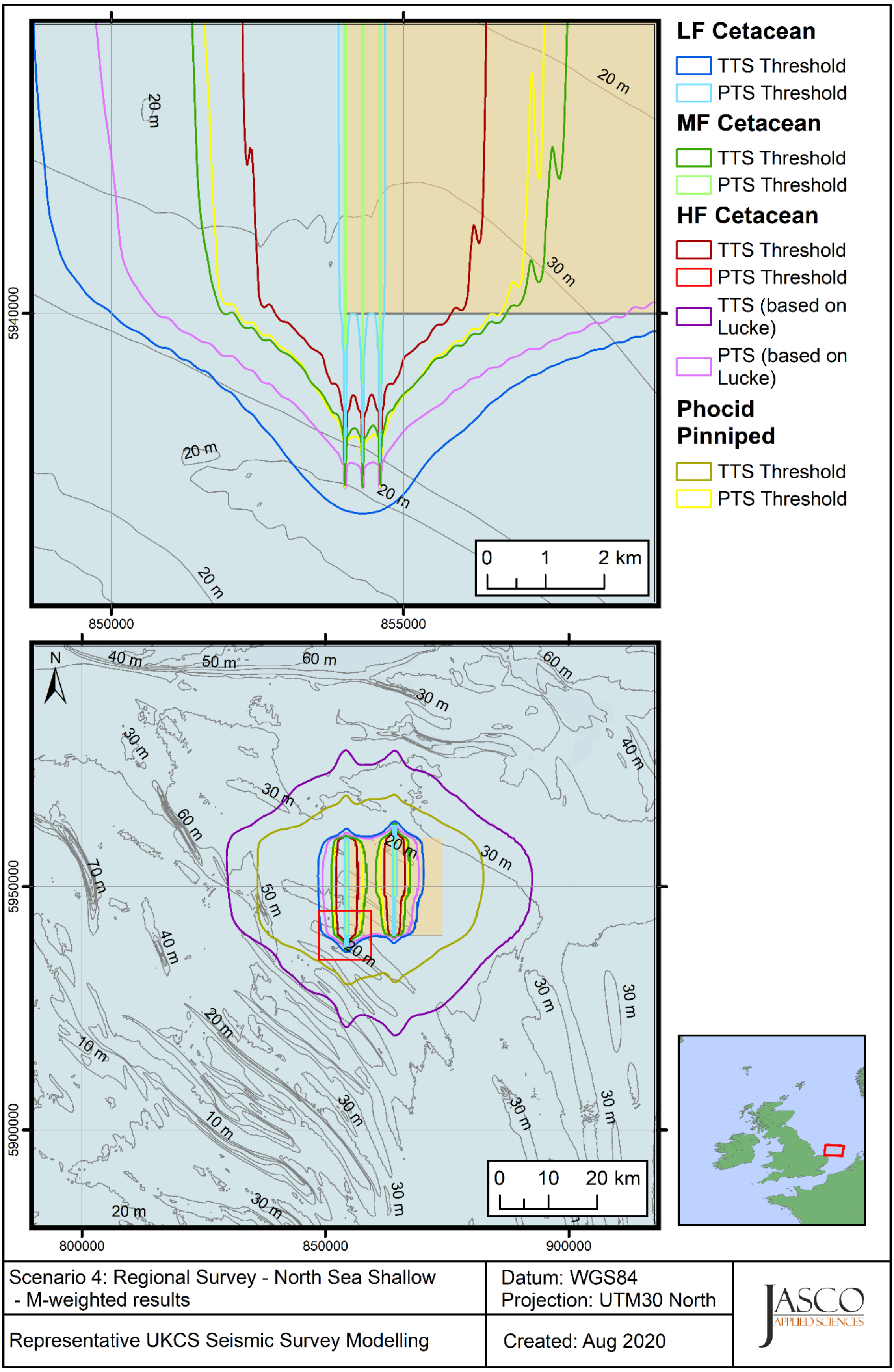

Figure J-22. Scenario 4: Isopleths to identified M-weighted sound impact thresholds.

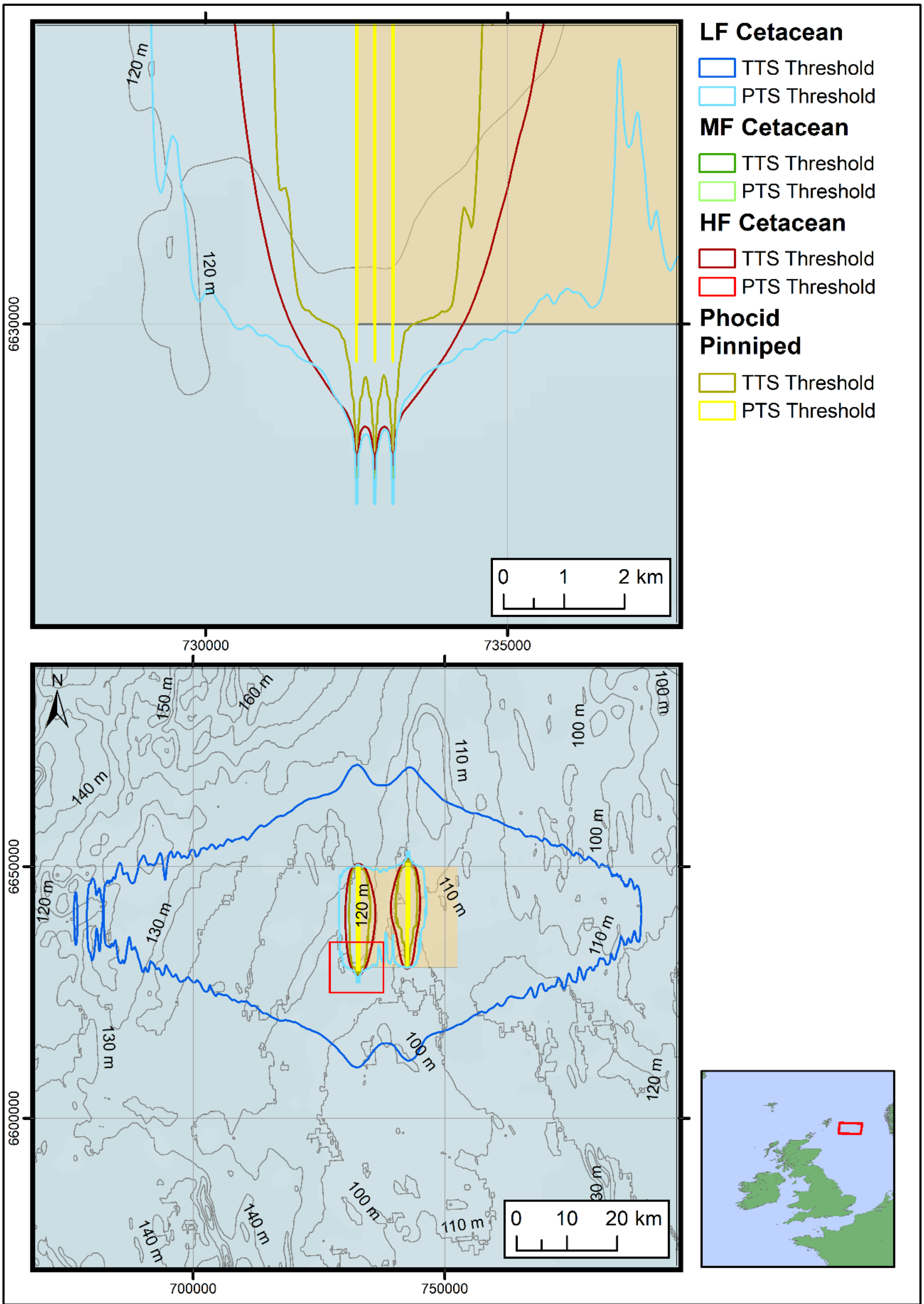

Scenario 5: Regional Survey - North Sea Deep - NMFS frequency-weighted results	Datum: WGS84 Projection: UTM30 North	JASCO APPLIED SCIENCES
Representative UKCS Seismic Survey Modelling	Created: Aug 2020	

Figure J-23. Scenario 5: Isopleths to identified frequency-weighted sound impact thresholds.

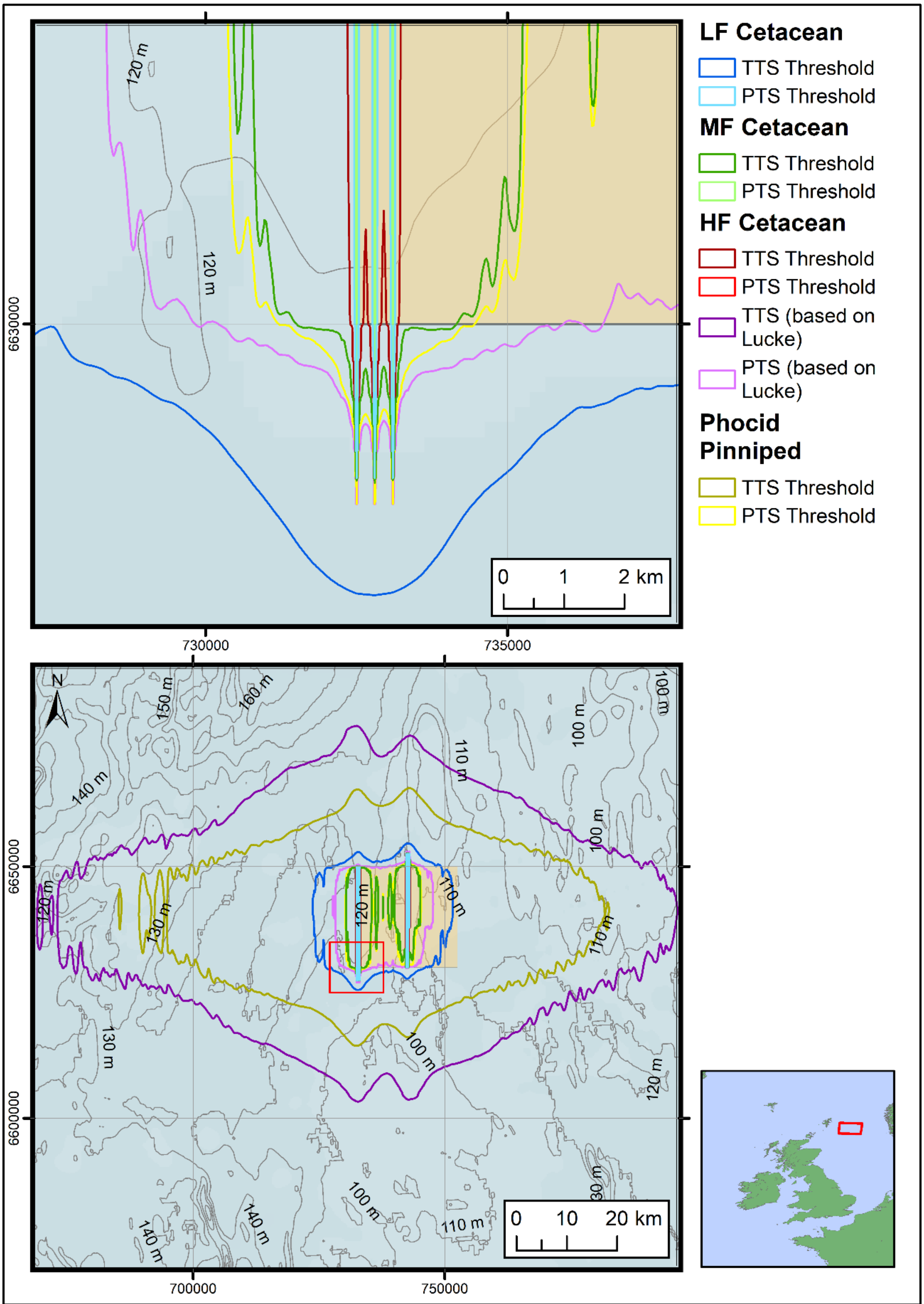

Scenario 5: Regional Survey - North Sea Deep - M-weighted results	Datum: WGS84 Projection: UTM30 North	JASCO APPLIED SCIENCES
Representative UKCS Seismic Survey Modelling	Created: Aug 2020	

Figure J-24. Scenario 5: Isopleths to identified M-weighted sound impact thresholds.

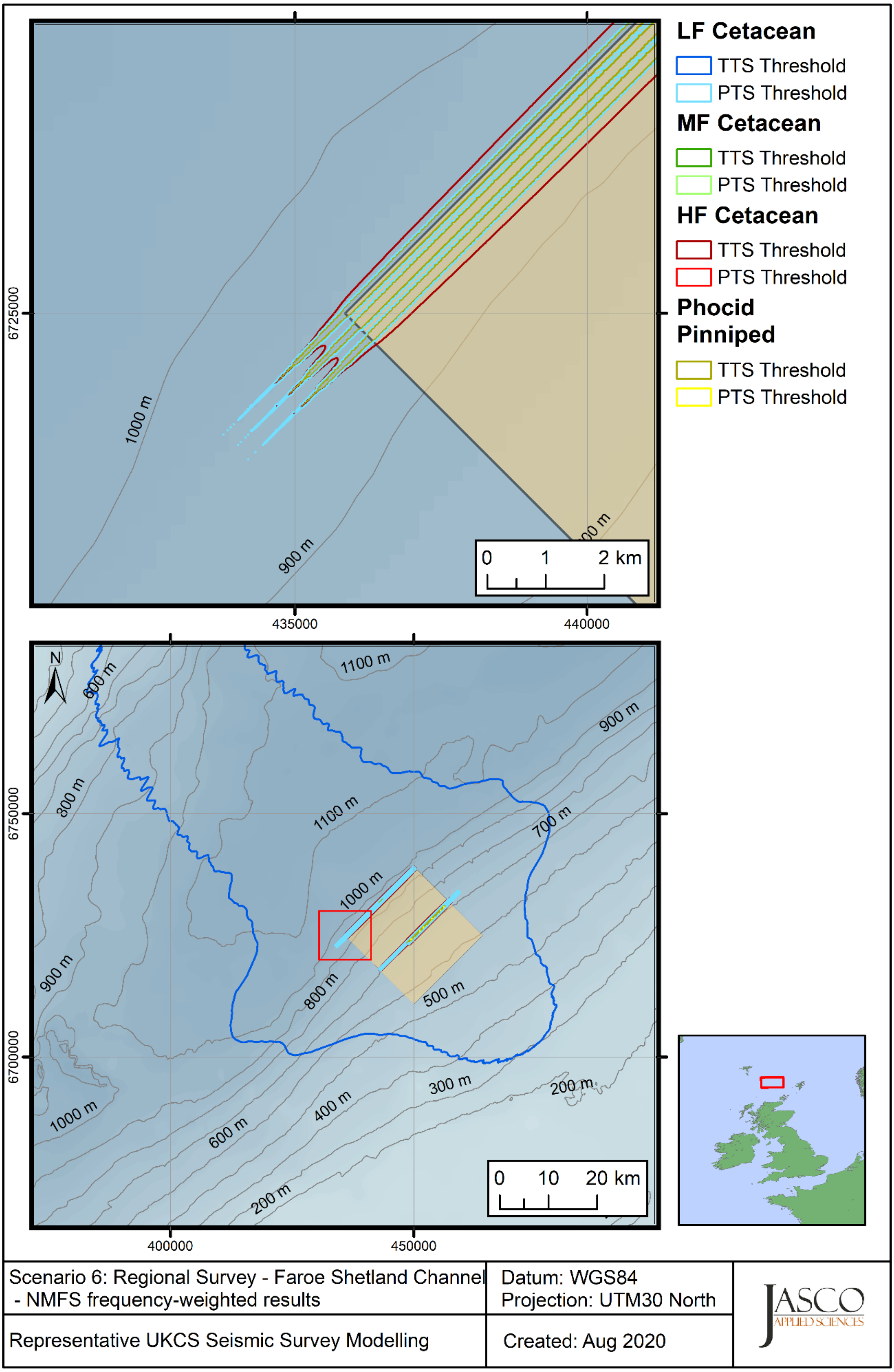

Figure J-25. Scenario 6: Isopleths to identified frequency-weighted sound impact thresholds.

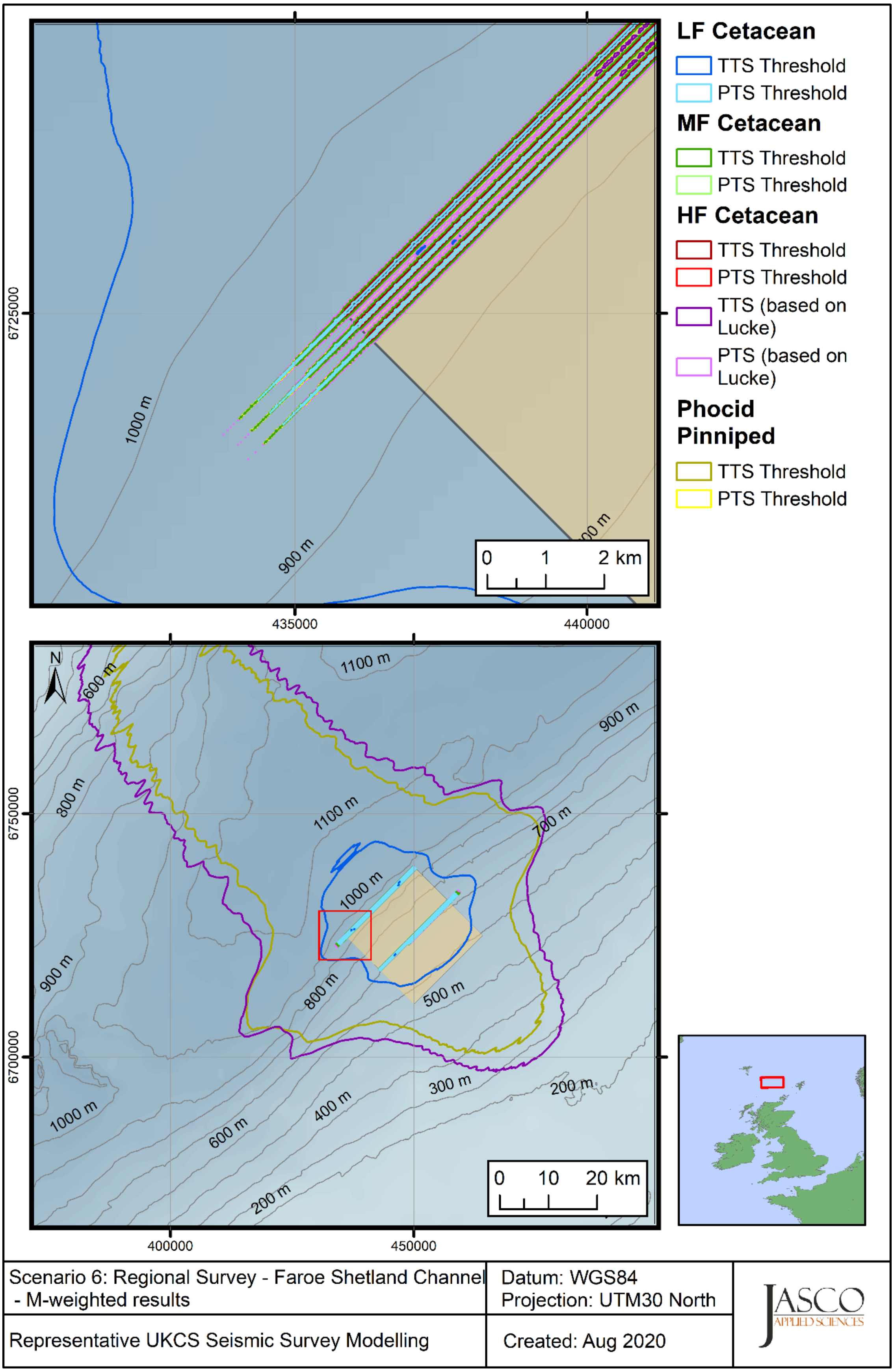

Figure J-26. Scenario 6: Isopleths to identified M-weighted sound impact thresholds.

Appendix K. Empirical Method Results

K.1. Peak Sound Pressure – NMFS criteria

K.1.1. Scenario 1

Table K-1. Scenario 1: Maximum ranges at 10 m depth to the peak sound pressure level threshold values defined by the NMFS 2018 criteria. Empirical approach using “$X \log R$” with X = (20, 18, and 15) with different nominal source level reductions relative to the vertical beam. Note that the “$X \log R$” approach typically does not make physical sense; the methodology presented here is provided only for indicative values and should not be taken out of context of the work presented in this report.

Type of animal	Effect	$L_{p,pk}$	$20 \log R$			$18 \log R$			$15 \log R$		
		(dB re 1 µPa)	vert. beam (0 dB)	horiz. beam (-12 dB)	horiz. beam (-20 dB)	vert. beam (0 dB)	horiz. beam (-12 dB)	horiz. beam (-20 dB)	vert. beam (0 dB)	horiz. beam (-12 dB)	horiz. beam (-20 dB)
			R_{max} (km)	R_{max} (km)	R_{max} (km)	R_{max} (km)	R_{max} (km)	R_{max} (km)	R_{max} (km)	R_{max} (km)	R_{max} (km)
Low-frequency cetaceans	PTS	219	0.01	0.00	0.00	0.01	0.00	0.00	0.02	0.00	0.00
	TTS	213	0.02	0.00	0.00	0.03	0.00	0.00	0.05	0.00	0.00
Mid-frequency cetaceans	PTS	230	0.00	0.00	0.00	0.00	0.00	0.00	0.00	0.00	0.00
	TTS	224	0.00	0.00	0.00	0.00	0.00	0.00	0.01	0.00	0.00
High-frequency cetaceans	PTS	202	0.07	0.02	0.00	0.11	0.02	0.00	0.27	0.04	0.01
	TTS	196	0.13	0.03	0.01	0.23	0.05	0.02	0.69	0.11	0.03
Phocid pinnipeds in water	PTS	218	0.01	0.00	0.00	0.01	0.00	0.00	0.02	0.00	0.00
	TTS	212	0.02	0.00	0.00	0.03	0.00	0.00	0.06	0.01	0.00

K.1.2. Scenario 2

Table K-2. Scenario 2: Maximum ranges at 10 m depth to the peak sound pressure level threshold values defined by the NMFS 2018 criteria. Empirical approach using "$X \log R$" with X = (20, 18, and 15) with different nominal source level reductions relative to the vertical beam. Note that the "$X \log R$" approach typically does not make physical sense; the methodology presented here is provided only for indicative values and should not be taken out of context of the work presented in this report.

Type of animal	Effect	$L_{p,pk}$	20 log R			18 log R			15 log R		
		(dB re 1 µPa)	vert. beam (0 dB)	horiz. beam (-12 dB)	horiz. beam (-20 dB)	vert. beam (0 dB)	horiz. beam (-12 dB)	horiz. beam (-20 dB)	vert. beam (0 dB)	horiz. beam (-12 dB)	horiz. beam (-20 dB)
			R_{max} (km)	R_{max} (km)	R_{max} (km)	R_{max} (km)	R_{max} (km)	R_{max} (km)	R_{max} (km)	R_{max} (km)	R_{max} (km)
Low-frequency cetaceans	PTS	219	0.01	0.00	0.00	0.01	0.00	0.00	0.02	0.00	0.00
	TTS	213	0.02	0.00	0.00	0.03	0.00	0.00	0.06	0.01	0.00
Mid-frequency cetaceans	PTS	230	0.00	0.00	0.00	0.00	0.00	0.00	0.00	0.00	0.00
	TTS	224	0.00	0.00	0.00	0.01	0.00	0.00	0.01	0.00	0.00
High-frequency cetaceans	PTS	202	0.08	0.02	0.01	0.12	0.03	0.01	0.32	0.05	0.02
	TTS	196	0.15	0.04	0.02	0.26	0.06	0.02	0.80	0.13	0.04
Phocid pinnipeds in water	PTS	218	0.01	0.00	0.00	0.02	0.00	0.00	0.03	0.00	0.00
	TTS	212	0.02	0.00	0.00	0.03	0.01	0.00	0.07	0.01	0.00

K.1.3. Scenarios 3–6

Table K-3. Scenario 3-6: Maximum ranges at 10 m depth to the peak sound pressure level threshold values defined by the NMFS 2018 criteria. Empirical approach using "$X \log R$" with X = (20, 18, and 15) with different nominal source level reductions relative to the vertical beam. Note that the "$X \log R$" approach typically does not make physical sense; the methodology presented here is provided only for indicative values and should not be taken out of context of the work presented in this report.

Type of animal	Effect	$L_{p,pk}$	$20 \log R$			$18 \log R$			$15 \log R$		
		(dB re 1 µPa)	vert. beam (0 dB)	horiz. beam (-12 dB)	horiz. beam (-20 dB)	vert. beam (0 dB)	horiz. beam (-12 dB)	horiz. beam (-20 dB)	vert. beam (0 dB)	horiz. beam (-12 dB)	horiz. beam (-20 dB)
			R_{max} (km)	R_{max} (km)	R_{max} (km)	R_{max} (km)	R_{max} (km)	R_{max} (km)	R_{max} (km)	R_{max} (km)	R_{max} (km)
Low-frequency cetaceans	PTS	219	0.09	0.02	0.01	0.15	0.03	0.01	0.42	0.07	0.02
	TTS	213	0.18	0.05	0.02	0.33	0.07	0.03	1.05	0.17	0.05
Mid-frequency cetaceans	PTS	230	0.03	0.01	0.00	0.04	0.01	0.00	0.08	0.01	0.00
	TTS	224	0.05	0.02	0.01	0.08	0.02	0.01	0.19	0.03	0.01
High-frequency cetaceans	PTS	202	0.65	0.16	0.07	1.35	0.29	0.10	5.68	0.90	0.26
	TTS	196	1.31	0.33	0.13	2.90	0.62	0.22	14.28	2.26	0.66
Phocid pinnipeds in water	PTS	218	0.10	0.03	0.01	0.17	0.04	0.02	0.49	0.08	0.02
	TTS	212	0.21	0.05	0.02	0.37	0.08	0.03	1.22	0.19	0.06

K.2. Peak Sound Pressure – Southall et al 2007 criteria

K.2.1. Scenario 1

Table K-4. Scenario 1: Maximum ranges at 10 m depth to the peak sound pressure threshold values defined by Southall (2007) and Lucke (2009). Empirical approach using "$X \log R$" with X = (20, 18, and 15) with different nominal source level reductions relative to the vertical beam. Note that the "$X \log R$" approach typically does not make physical sense; the methodology presented here is provided only for indicative values and should not be taken out of context of the work presented in this report.

Type of animal	Effect	$L_{p,pk}$ (dB re 1 μPa)	20 log R			18 log R			15 log R		
			vert. beam (0 dB)	horiz. beam (-12 dB)	horiz. beam (-20 dB)	vert. beam (0 dB)	horiz. beam (-12 dB)	horiz. beam (-20 dB)	vert. beam (0 dB)	horiz. beam (-12 dB)	horiz. beam (-20 dB)
			R_{max} (km)	R_{max} (km)	R_{max} (km)	R_{max} (km)	R_{max} (km)	R_{max} (km)	R_{max} (km)	R_{max} (km)	R_{max} (km)
Low-frequency cetaceans	PTS	230	0.00	0.00	0.00	0.00	0.00	0.00	0.00	0.00	0.00
	TTS	224	0.00	0.00	0.00	0.00	0.00	0.00	0.01	0.00	0.00
Mid-frequency cetaceans	PTS	230	0.00	0.00	0.00	0.00	0.00	0.00	0.00	0.00	0.00
	TTS	224	0.00	0.00	0.00	0.00	0.00	0.00	0.01	0.00	0.00
High-frequency cetaceans	PTS	230	0.00	0.00	0.00	0.00	0.00	0.00	0.00	0.00	0.00
	TTS	224	0.00	0.00	0.00	0.00	0.00	0.00	0.01	0.00	0.00
High-frequency cetaceans (based on Lucke)	PTS	200	0.08	0.02	0.00	0.14	0.03	0.01	0.37	0.06	0.02
	TTS	194	0.17	0.04	0.02	0.30	0.06	0.02	0.94	0.15	0.04
Phocid pinnipeds in water	PTS	218	0.01	0.00	0.00	0.01	0.00	0.00	0.02	0.00	0.00
	TTS	212	0.02	0.00	0.00	0.03	0.00	0.00	0.06	0.01	0.00

K.2.2. Scenario 2

Table K-5. Scenario 2: Maximum ranges at 10 m depth to the peak sound pressure threshold values defined by Southall (2007) and Lucke (2009). Empirical approach using "$X \log R$" with X = (20, 18, and 15) with different nominal source level reductions relative to the vertical beam. Note that the "$X \log R$" approach typically does not make physical sense; the methodology presented here is provided only for indicative values and should not be taken out of context of the work presented in this report.

Type of animal	Effect	$L_{p,pk}$	20 log R			18 log R			15 log R		
		(dB re 1 μPa)	vert. beam (0 dB)	horiz. beam (-12 dB)	horiz. beam (-20 dB)	vert. beam (0 dB)	horiz. beam (-12 dB)	horiz. beam (-20 dB)	vert. beam (0 dB)	horiz. beam (-12 dB)	horiz. beam (-20 dB)
			R_{max} (km)	R_{max} (km)	R_{max} (km)	R_{max} (km)	R_{max} (km)	R_{max} (km)	R_{max} (km)	R_{max} (km)	R_{max} (km)
Low-frequency cetaceans	PTS	230	0.00	0.00	0.00	0.00	0.00	0.00	0.00	0.00	0.00
	TTS	224	0.00	0.00	0.00	0.01	0.00	0.00	0.01	0.00	0.00
Mid-frequency cetaceans	PTS	230	0.00	0.00	0.00	0.00	0.00	0.00	0.00	0.00	0.00
	TTS	224	0.00	0.00	0.00	0.01	0.00	0.00	0.01	0.00	0.00
High-frequency cetaceans	PTS	230	0.00	0.00	0.00	0.00	0.00	0.00	0.00	0.00	0.00
	TTS	224	0.00	0.00	0.00	0.01	0.00	0.00	0.01	0.00	0.00
High-frequency cetaceans (based on Lucke)	PTS	200	0.10	0.02	0.01	0.16	0.03	0.01	0.43	0.07	0.02
	TTS	194	0.19	0.05	0.02	0.34	0.07	0.03	1.08	0.17	0.05
Phocid pinnipeds in water	PTS	218	0.01	0.00	0.00	0.02	0.00	0.00	0.03	0.00	0.00
	TTS	212	0.02	0.00	0.00	0.03	0.01	0.00	0.07	0.01	0.00

K.2.3. Scenarios 3–6

Table K-6. Scenario 3-6: Maximum ranges at 10 m depth to the peak sound pressure threshold values defined by Southall (2007) and Lucke (2009). Empirical approach using “$X \log R$” with X = (20, 18, and 15) with different nominal source level reductions relative to the vertical beam. Note that the “$X \log R$” approach typically does not make physical sense; the methodology presented here is provided only for indicative values and should not be taken out of context of the work presented in this report.

Type of animal	Effect	$L_{p,pk}$ (dB re 1 μPa)	20 log R			18 log R			15 log R		
			vert. beam (0 dB)	horiz. beam (-12 dB)	horiz. beam (-20 dB)	vert. beam (0 dB)	horiz. beam (-12 dB)	horiz. beam (-20 dB)	vert. beam (0 dB)	horiz. beam (-12 dB)	horiz. beam (-20 dB)
			R_{max} (km)	R_{max} (km)	R_{max} (km)	R_{max} (km)	R_{max} (km)	R_{max} (km)	R_{max} (km)	R_{max} (km)	R_{max} (km)
Low-frequency cetaceans	PTS	230	0.03	0.01	0.00	0.04	0.01	0.00	0.08	0.01	0.00
	TTS	224	0.05	0.02	0.01	0.08	0.02	0.01	0.19	0.03	0.01
Mid-frequency cetaceans	PTS	230	0.03	0.01	0.00	0.04	0.01	0.00	0.08	0.01	0.00
	TTS	224	0.05	0.02	0.01	0.08	0.02	0.01	0.19	0.03	0.01
High-frequency cetaceans	PTS	230	0.03	0.01	0.00	0.04	0.01	0.00	0.08	0.01	0.00
	TTS	224	0.05	0.02	0.01	0.08	0.02	0.01	0.19	0.03	0.01
High-frequency cetaceans (based on Lucke)	PTS	200	0.82	0.21	0.08	1.74	0.37	0.13	7.73	1.22	0.36
	TTS	194	1.64	0.41	0.16	3.74	0.81	0.29	15.00	3.08	0.90
Phocid pinnipeds in water	PTS	218	0.10	0.03	0.01	0.17	0.04	0.02	0.49	0.08	0.02
	TTS	212	0.21	0.05	0.02	0.37	0.08	0.03	1.22	0.19	0.06

K.3. SEL_{24h} – NMFS criteria Scenarios 3–6

Table K-7. Maximum ranges at 10 m depth to the frequency-weighted SEL_{24h} threshold values defined by NMFS (2018). All sound exposure levels are frequency-weighted. Model predictions are based on accumulation over all shots points, using empirical approach for propagation loss using "$X \log R$" with X = (20, 18, and 15) and nominal vertical beam corrections of 0 dB (downward) and -12 dB (horizontal). Note that the "$X \log R$" approach typically does not make physical sense; the methodology presented here is provided only for indicative values and should not be taken out of context of the work presented in this report.

Type of animal	Effect	$SEL_{24h,Weighted}$	$20 \log R$		$18 \log R$		$15 \log R$	
		(dB re 1 µPa²s)	*0 dB*	*-12 dB*	*0 dB*	*-12 dB*	*0 dB*	*-12 dB*
			R_{max} (km)	R_{max} (km)	R_{max} (km)	R_{max} (km)	R_{max} (km)	R_{max} (km)
Low-frequency cetaceans	PTS	183	10.0	1.9	26.2	5.3	178	31.6
	TTS	168	52.4	13.0	147	38.1	†	268
Mid-frequency cetaceans	PTS	185	0.01	0.0	0.01	0.0	0.01	0.0
	TTS	170	0.05	0.01	0.18	0.01	5.3	0.03
High-frequency cetaceans	PTS	155	2.6	0.12	8.9	0.60	23	9.5
	TTS	140	19.4	5.3	27.7	12.0	110	31.8
Phocid pinnipeds in water	PTS	185	0.29	0.02	2.2	0.04	15.4	1.4
	TTS	170	7.5	0.73	19.4	3.8	120	22.8

† indicates ranges were greater than the calculation domain

K.4. SEL_{24h} – Southall et al. 2007 criteria Scenarios 3–6

Table K-8. Maximum ranges at 10 m depth to the M-weighted SEL_{24h} threshold values defined by Southall (2007) and Lucke (2009). All sound exposure levels are M-weighted. Model predictions are based on accumulation over all shots points, using empirical approach for propagation loss using "$X \log R$" with X = (20, 18, and 15) and nominal vertical beam corrections of 0 dB (downward) and -12 dB (horizontal). Note that the "$X \log R$" approach typically does not make physical sense; the methodology presented here is provided only for indicative values and should not be taken out of context of the work presented in this report.

Type of animal	Effect	$SEL_{24h,MW}$	$20 \log R$		$18 \log R$		$15 \log R$	
		(dB re 1 µPa²s)	*0 dB*	*-12 dB*	*0 dB*	*-12 dB*	*0 dB*	*-12 dB*
			R_{max} (km)	R_{max} (km)	R_{max} (km)	R_{max} (km)	R_{max} (km)	R_{max} (km)
Low-frequency cetaceans	PTS	198	3.3	0.10	10.4	0.85	60	10.4
	TTS	183	21.9	5.3	66	14.0	552	95
Mid-frequency cetaceans	PTS	198	0.27	0.02	2.1	0.04	15.0	1.3
	TTS	183	7.2	0.69	19.4	4.2	131	23.3
High-frequency cetaceans	PTS	198	0.14	0.02	1.1	0.02	10.9	0.49
	TTS	183	5.3	0.38	15.9	2.8	97	17.9
High-frequency cetaceans (based on Lucke)	PTS	179	10.1	1.2	26.0	5.3	165	23.3
	TTS	164	51.4	13.8	154	37.6	520	242
Phocid pinnipeds in water	PTS	186	8.4	0.89	23.0	5.3	157	27.1
	TTS	171	46.8	11.2	147	33.5	†	238

† indicates ranges were greater than the calculation domain

Appendix L. Spectral Differences Between Sources

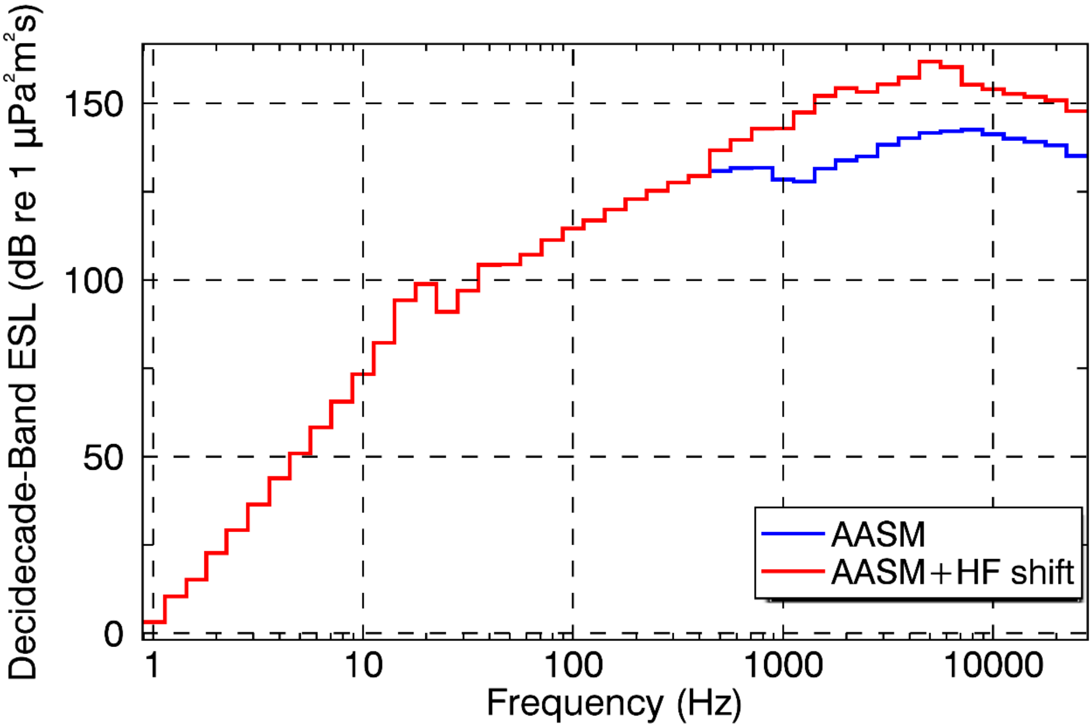

Figure L-1. Horizontal array energy source levels weighted for high-frequency cetaceans. Levels are maximum over all modelled azimuths. Results shown for soft-start step 1. Results are for the AASM spectrum (blue) and for the modified AASM spectrum, shifted by the amount indicated in Figure 34 and Table 45.

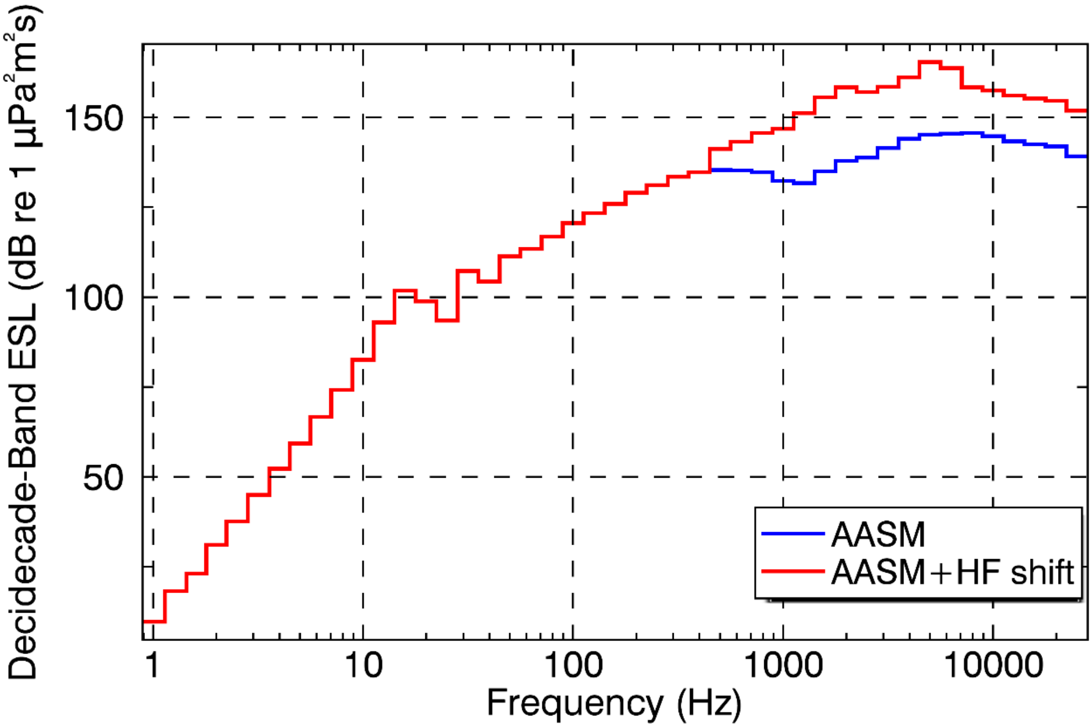

Figure L-2. Horizontal array energy source levels weighted for high-frequency cetaceans. Levels are maximum over all modelled azimuths. Results shown for soft-start step 2.

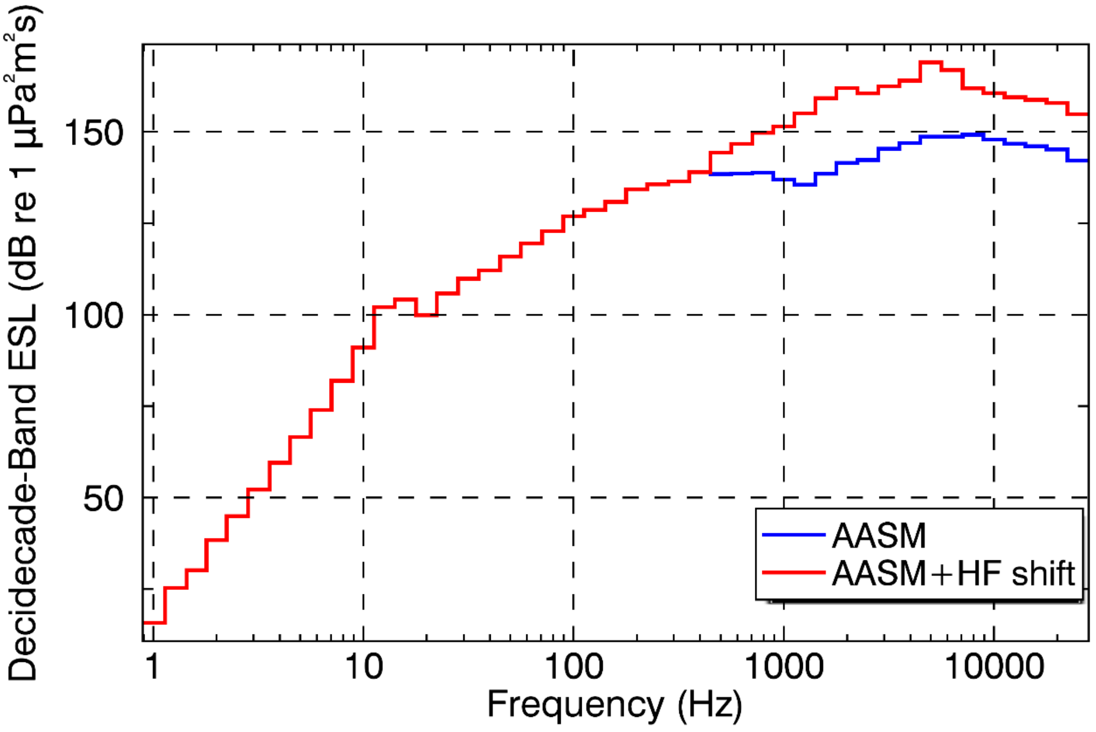

Figure L-3. Horizontal array energy source levels weighted for high-frequency cetaceans. Levels are maximum over all modelled azimuths. Results shown for soft-start step 3.

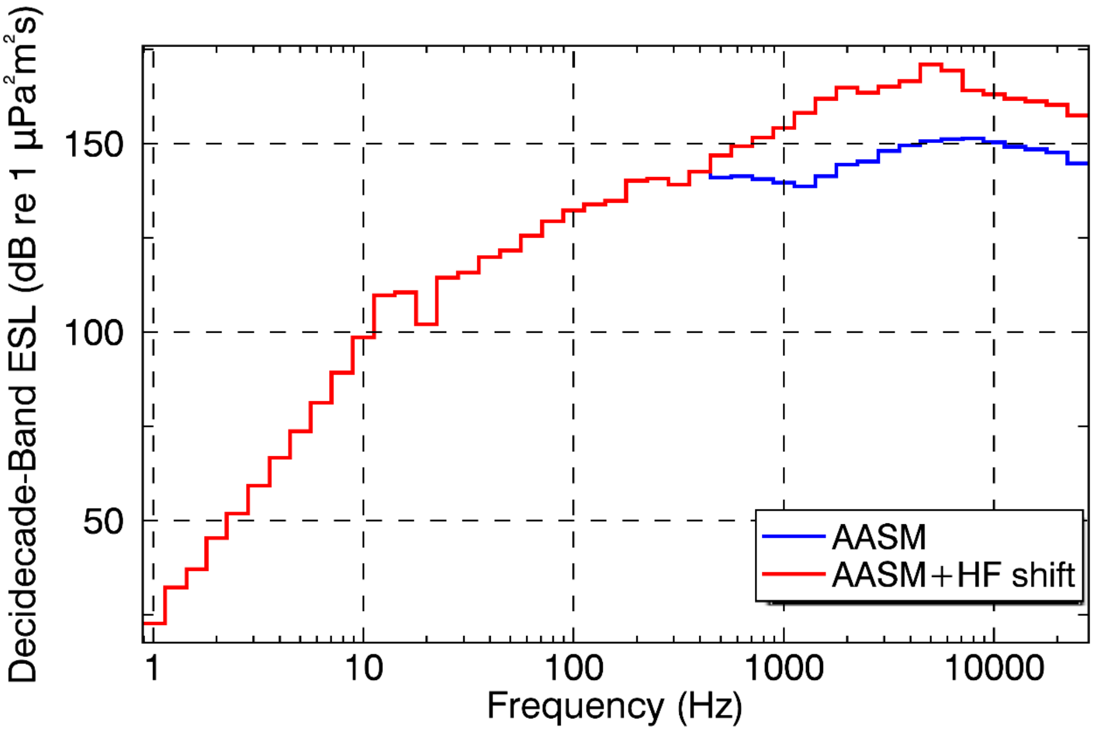

Figure L-4. Horizontal array energy source levels weighted for high-frequency cetaceans. Levels are maximum over all modelled azimuths. Results shown for soft-start step 4.

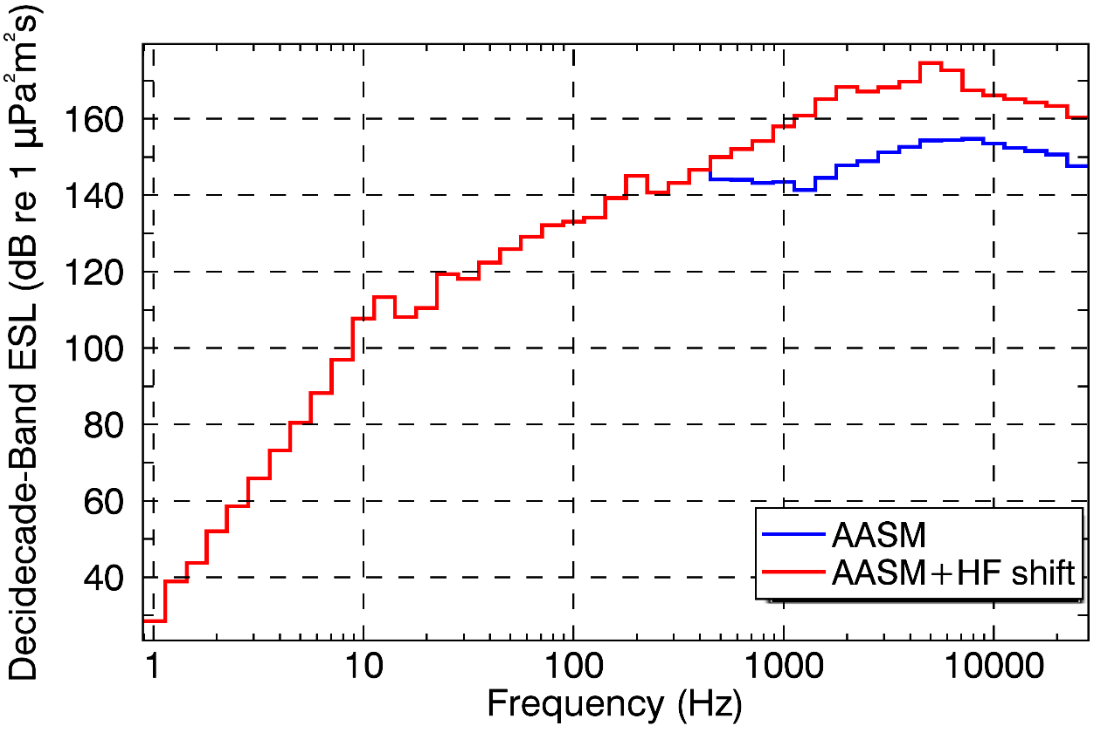

Figure L-5. Horizontal array energy source levels weighted for high-frequency cetaceans. Levels are maximum over all modelled azimuths. Results shown for soft-start step 5.

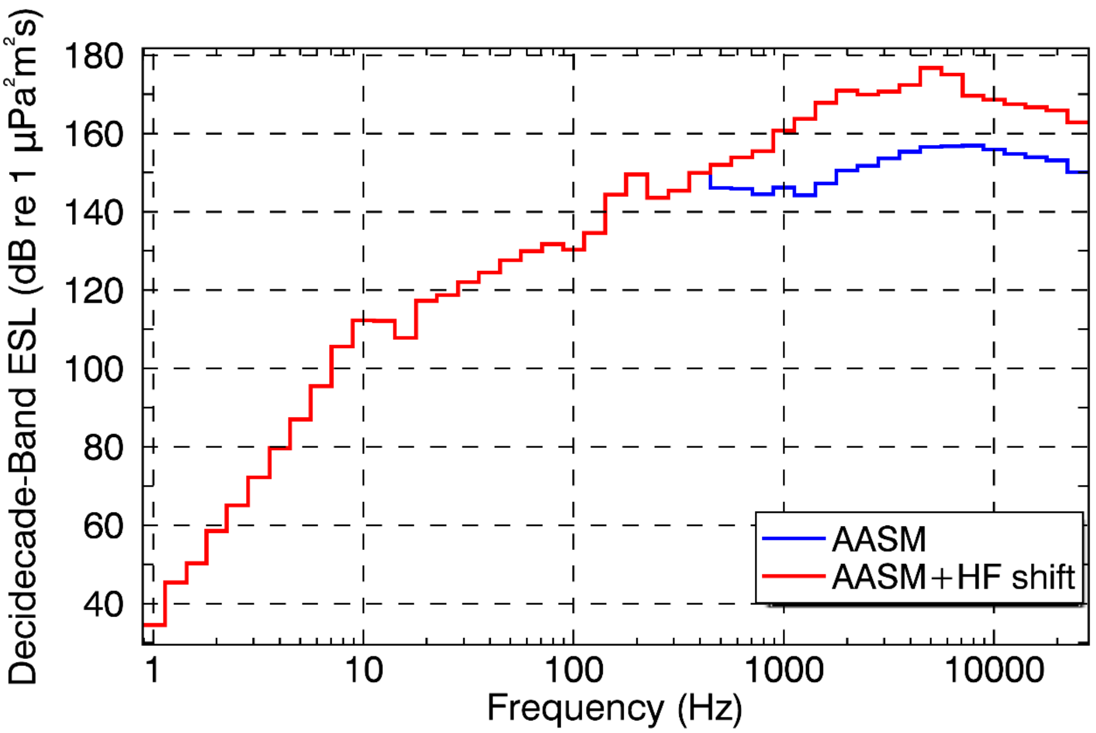

Figure L-6. Horizontal array energy source levels weighted for high-frequency cetaceans. Levels are maximum over all modelled azimuths. Results shown for soft-start step 6.

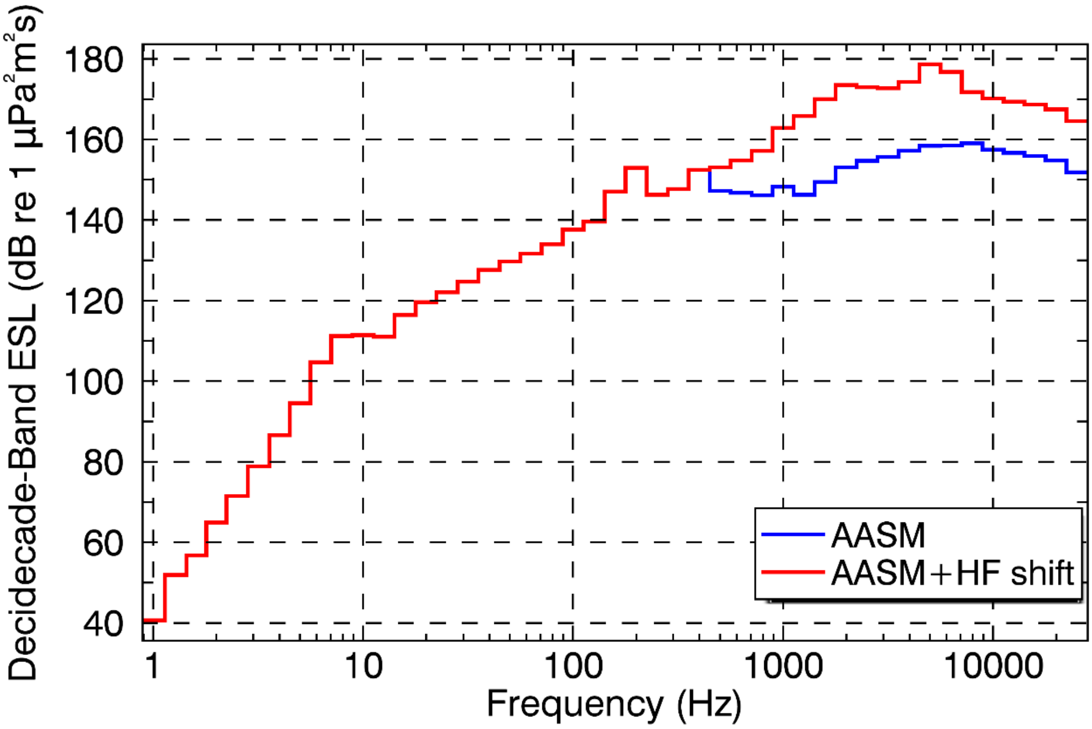

Figure L-7. Horizontal array energy source levels weighted for high-frequency cetaceans. Levels are maximum over all modelled azimuths. Results shown for soft-start step 7.

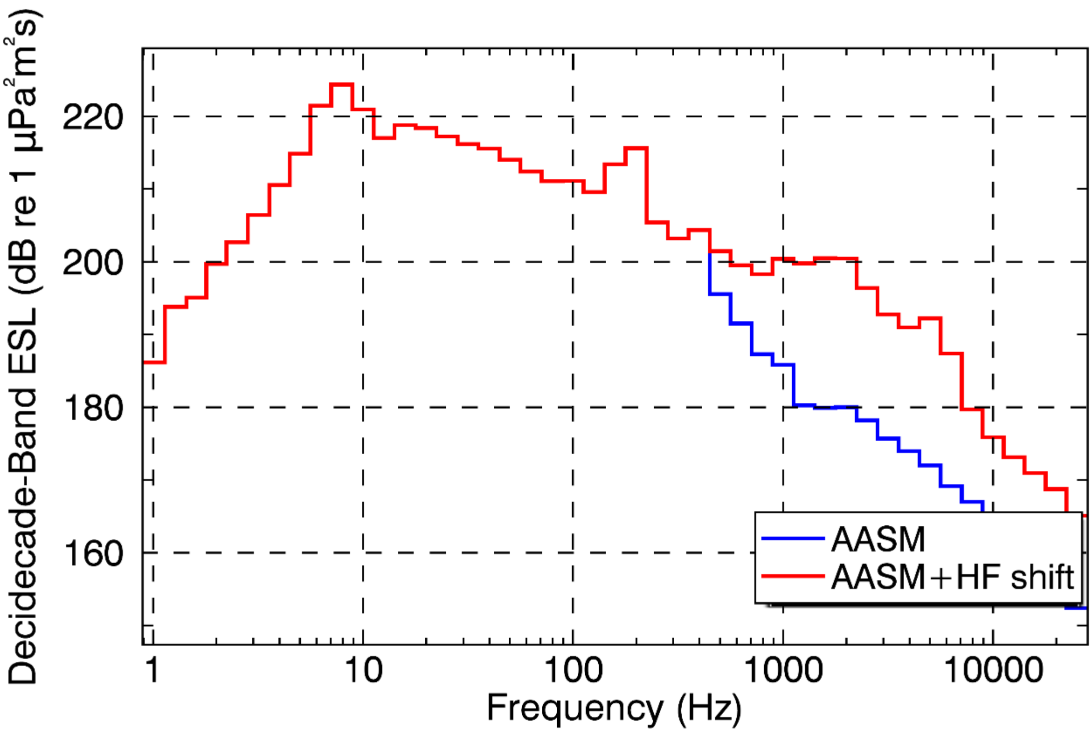

Figure L-8. Horizontal array energy unweighted source levels. Levels are maximum over all modelled azimuths. Results shown for full array.

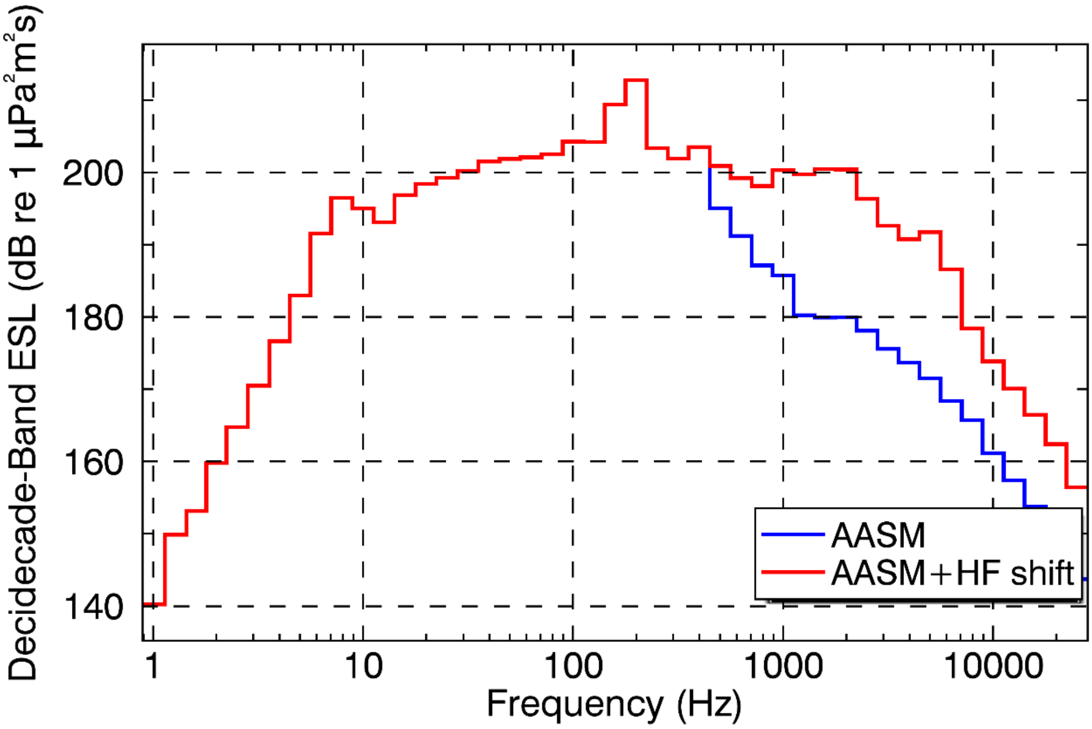

Figure L-9. Horizontal array energy source levels weighted for low-frequency cetaceans. Levels are maximum over all modelled azimuths. Results shown for full array.

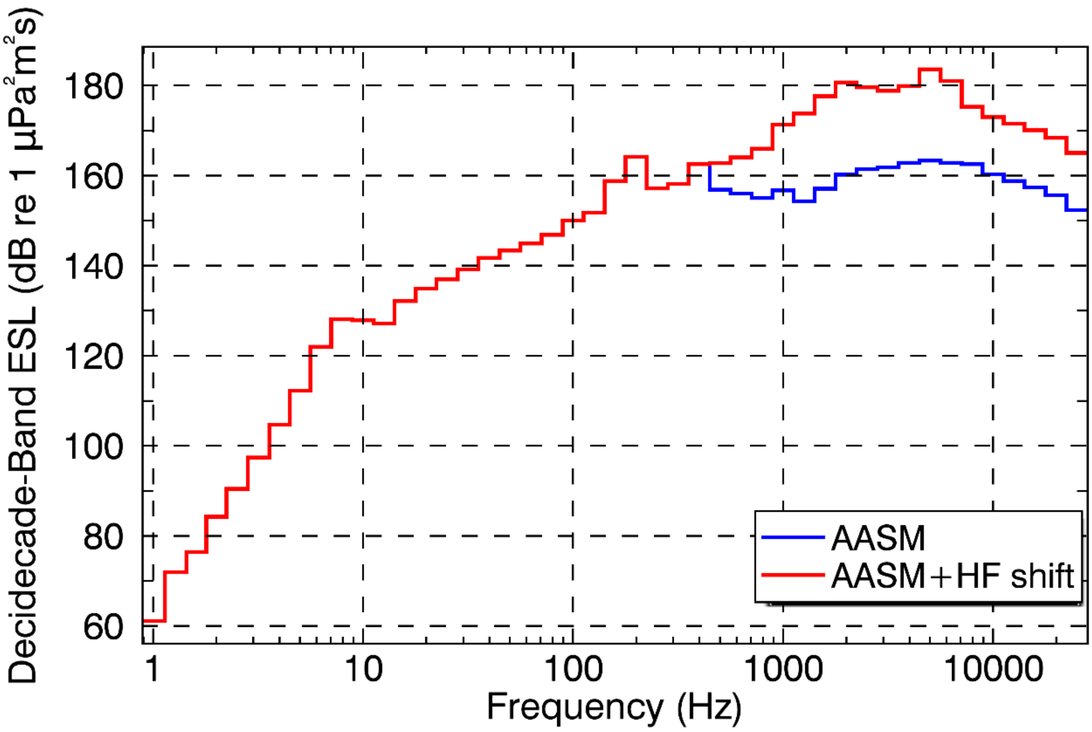

Figure L-10. Horizontal array energy source levels weighted for mid-frequency cetaceans. Levels are maximum over all modelled azimuths. Results shown for full array.

Appendix M. Results for High-Frequency Shifted Source

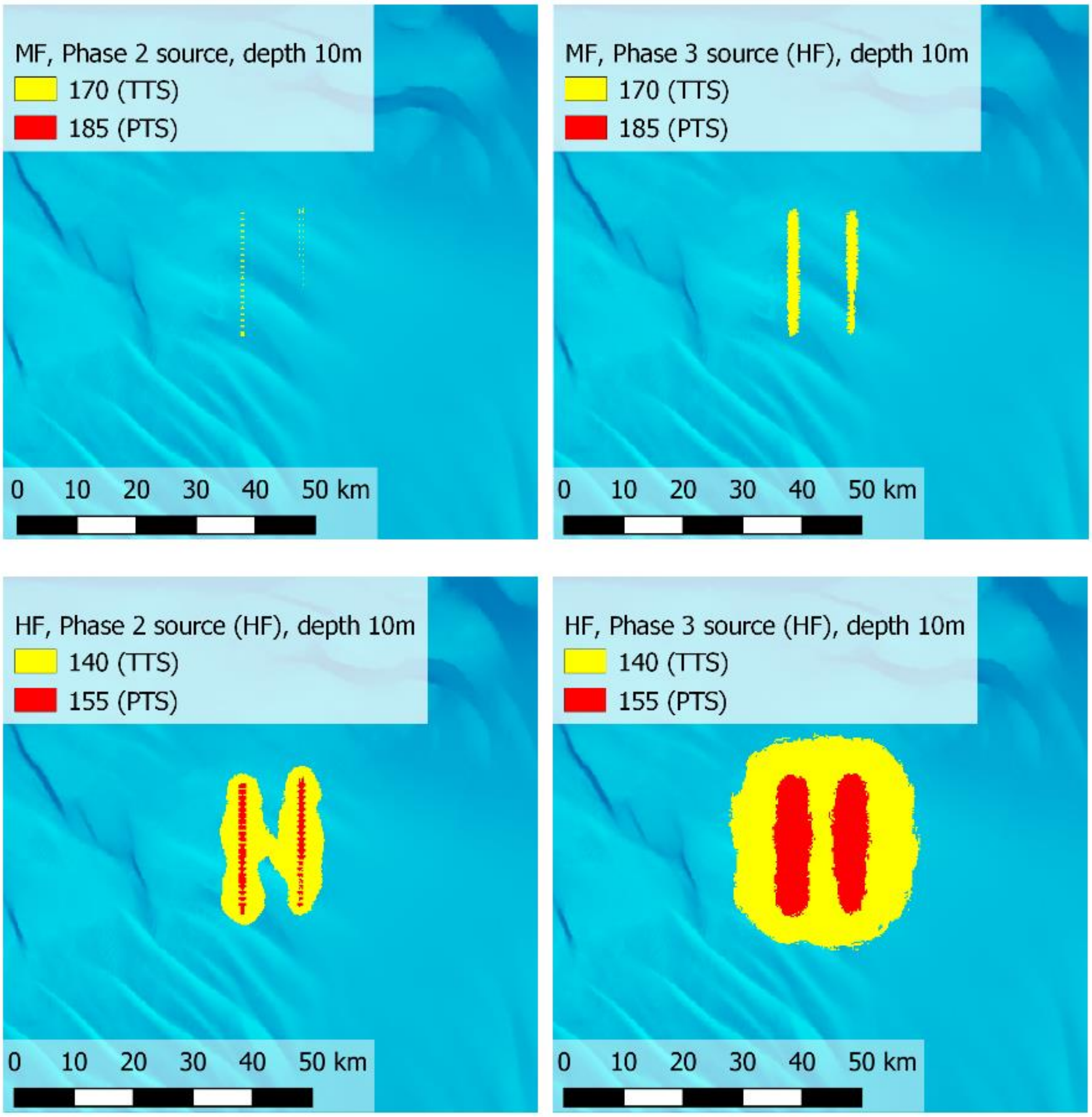

Figure M-1. Sound fields from the source without and with high-frequency shift indicating PTS and TTS thresholds weighted for HF cetaceans and MF cetaceans. Results from dBSea.

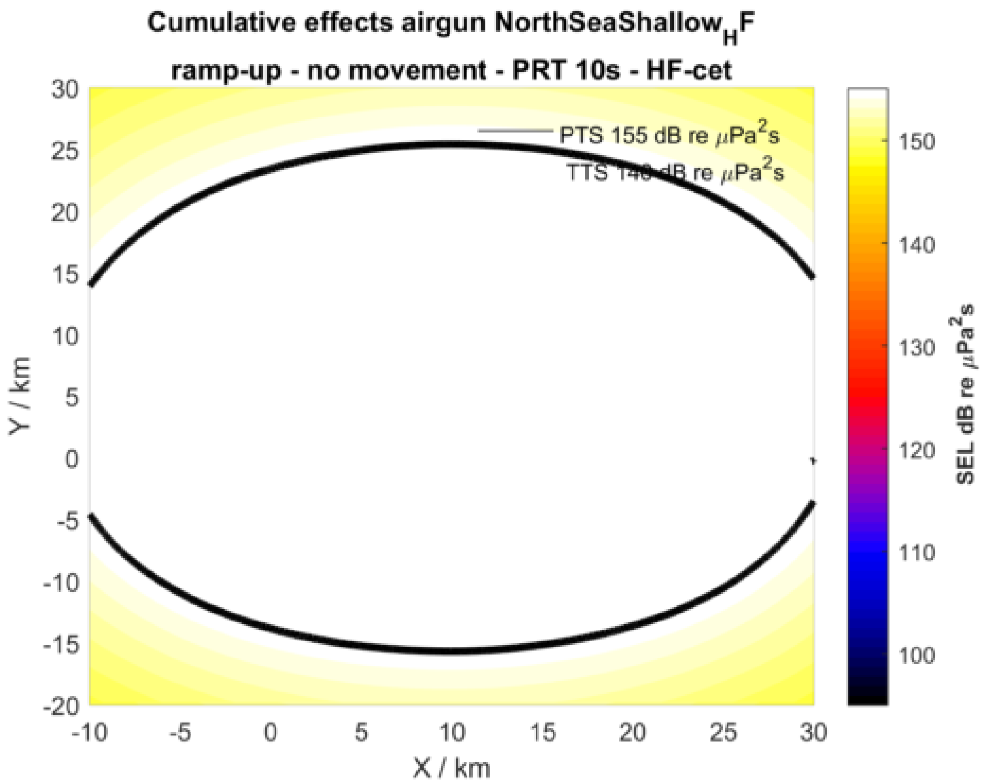

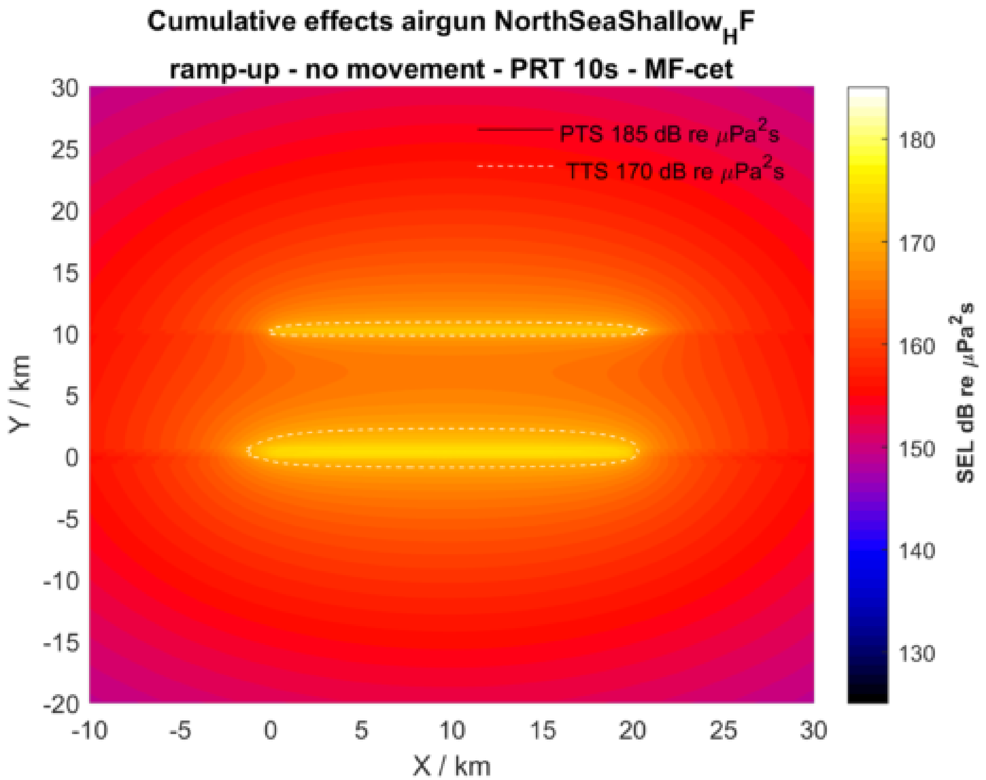

Figure M-2. Sound fields from the source with high-frequency shift indicating PTS and TTS thresholds weighted for HF cetaceans (top) and MF cetaceans (bottom). Results from Soprano.

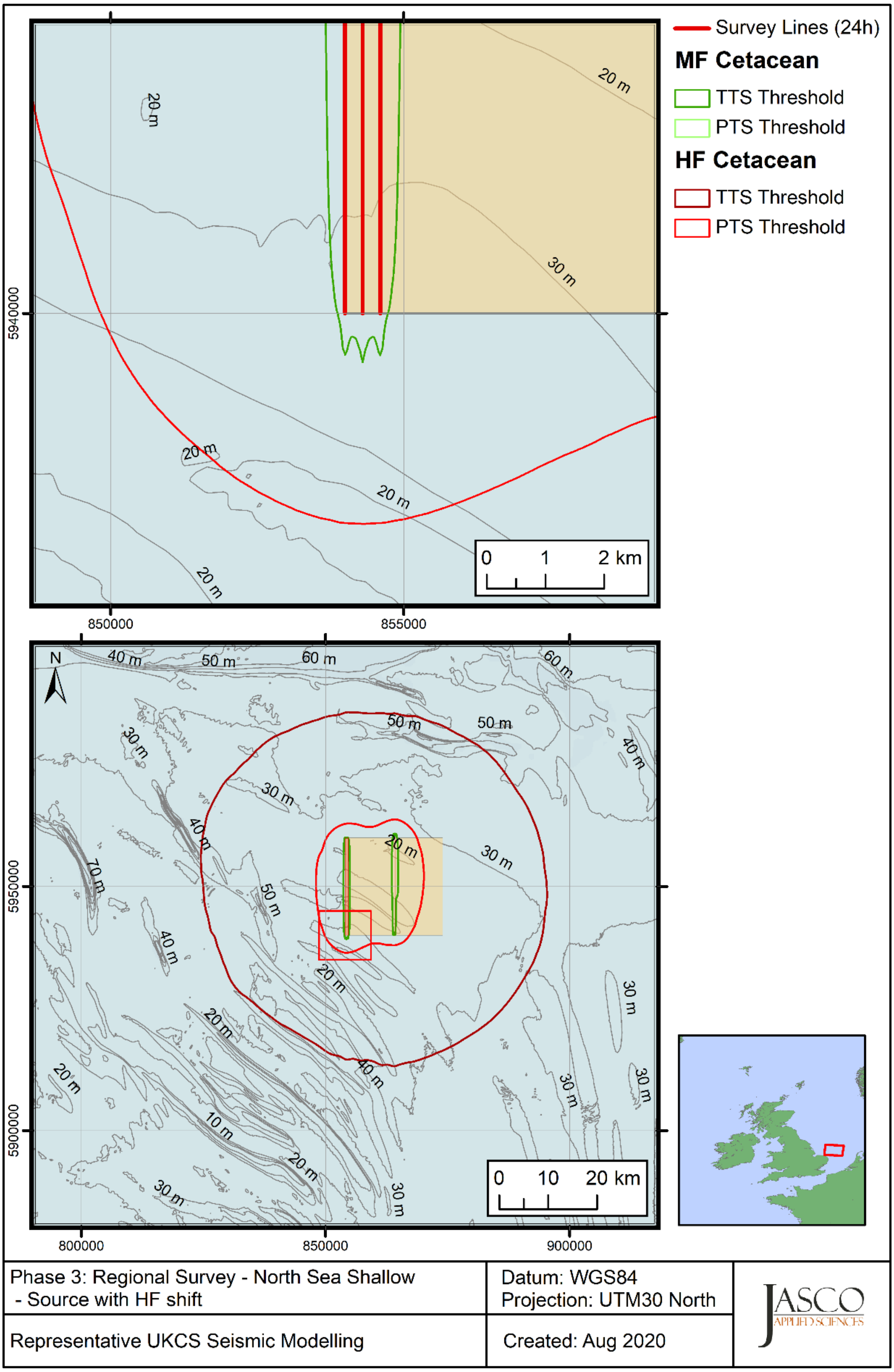

Figure M-3. Sound fields from the source with high-frequency shift indicating PTS and TTS thresholds weighted for HF cetaceans and MF cetaceans. Results from MONM-BELLHOP.

Appendix N. Tabulated Summer Sound Speed Profiles

Water depth (m)	North Sea Deep (m/s)	Faroe-Shetland Channel (m/s)
0	1496.63	1488.30
2	1496.54	1488.28
4	1496.45	1488.27
6	1496.33	1488.24
8	1496.18	1488.22
10	1496.01	1488.19
15	1495.16	1487.94
20	1494.04	1487.64
25	1492.01	1487.31
30	1489.99	1487.04
35	1488.38	1486.79
40	1486.84	1486.54
45	1485.48	1486.31
50	1484.45	1486.11
55	1483.72	1485.98
60	1483.21	1485.86
65	1482.77	1485.74
70	1482.38	1485.62
75	1482.01	1485.53
80	1481.75	1485.45
85	1481.52	1485.36
90	1481.31	1485.28
95	1481.11	1485.21
100	1480.91	1485.16
110	1480.66	1485.08
120	1480.56	1485.02
130	1480.28	1484.96
140	1479.98	1484.90
150	1479.90	1484.82
160	1479.94	1484.74
170	1479.99	1484.66
180		1484.56
190		1484.44
200		1484.33
220		1484.08
240		1483.79

Water depth (m)	Faroe-Shetland Channel (m/s)
260	1483.45
280	1483.04
300	1482.53
350	1480.52
400	1477.66
500	1468.81
600	1461.27
700	1458.93
800	1459.64
900	1460.73
1000	1461.91
1100	1463.09
1200	1464.27

Appendix O. Results for Summer Sound Speed Profile

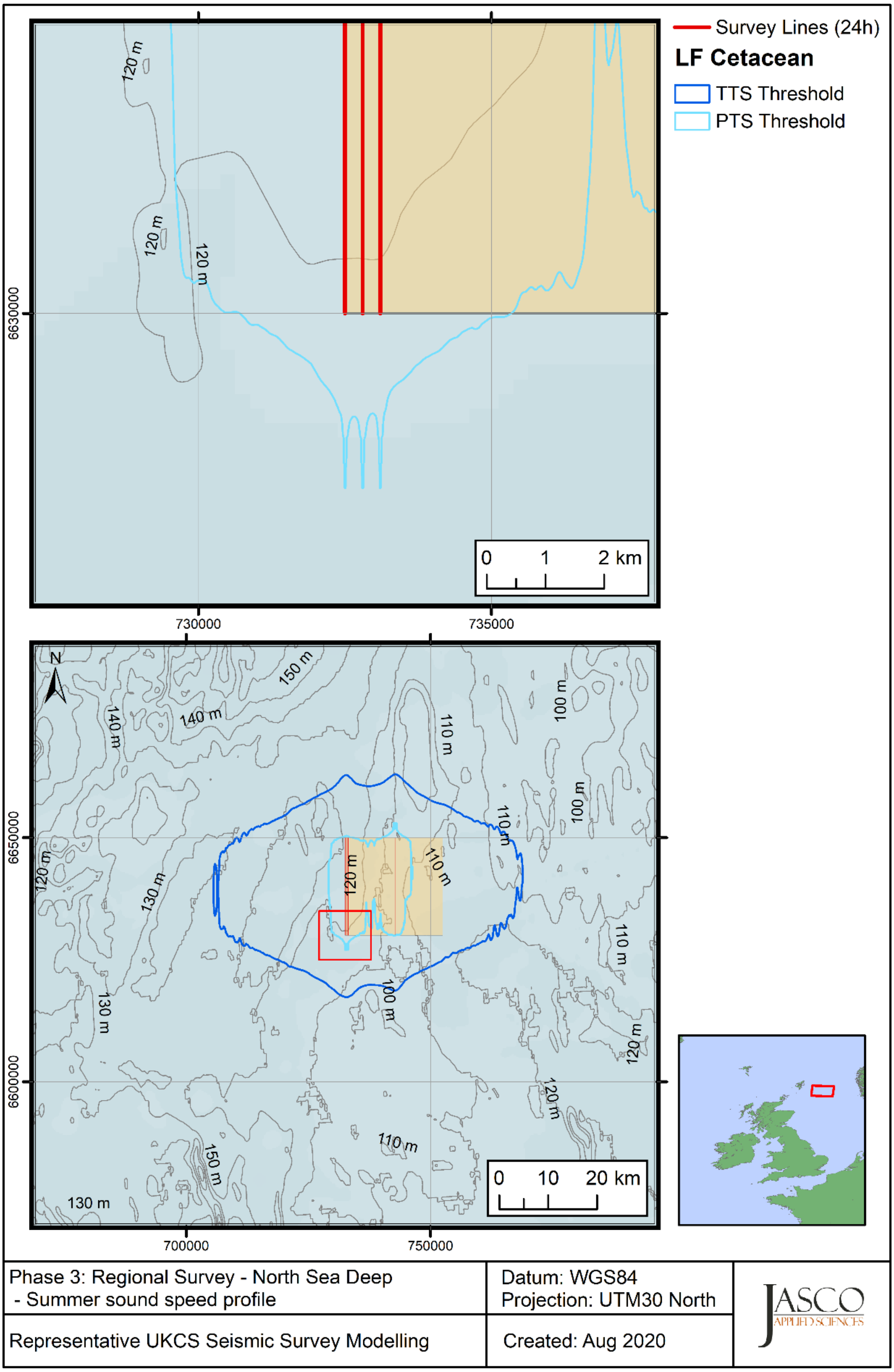

Figure O-1. Sound fields from the source at 10 m depth indicating ranges to PTS and TTS thresholds weighted for LF cetaceans for a summer sound speed profile for Scenario 5: North Sea Deep. Results from MONM-BELLHOP.

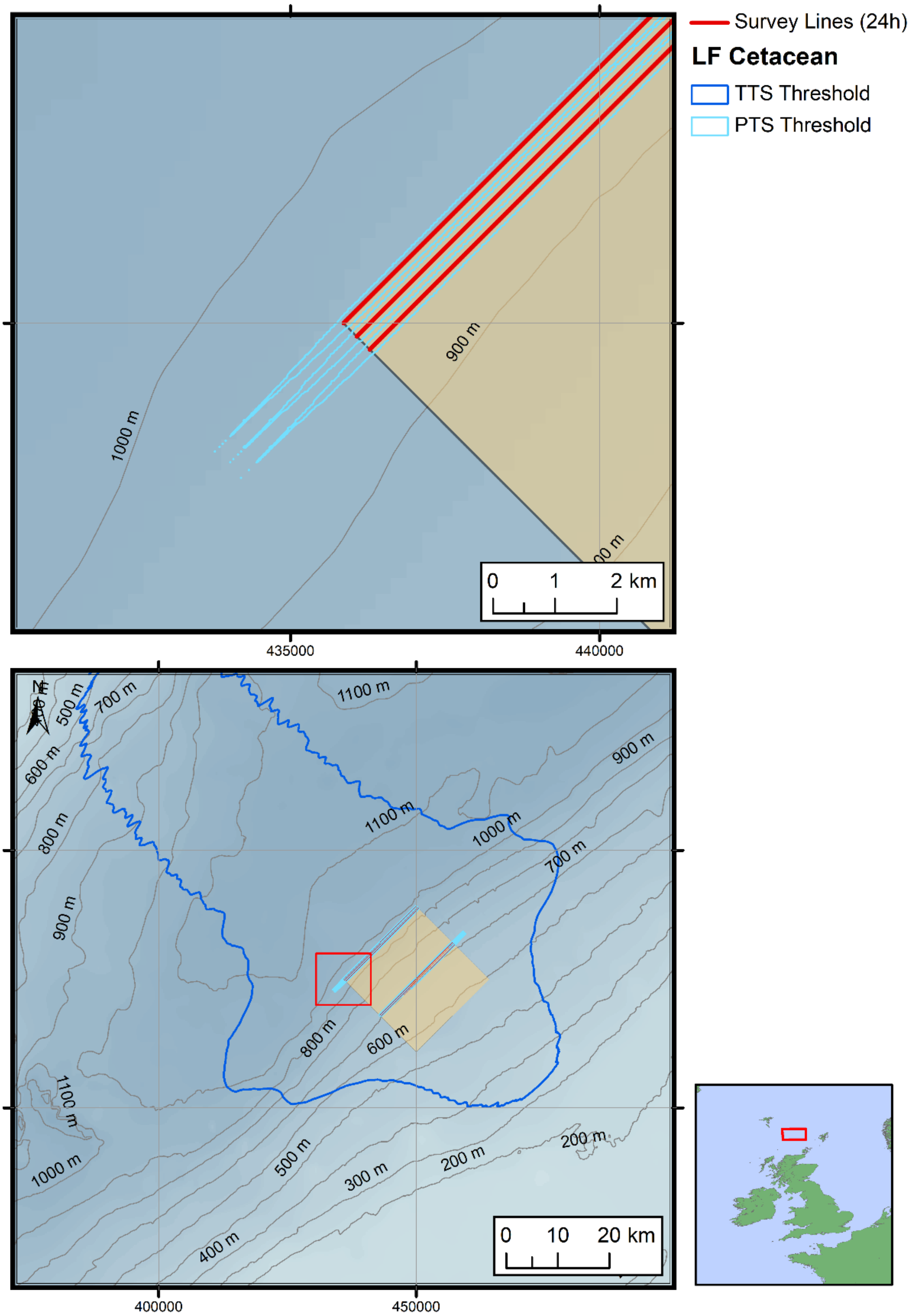

Phase 3: Regional Survey - Faroe Shetland Channel - Summer sound speed profile	Datum: WGS84 Projection: UTM30 North	JASCO APPLIED SCIENCES
Representative UKCS Seismic Survey Modelling	Created: Aug 2020	

Figure O-2. Sound fields from the source at 10 m depth indicating ranges to PTS and TTS thresholds weighted for LF cetaceans for a summer sound speed profile for Scenario 6: Faroe Shetland Channel. Results from MONM-BELLHOP.

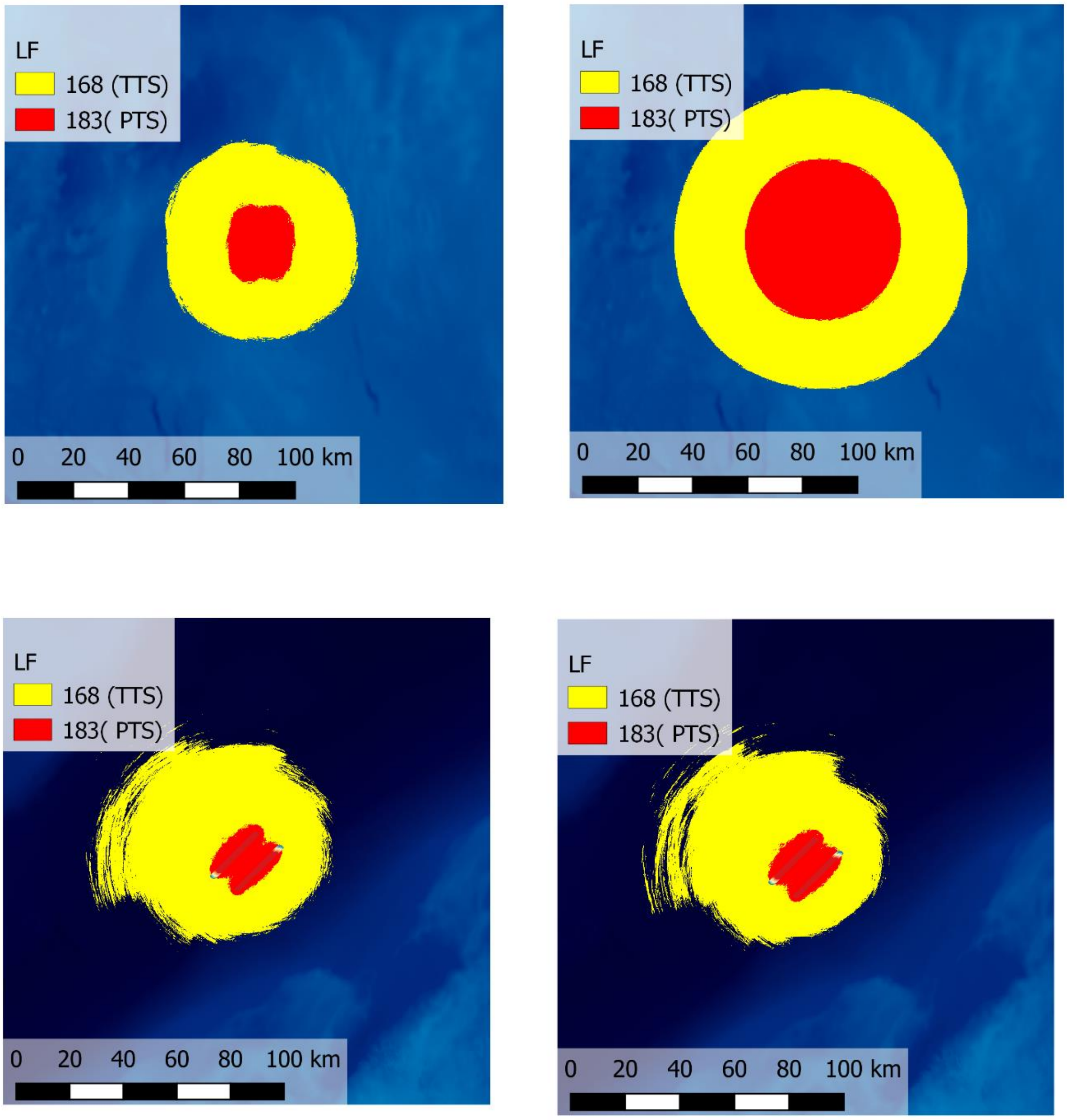

Figure O-3. Sound fields from the source at 10 m depth indicating ranges to PTS and TTS thresholds weighted for LF cetaceans for winter(left) and summer (right) sound speed profiles for Scenario 5 (top) and Scenario 6 (bottom). Results from dBSea.

Appendix P. Results for Maximum Level Over Depth

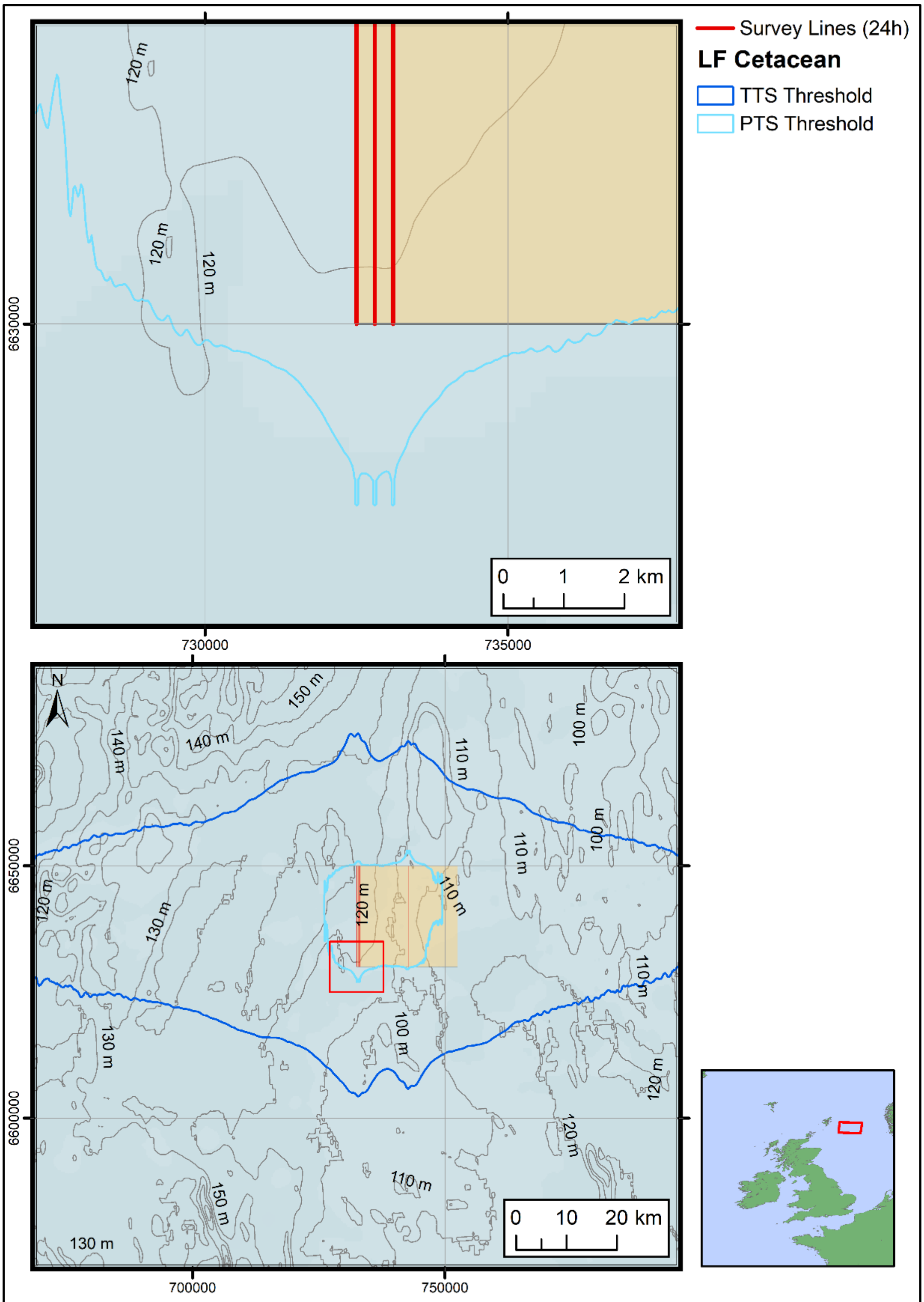

Phase 3: Regional Survey - North Sea Deep - Maximum sound level over depth	Datum: WGS84 Projection: UTM30 North	JASCO APPLIED SCIENCES
Representative UKCS Seismic Survey Modelling	Created: Aug 2020	

Figure P-1. Sound fields from the source taking maximum sound level over depth indicating PTS and TTS thresholds weighted for LF cetaceans for Scenario 5: North Sea Deep. Results from MONM-BELLHOP.

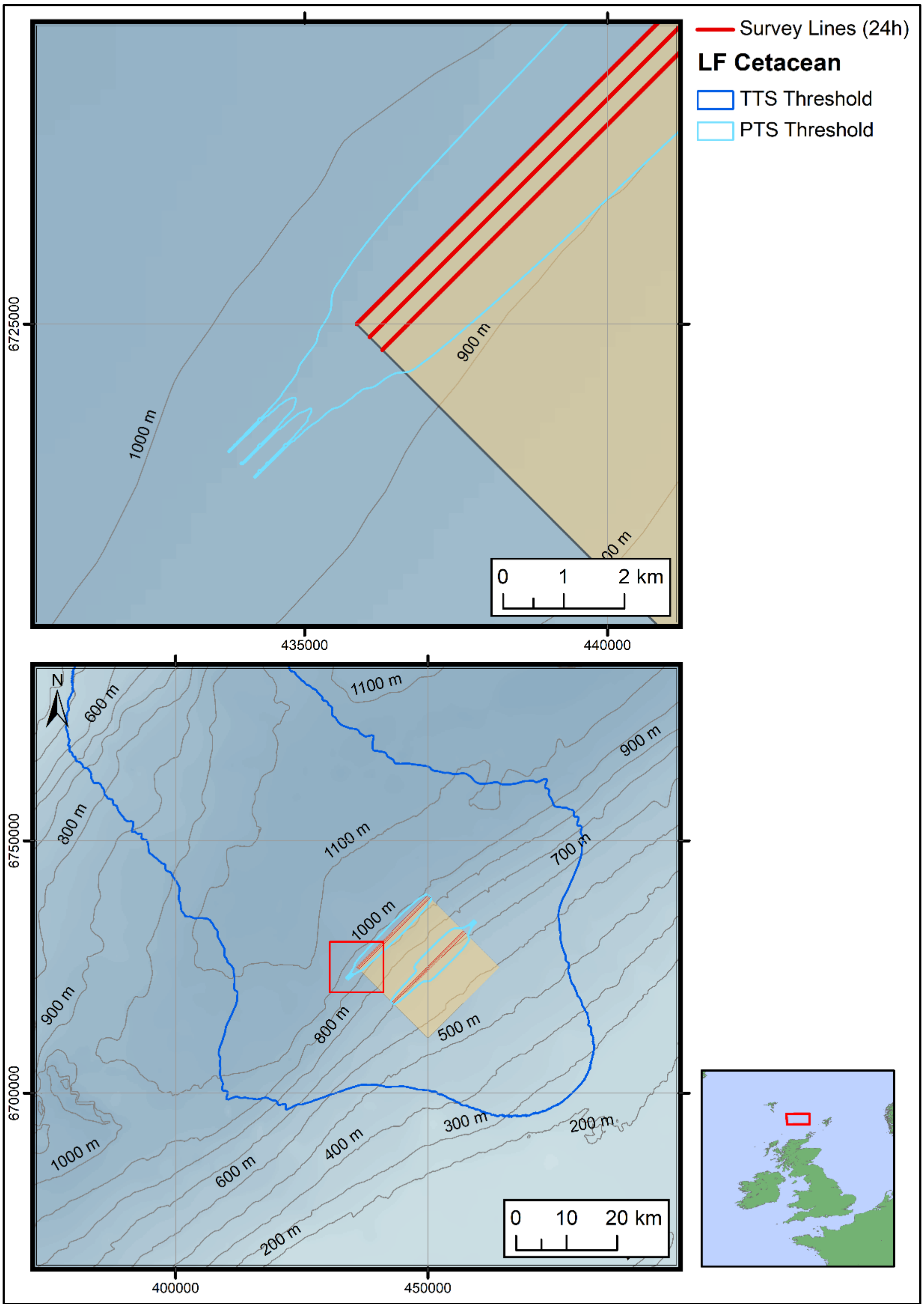

Phase 3: Regional Survey - Faroe Shetland Channel - Maximum sound level over depth	Datum: WGS84 Projection: UTM30 North	JASCO APPLIED SCIENCES
Representative UKCS Seismic Survey Modelling	Created: Aug 2020	

Figure P-2. Sound fields from the source taking maximum sound level over depth indicating PTS and TTS thresholds weighted for LF cetaceans for Scenario 6: Faroe Shetland Channel. Results from MONM-BELLHOP.

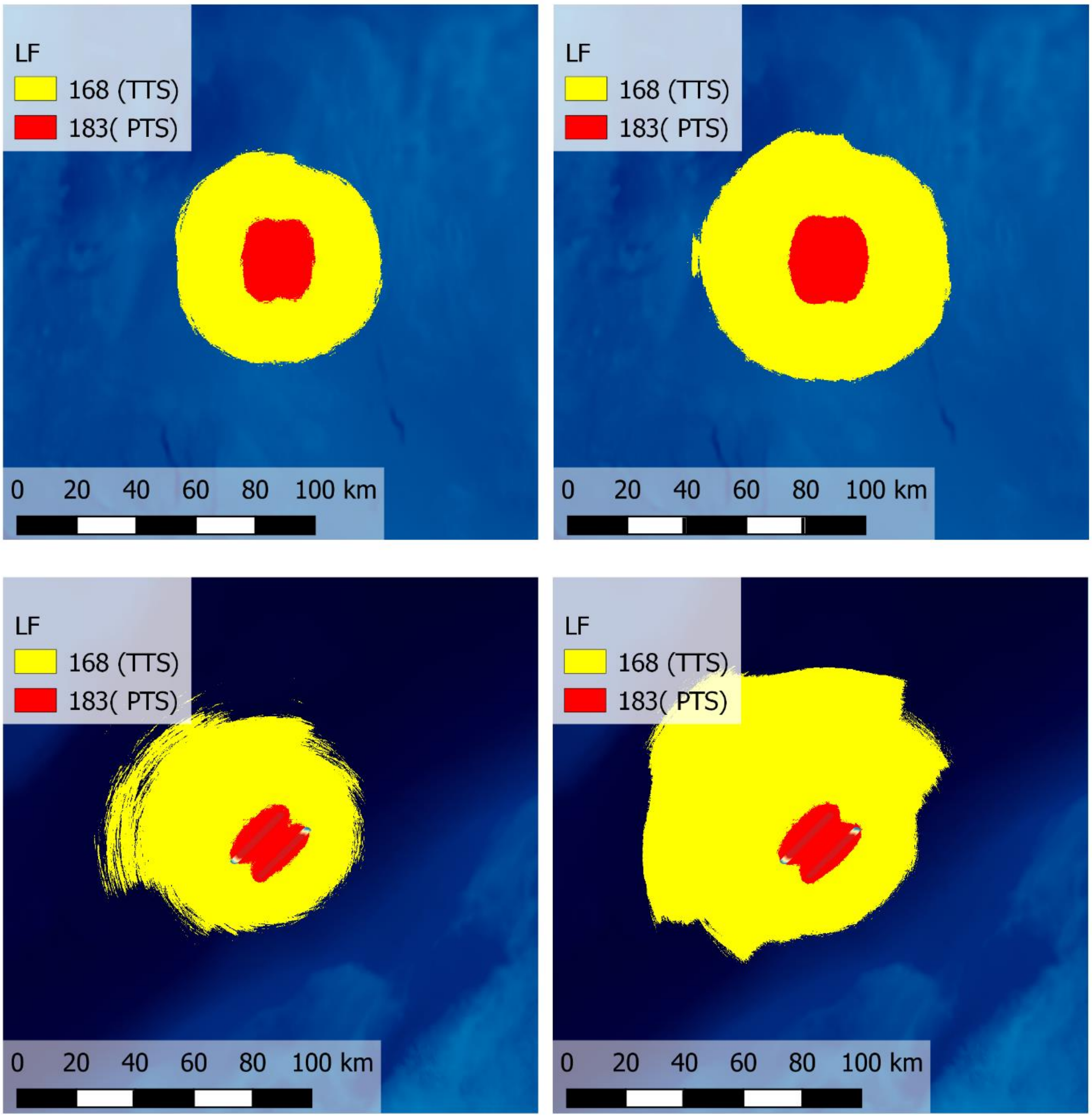

Figure P-3. Sound fields for Scenario 5 (top) and Scenario 6 (bottom) for levels at 10 m depth (left) and maximum level over all depths (right). Shown are areas ensonified to PTS and TTS thresholds weighted for LF cetaceans. Results from dBSea.

Appendix Q. Results for High-frequency Shifted Source and Surface Roughness

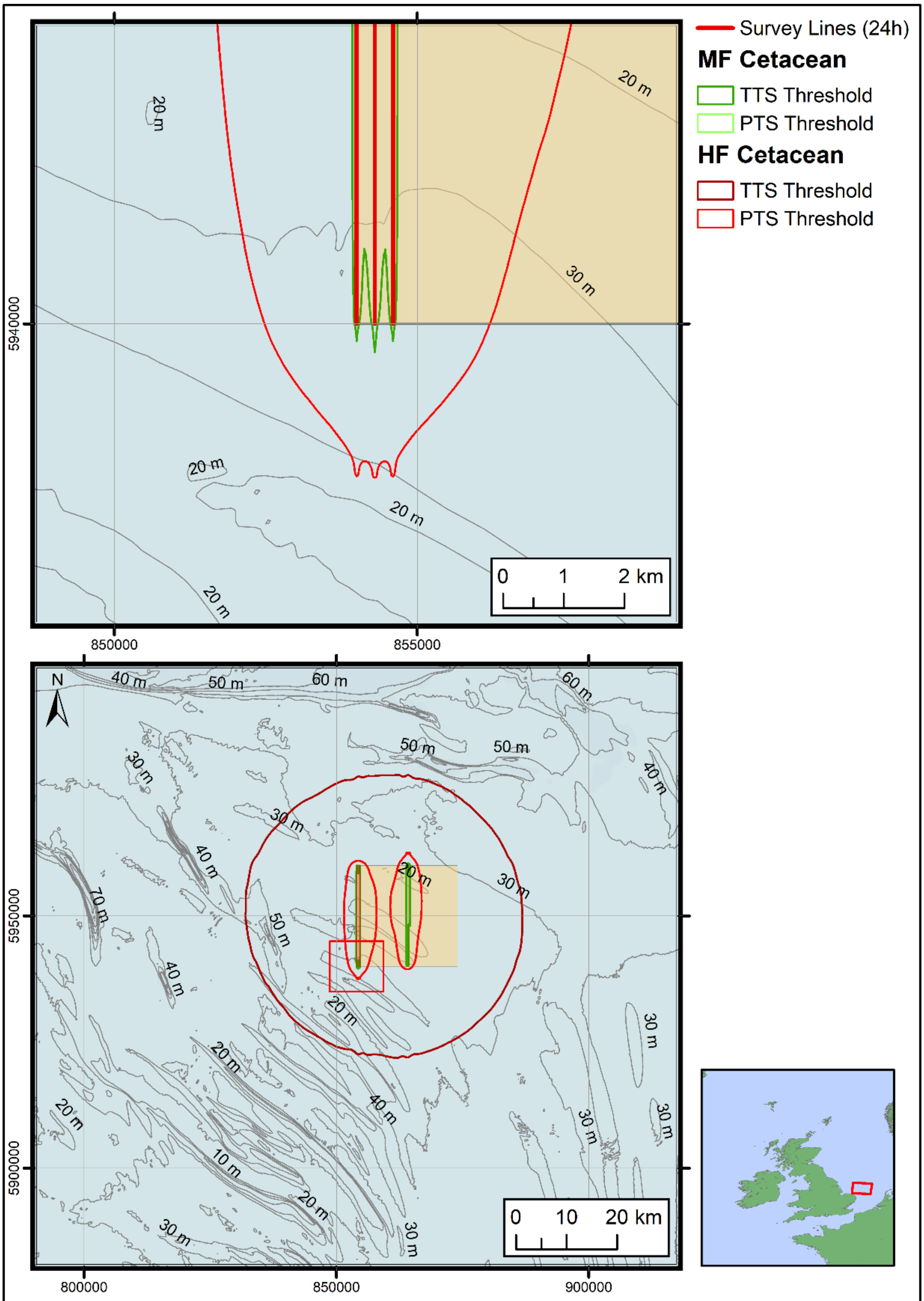

Phase 3: Regional Survey - North Sea Shallow - Source with HF shift; wind speed of 9.5 knots	Datum: WGS84 Projection: UTM30 North	JASCO APPLIED SCIENCES
Representative UKCS Seismic Survey Modelling	Created: Aug 2020	

Figure Q-1. Sound fields from the source with high-frequency shift and surface loss (9.5 knot wind) indicating PTS and TTS thresholds weighted for HF cetaceans and MF cetaceans. Results from MONM-BELLHOP.

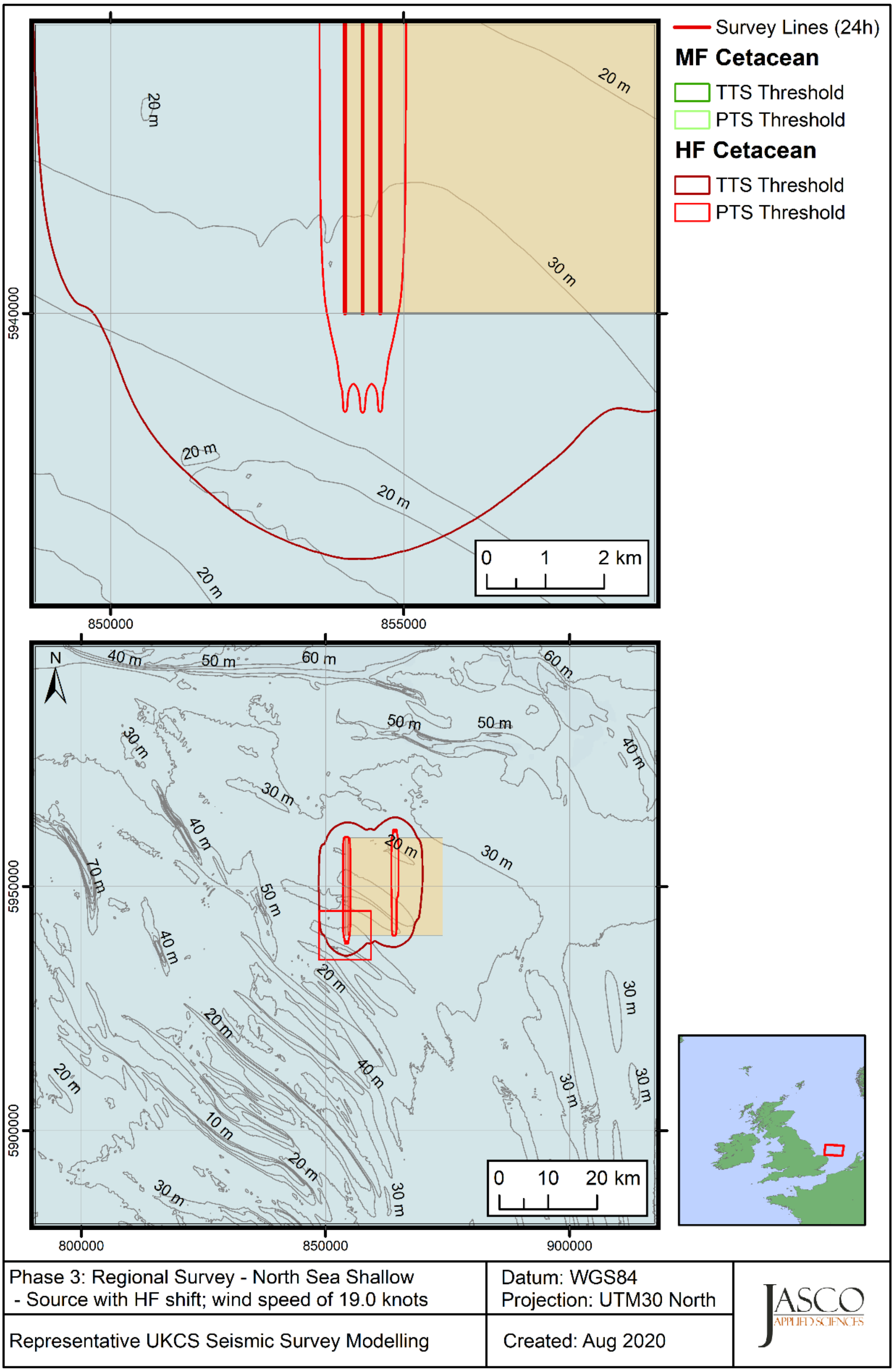

Figure Q-2. Sound fields from the source with high-frequency shift and surface loss (9.5 knot wind) indicating PTS and TTS thresholds weighted for HF cetaceans and MF cetaceans. Results from MONM-BELLHOP.

Appendix R. Supplemental information - JASMINE

The JASCO Animal Simulation Model Including Noise Exposure (JASMINE) was used to predict the exposure of animats (virtual marine mammals and sea turtles) to sound arising from the simulated seismic survey. Sound exposure models like JASMINE integrate the predicted sound field with biologically meaningful movement rules for each marine mammal species that result in an exposure history for each animat in the model. Inside JASMINE, the sound fields are those predicted from the Phase 2 results. The parameters used for forecasting realistic behaviours (e.g., diving, foraging, aversion, surface times) are determined and interpreted from marine species studies (e.g., tagging studies) where available, or reasonably extrapolated from related species. An individual animat's sound exposure levels are summed over a specified duration, such as 24 hours or the entire simulation, to determine its total received energy, and then compared to the threshold criteria.

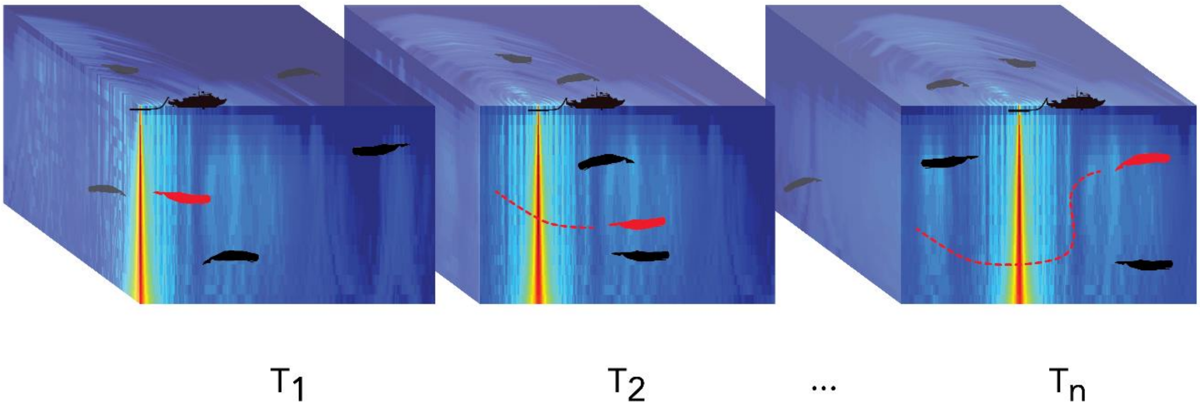

Figure R-1. Illustration of animats in a moving sound field. Example animat (red) shown moving with each time step. The acoustic exposure of each animat is determined by where it is in the sound field, and its exposure history is accumulated as the simulation steps through time.

R.1. Animal Movement Modelling

To assess the risk of impacts from exposure, an estimate of received sound levels for the animals in the area during operations is required. Sound sources often move and so do animals. The sound fields may be complex, and the sound received by an animal is a function of where the animal is at any given time. To a reasonable approximation, the location of the sound source(s) is known and acoustic modelling can be used to predict the 3-D sound field. The location and movement of animals within the sound field, however, is unknown. Realistic animal movement within the sound field can be simulated, and repeated random sampling (Monte Carlo)—achieved by simulating many animals within the operations area—used to estimate the sound exposure history of animals during the operation. Monte Carlo methods provide a heuristic approach for determining the probability distribution function (PDF) of complex situations, such as animals moving in a sound field. The probability of an event's occurrence is determined by the frequency with which it occurs in the simulation. The greater the number of random samples, in this case the more simulated animals (animats), the better the approximation of the PDF. Animats are randomly placed, or seeded, within the simulation boundary at a specified density (animats/km^2). The animat density is much higher than the real-world density to ensure good representation of the PDF. The resulting PDF is scaled using the real-world density.

Several models for marine mammal movement have been developed (Ellison et al. 1987, Frankel et al. 2002, Houser 2006). These models use an underlying Markov chain to transition from one state to another based on probabilities determined from measured swimming behaviour. The parameters may represent simple states, such as the speed or heading of the animal, or complex states, such as likelihood of participating in foraging, play, rest, or travel. Attractions and aversions to variables like anthropogenic sounds and different depth ranges can be included in the models.

Analysis in this report uses the JASCO Animal Simulation Model Including Noise Exposure (JASMINE) 2017. JASMINE uses the same animal movement algorithms as the Marine Mammal

Movement and Behavior (3MB) model (Houser 2006) but has been extended for use with JASCO-formatted acoustic fields, inclusion of source tracks, and for animats to change behavioural states based on modelled variables such as received level. JASMINE can also include aversion in response to realistic received levels.

R.1.1. Animal Movement Parameters

JASMINE uses previously measured behaviour to forecast behaviour in new situations and locations. The parameters used for forecasting realistic behaviour are determined (and interpreted) from marine species studies (e.g., tagging studies). Each parameter in the model is described as a probability distribution. When limited or no information is available for a species parameter, a Gaussian or uniform distribution may be chosen for that parameter. For the Gaussian distribution, the user determines the mean and standard deviation of the distribution from which parameter values are drawn. For the uniform distribution, the user determines the maximum and minimum distribution from which parameter values are drawn. When detailed information about the movement and behaviour of a species are available, a user-created distribution vector, including cumulative transition probabilities, may be used (referred to here as a vector model; Houser 2006). Different sets of parameters can be defined for different behaviour states. The probability of an animat starting out in or transitioning into a given behaviour state can in turn be defined in terms of the animat’s current behavioural state, depth, and the time of day. In addition, each travel parameter and behavioural state has a termination function that governs how long the parameter value or overall behavioural state persists in simulation.

The parameters used in JASMINE describe animal movement in both the vertical and horizontal planes. The parameters relating to travel in these two planes are briefly described below.

R.1.2. Travel sub-models

- Direction – determines the animat’s choice of direction in the horizontal plane. Sub-models are available for determining the bearing of animats, allowing for movement to range from strongly biased to undirected. A random walk model can be used for behaviours with no directional preference, such as feeding and playing. In a random walk, all bearings are equally likely at each parameter transition time step. A correlated random walk can be used to smooth the changes in bearing by using the current bearing as the mean of the distribution from which to draw the next heading. An additional variant of the correlated random walk is available that includes a directional bias for use in situations where animals have a preferred absolute direction, such as migration. A user-defined vector of directional probabilities can also be defined to control animat bearing. For more detailed discussion of these parameters, see Houser (2006) and Houser and Cross (1999).
- Travel rate – defines the rate of travel of an animat in the horizontal plane. When combined with vertical speed and dive depth, the dive profile of the animat is produced.

R.1.3. Dive sub-models

- Ascent Rate – defines the rate of travel of an animat in the vertical plane during the ascent portion of a dive.
- Descent Rate – defines the rate of travel of an animat in the vertical plane during the descent portion of a dive.
- Depth – defines the maximum depth to which an animat will dive.
- Bottom Following – determines whether an animat returns to the surface once reaching the ocean floor, or whether it follows the contours of the bathymetry.
- Reversals – determines whether multiple vertical excursions occur once reaching the maximum dive depth. This behaviour is used to emulate the foraging behaviour of some marine mammal species at depth. Reversal-specific ascent and descent rates may be specified.
- Surface Interval – determines the amount of time spent at the surface prior to performing another dive.

R.2. Parameters for Animal Movement Modelling

This section provides the parameters describing the animal behavioural model inputs. Parameters for the animal movement modelling are generated for specific projects and are continuously updated and revised; consequently, the parameters may not be appropriate in other locations or for future projects.

R.2.1. Minke Whales (Balaenoptera acutorostrata)

Table R-1. *Minke Whales:* Data values and references input in JASMINE to create diving behaviour.

Behaviour	Variable	Value	Reference
Feeding dive	Travel direction	Correlated random walk	Approximated (based on fin whale - Watwood and Buonantony 2012)
	Perturbation value	10	Approximated (based on fin whale - Watwood and Buonantony 2012)
	Termination coefficient	0.2	Approximated (based on fin whale - Watwood and Buonantony 2012)
	Travel rate (m/s)	Gaussian 3.25 (0.3)	Approximated (Blix and Folkow 1995)
	Ascent rate (m/s)	Gaussian 2.1 (0.3)	Approximated (fin whale - Goldbogen et al. 2011)
	Descent rate (m/s)	Gaussian 3 (0.2)	Approximated (fin whale - Goldbogen et al. 2011)
	Average depth (m)	Gaussian 35 (20)	Approximated (best guess based on figure in Blix and Folkow 1995)
	Bottom following	No	Approximated (Blix and Folkow 1995)
	Reversals	Gaussian 3.1 (1.1)	Approximated (fin whale - Croll et al. 2001, Goldbogen et al. 2006)
	Probability of reversal	0.95	Approximated (Blix and Folkow 1995)
	Reversal ascent dive rate (m/s)	Gaussian 1.7 (0.4)	Fin whale–Croll et al. (2001)
	Reversal descent dive rate (m/s)	Gaussian 1.4 (0.5)	Fin whale–Croll et al. (2001)
	Time in reversal (s)	Gaussian 13.7 (2.8)	Fin whale–Croll et al. (2001)
	Surface interval (s)	Gaussian 66.1 (96.7)	Stockin et al. (2001)
	Bout duration (s)	Gaussian 1500 (500)	Approximated (best guess based on figure in Blix and Folkow 1995)
Cruising dive	Travel direction	Correlated random walk	Approximated (based on fin whale - Watwood and Buonantony 2012)
	Perturbation value	10	Approximated (based on fin whale - Watwood and Buonantony 2012)
	Termination coefficient	0.2	Approximated (based on fin whale - Watwood and Buonantony 2012)
	Travel rate (m/s)	Gaussian 3.25 (0.3)	Approximated (Blix and Folkow 1995)

Behaviour	Variable	Value	Reference
	Ascent rate (m/s)	Gaussian 1.7 (0.4)	Approximated (fin whale - Goldbogen et al. 2011)
	Descent rate (m/s)	Gaussian 2.0 (0.2)	Approximated (fin whale - Goldbogen et al. 2011)
	Average depth (m)	Gaussian 15 (10)	Approximated (best guess based on figure in Blix and Folkow 1995)
	Bottom following	No	Approximated (best guess based on figure in Blix and Folkow 1995)
	Reversals	No	Approximated (best guess based on figure in Blix and Folkow 1995)
	Surface interval (s)	Gaussian 66.1 (96.7)	Stockin et al. (2001)
	Bout duration (s)	Gaussian 1000 (600)	Approximated (best guess based on figure in Blix and Folkow 1995)
Sleeping	Travel direction	Correlated random walk	Approximated (based on fin whale - Watwood and Buonantony 2012)
	Perturbation value	10	Approximated (based on fin whale - Watwood and Buonantony 2012)
	Termination coefficient	0.2	Approximated (based on fin whale - Watwood and Buonantony 2012)
	Travel rate (m/s)	Gaussian 3.25 (0.3)	Approximated (Blix and Folkow 1995)
	Ascent rate (m/s)	Gaussian 1.7 (0.4)	Approximated (fin whale - Goldbogen et al. 2011)
	Descent rate (m/s)	Gaussian 2.0 (0.2)	Approximated (fin whale - Goldbogen et al. 2011)
	Average depth (m)	Gaussian 10 (5)	Approximated (best guess based on figure in Blix and Folkow 1995)
	Bottom following	No	Approximated (best guess based on figure in Blix and Folkow 1995)
	Reversals	No	Approximated (best guess based on figure in Blix and Folkow 1995)
	Surface interval (s)	Gaussian 66.1 (96.7)	Stockin et al. (2001)
	Bout duration (s)	Gaussian 2000 (400)	Approximated (best guess based on figure in Blix and Folkow 1995)
Unknown	Travel direction	Correlated random walk	Approximated (based on fin whale - Watwood and Buonantony 2012)
	Perturbation value	10	Approximated (based on fin whale - Watwood and Buonantony 2012)

Behaviour	Variable	Value	Reference
	Termination coefficient	0.2	Approximated (based on fin whale - Watwood and Buonantony 2012)
	Travel rate (m/s)	Gaussian 3.25 (0.3)	Approximated (Blix and Folkow 1995)
	Ascent rate (m/s)	Gaussian 1.7 (0.4)	Approximated (fin whale - Goldbogen et al. 2011)
	Descent rate (m/s)	Gaussian 2.0 (0.2)	Approximated (fin whale - Goldbogen et al. 2011)
	Average depth (m)	Gaussian 20 (10)	Approximated (best guess based on figure in Blix and Folkow 1995)
	Bottom following	No	Approximated (best guess based on figure in Blix and Folkow 1995)
	Reversals	No	Approximated (best guess based on figure in Blix and Folkow 1995)
	Surface interval (s)	Gaussian 66.1 (96.7)	Stockin et al. (2001)
	Bout duration (s)	Gaussian 1500 (500)	Approximated (best guess based on figure in Blix and Folkow 1995)
General	Shore following (m)	80	Approximated (Hooker et al. 1999)
	Depth limit on seeding (m)	20 (minimum), 10000 (maximum)	Approximated (Kraus et al. 2016)

Approximated: Value based on the best fit for diving profile. Those values were unavailable from literature, but they were estimated to produce a diving profile similar to D-tag results, for example.

R.2.2. Harbour Porpoises (*Phocoena phocoena*)

Table R-2. *Harbour Porpoises*: Data values and references input in JASMINE to create diving behaviour (number values represent means [standard deviations] unless otherwise indicated).

Behaviour	Variable	Value	Reference
Daytime	Travel direction	Correlated Random Walk	Approximated (Watwood and Buonantony 2012)
	Perturbation value	10	Approximated (Watwood and Buonantony 2012)
	Termination coefficient	0.2	Approximated (Watwood and Buonantony 2012)
	Travel rate (m/s)	Gaussian 0.9 (0.3)	Otani et al. (2000)
	Ascent rate (m/s)	Gaussian 0.87 (0.38)	Westgate et al. (1995)
	Descent rate (m/s)	Gaussian 0.99 (0.34)	Westgate et al. (1995)
	Average depth (m)	Gaussian 22.5 (11.6)	Westgate et al. (1995)
	Bottom following	Yes	Approximated (Watwood and Buonantony 2012)

Behaviour	Variable	Value	Reference
	Reversals	Gaussian 1 (0)	Approximated (Watwood and Buonantony 2012)
	Probability of reversal	0.84	Westgate et al. (1995)
	Reversal ascent dive rate (m/s)	Gaussian 0.0 (0.0)	Approximated (Watwood and Buonantony 2012)
	Reversal descent dive rate (m/s)	Gaussian 0.0 (0.0)	Approximated (Watwood and Buonantony 2012)
	Time in reversal (s)	Gaussian 20.5 (27.8)	Westgate et al. (1995)
	Surface interval (s)	Gaussian 31.6 (73.8)	Otani et al. (1998) Otani et al. (2000)
	Bout duration (s)	T_{50} = 600 (s), k = 1	Approximated (Watwood and Buonantony 2012)
Nighttime	Travel direction	Correlated Random Walk	Approximated (Watwood and Buonantony 2012)
	Perturbation value	10	Approximated (Watwood and Buonantony 2012)
	Termination coefficient	0.2	Approximated (Watwood and Buonantony 2012)
	Travel rate (m/s)	Gaussian 0.9 (0.3)	Westgate et al. (1995)
	Ascent rate (m/s)	Gaussian 1.34 (0.53)	Westgate et al. (1995)
	Descent rate (m/s)	Gaussian 1.44 (0.51)	Westgate et al. (1995)
	Average depth (m)	Gaussian 37.5 (12.5)	Westgate et al. (1995)
	Bottom following	Yes	Approximated (Watwood and Buonantony 2012)
	Reversals	Gaussian 1 (0)	Approximated (Watwood and Buonantony 2012)
	Probability of reversal	0.84	Approximated (Watwood and Buonantony 2012)
	Reversal ascent dive rate (m/s)	Gaussian 0.0 (0.0)	Approximated (Watwood and Buonantony 2012)
	Reversal descent dive rate (m/s)	Gaussian 0.0 (0.0)	Approximated (Watwood and Buonantony 2012)
	Time in reversal (s)	Gaussian 10.3 (13.9)	Westgate et al. (1995)
	Surface interval (s)	Gaussian 31.6 (73.8)	Otani et al. (1998) Otani et al. (2000)
	Bout duration (s)	T_{50} = 600 (s), k = 1	Approximated (Watwood and Buonantony 2012)

Behaviour	Variable	Value	Reference
General	Shore following (m)	10	Approximated (Watwood and Buonantony 2012)
	Depth limit on seeding (m)	10 (minimum), 1000 (maximum)	Approximated Osmek et al. (1996)

Approximated: Value based on the best fit for diving profile. Those values were unavailable from literature, but they were estimated to produce a diving profile similar to D-tag results, for example.

Appendix S. Animat Modelling TTS results

S.1. Low-frequency Cetaceans – North Sea Deep Environment

These are supplemental results to those in Section 12.1. In total, 38,917 animats were exposed to cumulative weighted sound levels greater than the TTS threshold of 168 dB re 1 µPa²s. The minimum CPA distance of an animat exceeding the TTS threshold but not the PTS threshold was 13 m, and the maximum CPA was 14.4 km; the 95th percentile range was 7.7 km. The histogram of the minimum CPA ranges for all animats exceeding the TTS threshold is shown in Figure S-1.

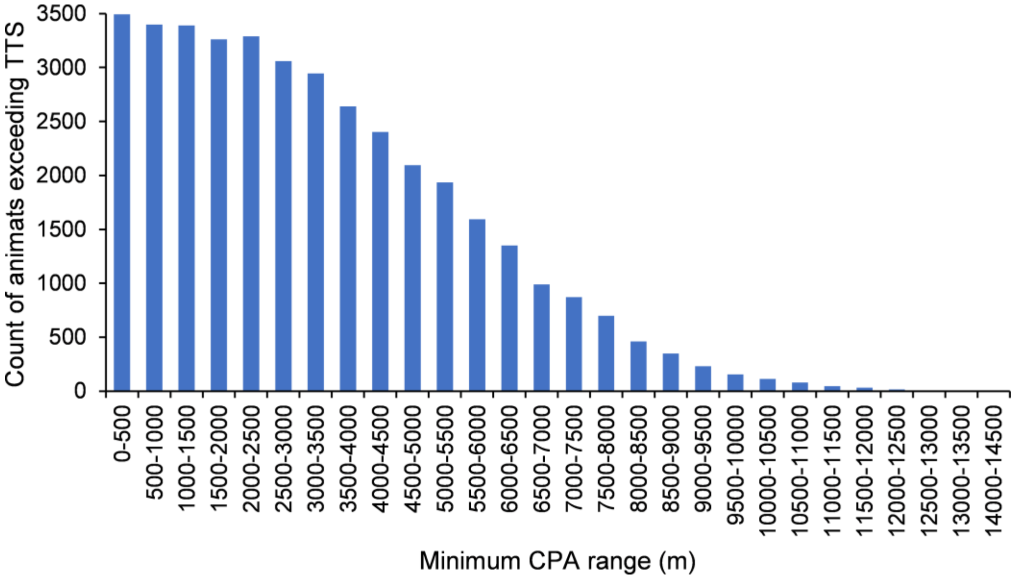

Figure S-1. Minimum CPA distances of animats exceeding TTS threshold.

The histogram of the received levels of all animats experiencing levels greater than the TTS threshold is shown in Figure S-2; again, the trend is that there are fewer receivers experiencing the higher levels – all animats exceeding the PTS threshold are shown as a single entry (>183).

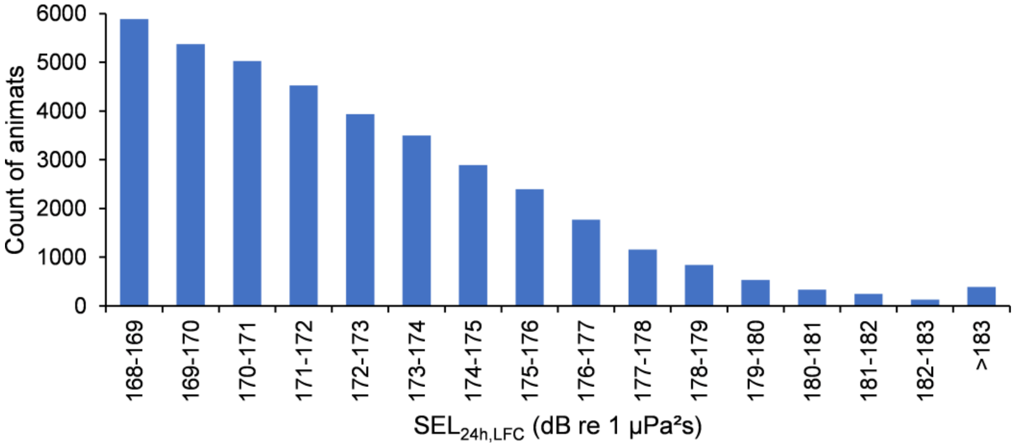

Figure S-2. Distribution of received levels of animats exceeding the TTS threshold.

S.2. High-frequency Cetaceans – North Sea Shallow Environment

Using the original source level functions, a total of 12 162 out of 260 000 animats were exposed to levels above the TTS threshold. Figure S-3 shows the histogram of number of animats exposed to discretised sound levels and Figure S-4 shows the histogram of distances of animats exposed to levels exceeding TTS thresholds; within 500 m, a total of 4823 out of 5240 animats were exposed to levels greater than the TTS threshold; of the exposed animats, 95% exceeded the TTS level within 1773 m of the source.

With the high-frequency shifted source, the number of animats exposed to levels exceeding the TTS threshold increased to a total of 99 530. Figure S-5 shows the distribution of levels received by animats; of the animats exceeding TTS thresholds, 20 432 also exceeded the PTS threshold. Within 500 m of the source, all animats were exposed to levels above the TTS threshold. Figure S-6 shows the distribution of minimum CPA ranges of animats exceeding the TTS threshold; of the animats exposed to levels above the TTS threshold, 95% did so within 13 392 m of the source.

With surface roughness included, again we see a significant reduction in the maximum ranges of animats exposed to TTS levels, and in the number of animats exposed to levels exceeding the TTS threshold. Figure S-7 shows the distribution of sound levels for animats exceeding the TTS threshold; the total numbers are similar to those in Figure S-3 but the distribution shows a peak at 143-144 dB re 1 µPa²s and has greater numbers at higher levels; the surface roughness produces a compound effect such that regions close to the source are mostly unaffected but the rate of propagation loss increases with increasing distance. The same phenomenon is exhibited in Figure S-8 which shows the distribution of minimum CPA distance for animats exceeding the TTS threshold; while the number of animats exceeding TTS levels are higher close to the source than for the equivalent for the original source array in Figure S-4, the drop-off rate is considerable greater. The maximum range at which any animat exceeded the TTS threshold was 4756 m, and of the animats exposed to levels above the TTS threshold, 95% did so within 2978 m of the source.

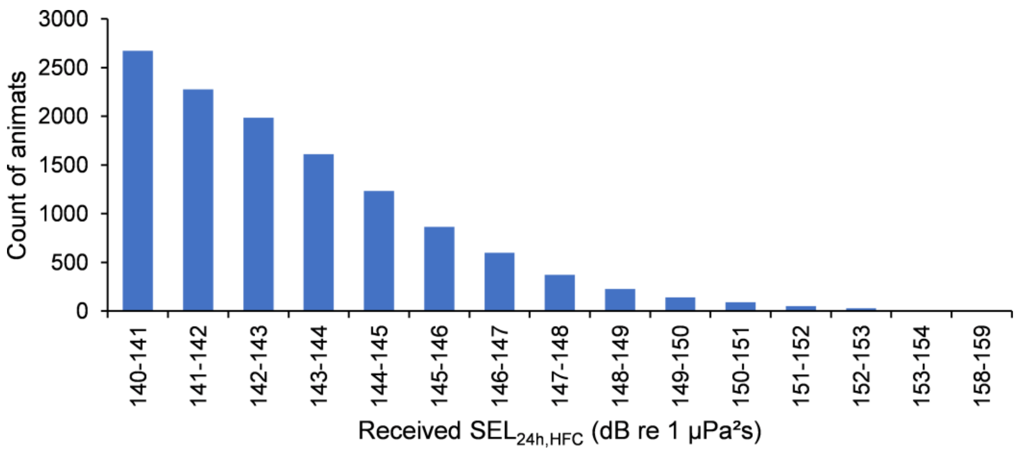

Figure S-3. Distribution of received cumulative levels exceeding the TTS threshold by animats (harbour porpoise) for Scenario 4 using the original airgun source and no surface roughness.

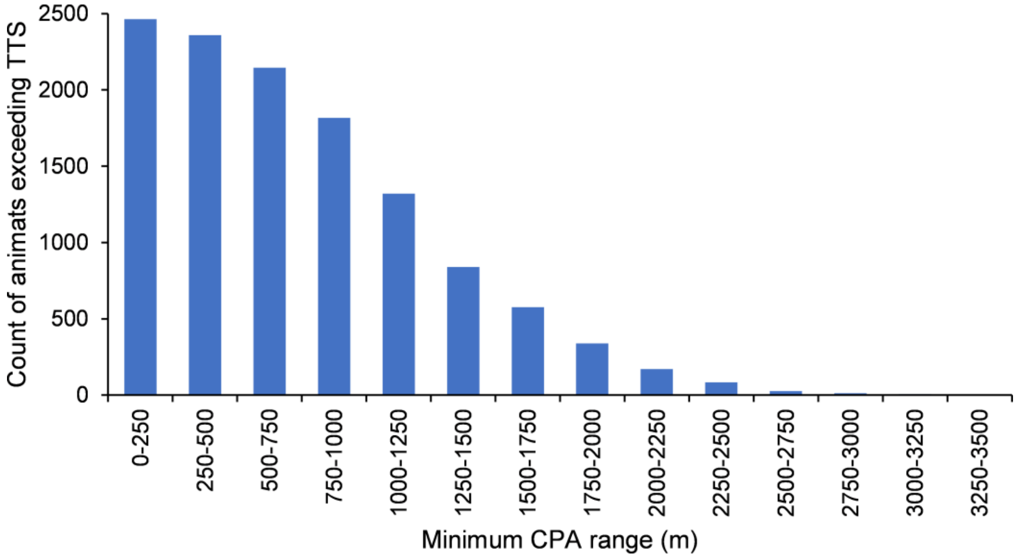

Figure S-4. Distribution of minimum CPA ranges for all animats (harbour porpoise) exceeding the TTS thresholds for the original airgun array source for Scenario 4.

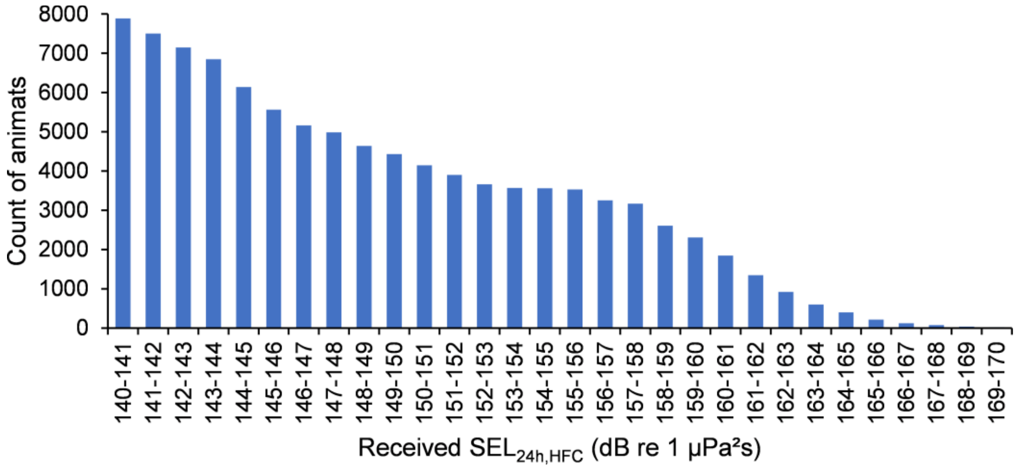

Figure S-5. Distribution of received cumulative levels exceeding the TTS threshold by animats (harbour porpoise) for Scenario 4 using the high-frequency shifted source and no surface roughness.

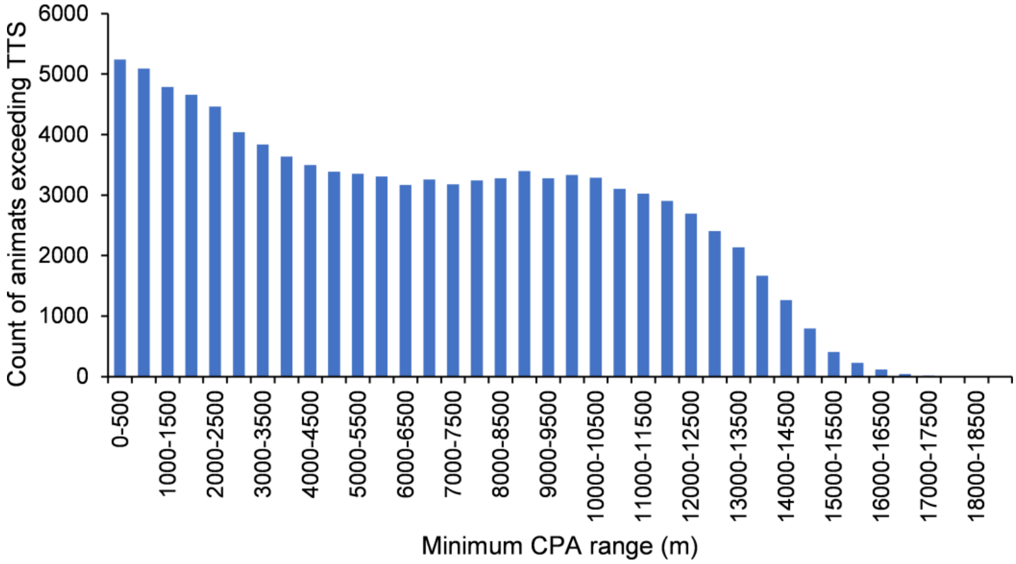

Figure S-6. Distribution of minimum CPA ranges for all animats (harbour porpoise) exceeding the PTS thresholds for the high-frequency shifted source for Scenario 4.

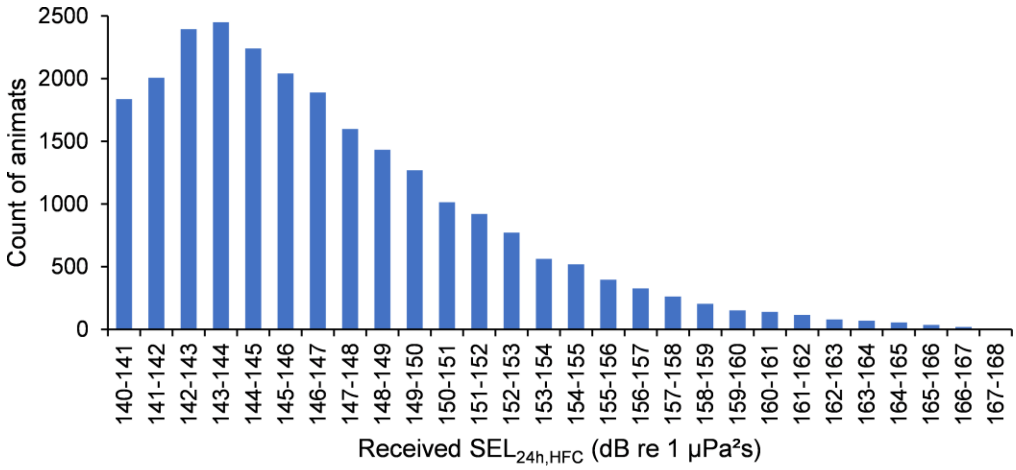

Figure S-7. Distribution of received cumulative levels exceeding the TTS threshold by animats (harbour porpoise) for Scenario 4 using the high-frequency shifted source and including surface roughness.

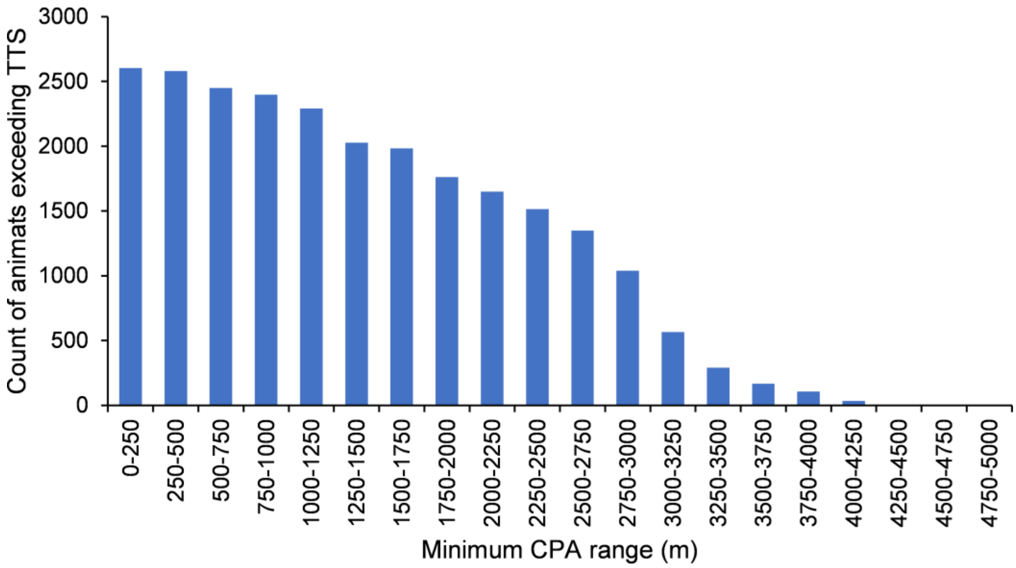

Figure S-8. Distribution of minimum CPA ranges for all animats (harbour porpoise) exceeding the TTS thresholds for the high-frequency shifted source for Scenario 4 with the inclusion of surface roughness.

Appendix T. High-frequency Animat Paths

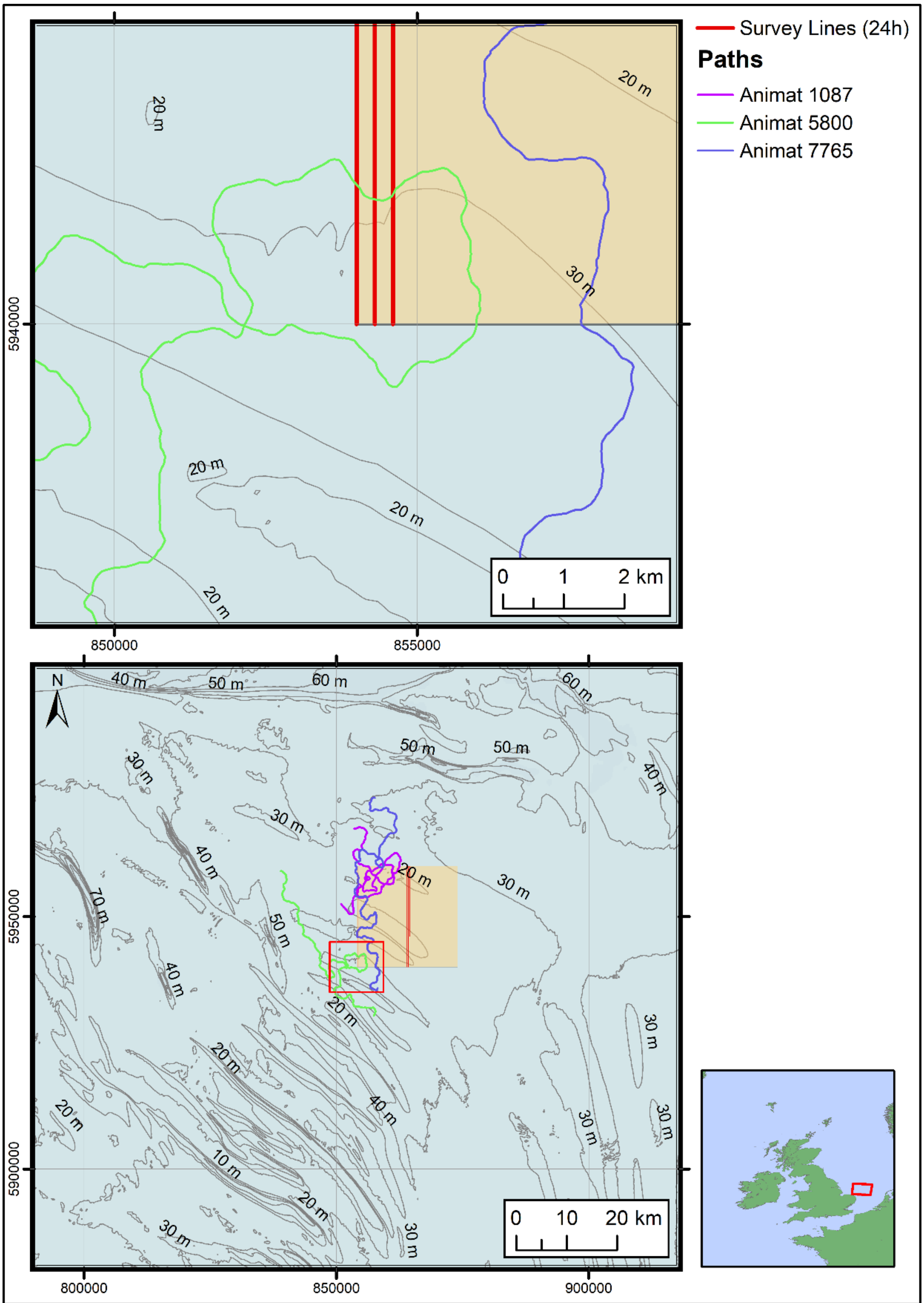

Phase 3: Regional Survey - North Sea Shallow - High-frequency Animat paths	Datum: WGS84 Projection: UTM30 North	JASCO APPLIED SCIENCES
Representative UKCS Seismic Survey Modelling	Created: Aug 2020	

Figure T-1. Paths of three selected animats relative to the seismic survey.

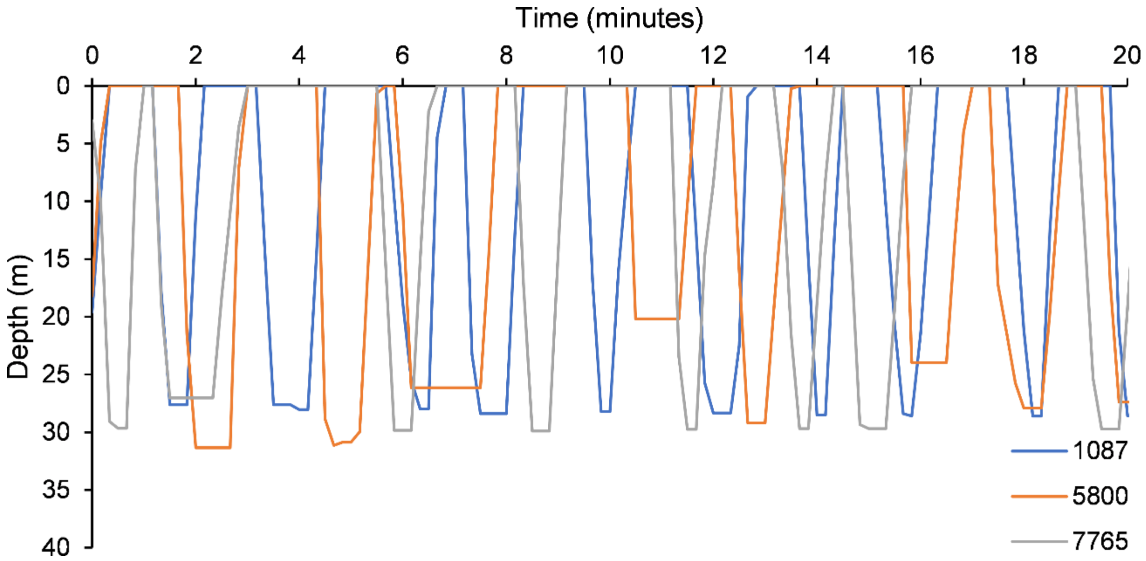

Figure T-2. Depth profiles for the selected animats over the first 20 minutes of the survey. These continue similarly throughout the 24-hour period.

Appendix U. Received Single Shot and Cumulative SEL for Selected Animats

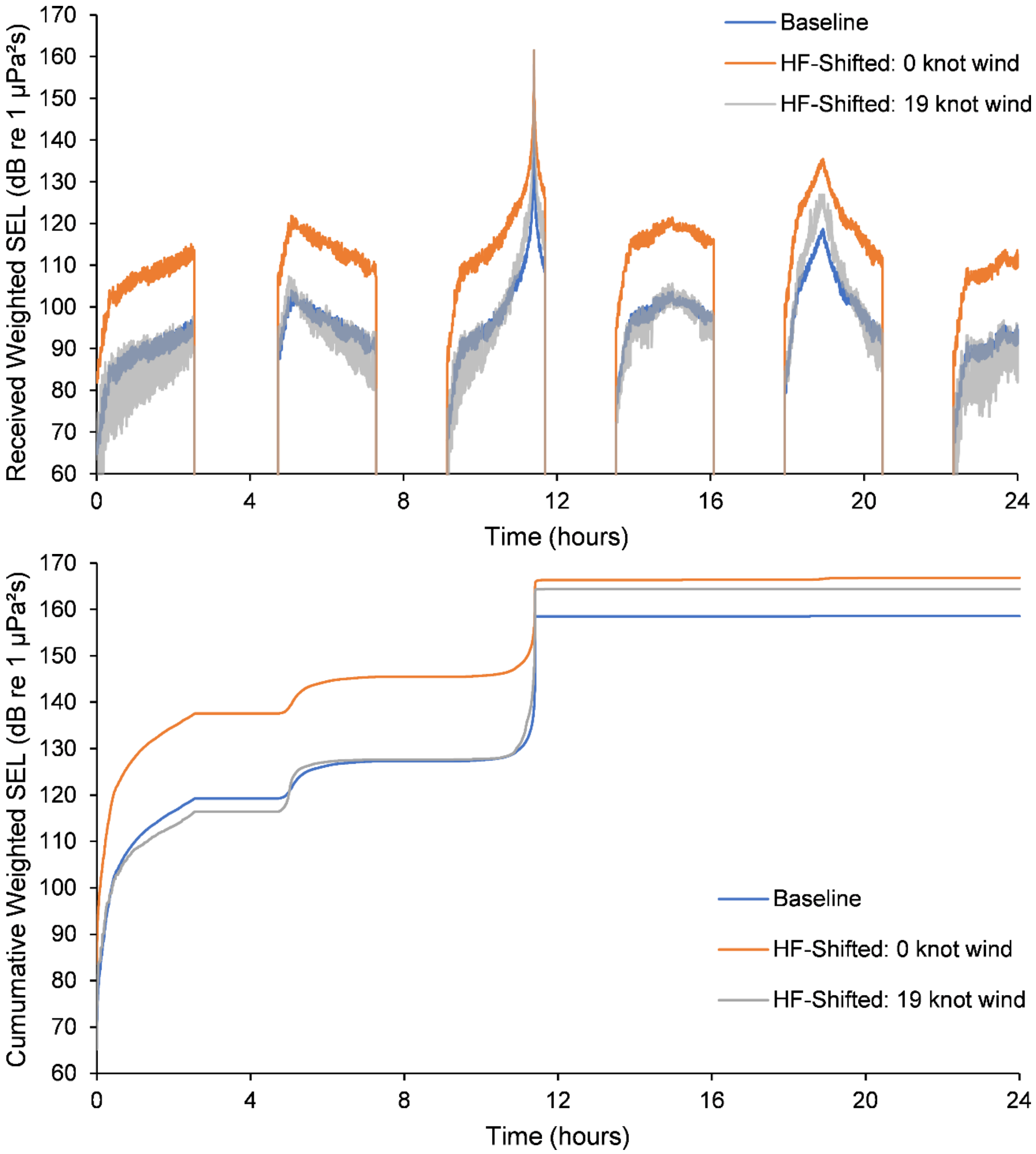

Figure U-1. Single shot SEL (Top) and the cumulative SEL (Bottom) for Animat 7765 for the three high-frequency animat studies in Section 12.2.

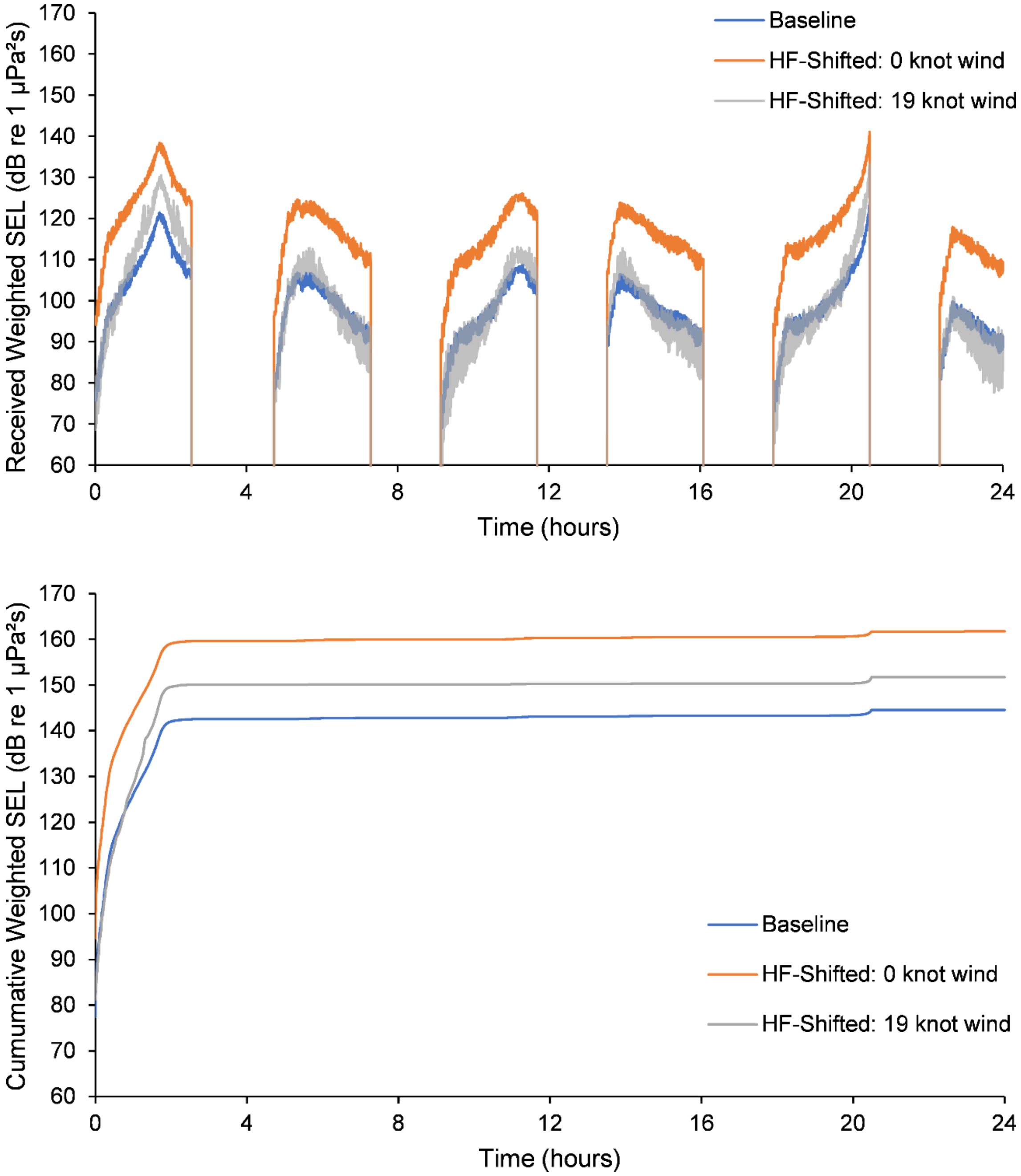

Figure U-2. Single shot SEL (Top) and the cumulative SEL (Bottom) for Animat 1087 for the three high-frequency animat studies in Section 12.2.

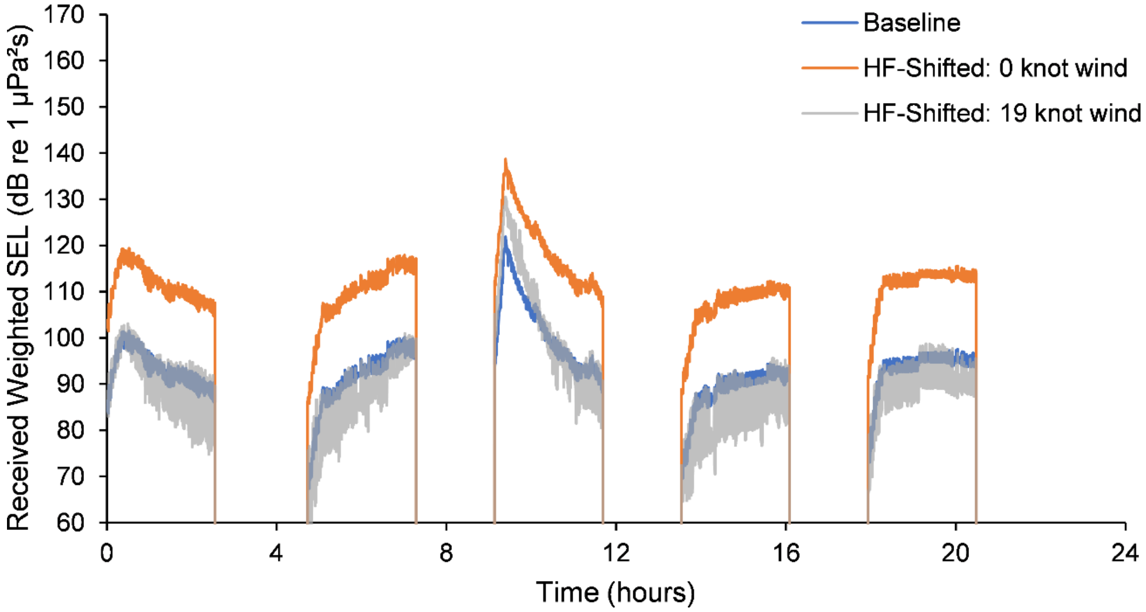

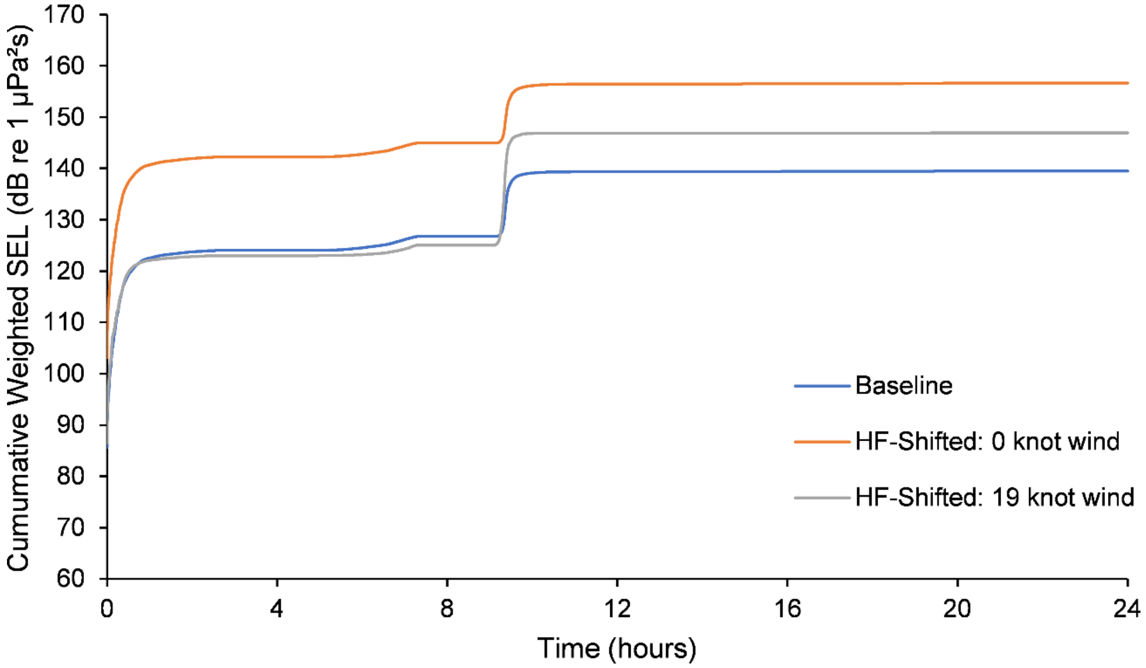

Figure U-3. Single shot SEL (Top) and the cumulative SEL (Bottom) for Animat 5800 for the three high-frequency animat studies in Section 12.2.